Fermion condensation and super pivotal categories

David Aasen[1,2], Ethan Lake[3], and Kevin Walker[4]

[1] Department of Physics and Institute for Quantum Information and Matter, California Institute of Technology, Pasadena, CA 91125, USA

[2]Kavli Institute for Theoretical Physics, University of California, Santa Barbara, CA 93106, USA

[3] Department of Physics and Astronomy, University of Utah, Salt Lake City, UT 84112, USA

[4] Station Q, Microsoft Research, Santa Barbara, California 93106-6105, USA

September 8, 2017

Abstract

We study fermionic topological phases using the technique of fermion condensation. We give a prescription for performing fermion condensation in bosonic topological phases which contain a fermion. Our approach to fermion condensation can roughly be understood as coupling the parent bosonic topological phase to a phase of physical fermions, and condensing pairs of physical and emergent fermions. There are two distinct types of objects in fermionic theories, which we call "m-type" and "q-type" particles. The endomorphism algebras of q-type particles are complex Clifford algebras, and they have no analogues in bosonic theories. We construct a fermionic generalization of the tube category, which allows us to compute the quasiparticle excitations in fermionic topological phases. We then prove a series of results relating data in condensed theories to data in their parent theories; for example, if $\mathcal{C}$ is a modular tensor category containing a fermion, then the tube category of the condensed theory satisfies $\mathbf{Tube}(\mathcal{C}/\psi) \cong \mathcal{C} \times (\mathcal{C}/\psi)$. We also study how modular transformations, fusion rules, and coherence relations are modified in the fermionic setting, prove a fermionic version of the Verlinde dimension formula, construct a commuting projector lattice Hamiltonian for fermionic theories, and write down a fermionic version of the Turaev-Viro-Barrett-Westbury state sum. A large portion of this work is devoted to three detailed examples of performing fermion condensation to produce fermionic topological phases: we condense fermions in the Ising theory, the $SO(3)_6$ theory, and the $\frac{1}{2}\mathrm{E}_6$ theory, and compute the quasiparticle excitation spectrum in each of these examples.

Contents

1 Introduction

A large program in condensed matter physics in recent years has been to classify topological phases of matter which host emergent quasiparticle excitations with topological properties like exotic braiding statistics. The mathematical framework of category theory has proven to provide the right framework needed to formally develop classification efforts. Thus far, the bulk of these efforts have focused on understanding bosonic topological phases. These phases are "bosonic" because the topological excitations emerge from bosonic local degrees of freedom.

By contrast, much less is known about how to complete a classification program for *fermionic* topological phases, in which fermions constitute the underlying degrees of freedom. Early work in this direction was presented by one of the authors in a series of talks [1, 2, 3]. Progress on understanding the coherence relations used to classify fermionic topological phases and the identification of a class of examples of such phases was made in [4, 5, 6]. Recently, Majorana dimer lattice models have appeared [7, 8], which give an explicit Hamiltonian construction of a non-trivial fermionic phase closely related to the Ising theory. There has also been some recent work in the math community [9, 10, 11, 12] devoted to studying the formal category-theoretic description of fermionic topological phases and spin-TQFTs.

Intimately related to the description of fermionic topological phases is the concept of fermion condensation, whereby one passes to a phase in which the emergent (anyonic) fermions have become local particles (meaning that they can be created and destroyed locally). There have been several recent approaches related to understanding fermionic topological phases with field theoretic methods, fermion condensation, and bosonization [13, 14, 15, 16, 17, 18, 19], with a more algebraic take on fermion condensation given in [20].

In this work, we perform a systematic study of fermionic topological phases and fermion condensation from a category-theoretic point of view. The strategy we will use to construct examples of fermionic topological phases will be to start with a bosonic phase described by a tensor category $\mathcal{C}$ which contains an emergent fermion ψ. To obtain a fermionic theory, we will "condense" ψ. The resulting fermionic topological phase is described by a super pivotal category, which we denote as $\mathcal{C}/\psi$. $\mathcal{C}/\psi$ is a fermionic phase because in order for a phase to support local fermionic excitations, its underlying degrees of freedom must be fermionic.

Due to their nontrivial spin and statistics, condensing fermions is not a straightforward business. From a mathematical perspective, in order to perform the condensation it is necessary to equip the configuration space of ψ worldline endpoints with a certain complex line bundle. Physically, the construction of this bundle amounts to attaching a phase of

physical (not emergent) fermions f to the parent bosonic theory: fermion condensation then heuristically proceeds by coupling the ψ fermions to the f fermions, and condensing ψf bound states. In most cases (when ψ is not transparent in $\mathcal{C}$), we will also need to perform the condensation with a construction we call the "back wall", which is a codimension-1 surface on which ψ worldlines are allowed to end.

An important difference between fermionic topological phases and their bosonic counterparts is that the former possesses two distinct classes of simple objects (or anyons). One class of simple objects, which we refer to as "m-type" objects, are identical in character to the simple objects found in bosonic theories. The other class of objects, which we call "q-type" objects, have no bosonic analogues. From a formal perspective, they are distinguished by their nontrivial endomorphism algebras – if a is a q-type simple object, then $\mathrm{End}(a) \cong \mathbb{C}\ell_1$, the first complex Clifford algebra. From a physical point of view, these can be thought of as "Majorana objects", which have the ability to "absorb" fermions. In string-net constructions, strings labeled by q-type objects behave like Kitaev wires in the topological phase: the fermion parity of a closed loop of such a string is determined by the spin structure inherited by the string, and is delocalized in the sense that fermions living on the q-type string are allowed to fluctuate freely along its length.

One rather trivial way to produce a fermionic phase is to simply form a non-interacting stack of a phase of physical fermions and a known bosonic topological phase. To obtain examples of fermionic phases that do not arise in this way (which are called "primitive" in [6]), it is essential to examine theories that contain q-type objects, which are fundamentally fermionic in nature and which are impossible to obtain in theories constructed through this stacking procedure.

A categorical description of the condensed phase $\mathcal{C}/\psi$ cannot be obtained within the framework of regular tensor categories, and one needs to instead adopt the framework of so-called *super pivotal tensor categories*. The fermionic nature of $\mathcal{C}/\psi$ means that the fusion spaces of the theory become super vector spaces (as opposed to normal vector spaces), tensor products of morphisms and coherence relations like the pentagon identity are modified to account for Koszul signs, the pivotal structure of the theory is changed to account for the presence of fermions, and so on.

We should stress that all of the constructions we employ in this paper are mathematically well-defined and self-contained, independent of their physical interpretations. Most of the paper uses techniques from category theory, TQFTs and string nets to construct what one might call fermionic Turaev-Viro theory. This paper is mostly about fermionic TQFTs from this perspective, rather than ground states of Hamiltonians. Indeed, not until near the end of the paper do we define a fermionic Levin-Wen style Hamiltonian whose ground states coincide with the Hilbert spaces of this TQFT. Foreshadowing the introduction of this Hamiltonian, we will, throughout the paper, talk about physical notions like "excitations", "ground state degeneracies", etc, even though strictly speaking this point of view does not make sense until after we have introduced the Hamiltonian. We emphasize that the Hamiltonian point of view is optional; most of the paper can be viewed as taking place in the self-contained world of (fermionic) string-net TQFTs.

In order to examine the quasiparticle excitation spectrum of fermionic phases, we use the tube category construction [21],[1] which is closely related to the Drinfeld center. In the fermionic context, we must modify the tube category construction to take into account different spin structures on the circle. For bosonic theories we have the isomorphism

[1] Again, it is technically imprecise to call the objects of the tube category "excitations" until after we have carefully defined a Hamiltonian.

$\mathbf{Tube}(\mathcal{C}) \cong \mathcal{C} \times \overline{\mathcal{C}}$ [22] if $\mathcal{C}$ is modular, where $\overline{\mathcal{C}}$ denotes the opposite category of $\mathcal{C}$. We prove a fermionic version of this isomorphism, namely that if $\mathcal{C}$ is modular then

$$\mathbf{Tube}(\mathcal{C}/\psi) \cong \mathcal{C} \times (\overline{\mathcal{C}/\psi}). \tag{1}$$

Because quasiparticle excitations are associated to circular boundary components of the ambient manifold on which the theory is defined, there are two distinct classes of quasiparticles (a.k.a. representations of the tube category) in fermionic theories: those with anti-periodic fermion boundary conditions around the circle, and those with periodic boundary conditions. The tubes in the tube category come equipped with spin structures, which gives the tube category a $\mathbb{Z}_2$ grading and separates the quasiparticle spectrum in to vortex quasiparticles (those which bind spin structure defects) and non-vortex quasiparticles (which are similar in character to the quasiparticles present in bosonic theories).

The analysis of things related to the tube category, like modular transformations, braiding statistics, and the computation of ground state degeneracies on various spin surfaces, is also modified in the fermionic setting. The behavior of the S and T modular transformations on the torus depends on the spin structure of the torus in question, and certain relations like $(ST)^3 = \mathrm{id}$ are modified in the fermionic setting, becoming $(ST)^3 = (-1)^F\mathrm{id}$ where $(-1)^F$ is the fermion parity operator.

We will also show how to construct a commuting projector lattice Hamiltonian for fermionic phases, whose excitation spectrum is given by the objects in the fermionic tube category. It is similar in character to the Levin-Wen Hamiltonian [23], except that it includes an extra edge term which is responsible for moving fermions along edges labeled by q-type objects. Spin structure defect excitations are realized as violations of this edge term, and are linearly confined.

Finally, we show how to construct a tensor network which produces the ground state wavefunction of our lattice Hamiltonian. We do this using a cut-and-glue approach to the construction of the Turaev-Viro-Barrett-Westbury state sum, which allows us to write the bosonic partition function as a tensor contraction. We then show how to modify this construction in order to obtain a fermionic version of the TVBW state sum and a corresponding fermionic tensor network.

A series of in-depth examples occupies a large portion of this paper. Our presentation is characterized by an emphasis on examples, and we often save formal definitions and more general statements for later sections after relevant examples have been presented. Many general observations are mixed in with the example sections, and we stress that the more general sections are intended as a supplement to the example sections; they are not stand-alone.

In several places in the paper we make use of a fermionic version of a Turaev-Viro type 2+1-dimensional TQFT. Constructing this TQFT using the techniques of [24] is straightforward – one simply replaces oriented manifolds with spin manifolds and allows for the possibility of non-trivial endomorphism algebras of minimal idempotents. In the interest of not further increasing the length of this paper, we have not repeated details found in [24] here.

We now give a quick section-by-section summary of the paper. Much of the content of Section 2 was presented at [1] in July 2013, and many of the ideas contained in Sections 3.1, 3.2, and 9 were presented at [2] and again at [3].

Sections 2 and 3 are devoted to a detailed study of fermion condensation in the Ising TQFT, which is a simple case study that allows us to build intuition for the condensation

procedure. This condensed theory has been examined before in [16, 18]; here we examine it in greater detail. In Section 2 we review the Ising TQFT, describe how to perform the fermion condensation, and write down the local string-net rules in the condensed theory, which we call the C_2 theory. In Section 3 we compute the simple objects of the tube category of the C_2 theory, determine their fusion rules, compute the ground state degeneracy on the torus, and study the modular transformations of the theory.

In Section 4, we present a collection of more general results on the machinery of fermionic theories. We show how to perform fermion condensation in more general settings and discuss the fermionic version of the tube category construction in more generality. We also discuss how to compute quantum dimensions and fusion rules, and we prove some general relations between the total quantum dimensions of condensed theories, their parent theories, and their tube categories. Additionally, we present a Verlinde-type dimension formula for fermionic theories.

We devote Section 5 to a detailed study of the tube category for fermionic theories which result from fermion condensation in a modular tensor category (MTC). We introduce several tools for performing calculations in tube categories, and use them to prove that if $\mathcal{C}$ is an MTC containing a fermion ψ, then $\mathbf{Tube}(\mathcal{C}/\psi) \cong \mathcal{C} \times (\overline{\mathcal{C}/\psi})$ as tensor categories. We also describe a way of easily computing the modular data for $\mathbf{Tube}(\mathcal{C}/\psi)$.

Section 6 is devoted to the example of performing condensation in the $SO(3)_6$ and $SU(2)_6$ theories, while Section 7 discusses fermion condensation in the $\frac{1}{2}\mathrm{E}_6$ theory. Both of these examples are more involved than the C_2 theory, and illustrate some of the more interesting features of general fermionic topological phases.

In Section 8 we discuss super pivotal categories from a more formal point of view. We show how fermionic fusion spaces are constructed and tensored together, how coherence relations like the pentagon identity are modified in the fermionic case, and explain various other modifications that are necessary in the fermionic case.

Section 9 is devoted to a discussion of a lattice Hamiltonian for fermionic theories, which is an extension of the Levin-Wen Hamiltonian. It differs most significantly from the Levin-Wen Hamiltonian due to the presence of an edge term, which is responsible for allowing fermions to fluctuate across q-type strings.

We show how to construct a tensor network realizing the ground state of our lattice Hamiltonian in Section 10. We first review how to write the partition function of a bosonic theory as a tensor contraction in a way amenable to generalization, and then show how our construction can be extended to cover the fermionic case.

In Section 11, we discuss the Kitaev chain within the framework of super pivotal categories. We show how the Kitaev chain Hamiltonian and ground-state wavefunctions can be succinctly written down using the diagrammatic calculus developed earlier in the paper, and discuss connections between the Kitaev chain and the C_2 theory. This section also provides a connection between our work and recent work on fermionic topological phases in the physics community [8, 7, 25]. The only prerequisite for this section is a brief reading of Section 2, and physically-inclined readers less interested in more general mathematical frameworks are invited to read this section after reading Section 2.

We end with a conclusion and discussion in Section 12. Several appendices contain miscellaneous results and mathematical background information.

1.1 Table of notation

In partial compensation for the unwieldy length of this paper, we give a table summarizing some of the most frequently used and/or least standard notation found herein.

$\mathcal{C}$	tensor category
$\mathcal{C}/\psi$	fermionic quotient of $\mathcal{C}$
$\mathcal{S}$	super pivotal tensor category, e.g. $\mathcal{C}/\psi$
$\mathcal{T}$	super linear category
$\mathrm{sob}_r(\mathcal{C})$	complete set of representatives of simple objects for $\mathcal{C}$
$\mathrm{mor}(x \to y)$	morphisms from x to y
$\mathrm{End}(x)$	endomorphism algebra of the object x; same as $\mathrm{mor}(x \to x)$
$\mathbb{C}\ell_1$	first complex Clifford algebra
$\mathbb{C}^{r\|s}$	Super vector space with even dimension r and odd dimension s
m-type	simple object with $\mathrm{End}(x) \cong \mathbb{C}$
q-type	simple object with $\mathrm{End}(x) \cong \mathbb{C}\ell_1$
n_x	$\dim \mathrm{End}(x)$, 1 if x is m-type and 2 if x is q-type
$\mathrm{cl}(x)$	closure of x in either an annulus or torus depending on context
$\mathrm{cl}_W(x)$	closure of x with spin structure W assigned to new cycle
$f \cdot g$	the composition of two morphisms $x \xrightarrow{f} y \xrightarrow{g} z$ (arrow order)
$g \circ f$	the composition of two morphisms $x \xrightarrow{f} y \xrightarrow{g} z$ (function order)
$A(Y)$	string nets modulo local relations on a 2-manifold Y; predual Hilbert space
$A(Y; c)$	string nets, with fixed boundary condition c on ∂Y, modulo local relations
$Z(Y)$	functions on string nets invariant under local relations on a 2-manifold Y; dual space $A(Y)^*$; Hilbert space
$Z(Y; c)$	functions on string nets, with fixed boundary condition c on ∂Y, invariant under local relations
$Z(M)$	path integral of a 3-manifold M
$Z(M)(c)$	path integral of a 3-manifold M, evaluated on a boundary condition $c \in A(\partial M)$
$\mathbf{Tube}(\mathcal{C})$	tube category of $\mathcal{C}$

$\mathbf{Tube}^B(\mathcal{C})$	bounding tube category
$\mathbf{Tube}^N(\mathcal{C})$	non-bounding tube category
$\mathbf{Tube}_{x\to y}$	morphisms from x to y in the tube category
B, N	bounding, nonbounding spin structures on the circle
S^1_B	spin circle with bounding (anti-periodic) spin structure
S^1_N	spin circle with nonbounding (periodic) spin structure
$\mathbb{1}$	tensor unit in a tensor category; trivial object
d_a	quantum dimension of the object a; loop value of a
θ_a	twist eigenvalue of the simple object a
$\mathcal{D}^2$	$\sum_{a\in \mathrm{sob}_r(\mathcal{C})} d_a^2$ in bosonic case; $\sum_{a\in \mathrm{sob}_r(\mathcal{S})} d_a^2/n_a$ in fermionic case

2 Fermion condensation in the Ising TQFT

Before discussing super pivotal categories in the abstract and general techniques for constructing examples thereof, we will give a detailed account of one of the simplest examples: the C_2 super pivotal category. This theory is obtained from the Ising TQFT by condensing the emergent fermion ψ, and provides a good demonstration of the qualitatively new features that occur as a result of fermion condensation. This section (and the next) is organized as follows: in 2.1 we briefly review the aspects of the Ising TQFT we will need in later sections. In 2.2 we comment on the general procedure of anyon condensation, and in 2.3 we show how to condense ψ in the Ising theory, obtaining the C_2 super pivotal theory. 2.4 details the diagrammatic properties of the C_2 theory, and in 3.1 we compute the quasiparticle excitations of the theory. In 3.2 we determine the fusion rules of these quasiparticles, and in 3.3 we compute the modular S and T matrices of the theory.

2.1 Ising TQFT

Here we provide a brief review the the Ising TQFT (see e.g. [26]). There are three particles in the theory, which we label as $\mathbb{1}$ (the trivial particle), σ (the non-abelian Ising anyon), and ψ (the emergent fermion). The nontrivial fusion rules of the theory are as follows:

$$\sigma \otimes \sigma \cong \mathbb{1} \oplus \psi, \quad \sigma \otimes \psi \cong \sigma, \quad \psi \otimes \psi \cong \mathbb{1}. \tag{2}$$

The quantum dimensions of the particles are

$$d_{\mathbb{1}} = 1 \quad d := d_\sigma = -A^2 - A^{-2} \quad d_\psi = 1, \tag{3}$$

where A is a primitive 16th root of unity. Graphically, this means that

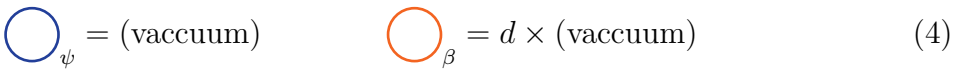

(4)

where the blue (orange) circle denotes a circular ψ (σ) worldline. $\mathbb{1}$ worldlines, being identified with the vaccuum, are not drawn in diagrams.

Out of the eight possible choices for A, the four different choices $A = ie^{\pm i\pi/8}, -ie^{\pm i\pi/8}$ all give a positive quantum dimension for the σ particle of $d = \sqrt{2}$. The other four choices of A give $d = -\sqrt{2}$, which can alternatively be defined with $d = \sqrt{2}$ but with a negative Frobenius-Schur indicator of $\kappa_\sigma = -1$. In what follows, we will specify to $A = ie^{\pm i\pi/8}, -ie^{\pm i\pi/8}$ so that $d_\sigma = \sqrt{2}, \kappa_\sigma = 1$.

We now turn our attention to the graphical calculus of the Ising TQFT. We pick a normalization more common in the physics literature, bubbles in diagrams can be eliminated by using the rule

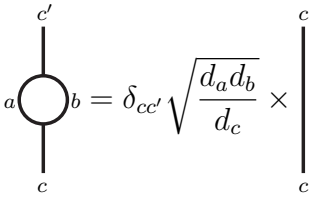

(5)

In particular, we have

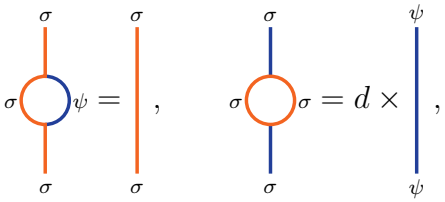

(6)

where again, we are marking ψ worldlines in dark blue and σ worldlines in orange.

The non-trivial F-moves in the theory are as follows:

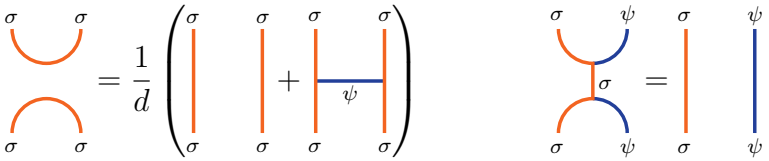

(7)

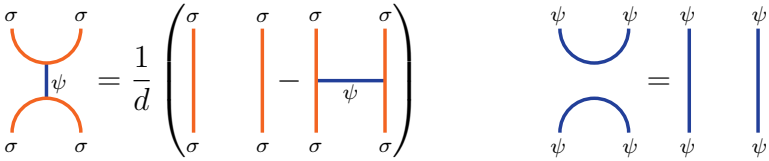

(8)

The twist and braiding of the σ particle are given by

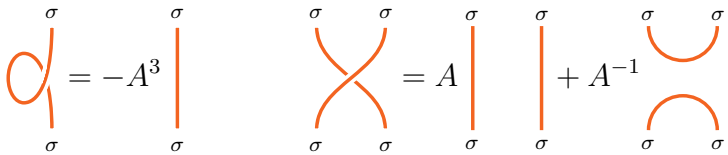

(9)

The formula for the topological twist on the left follows from the relation given on the right. Using that $\sigma \otimes \sigma = \mathbb{1} \oplus \psi$ and (9) we can derive the braiding data for the ψ particle. Most importantly for us, the ψ particle is fermionic in both its topological twist and statistics, regardless of the choice of A:

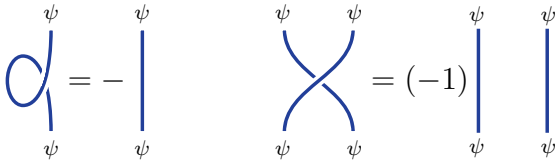

(10)

Additionally, ψ is not transparent, as it braids nontrivially with σ:

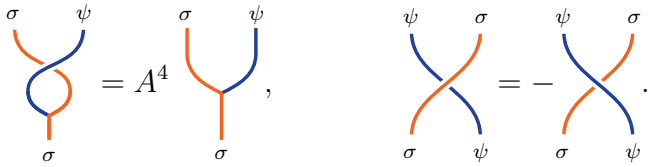

(11)

Our goal in what follows is to describe how to condense the ψ particle in the Ising TQFT. To put this in context, we will first make a few remarks on the more familiar bosonic condensation.

2.2 Condensation of transparent bosons

We now briefly review how to perform condensation with transparent bosons (see e.g. [27]). Let $\mathcal{C}$ be a ribbon category and let α be a particle (simple object) of $\mathcal{C}$ which we hope to condense. In category theoretic terms, we want to add morphisms to $\mathcal{C}$ so that α becomes isomorphic to the trivial particle $\mathbb{1}$ (or, more generally, to a direct sum of several copies of $\mathbb{1}$). We can think of this as a categorical quotient, denoted $\mathcal{C}/\langle\alpha \cong \mathbb{1}\rangle$ or more simply as $\mathcal{C}/\alpha$. Physically, this amounts to turning the anyon α into a *local* particle (one which can be created locally).

In our graphical calculus, condensing α means that α worldlines are allowed to have endpoints at locations where they are "absorbed" into the condensate (allowing them to be created locally). We will mark the locations where α particles are absorbed into the condensate with boxes

(12)

where the horizontal blue line is an α worldline. We can also think of these boxes as morphisms from α to the trivial particle. For simplicity, we will assume that $\alpha \otimes \alpha \cong \mathbb{1}$ (which will be true in the examples considered in this paper), although most of the following discussion can be made to work more generally.

In order for this condensation procedure to not cause unintended collapse in $\mathcal{C}$ (e.g. confine other particles of $\mathcal{C}$, or result in a trivial theory), α must satisfy three conditions:

- First, the twist of α must be 1. This is because

(13)

  and so if $\theta_\alpha \neq 1$, diagrams in which α worldlines are absorbed into the condensate are identically zero, and condensation is impossible.

- Secondly, α must be statistically bosonic, i.e. it must braid trivially with itself. This is because

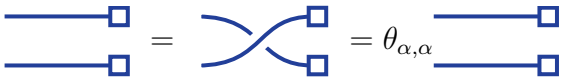

(14)

  where $\theta_{\alpha,\alpha}$ is the self-statistics of α. (By our assumption that $\alpha \otimes \alpha \cong \mathbb{1}$, the last equality must hold with $\theta_{\alpha,\alpha} = \pm 1$.) By the spin-statistics relation this condition is not independent of the previous one, but it will be useful to regard them as separate constraints for the purpose of the fermion condensation procedure described in the next section.[2]

[2] If we drop positivity requirements, we can violate the spin-statistics theorem and have particles which are fermionic in spin but not statistics or vice-versa; see [28] for a discussion of this.

- Finally, α must braid trivially with every particle in $\mathcal{C}$. In category-theoretic language, this means that α must lie in the transparent subcategory of $\mathcal{C}$. If a particle β braids non-trivially with α (i.e. if the left and right braidings are not equal), then any string diagram which includes a β particle must be zero: (we assume the quantum dimension of alpha is one for convenience)

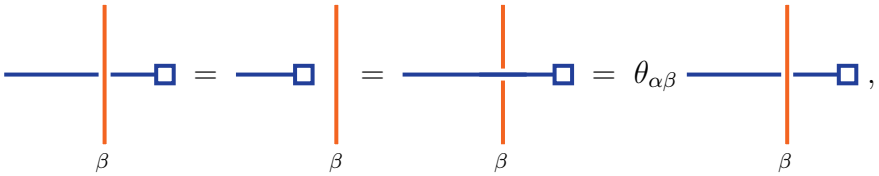

(15)

where the orange line is a β worldline and $\theta_{\alpha,\beta}$ is the mutual statistics of α and β. The first two equalities follow from the fact that the location of a particle being absorbed into the condensate is not physically significant: no operator can distinguish between states that differ only by the location of an α endpoint. Therefore, if $\theta_{\alpha,\beta} \neq 1$, condensing α causes unintended collapse in $\mathcal{C}$, since it confines β.

To summarize, in order to condense α, α must have a twist of 1, have bosonic self-statistics, and braid trivially with every other particle in the theory. If any of these conditions are violated, we will have to work harder to construct $\mathcal{C}/\alpha$.

2.3 Condensing ψ in Ising

In this subsection we describe our procedure for condensing ψ in the Ising theory. While we will focus on the Ising theory in this section, our discussion will be fairly general, and can be applied to perform fermion condensation in more general scenarios.

We would like to "condense" the ψ particle by constructing the quotient theory $\mathcal{C}/\psi$. We will denote the condensed theory by C_2, since the fusion rules are described by the C_2 Dynkin diagram; see below. We will denote the image of σ in the condensed theory C_2 as β.

First, from (10), we recall that ψ is fermionic in both spin and statistics, Additionally, we recall that ψ has nontrivial braiding with σ, and as such ψ is not transparent. Thus, ψ violates all three of the conditions that particles in a condensate must satisfy! To condense ψ, we will clearly need some new tricks.

We will first examine how to address the non-transparency of ψ. As we saw above in (15), we can't allow world lines of ψ to disappear at arbitrary points in the 3-dimensional spacetime, since this would confine β (a.k.a. σ).

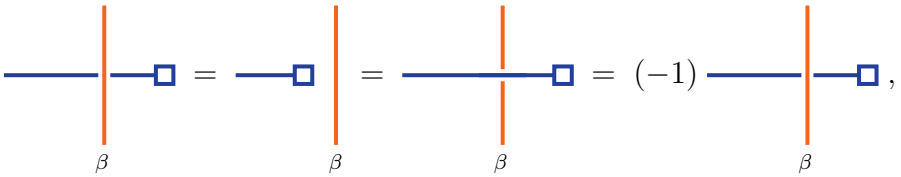

(16)

However, if we restrict the ψ worldline endpoints to lie on a 2-dimensional subset of the boundary of the ambient 3-dimensional spacetime, we *can* obtain a consistent graphical calculus.

In this paper, we will adopt the convention that ψ world lines are allowed to terminate on a codimension-1 "back wall", located on a boundary of the system that is positioned "behind" all other world lines drawn in our graphical calculus.

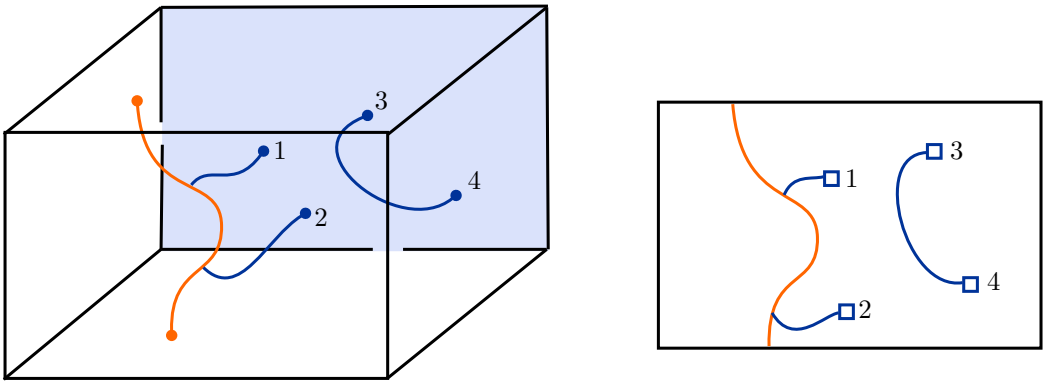

(a) (b)

Figure 2.3.1: (a) The "back wall" picture. The box represents a section of a (2+1)D Ising TQFT, with the codimension-1 back wall indicated by the blue back side of the box. ψ worldlines are absorbed into (or emitted from) the back wall at marked points labelled by $1, 2, 3, 4$. Free ψ endpoints which do not terminate on the back wall are not allowed. (b) Our way of representing the picture (a) in a (1+1)D graphical calculus. We have squashed the box down to a two dimensional plane, with the blue boxes representing the points at which the ψ lines "go straight back and hit the back wall".

Figure 2.3.1(a) demonstrates this graphically, with the light blue back section of the box denoting the back wall, on which the ψ worldlines can be absorbed or emitted. String-net graphs in our (2+1)D spacetime can be reduced to string-net graphs in (1+1)D spacetime by introducing a shorthand notation for ψ-lines terminating on the back wall. This notation is shown in Figure 2.3.1(b), where we use boxes to denote places where ψ worldlines head straight back into the back wall and terminate.

Even though we use the same box-at-the-end-of-the-string graphical convention to denote ordinary condensation and back wall condensation, there is an important difference. In both cases, we can slide a box behind another strand, with the before and after pictures differing by an isotopy:

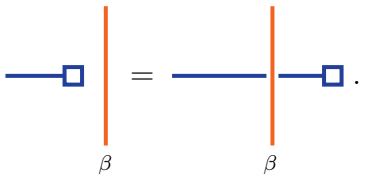

(17)

However, in the back wall case, we cannot slide a box in front of another strand

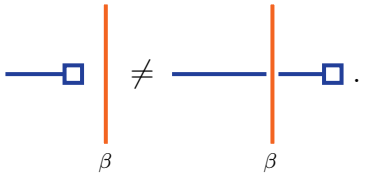

(18)

This is because doing so would involve the other strand crossing the ψ strand as it heads into the page en route to the back wall; the before and after pictures are not isotopic. Thus restricting ψ emission/absorption to the back wall disallows the series of diagram equalities in Figure 16.

An important consequence of the existence of the back wall this is that the quotient category C_2 is not braided (although there is a way to perform the condensation so that the resulting theory is braided, which we mention briefly in 4.1.4). String diagrams for braided categories (such as Ising) can be glued together in three independent dimensions: right/left, top/bottom, and back/front. In more formal terms, braided categories are (special cases of) 3-categories. Because of the back wall, it does not make sense to glue string diagrams for the C_2 category in the back/front dimension. In more formal terms, C_2 is a mere 2-category, or, more specifically, a (super) tensor category. We can, however, glue an Ising string diagram to the front (but not back) of a C_2 diagram. In category theoretic language, C_2 is a module 2-category for the Ising 3-category; equivalently, C_2 is a codimension 1 defect connecting Ising to the vacuum.

The back wall construction fixes the problems caused by ψ not being transparent. However, we have not yet addressed the spin and statistics inconsistencies (13) and (14). To fix these inconsistencies, we will couple the boxes marking the ψ endpoints to a complex line bundle associated to a spin structure. (When we later consider reflections, this spin structure will be promoted to a pin_+ structure.) Readers unfamiliar with spin and pin structures are referred to Appendix A. The spin structure will enable us to cancel out the factors of -1 arising from the endpoints of ψ worldlines twisting through 2π as in (13). This "bosonizes" the ψ endpoints and allowing the condensation process to go through.

To make this precise, let Y be an oriented 2-manifold, let $M = Y \times [0, 1]$, and let $B = Y \times \{1\}$. (Everything we do in this subsection will work more generally for M any oriented 3-manifold and B some codimension 0 submanifold of ∂M.) In addition, choose a spin structure on B. Our goal is to associate a Hilbert space to Y based on string nets in $M = Y \times I$ and some extra data on the back wall B.

Consider the configuration space $\mathcal{R}(B)$ of all ψ ribbon endpoints on B. Let $\mathcal{R}(B)_k$ denote the subspace of $\mathcal{R}(B)$ corresponding to configurations with exactly k endpoints. (If B is connected, then these are the connected components of $\mathcal{R}(B)$.) We can think of the ribbon endpoint as a point p of B plus a tangent vector at p which points in the direction of the "front" of the ribbon.[3] This means that $\mathcal{R}(B)_1$ is diffeomorphic to the unit tangent bundle of B. We also stipulate that $\mathcal{R}(B)_0$ consists of a single point.

In the next subsection we will construct a complex line bundle $F(B)$, with flat connection, over $\mathcal{R}(B)$, which will provide us with the additional structure we need to perform the condensation. The extra data alluded to above will be a vector in this vector bundle. More specifically, for each string net S in M, we have and endpoint configuration $e(S) \in \mathcal{R}(B)$. Our Hilbert space will be generated by pairs (S, v), where $v \in F(B)_{e(S)}$, the fiber of the bundle $F(B)$ at the configuration $e(S)$.

We impose the usual local string net relations in the interior of M. (Ribbon end points are fixed for these relations.) We also impose the following additional relation: Let $\{S_t\}$, with $0 \leq t \leq 1$, be a 1-parameter family of string nets. The ψ endpoints on B are allowed to move, but any other ribbon endpoints must remain fixed. Let $v \in F(B)_{e(S_0)}$. Using parallel translation for the connection on $F(B)$ and the path of configurations $\{e(S_t)\}$, we obtain $v' \in F(B)_{e(S_1)}$. We now identify these configurations by imposing the relation

$$(S_0, v) = (S_1, v'). \tag{19}$$

[3]Ribbons have a distinguished front and back; if they did not, then we would have to assign phases $\theta_a^{1/2}$ corresponding to half twists of ribbons.

Let us now see how coupling the system to $F(B)$ fixes the inconsistencies (13) and (14). The crucial property of the flat connection on $F(B)$ is the the holonomies around loops corresponding to (13) and (14) is -1. In other words, in (19), we have $v = -v'$ if $\{S_t\}$ is the family of string nets depicted in (13) or (14).

So, (13) now becomes

(20)

and (14) becomes

(21)

Is the choice of $F(B)$ together with its flat connection uniquely determined by the above holonomy requirements? No: in fact, there is a natural bijection between the set of spin structures on B and flat connections fulfilling the above holonomy requirements. In other words, in order to perform this sort of fermionic condensation, we we need to choose a spin structure on B (or on Y, in the main case where $M = Y \times I$ and $B \cong Y$).

The details of the construction of the bundle-with-connection $F(B)$ are somewhat technical, and can be found in in Appendix B. Some of the key properties of $F(B)$ are:

- In order to specify an element $v \in F(B)_{e(S)}$, it suffices to (a) assign an ordering to the ψ-endpoints, and (b) choose a spin-framing at each such endpoint. Recall that a spin structure can be thought of as a double-covering of the unit tangent bundle of B. By "spin framing" we mean a choice of lift to this double cover from the unit tangent vector determined by the ribbon orientation.

- The most general way of specifying a spin framing is via a "Dirac belt" connecting a base framing on B to the tangent vector in question. For manifolds equipped with global framings there are no ambiguities, and we can choose a "gauge" in which the orientation of the belt is consistent with the global framing, allowing us to drop the belts from the figures. The standard Euclidean structure on a page of this paper determines a global framing (the "blackboard framing"), and unless stated otherwise we implicitly equip each ψ endpoint with a spin framing determined by this choice of global framing. In some figures we have in mind a spin structure with a different global framing, and in these cases we will draw dashed "branch cut" lines to indicate how the framing differs from the standard blackboard framing. The branch cuts will be chosen such that the spin framing rotates by 2π (switches sheets on the double cover) across a branch cut.

- Another important property of $F(B)$ is locality: The bundles behave well with respect to gluing surfaces. By "behave well", we roughly mean that for $B = B' \cup B''$, there is an isomorphism between $F(B)$ and $F(B') \otimes F(B'')$.

- $F(B)$ comes equipped with a way to cancel pairs of ψ endpoints, which is required since the fermion ψ we will be condensing satisfies the fusion rule $\psi \otimes \psi \cong \mathbb{1}$. This requires us to supplement the parallel transport of the flat connection with additional isomorphisms of fibers of $F(B)$ connecting points of $\mathcal{R}(B)_k$ to $\mathcal{R}(B)_{k-2}$.

- Finally, in order to define Hermitian inner products on our Hilbert spaces, $F(B)$ comes equipped with an antilinear bundle map $F(B) \to F(B')$ for all orientation-reversing maps $B \to B'$.

Our spin-structure-equipped back wall construction admits a simple physical interpretation: coupling the theory to the bundle $F(B)$ is equivalent to adding a phase of *physical* (not emergent) fermions to the theory, and binding single physical fermions to each ψ endpoint. The physical fermion attached to each ψ endpoint compensates for the fermionic nature of the ψ particle in the condensate: the factors of -1 that relate two different orderings of the ψ endpoints are the Koszul signs associated with the physical fermions, and the factors of -1 that we pick up when rotating the ψ endpoint framing by 2π come from the spin $1/2$ of the physical fermions. Thus, attaching physical fermions to the ψ endpoints transforms them into bosonic objects, which are then allowed to undergo normal boson condensation. Therefore, although we are indeed identifying emergent fermions with the vacuum, the term "fermion condensation" is a bit misleading, as what we are actually doing is closer to *boson* condensation of bound states of ψ and a physical fermion. However, we reiterate that the ψ endpoints are not technically bosons, since they see the background spin structure: the emergent ψ fermions do not see the spin structure, but the physical fermions attached to their endpoints do.

To summarize, we have seen that by introducing the back wall and equipping it with a spin structure, all three conditions necessary for ψ endpoints to condense are satisfied. We emphasize that we have utilized the back wall and the spin structure for two *independent* reasons (the non-transparency of ψ and ψ's fermionic spin and statistics, respectively). For example, if ψ were non-transparent but bosonic, we would still need a back wall, but the back wall would not need a spin structure. Conversely, if ψ were transparent but fermionic, then we would not need a back wall, but we would still need to introduce spin structures.

2.4 Local relations in the C_2 theory

Now that we have worked out how to condense ψ, we can determine the graphical rules that govern the condensed theory.

We have already seen that in order for the condensation procedure to go through, the manifold on which we define the C_2 theory must be equipped with a spin structure. The interaction of fermionic morphisms with this spin structure leads to relations in the diagrammatic calculus that are not present in bosonic theories.

First, we first observe that any ψ strands can be absorbed into the condensate at the expense of phase factors, and so in the condensed theory the only object remaining will be the image of σ under condensation, which will denote by β. β lines will be drawn in orange, and ψ lines will be drawn in blue (and can also be distinguished from β lines through their termination points). In the condensed theory, the β line may or may not have ψ fermions attached to them. We will introduce a blue dot as a compact notation for a ψ worldline that terminates on a β line:

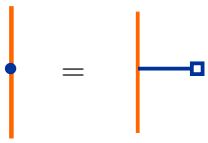

(22)

Note that in order for the dot notation to be unambiguous, we must specify a spin-framing at the dot. We will usually do this implicitly as follows. The dots are only allowed to occur on vertical strands, and the spin framing at the dot is obtained from the base framing of the manifold by rigidly translating with respect to the "blackboard framing" of the page. For diagrams which do not inherit their spin structure from the blackboard, we will have to use other means to specify the spin-framing.

Because β lines in the condensed theory can have fermionic dots on them, there are several new diagrammatic rules involving them that need to be included in our graphical calculus. One of the most important local relations is the addition and removal of an even number of fermions on β lines. The process of removing two fermions can be done at the cost of a phase factor:

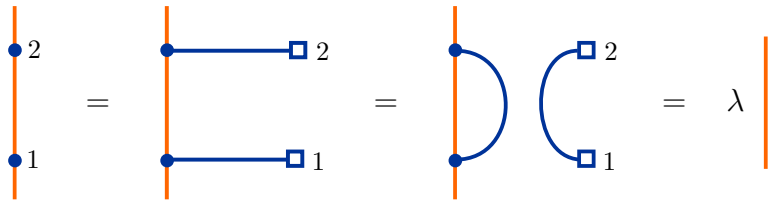

(23)

where the labels 1 and 2 denote the ordering of the fermions in question. We have performed an F-move on the ψ worldlines to get the second equality, used (6) to remove the ψ line attached to the σ line in the third diagram, and have used

$$= \lambda \times (\text{vaccuum}), \tag{24}$$

in the last step to remove the semicircular ψ line, where $\lambda \in \mathbb{C}$ is some complex number. We show in Appendix B that we must have $\lambda = \pm i$, and since $A^4 = \pm i$ in the Ising theory, we may choose either $\lambda = A^4$ or $\lambda = -A^4$ (the choice of A does not constrain the choice of λ). The choice of $\lambda = \pm A^4$ affects the F-symbols in the condensed theory, but does not affect observable quantities like the twists or mutual statistics of the quasiparticles in the theory.[4] Therefore without loss of generality we may choose a gauge in which $\lambda = A^4$, and so

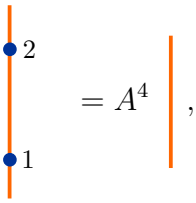

(25)

Since ψ is statistically fermionic, exchanging two fermions on a β line results in a minus sign:

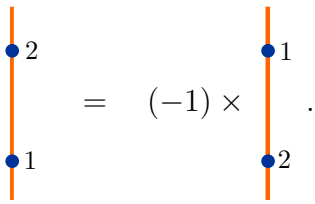

(26)

[4] This is because the choice of $\lambda = \pm A^4$ doesn't change the "multiplication table" of the tube category, which we will discuss below. Essentially, changing λ just performs a scaling on the ψ endpoints in the figures.

The braiding in the parent Ising theory means that we pick up non-trivial phase factors when sliding fermion dots over and around β caps and cups. For example, we can compute

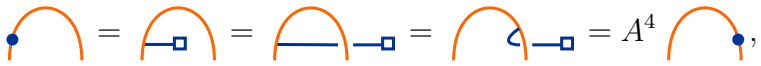

(27)

where in the last step we have used (11). Since in the Ising theory $A^4 = \pm i$, we can invert (27) to find

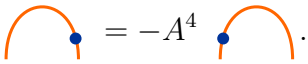

(28)

By a similar argument we find

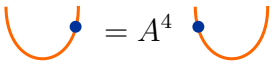

(29)

Because of the nontrivial rules for sliding dots through cups and caps, dots which live on the apex of a cup or the bottom of a cap (where the β line is horizontal) are ambiguous, and we will not allow them to be drawn in our fusion diagrams. We stress that these phases are derived completely from the *braiding data* of the Ising theory.

Note that the above relations imply that even-parity β loops are non-zero, while odd-parity β loops vanish:

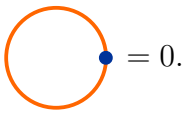

(30)

This is as expected – dragging the fermionic dot around the circle rotates it through 2π.

The final local relations that will be important in what follows are the F-moves, which provide linear relations between different isotopy classes of diagrams. The F-symbols in the condensed C_2 theory can be worked out using our rules for manipulating condensed ψ worldlines and our knowledge of the F-symbols in the parent Ising theory. We begin with a diagram in the Ising theory, apply an F-move, and then remove all ψ lines through condensation to evaluate the F-move in the C_2 theory. For example, in the parent Ising theory we have

(31)

When we condense ψ, the second diagram on the left hand side becomes

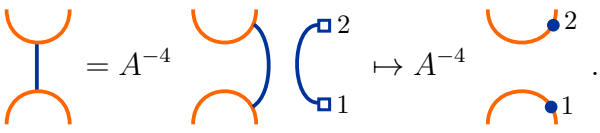

(32)

Note that in the first step of (32) we have displaced the vertical ψ line to the right, so that it never intersects the β line at the apex of a cap or the bottom of a cup. We do this to avoid ambiguities in the fermion framing, which as discussed earlier always points "to the left", meaning that dots living on horizontal β lines are not well-defined. While we

choose to displace the ψ line to the right in (32), this is merely a gauge choice: we could have equally well chosen it to be displaced to the left. Recapitulating, we see that in the C_2 theory we have the F-move

(33)

By similar reasoning we can derive the other nontrivial F-move in the C_2 theory, which is

(34)

The fact that β lines can host dots means that β has an endomorphism which is not a multiple of the identity, which is a hallmark of physics that cannot be found in bosonic topological phases. Indeed, any section of a given β worldline may look like

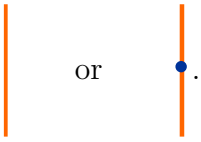

(35)

The two diagrams in (35) are the generators of the endorphism algebra of β. Since we have one even generator and one odd generator we see that $\mathrm{End}(\beta) \cong \mathbb{C}\ell_1$, where $\mathbb{C}\ell_1$ is the first complex Clifford algebra (generated by 1 and a single odd-parity generator). More generally, the vector space assigned to a disk with $2n$ β strings ending on its boundary is has dimension 2^n, and the endomorphism algebra of $\beta^{\otimes n}$ (i.e. n copies of β on a line) is isomorphic to $\mathbb{C}\ell_n$.

In more general contexts, we will refer to simple objects whose endomorphism algebras are isomorphic to $\mathbb{C}\ell_1$ as "q-type objects", and those whose endomorphism algebras are isomorphic to $\mathbb{C}$ as "m-type objects". From the above information, we can infer the fusion rule

$$\beta \otimes \beta \cong \mathbb{C}^{1|1} \cdot \mathbb{1}, \tag{36}$$

where $\mathbb{C}^{1|1}$ is the complex vector space with a single even generator and a single odd generator, corresponding to the even and odd channels of the fusion product $\beta \otimes \beta$.

In bosonic theories, having $\mathrm{End}(\beta) \cong \mathbb{C}\ell_1$ would imply that β is not a simple object, since by Shur's lemma the endomorphism algebra of any simple object must be a division algebra, and since $\mathbb{C}$ is the only ungraded division algebra. Nevertheless, β *is* a simple object.[5] This is possible because in fermionic theories, the Hilbert spaces we use are supervector spaces, compared to the regular vector spaces of bosonic theories. Unlike in the bosonic case, there are *two* super division algebras, $\mathbb{C}$ and $\mathbb{C}\ell_1$. This means that simple objects in the fermionic setting can have endomorphism algebras of either $\mathbb{C}$ or $\mathbb{C}\ell_1$. Later on, we will see that the existence of simple objects with $\mathbb{C}\ell_1$ endomorphism algebras is responsible for a large part of the novel physics that occurs as a result of fermion condensation.

[5] Indeed, if we tried to decompose β into two idempotents, they would each be linear combinations of the two pictures in (35), which have different fermion parity. But idempotents must have even parity.

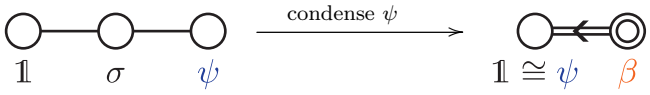

Basic data:

simple objects	fusion rules	dimensions	Koszul signs
$\mathbb{1}$ and β	$\beta \otimes \beta \cong \mathbb{C}^{1\|1} \cdot \mathbb{1}$	$= d$	$= -$

Linear relations:

F-symbols d $= + A^{12}$ d $= +$ (33)

Fermion pairing $= A^4$ (25) $= A^4$ $= A^4$ (28)

$A^2 = -e^{\pm i\pi/4}$ $d = -A^2 - A^{-2}$ (3)

Table 2.4.1: Summary of C_2 data

Finally, we mention a higher-level way of understanding the content of the C_2 theory from the parent Ising theory. We begin by noting that the principle graph for the Ising theory is given by the A_3 Dynkin diagram (see the top left of Table 2.4.1). Condensing ψ means establishing an isomorphism between ψ and $\mathbb{1}$, so that in the condensed theory $\mathbb{1}$ and ψ correspond to the same node of the principal graph. This identification can be done by "folding" the A_3 principal graph about the central node so that the $\mathbb{1}$ and ψ nodes are identified. Note that σ is preserved under the folding, which translates into the fact that the image of σ in the condensed theory (namely β) has a nontrivial endomorphism algebra. The resulting folded principal graph is shown in the top right of Table 2.4.1: the double line indicates the two fusion channels in $\beta \otimes \beta \cong \mathbb{C}^{1|1} \cdot \mathbb{1}$, the double circle indicates that β has a two-dimensional endomorphism algebra, and the arrows have been chosen to point away from the object with larger endomorphism algebra. The resulting principal graph is precisely the C_2 Dynkin diagram, which is why we call the condensed theory the C_2 theory. This idea can be applied to perform fermion condensation in many other theories (most straightforwardly the other theories in the A_n series which contain a fermion). We will explore several examples along these lines in later sections.

3 Quasiparticle excitations and the tube category of C_2

In this section, we identify the quasiparticle excitations in the C_2 theory. We will discuss the quasiparticles in the theory, their fusion rules, their statistics, and the modular trans-

formations of the ground states on the torus. We will identify the excitations using a fermionic generalization of a device known as the *tube category*. We will briefly review the tube category as applied to the C_2 theory below; for a more detailed overview and for an explanation of why the fermionic version of the tube category computes the excitations, we refer the reader to Section 5, where we discuss the construction in full generality.

For the benefit of more physically-inclined readers we will use the "Hamiltonian/ground-state/excitation" terminology in this section, even though (as discussed in the introduction) we will not define the relevant Hamiltonian until Section 9. The constructions in this section all take place within the self-contained world of TQFTs defined via string nets; the Hamiltonian/ground-state/excitation interpretation is optional.

3.1 Finding the quasiparticle excitations

We now turn to a detailed study of the tube category for C_2. The objects of $\mathbf{Tube}(C_2)$ are given by spin circles with a finite number of marked points labeled by simple objects of C_2. There are two spin structures on the circle: bounding (anti-periodic boundary conditions; non-vortex) and non-bounding (periodic boundary conditions; vortex). Each object in $\mathbf{Tube}(C_2)$ thus determines a choice of spin structure of the underlying circle.

It suffices to consider only objects with at most one labeled point. This is because any other object is isomorphic to a direct sum of objects with at most one labeled point. Note also that an object with a point labeled by $\mathbb{1}$ (the trivial object of C_2) is isomorphic to the object obtained by erasing that marked point. In particular, a circle with no marked points is isomorphic to a circle with a single point labeled by $\mathbb{1}$.

Since there are two simple objects in C_2, for a fixed spin structure there are only two possible labels that can be assigned to a marked point,

(37)

where B, N denote bounding and non-bounding spin structures respectively.

Morphisms of $\mathbf{Tube}(C_2)$ are defined to be cylinders (which we will draw as annuli) decorated by C_2 string-nets. A given morphism $a \to b$ is thus an annulus whose outer (inner) boundary conditions are determined by the object a (b).

After applying local relations (F-moves, dot-cancellations, removing trivial loops), an arbitrary string-net diagram on any tube can be reduced to a linear combination of the following diagrams:

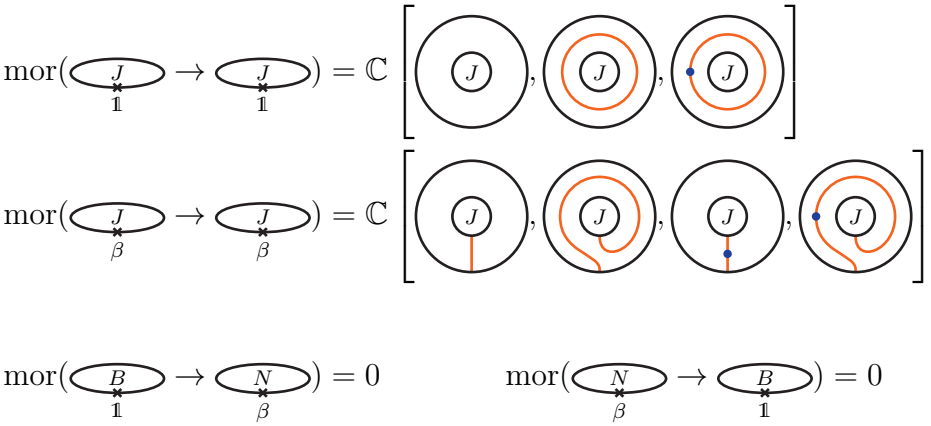

(38)

with $J = B$ for bounding spin structure, and $J = N$ for non-bounding spin structure. In the first row we have listed all possible tubes which take the trivial boundary condition

back to itself, and in the second row the tubes which take the β marked point back to itself. Notice that all non-zero tubes for C_2 have the same label at the two marked points. For general input categories this won't happen; see Sections 6 and 7 for examples.

Depending on the spin structure on the annulus, some of the above diagrams may be zero. With a bounding spin structure, a fermionic dot picks up a factor of -1 if it moves around the annulus. On the other hand a fermionic dot picks up a factor of $+1$ if it moves around the annulus with non-bounding spin structure.

As we said above, not every string diagram in the annulus is consistent with a given spin structure. For example,

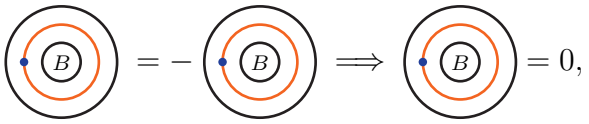

(39)

where we have simply pulled the fermion around the non-contractible loop on the tube. A non-bounding tube with a horizontal β line is also zero, since

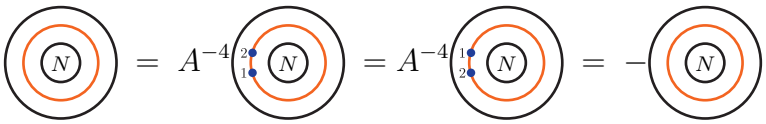

(40)

Where in the second step we have dragged one of the two fermions around the annulus. All other tubes are nonzero for both spin structures, and so a complete basis for tubes in the bounding sector is given by

$$\mathbf{Tube}^{B}_{\mathbb{1}\to\mathbb{1}} = \mathbb{C}\left[\quad,\quad\right] \tag{41}$$

$$\mathbf{Tube}^{B}_{\beta\to\beta} = \mathbb{C}\left[\quad,\quad,\quad,\quad\right] \tag{42}$$

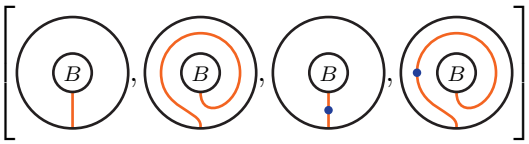

while a basis for the non-bounding sector is given by

$$\mathbf{Tube}^{N}_{\mathbb{1}\to\mathbb{1}} = \mathbb{C}\left[\quad,\quad\right] \tag{43}$$

$$\mathbf{Tube}^{N}_{\beta\to\beta} = \mathbb{C}\left[\quad,\quad,\quad,\quad\right] \tag{44}$$

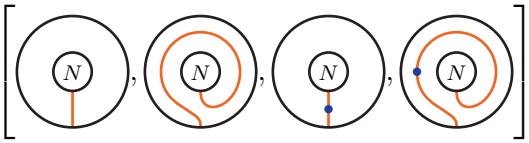

The multiplication operation in the tube category is given by stacking tubes on top of one another and simplifying the resulting tube using local relations. For example, in the non-bounding sector we have

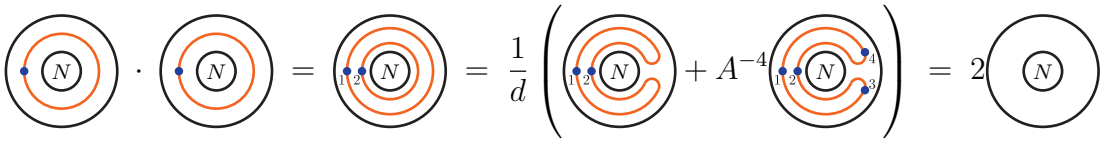

(45)

Note that since the spin structures on two tubes being fused must agree on the boundary at which they are fused, non-bounding tubes can only be stacked on top of non-bounding tubes, and similarly for bounding tubes.

Relations like the ones above allow us to find the (isomorphism classes of) minimal idempotents of the tube category. First, we turn to an analysis of tubes with bounding spin structure.

3.1.1 Non-vortex spin structure

Let us first examine the tubes with no charge,[6] that is, cylinders with bounding spin structures and empty boundary conditions on both their top and bottom, which are the cylinders in $\mathbf{Tube}^B_{\mathbb{1}\to\mathbb{1}}$. We see that this algeba (41) has two even generators, and so as a vector space

$$\mathbf{Tube}^B_{\mathbb{1}\to\mathbb{1}} \cong \mathbb{C}^{2|0} \tag{46}$$

There is only one possible super algebra structure on $\mathbb{C}^{2|0}$; it is the sum of two trivial 1-dimensional algebras $\mathrm{End}(\mathbb{C}) \oplus \mathrm{End}(\mathbb{C})$ (or $\mathbb{C} \oplus \mathbb{C}$ for short, where here $\mathbb{C}$ denotes a 1-dimensional algebra rather than a 1-dimensional vector space). This sector therefore contains two minimal idempotents, which we will call $m_{\mathbb{1}}$ and m_ψ. Explicitly, they are

$m_{\mathbb{1}} = \frac{1}{2}\Bigg($ 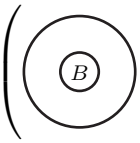 $+ \frac{1}{d}$ 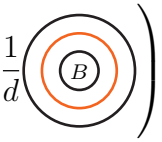 $\Bigg)$, $\qquad m_\psi = \frac{1}{2}\Bigg($ 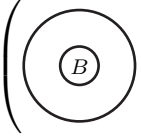 $- \frac{1}{d}$ 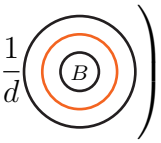 $\Bigg)$. (47)

One can check that the action of any element from $\mathbf{Tube}^B_{\mathbb{1}\to\mathbb{1}}$ on both $m_{\mathbb{1}}$ and m_ψ is simply scalar multiplication.

Now we turn to the endomorphism algebra $\mathbf{Tube}^B_{\beta\to\beta}$, defined in (41), of charged tubes: those whose top and bottom boundary conditions consist of a single marked β point. There are two non-zero even tubes and two non-zero odd tubes, hence as a vector space we have,

$$\mathbf{Tube}^B_{\beta\to\beta} \cong \mathbb{C}^{2|2}. \tag{48}$$

This means that as an algebra $\mathbf{Tube}^B_{\beta\to\beta}$ is either $\mathbb{C}\ell_2$ (a.k.a. $\mathrm{End}(\mathbb{C}^{1|1})$) or $\mathbb{C}\ell_1 \oplus \mathbb{C}\ell_1$.

To figure out which case we have, we begin by writing down the multiplication rules. By using the local relations in the C_2 theory we can work out the multiplication table, which is presented in the following table. In the table, $A \times B$ means "stack A (left most column) on top of B (top most row)". For multiplications involving odd tubes, we always take fermions in the A tube to have a higher ordering than the fermions in the B tube.

[6] We define the "charge" of a tube to be the label of the marked point of the upper boundary of the tube, so that tubes in $\mathbf{Tube}_{a\to b}$ have charge b. This is slightly misleading however, because charge is not a good quantum number: in more general theories, $\mathbf{Tube}_{a\to b}$ will be nonzero even when $a \neq b$.

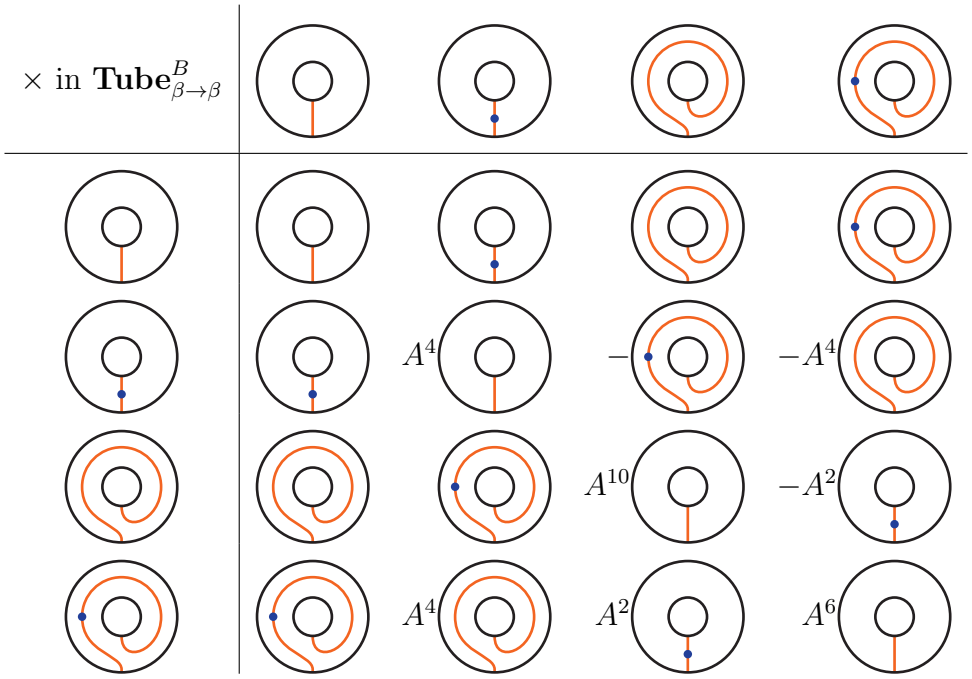

(49)

Since the multiplication table for $\mathbf{Tube}^B_\beta$ is non-abelian, as an algebra it must be $\mathbb{C}\ell_2$, as the other possibility (namely $\mathbb{C}\ell_1 \oplus \mathbb{C}\ell_1$) is abelian. In order to show that the previous table is indeed the multiplication table of $\mathbb{C}\ell_2$, one can identify,

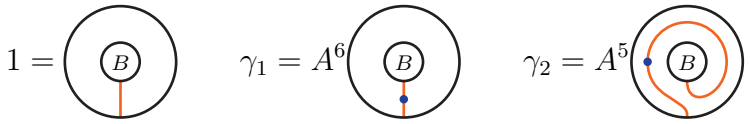

(50)

and check that the odd generators γ_1 and γ_2 satisfy $\gamma_1^2 = \gamma_2^2 = 1$, and $\{\gamma_i, \gamma_j\} = 2\delta_{ij}$. These are precisely the defining relations of $\mathbb{C}\ell_2 \cong \langle 1, \gamma_1, \gamma_2 \rangle$, and so we have $\mathbf{Tube}^B_{\beta\to\beta} \cong \mathbb{C}\ell_2$.

The super algebra $\mathbb{C}\ell_2$ contains exactly two minimal idempotents, which we will call m_σ^+ and m_σ^-. Explicitly,

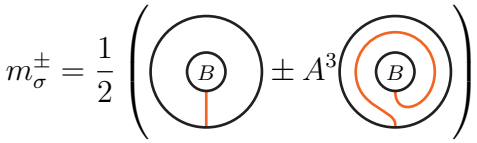

(51)

These two idempotents are isomorphic, in the sense that there exist endomorphisms (tubes) u and v such that $uv = m_\sigma^+$ and $vu = m_\sigma^-$.[7] The existence of this isomorphism means that m_σ^+ and m_σ^- correspond to isomorphic simple modules and so represent the same quasiparticle type. Note that in this case u and v are necessarily odd; we say that m_σ^+ and m_σ^- are *oddly* isomorphic. When doing calculations we fix a particular representative of the $m_\sigma^\pm$ equivalence class, which we will choose to be m_σ^+.

3.1.2 Vortex spin structure

As in the last section, we first examine the endomorphism algebra $\mathbf{Tube}^N_{\mathbb{1}\to\mathbb{1}}$, consisting of tubes with no charge and non-bounding spin structure. As we saw in (43), this algebra

[7] Indeed this must be the case, since $\mathbb{C}\ell_2$ is Morita equivalent to $\mathbb{C}$, which has only one minimal idempotent.

is two dimensional, and generated by a single even vector and a single odd vector, so as a vector space we have

$$\mathbf{Tube}^N_{\mathbb{1}\to\mathbb{1}} \cong \mathbb{C}^{1|1} \tag{52}$$

The only possible algebra structure on $\mathbb{C}^{1|1}$ is $\mathbb{C}\ell_1$. $\mathbb{C}\ell_1 = \langle 1, \gamma\rangle$ has only one simple module, namely $\mathbb{C}^{1|1}$ with the matrix representation $\rho(1) = \sigma^0, \rho(\gamma) = \sigma^x$. Therefore, this endomorphism algebra will support only one quasiparticle. Since idempotents must always be even, the explicit presentation of this quasiparticle is simply the empty tube. We will denote this quasiparticle by q_σ:

$q_\sigma =$ 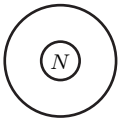

(53)

Now we examine the charge sector, corresponding to the algebra $\mathbf{Tube}^N_{\beta\to\beta}$ of vortex tubes with nontrivial charge. As we have seen in (43) this subalgebra again has two even generators and two odd generators, and so as a vector space:

$$\mathbf{Tube}^N_{\beta\to\beta} \cong \mathbb{C}^{2|2} \tag{54}$$

Therefore, as an algebra, we must have $\mathbf{Tube}^N_{\beta\to\beta} \cong \mathbb{C}\ell_2$ or $\mathbf{Tube}^N_{\beta\to\beta} \cong \mathbb{C}\ell_1 \oplus \mathbb{C}\ell_1$. To determine which choice is correct, we work out the multiplication table, which is

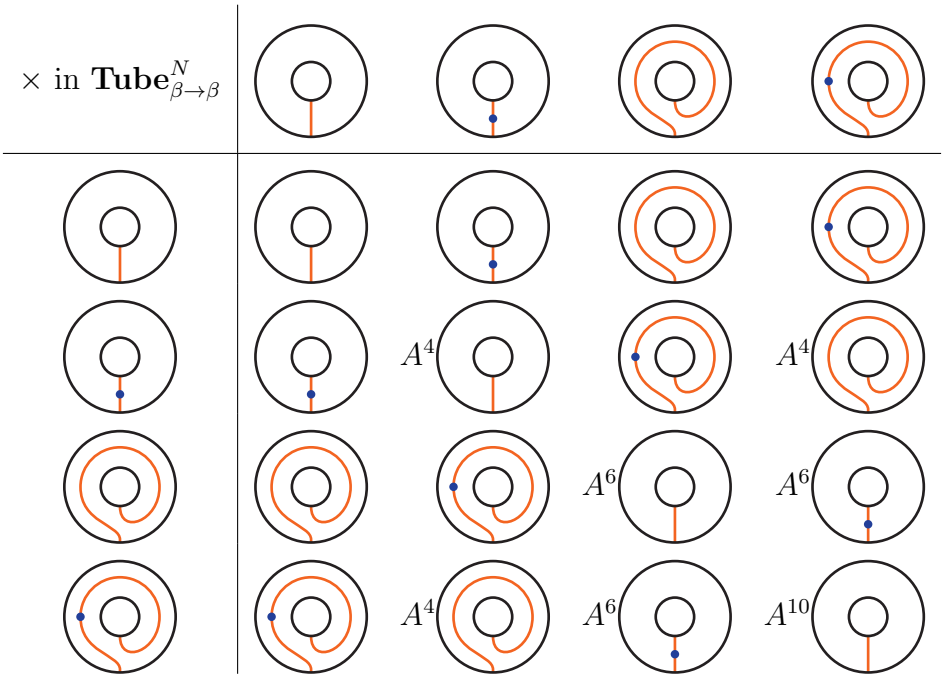

(55)

Since the multiplication table is abelian, we must have $\mathbf{Tube}^N_\beta \cong \mathbb{C}\ell_1 \oplus \mathbb{C}\ell_1$ (as the other choice, $\mathbb{C}\ell_2$, is non-abelian). To see this explicitly, we make the identifications

$$\mathbb{1}^\pm = \frac{1}{2}\left(\text{ 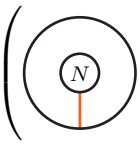 } \pm A^5 \text{ 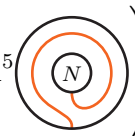 } \right), \qquad \gamma^\pm = \frac{A^6}{2}\left(\text{ 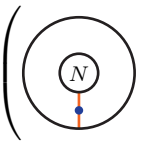 } \pm A^5 \text{ 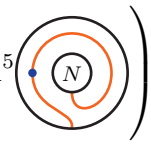 } \right). \tag{56}$$

If we then re-write the multiplication table for $\mathbf{Tube}^N_{\beta\to\beta}$ in terms of these generators, we see that it is indeed isomorphic to $\langle \mathbb{1}^+, \gamma^+\rangle \oplus \langle \mathbb{1}^-, \gamma^-\rangle = \mathbb{C}\ell_1 \oplus \mathbb{C}\ell_1$, with $(\gamma^\pm)^2 = \mathbb{1}^\pm$.

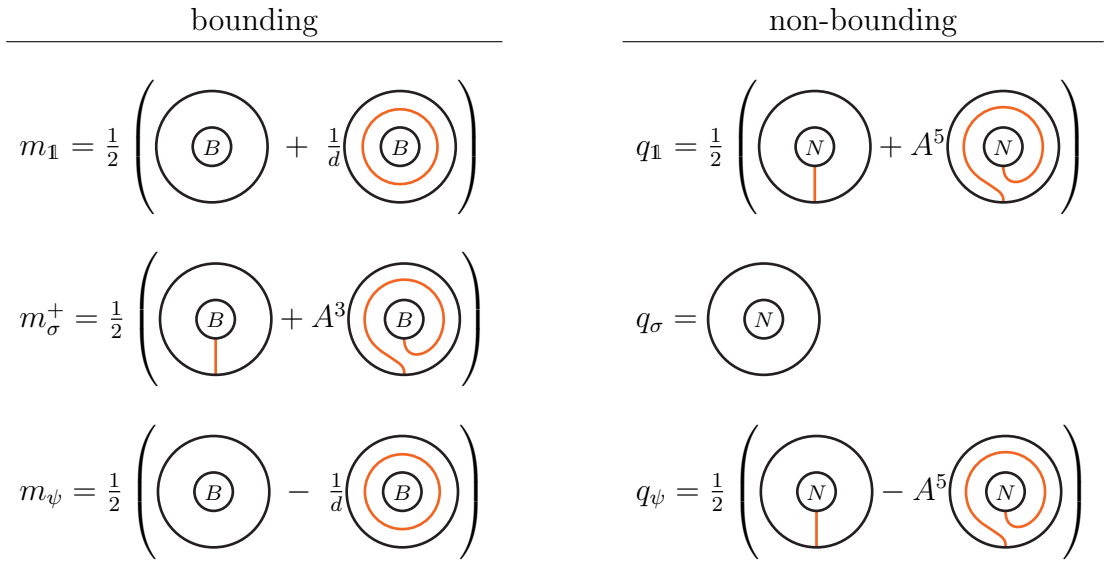

Table 3.1.1: Representative idempotents for the six quasiparticles in the C_2 theory. The non-bounding (i.e., vortices) are all q-type particles, while the bounding (i.e., non-vortex) particles are all m-type. We have chosen m_σ^+ as the representative of the isomorphism class given by m_σ^+ and m_σ^-.

particle	$m_{\mathbb{1}}$	m_σ^+	m_ψ	$q_{\mathbb{1}}$	q_σ	q_ψ
quantum dimension	1	$\sqrt{2}$	1	$\sqrt{2}$	2	$\sqrt{2}$

Table 3.1.2: **Tube**(C_2) quantum dimensions. The total quantum dimension is $\mathcal{D} = \sqrt{8}$. The quantum dimensions above have been normalized so that the trivial idempotent $m_{\mathbb{1}}$ has unit quantum dimension.

We therefore have two (non-isomorphic) idempotents, $q_{\mathbb{1}} = \mathbb{1}^+$ and $q_\psi = \mathbb{1}^-$. Thus, the $\mathbf{Tube}^N_{\beta\to\beta}$ endomorphism algebra gives rise to two q-type quasiparticles. (Recall that a q-type object is a simple object whose endomorphism algebra is $\mathbb{C}^{1|1}$. Simple objects whose endomorphism algebras are isomorphic to $\mathbb{C}$ are referred to as m-type.)

To summarize, we have found six types of quasiparticles in the theory: three non-vortex quasiparticles associated with tubes possessing bounding spin structures, and three vortex quasiparticles associated with tubes possessing non-bounding spin structures. They are displayed in Table 3.1.1. The quantum dimension of these excitations can be computed by tracing out the idempotents associated with each excitation, which we elaborate on in Section 4.2.1. The quantum dimensions are displayed in Table 3.1.2.

3.2 Quasiparticle fusion rules

With all quasiparticles in hand, we are ready to compute their fusion rules. We postpone a more general discussion of how to compute fusion rules in fermionic theories to Section 4.4, and in this section restrict ourselves to working out examples for the C_2 theory.

Recall that to each minimal idempotent e we can associate an irreducible module (a.k.a. irreducible representation) M_e as follows. Let $\mathcal{T}$ denote the tube category, and let x be object of $\mathcal{T}$ which hosts e (i.e. $e \in \mathrm{End}(x)$). To each object y of $\mathcal{T}$, the module M_e associates the subspace of $\mathrm{mor}(x \to y)$ consisting of morphisms of the form ef, where e is our chosen idempotent and f is an arbitrary morphism from x to y. We can express this compactly as

$$M_e = e\mathcal{T}. \tag{57}$$

It is easy to check that if e and e' are isomorphic idempotents, then M_e and $M_{e'}$ are isomorphic modules, and conversely. Geometrically, the module M_e consists of tubes with e fixed at one end and arbitrary string nets (f above) at the other end.

We will frequently simplify notation and denote both the idempotent e and the corresponding module M_e as simply e.

It is important to note that there many idempotents within a given equivalence class, and these idempotents might be hosted at different objects. Furthermore, the isomorphism relating two idempotents might be odd (i.e. it reverses fermion parity). Despite these differences, all of the idempotents within an equivalence class should be thought of as representing the same anyon type. To do calculations, we must choose a particular idempotent within the equivalence class. This is analogous to a gauge choice. For example, the idempotent given by m_σ^+ constitutes a choice of representative of the equivalence class containing m_σ^+ and m_σ^-, but we could have just as easily chosen m_σ^- as a representative.

Given two modules a and b of $\mathcal{T}$, we can construct a tensor product module $a \otimes b$. Intuitively, forming $a \otimes b$ amounts to fusing the quasiparticles a and b together by bringing them close to one another, and "zooming out" to view a and b as a single composite quasiparticle. To make this precise, we can impost the idempotent versions of a and b as boundary conditions on the two inner boundary components of a twice-punctured disk P (a.k.a. pair of pants). Adding tubes to the outer boundary component of P gives a module for the tube category, and this module is, by definition $a \otimes b$. We will discuss this in more detail in 4.4.

We define the fusion space V_c^{ab} as the space

$$V_c^{ab} \equiv \mathrm{mor}(c \to a \otimes b). \tag{58}$$

Geometrically, V_c^{ab} corresponds to the space of all string-net configurations (modulo local relations) on a pair of pants whose outgoing legs are labeled by the quasiparticles a and b, and whose incoming leg is labelled by c.

One subtle property of fermion theories is that the vector spaces V_c^{ab} are *not* the vector spaces which appear in the direct sum decomposition of $a \otimes b$. Instead, we define the fusion rule coefficients Δ_c^{ab} via[8]

$$a \otimes b \cong \bigoplus_c \Delta_c^{ab} c, \tag{59}$$

where the sum runs over a set of representatives for the equivalence classes of irreducible representations (equivalently, of minimal idempotents). In bosonic theories $V_c^{ab} = \Delta_c^{ab}$, but in fermionic theories the fusion spaces can be larger than the the fusion coefficients:

$$V_c^{ab} \cong \Delta_c^{ab} \otimes \mathrm{End}(c). \tag{60}$$

[8]The Δ_c^{ab} are complex super vector spaces, not numbers. They are a categorified version of the coefficients used to write a general vector as a linear combination of basis vectors.

We demonstrate and elaborate on this in Section 8.4.

We will now illustrate how to compute the fusion spaces with simple examples in the C_2 theory. Suppose we want to find the fusion rule for $q_\sigma \otimes m_{\mathbb{1}}$. We first note that spin structure considerations on the pair of pants require that any quasiparticle appearing in $q_\sigma \otimes m_{\mathbb{1}}$ be a vortex-type quasiparticle (one with a non-bounding spin structure). Furthermore, since both $m_{\mathbb{1}}$ and q_σ have no charge (no β lines fixed to the boundaries of their tubes), we know that their fusion products cannot have any charge. Since q_σ is the only vortex-type quasi particle with no charge we know that it is the only particle which can appear in the tensor product of q_σ and $m_{\mathbb{1}}$. By searching for pants invariant under the applications of the appropriate idempotents, we see that the super vector space $V_{q_\sigma}^{q_\sigma m_{\mathbb{1}}}$ is isomorphic to $\mathbb{C}^{1|1}$, with the even subspace generated by a single even vector

$$[V_{q_\sigma}^{q_\sigma m_1}]^0 = \Big\langle$$ 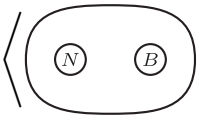 $$+ \frac{1}{d}$$ 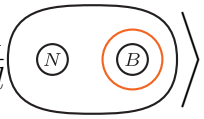 $$\Big\rangle \tag{61}$$

and the odd subspace generated by a single odd vector

$$[V_{q_\sigma}^{q_\sigma m_1}]^1 = \Big\langle$$ 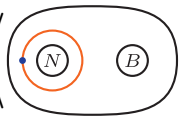 $$+ \frac{1}{d}$$ 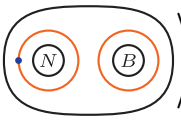 $$\Big\rangle . \tag{62}$$

Notice that to find the odd generator from the even one, we apply the odd endomorphism of q_σ to the "exterior" boundary of the pair of pants. Graphically, this corresponds to taking a β loop with a single dot on it and inserting it in a position parallel to the outer boundary of the pair of pants.

A more nontrivial fusion rule is $q_\sigma \otimes q_\sigma$. Since q_σ has no charge, any quasiparticles appearing in $q_\sigma \otimes q_\sigma$ must also carry no charge, since for the C_2 theory charge is a good quantum number. Additionally, any quasiparticles in $q_\sigma \otimes q_\sigma$ must have non-vortex spin structures, so we know that only $m_{\mathbb{1}}$ and m_ψ can appear in $q_\sigma \otimes q_\sigma$. This lets us work out the fusion spaces explicitly. We first work out the fusion space for $V_{m_{\mathbb{1}}}^{q_\sigma q_\sigma}$. The even part is generated by a single vector:

$$[V_{m_{\mathbb{1}}}^{q_\sigma q_\sigma}]^0 = \Big\langle$$ 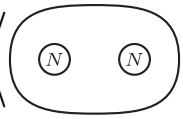 $$+ \frac{1}{\sqrt{2}}$$ 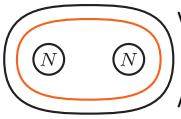 $$\Big\rangle . \tag{63}$$

As with (62), we find the odd generator by using the odd endomorphism coming from q_σ:

$$[V_{m_{\mathbb{1}}}^{q_\sigma q_\sigma}]^1 = \Big\langle$$ 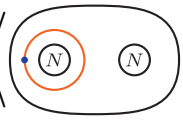 $$+ \frac{1}{\sqrt{2}}$$ 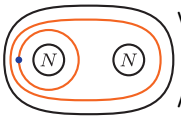 $$\Big\rangle . \tag{64}$$

Therefore, $V_{m_{\mathbb{1}}}^{q_\sigma q_\sigma} = [V_{m_{\mathbb{1}}}^{q_\sigma \otimes q_\sigma}]^0 \oplus [V_{m_{\mathbb{1}}}^{q_\sigma \otimes q_\sigma}]^1 \cong \mathbb{C}^{1|1}$. An analogous calculation shows that $V_{m_\psi}^{q_\sigma q_\sigma} \cong \mathbb{C}^{1|1}$, and is generated by the two vectors

$$V_{m_\psi}^{q_\sigma q_\sigma} = \Big\langle$$ 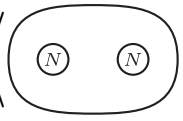 $$- \frac{1}{\sqrt{2}}$$ 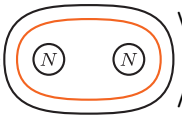 $$\Big\rangle \oplus \Big\langle$$ 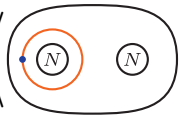 $$- \frac{1}{\sqrt{2}}$$ 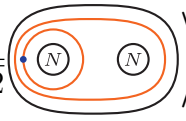 $$\Big\rangle . \tag{65}$$

Summarizing, we have $q_\sigma \otimes q_\sigma \cong \mathbb{C}^{1|1} m_{\mathbb{1}} \oplus \mathbb{C}^{1|1} m_\psi$, with $V_{m_{\mathbb{1}}}^{q_\sigma q_\sigma} \cong V_{m_\psi}^{q_\sigma q_\sigma} \cong \mathbb{C}^{1|1}$.

As a final example, we will examine the fusion channel $m_\sigma^+ \otimes m_\psi$. Since m_σ^+ has nonzero charge while m_ψ has no charge, anything appearing in $m_\sigma^+ \otimes m_\psi$ must carry nonzero charge. Additionally, since both m_σ^+ and m_ψ have non-vortex spin structures, their fusion products must possess non-vortex spin structures as well. Therefore, they must fuse to $m_\sigma^\pm$. Determining the fusion space $V_{m_\sigma^\pm}^{m_\sigma^+ m_\psi}$ thus amounts to identifying string-nets on the pair of pants which are invariant under the application of m_σ^+ and m_ψ on the inner legs of the pants and invariant under the application of $m_\sigma^\pm$ on the outer leg of the pants.

First apply m_σ^+ and m_ψ on the inner legs, and m_σ^+ on the outer leg to a generic linear combination of string nets on the pants. By using the linear relation,

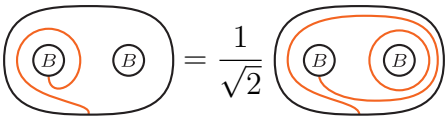

(66)

one can check that the resulting vector space will be zero dimensional if the the pair of pants has even parity, and will be one dimensional if the pair of pants has odd parity, generated as follows:

$$V_{m_\sigma^+}^{m_\sigma^+ m_\psi} =$$

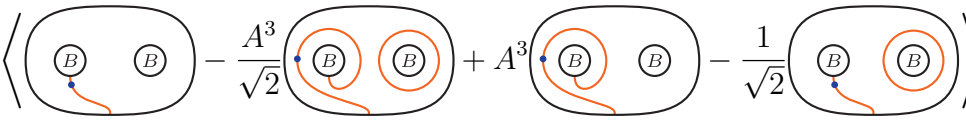

(67)

Hence $m_\sigma^+ \otimes m_\psi \cong \mathbb{C}^{0|1} m_\sigma^+$. Repeating the calculation for m_σ^- on the outer leg results in a one dimensional vector space if the pair of pants has even parity, and zero otherwise; $m_\sigma^+ \otimes m_\psi \cong \mathbb{C}^{1|0} m_\sigma^-$. This reflects the fact that m_σ^- is oddly isomorphic to m_σ^+. We emphasize that to write the fusion rules, we need to work with actual idempotents, not merely equivalence classes of idempotents.

By following the approach outlined in these examples, it is straightforward to write down the table of fusion rules in the theory, which we present in Table 3.2.1. In the table, we list the fusion rule coefficients from (59), with the bullets (•) representing cases where $\Delta_c^{ab} \cong \mathbb{C}^{1|1}$, and the appearance of $\mathbb{C}^{0|1}$ indicating a purely odd fusion channel. The fusion spaces V_c^{ab} can then be obtained through the use of $V_c^{ab} \cong \Delta_c^{ab} \otimes \mathrm{End}(c)$.

3.3 Modular transformations and ground states on the torus

3.3.1 C_2 string-nets on the torus

In this section, we compute a standard basis for C_2 string-nets-modulo-local-relations on spin tori as well as the action of the mapping class groupoid (i.e. the modular S and T matrices).

Because the C_2 theory is dependent on the existence of a spin structure, in order to talk about ground states on a torus we must first specify the spin structure on the torus. There are $|H^1(T^2; \mathbb{Z}_2)| = 4$ different spin structures on the torus, obtained by choosing either bounding or non-bounding spin structures for two of the torus's three non-contractible cycles (with the spin structure along the third non-contractible cycle

$\mathcal{A}\otimes\mathcal{A}$	$m_{\mathbb{1}}$	m_σ^+	m_ψ
$m_{\mathbb{1}}$	$m_{\mathbb{1}}$	m_σ^+	m_ψ
m_σ^+	m_σ^+	$m_{\mathbb{1}}\oplus\mathbb{C}^{0\vert1}m_\psi$	$\mathbb{C}^{0\vert1}m_\sigma^+$
m_ψ	m_ψ	$\mathbb{C}^{0\vert1}m_\sigma^+$	$m_{\mathbb{1}}$

$\mathcal{V}\otimes\mathcal{A}$	$m_{\mathbb{1}}$	m_σ^+	m_ψ
$q_{\mathbb{1}}$	$q_{\mathbb{1}}$	q_σ	q_ψ
q_σ	q_σ	$q_{\mathbb{1}}\oplus q_\psi$	q_σ
q_ψ	q_ψ	q_σ	$q_{\mathbb{1}}$

$\mathcal{A}\otimes\mathcal{V}$	$q_{\mathbb{1}}$	q_σ	q_ψ
$m_{\mathbb{1}}$	$q_{\mathbb{1}}$	q_σ	q_ψ
m_σ^+	q_σ	$q_{\mathbb{1}}\oplus q_\psi$	q_σ
m_ψ	q_ψ	q_σ	$q_{\mathbb{1}}$

$\mathcal{V}\otimes\mathcal{V}$	$q_{\mathbb{1}}$	q_σ	q_ψ
$q_{\mathbb{1}}$	$\bullet m_{\mathbb{1}}$	$\bullet m_\sigma^+$	$\bullet m_\psi$
q_σ	$\bullet m_\sigma^+$	$\bullet(m_{\mathbb{1}}\oplus m_\psi)$	$\bullet m_\sigma^+$
q_ψ	$\bullet m_\psi$	$\bullet m_\sigma^+$	$\bullet m_{\mathbb{1}}$

Table 3.2.1: The fusion rules in $\mathbf{Tube}(C_2)$. We have defined $\mathcal{A}=\{m_{\mathbb{1}},m_\sigma^+,m_\psi\}$ and $\mathcal{V}=\{q_{\mathbb{1}},q_\sigma,q_\psi\}$ as the set of anyons and set of vortices, respectively. The $(a\text{-}b)$th entry in each table is the sum $\oplus_c\Delta_c^{ab}c$, where we have omitted any Δ_c^{ab} that is equal to $\mathbb{C}$ and used $\bullet=\mathbb{C}^{1|1}$ to signify that the associated Δ_c^{ab} is isomorphic to $\mathbb{C}^{1|1}$. Entries with $\mathbb{C}^{0|1}$ indicate that the fusion channel is purely odd. The fusion spaces can be obtained from this table according to $V_c^{ab}\cong\Delta_c^{ab}\otimes\mathrm{End}(c)$. For example, $V_{q_\sigma}^{m_\psi q_\sigma}\cong\mathbb{C}\otimes\mathbb{C}^{1|1}=\mathbb{C}^{1|1}$.

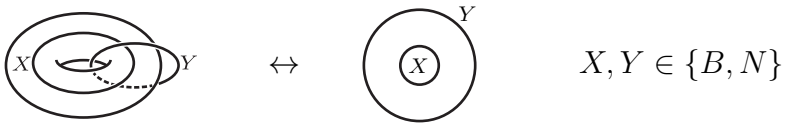

Figure 3.3.1: To go from the annulus to the torus we identify the inner and outer circles, and label the different spin structures by X and Y for the longitudinal and meridional cycles on the torus, respectively.

determined by those of the other two). To go from the annulus to the torus we identify the inner and outer circles, and label the different spin structures by

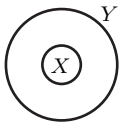

$$X,Y\in\{B,N\} \tag{68}$$

where X and Y specify the spin structure along the longitudinal and meridional cycles, respectively (see Figure 3.3.1).

If there was no interplay between a chosen spin structure and the string-net pictures drawn on the torus, and if the fermion parity of a ground state is fixed by the spin structure and the string-net picture drawn on the torus, we would expect $|H_1(T^2;\mathbb{Z}_2)|=4$ degenerate ground states for each choice of spin structure, since the β lines obey $\mathbb{Z}_2$ fusion rules. We will see that naive guess is incorrect: instead, for each spin structure, one of the four putative states is a null vector, meaning that there is only a 3-dimensional groundstate for each choice spin structure.

We will first use elementary arguments to find a spanning set for each of the four spin tori. Later, using more sophisticated techniques, we will prove that these spanning sets are in fact bases.

Since β lines obey $\mathbb{Z}/2$ fusion rules (see 2.4.1), it is easy to see that any string net on

a spin torus is a linear combination of the following seven diagrams:

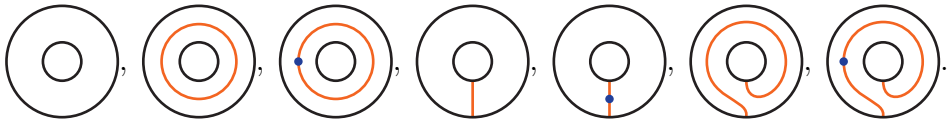

(69)

Indeed, using (33) and the ability to remove topologically trivial β loops, we can transform the β loops into a standard representative of their $\mathbb{Z}/2$ homology class. The resulting loop will be decorated by some number of fermionic dots; using dot cancellation we can assume that the loop will contain either 0 or 1 dot. The seven diagrams listed above are the only independent diagrams that remain after applying these relations.

However, for a given spin structure, some of the diagrams in (69) will be zero. To determine which of the diagrams are zero, we use the following three obervations:

1. If one of the non-trivial cycles of the torus has an antiperiodic spin structure, then any odd diagram is zero. This is because we can translate the entire string net in the direction of the antiperiodic cycle. When we arrive back at our starting point, we have picked up a factor of -1 from the antiperiodicity. Thus odd diagrams are equal to -1 times themselves and are therefore zero. In particular, the three odd diagrams of (69) are zero in the BB, BN and NB spin structures.

2. If a diagram contains a β loop without a dot (even fermion parity), and if that loop inherits the periodic spin structure, then the diagram is zero. To see this, we create two dots on the loop, slide one around the loop, and then cancel the dots again. Because of the Koszul sign, we see that the diagram is equal to -1 times itself. (If the spin structure along the cycle were antiperiodic, there would be an additional sign to cancel the Koszul sign.) In particular, in the NN spin structure all three of the even β loops are zero. For the BB, BN and NB spin structures, exactly one of the three even β loops fails this test and is zero.

3. Finally, the empty diagram with NN spin structure is zero. To show this, we first create a topologically trivial circular β loop. We then wrap it around the tube and fuse it with itself to get the sum of two diagrams with parallel β loops wrapping around the tube, one of which has no fermion dots (the even channel of $\beta \otimes \beta$) and one which has one dot on each β loop (the odd fusion channel of $\beta \otimes \beta$). The diagram corresponding to the even fusion channel is zero by observation 2 above, while the diagram with two odd loops is zero by an argument similar to observation 2: we slide one of the loops in the direction orthogonal to itself and pick up a Koszul sign, showing that the diagram must be zero.

Figure 3.3.2 shows the remaining non-zero diagrams for each spin structure. It is easy to see that these diagrams are linearly independent if they are non-zero, but we have not yet proved that they are in fact non-zero. To do this, we will employ a fancier argument relating a basis of the torus Hilbert space to minimal idempotents of the tube category.

Let $\mathbf{Tube}^B$ denote the bounding tube category and $\mathbf{Tube}^N$ denote the non-bounding tube category. We can make use of the following results, which we prove in a more general context in Section 4.3.1: The ground state spaces of the BB, NB, and BN tori are purely even, with an orthogonal basis given by closed-up minimal idempotents of $\mathbf{Tube}^B$. Additionally, the ground state space of the NN torus is isomorphic to $\mathbb{C}^{p|q}$, where p is the number of m-type idempotents of $\mathbf{Tube}^N$ and q is the number of q-type idempotents of $\mathbf{Tube}^N$. An orthogonal basis is given by (representatives of) the

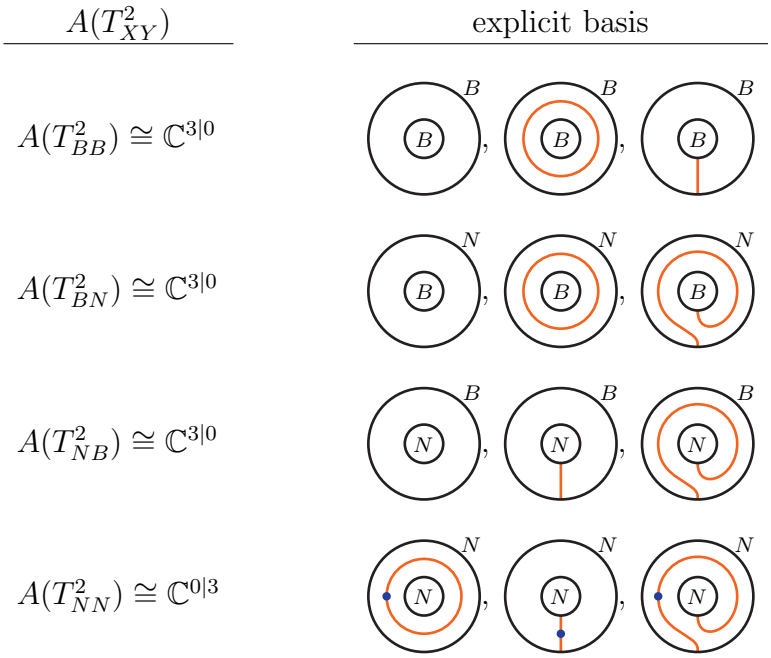

Figure 3.3.2: The ground states on the four different spin tori. Notice that the non-bounding torus (with NN spin structure) has only odd fermion parity ground states.

minimal m-type idempotents of $\mathbf{Tube}^N$, union $\{\mathrm{cl}(\gamma_j)\}$, where γ_j runs through a set of representatives of odd endomorphisms of the minimal q-type idempotents of $\mathbf{Tube}^N$. We use cl to denote the closure of an annular diagram on the torus.

For the C_2 theory, we have shown that $\mathbf{Tube}^B$ has three m-type minimal idempotents, and $\mathbf{Tube}^N$ has three q-type minimal idempotents. Letting $A(T^2_{JK})$ denote the Hilbert space on the torus with JK spin structure, it follows that $A(T^2_{BB}) \cong A(T^2_{NB}) \cong A(T^2_{BN}) \cong \mathbb{C}^{3|0}$ and $A(T^2_{NN}) \cong \mathbb{C}^{0|3}$, and so the diagrams of Figure 3.3.2 must indeed all be non-zero.

For future reference we also tabulate the change of basis between the ground-state tori in Figure 3.3.2 and the closed-up primitive idempotents. To form string-net pictures drawn on tori from the idempotents, we close up the idempotents along the longitudinal direction by identifying the inner boundary of the annulus on which the idempotent lives with the outer boundary, specifying a choice of spin structure along the newly made cycle. We then express the result as a linear combination of the tori in Figure 3.3.2. For simplicity of notation, we will define

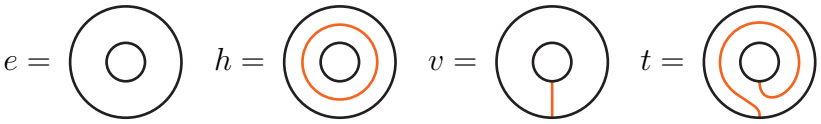

(70)

and append subscripts to denote a particular spin structure. We will also use an overscript $\bullet$ if we are closing up an odd endomorphism rather than the idempotent itself. For example,

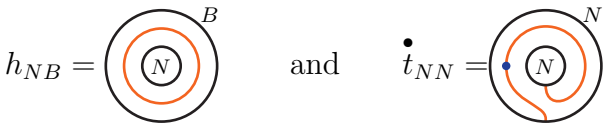

(71)

$$\begin{pmatrix} m_{\mathbb{1}} \\ m_\sigma^+ \\ m_\psi \end{pmatrix}_{BB} = \frac{1}{2}\begin{pmatrix} 1 & 1/d & 0 \\ 0 & 0 & 1 \\ 1 & -1/d & 0 \end{pmatrix}\begin{pmatrix} e \\ h \\ v \end{pmatrix}_{BB} \qquad \begin{pmatrix} m_{\mathbb{1}} \\ m_\sigma^+ \\ m_\psi \end{pmatrix}_{BN} = \frac{1}{2}\begin{pmatrix} 1 & 1/d & 0 \\ 0 & 0 & A^3 \\ 1 & -1/d & 0 \end{pmatrix}\begin{pmatrix} e \\ h \\ t \end{pmatrix}_{BN}$$

$$\begin{pmatrix} q_{\mathbb{1}} \\ q_\sigma \\ q_\psi \end{pmatrix}_{NB} = \frac{1}{2}\begin{pmatrix} 0 & 1 & A^5 \\ 2 & 0 & 0 \\ 0 & 1 & -A^5 \end{pmatrix}\begin{pmatrix} e \\ v \\ t \end{pmatrix}_{NB} \qquad \begin{pmatrix} \overset{\bullet}{q}_{\mathbb{1}} \\ \overset{\bullet}{q}_\sigma \\ \overset{\bullet}{q}_\psi \end{pmatrix}_{NN} = \frac{1}{2}\begin{pmatrix} 0 & A^6 & -A^3 \\ \sqrt{2} & 0 & 0 \\ 0 & A^6 & A^3 \end{pmatrix}\begin{pmatrix} \overset{\bullet}{h} \\ \overset{\bullet}{v} \\ \overset{\bullet}{t} \end{pmatrix}_{NN}$$

Figure 3.3.3: Change of basis between the quasiparticle (idempotent) basis given in Table (3.1.1) and the topological bases in Figure (3.3.2) for the torus. These are simply given by expressing the idempotents in the topological bases. Note that the odd torus has a sign ambiguity on each of the of the idempotents. We can require that $(\overset{\bullet}{q})^2 = q$, but that leaves $\overset{\bullet}{q}$ ambiguous up to a $\pm$ sign. This ambiguity can lead to different S matrices, see (82) and surrounding text for more details.

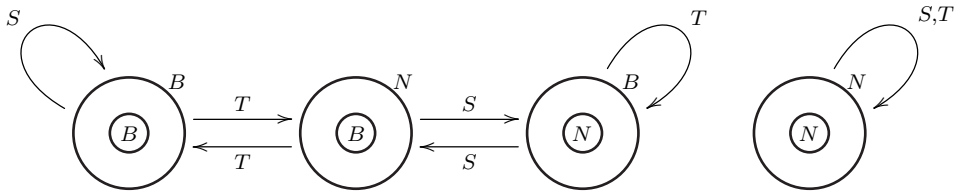

Figure 3.3.4: The action of the mapping class group on the four spin tori.

We can then compute the change of basis shown in Figure 3.3.3.

3.3.2 The modular S and T matrices

In this section, we will compute the representation of the modular S and T matrices in the C_2 theory, which together generate the modular groupoid. The modular S-matrix acts on states on the torus by interchanging the meridional and longitudinal cycles of the torus. If we draw the torus as a square with opposite sides identified, then S acts by rotating the square by $\pi/2$ clockwise. The modular T matrix represents the action of the Dehn twist on the torus, which corresponds to cutting the torus along a meridional cycle, twisting the boundary conditions at the cut by 2π relative to one another, and gluing the torus back together. In terms the annular pictures we have been drawing of the tubes, the twist is accomplished by twisting the inner boundary of the annulus by 2π counterclockwise relative to the outer boundary.

Importantly, the S and T modular transformations do *not* always preserve the spin structure of the torus they act on. Figure 3.3.4 shows how the different possible spin structures are permuted under S and T. Since T does not preserve the spin structures, it cannot have well-defined eigenstates with a definite spin structure, meaning that it will not be diagonal in the idempotent (quasiparticle) basis. This means that the topological spins of bounding (non-vortex) quasiparticles, defined as their eigenvalues under T, will not be well-defined. In contrast with T, the action of T^2 preserves spin structures, and so we are still able to associate definite T^2 eigenvalues to the quasiparticles in the theory.

Putting aside the issue of spin structures, the twist of an idempotent (defined as the phase acquired when performing a 2π twist on the tubes in a given idempotent) is in general only defined up to a $\pm$ sign (which has been discussed in e.g. [29, 11, 5]). More precisely, the twist of a given simple object in the tube category is ambiguous across the isomorphism class of that object. Indeed, we will see that the twists of the two idempotents in the m_σ isomorphism class (namely m_σ^+ and m_σ^-) have twists that differ by a factor of -1.

We now proceed to examine the action of the S and T modular transformations on the four spin tori which compose the 12-dimensional space listed in Figure 3.3.2. Although the calculations are most easily performed in the topological basis in Figure 3.3.2, it is more natural to analyze the resulting transformations in the idempotent basis given in Table 3.1.1. As mentioned earlier, the basis vectors in the idempotent basis are constructed by taking the idempotents associated with the quasiparticles identified in the previous section and closing them up (with different choices of spin structure) along the longitudinal direction. The change of basis between the topological and idempotent bases are written explicitly in Figure 3.3.3.

We'll start with the BB spin structure, which is preserved under the action of S. In the topological basis $(e, v, h)^T$ we find

$$\begin{pmatrix} e \\ v \\ h \end{pmatrix}_{BB} \xrightarrow{S^{BB\to BB}} \begin{pmatrix} 1 & 0 & 0 \\ 0 & 0 & 1 \\ 0 & 1 & 0 \end{pmatrix} \begin{pmatrix} e \\ v \\ h \end{pmatrix}_{BB} . \tag{72}$$

To transform $S^{BB\to BB}$ into the quasiparticle basis we use Figure 3.3.3. After the change of basis we find the familiar matrix

$$\begin{pmatrix} m_{\mathbb{1}} \\ m_\sigma^+ \\ m_\psi \end{pmatrix}_{BB} \xrightarrow{S^{BB\to BB}} \frac{1}{2} \begin{pmatrix} 1 & d & 1 \\ d & 0 & -d \\ 1 & -d & 1 \end{pmatrix} \begin{pmatrix} m_{\mathbb{1}} \\ m_\sigma^+ \\ m_\psi \end{pmatrix}_{BB} \tag{73}$$

which is identical to the S-matrix for the Ising TQFT.

Now for the BN and NB spin structures. These are interchanged by the S-matrix, as indicated in Figure 3.3.4. In the idempotent bases these induce transformations between the non-vortex and vortex quasi-particles. We obtain

$$\begin{pmatrix} e \\ h \\ t \end{pmatrix}_{BN} \xrightarrow{S^{BN\to NB}} \begin{pmatrix} 1 & 0 & 0 \\ 0 & 1 & 0 \\ 0 & 0 & A^{10} \end{pmatrix} \begin{pmatrix} e \\ v \\ t \end{pmatrix}_{NB} \quad \text{and} \quad \begin{pmatrix} e \\ v \\ t \end{pmatrix}_{NB} \xrightarrow{S^{NB\to BN}} \begin{pmatrix} 1 & 0 & 0 \\ 0 & 1 & 0 \\ 0 & 0 & A^{6} \end{pmatrix} \begin{pmatrix} e \\ h \\ t \end{pmatrix}_{BN} . \tag{74}$$

Notice that if we compose both transformations we get the identity. These can each be transformed into the idempotent bases using (3.3.3), where one finds,

$$\begin{pmatrix} m_{\mathbb{1}} \\ m_\sigma^+ \\ m_\psi \end{pmatrix}_{BN} \xrightarrow{S^{BN\to NB}} \frac{1}{2} \begin{pmatrix} 1 & d & 1 \\ -d & 0 & d \\ -1 & d & -1 \end{pmatrix} \begin{pmatrix} \hat{q}_{\mathbb{1}} \\ \hat{q}_\sigma^+ \\ \hat{q}_\psi \end{pmatrix}_{NB} \tag{75}$$

and

$$\begin{pmatrix} \hat{q}_{\mathbb{1}} \\ \hat{q}_\sigma^+ \\ \hat{q}_\psi \end{pmatrix}_{NB} \xrightarrow{S^{NB\to BN}} \frac{1}{2} \begin{pmatrix} 1 & -d & -1 \\ d & 0 & d \\ 1 & d & -1 \end{pmatrix} \begin{pmatrix} m_{\mathbb{1}} \\ m_\sigma^+ \\ m_\psi \end{pmatrix}_{BN} . \tag{76}$$

In order to make the matrix unitary, we have defined $\hat{q} = q/\sqrt{2}$ so that each $\hat{q}$ idempotent has unit norm (how to compute the norms of idempotents will be discussed in Section 4.2.1). To collect the results we've arrived at so far, we define

$$\mathbf{M} = [m_{\mathbb{1}}\ m_\sigma^+\ m_\psi]^T \qquad \widehat{\mathbf{Q}} = [\hat{q}_{\mathbb{1}}\ \hat{q}_\sigma\ \hat{q}_\psi]^T \tag{77}$$

Then we have,

$$\begin{pmatrix} \mathbf{M}_{BN} \\ \widehat{\mathbf{Q}}_{NB} \\ \mathbf{M}_{BB} \end{pmatrix} \xrightarrow{S} \begin{pmatrix} & S^{BN\to NB} & \\ S^{NB\to BN} & & \\ & & S^{BB\to BB} \end{pmatrix} \begin{pmatrix} \mathbf{M}_{BN} \\ \widehat{\mathbf{Q}}_{NB} \\ \mathbf{M}_{BB} \end{pmatrix}. \tag{78}$$

Similarly we can compute the modular T-matrix, the action of which twists the inner boundary of an annulus by an angle of 2π counterclockwise with respect to its outer boundary. This definition ensures that the T-matrix acts as the identity on tubes with no charge line (i.e. with no strings ending on their inner annular boundaries). Within each spin structure sector the T-matrix is diagonal in the idempotent basis. We can read off the structure of the T-matrix with the help of Figure 3.3.4 to find

$$\begin{pmatrix} \mathbf{M}_{BN} \\ \widehat{\mathbf{Q}}_{NB} \\ \mathbf{M}_{BB} \end{pmatrix} \xrightarrow{T} \begin{pmatrix} & & T^{BN\to BB} \\ T^{BB\to BN} & & \\ & T^{NB\to NB} & \end{pmatrix} \begin{pmatrix} \mathbf{M}_{BN} \\ \widehat{\mathbf{Q}}_{NB} \\ \mathbf{M}_{BB} \end{pmatrix}. \tag{79}$$

With

$$T^{BN\to BB} = \begin{pmatrix} 1 & & \\ & A^3 & \\ & & 1 \end{pmatrix} \quad T^{NB\to NB} = \begin{pmatrix} A^5 & & \\ & 1 & \\ & & -A^5 \end{pmatrix} \quad T^{BB\to BN} = \begin{pmatrix} 1 & & \\ & A^3 & \\ & & 1 \end{pmatrix} \tag{80}$$

One can check that the usual modular group relation $(ST)^3 = \mathbb{1}$ holds as expected.

More interesting is the NN torus, whose spin structure is preserved under both S and T. This has been investigated before in [8], and our results agree with theirs in this case. According to Figure 3.3.2, the Hilbert space is spanned by $\overset{\bullet}{h}$, $\overset{\bullet}{v}$, and $\overset{\bullet}{t}$, where as before the $\bullet$ means that the associated tubes have odd fermion parity. In the topological basis, we obtain

$$\begin{pmatrix} \overset{\bullet}{h} \\ \overset{\bullet}{v} \\ \overset{\bullet}{t} \end{pmatrix}_{NN} \xrightarrow{S^{NN\to NN}} \begin{pmatrix} 0 & 1 & 0 \\ A^4 & 0 & 0 \\ 0 & 0 & A^{10} \end{pmatrix} \begin{pmatrix} \overset{\bullet}{h} \\ \overset{\bullet}{v} \\ \overset{\bullet}{t} \end{pmatrix}_{NN} \tag{81}$$

Now we need to transform into the idempotent (quasiparticle) basis. With the choice of basis in Figure 3.3.3 we find

$$\begin{pmatrix} \overset{\bullet}{q}_{\mathbb{1}} \\ \overset{\bullet}{q}_\sigma \\ \overset{\bullet}{q}_\psi \end{pmatrix}_{NN} \xrightarrow{S^{NN\to NN}} \frac{-A^2}{2} \begin{pmatrix} 1 & d & -1 \\ d & 0 & d \\ -1 & d & 1 \end{pmatrix} \begin{pmatrix} \overset{\bullet}{q}_{\mathbb{1}} \\ \overset{\bullet}{q}_\sigma \\ \overset{\bullet}{q}_\psi \end{pmatrix}_{NN}. \tag{82}$$

Note that the requirement $\overset{\bullet}{q}^2 = q$ only determines $\overset{\bullet}{q}$ up to a $\pm$ sign. Consequently the off-diagonal matrix elements $(S^{NN\to NN})_{ij}$ between q-type idempotents are only determined

up to a sign (indeed, sending $\overset{\bullet}{q}_j \to s_j \overset{\bullet}{q}_j$, $s_j = \pm 1$ conjugates the S-matrix by a diagonal matrix of ± 1's). Similarly, we can compute the modular T-matrix,

$$\begin{pmatrix} \overset{\bullet}{q}_{\mathbb{1}} \\ \overset{\bullet}{q}_{\sigma} \\ \overset{\bullet}{q}_{\psi} \end{pmatrix}_{NN} \xrightarrow{T^{NN\to NN}} \begin{pmatrix} A^5 & & \\ & 1 & \\ & & -A^5 \end{pmatrix} \begin{pmatrix} \overset{\bullet}{q}_{\mathbb{1}} \\ \overset{\bullet}{q}_{\sigma} \\ \overset{\bullet}{q}_{\psi} \end{pmatrix}_{NN} \tag{83}$$

One can check that we have the modular relations

$$(S^{NN\to NN}T^{NN\to NN})^3 = (S^{NN\to NN})^4 = A^8\mathrm{id} = -\mathrm{id} \tag{84}$$

The minus sign comes from the fact that acting by S^4 or $(ST)^3$ performs a 2π rotation of the fermion framing, resulting in a phase of -1, since all states on the NN torus have odd fermion parity. For general theories, these relations become $(ST)^3 = S^4 = (-1)^F$, where $(-1)^F$ is the fermion parity operator. See Sections 6.4 and 7.5.2 for examples of this more general scenario.

Collecting these results, we can now write down the complete modular S and T matrices in the C_2 theory, which act across all spin structures. In the quasiparticle basis $[(m_{\mathbb{1}}, m_\sigma^+, m_\psi)_{BB}, (m_{\mathbb{1}}, m_\sigma^+, m_\psi)_{BN}, (q_{\mathbb{1}}, q_\sigma, q_\psi)_{NB}, (\overset{\bullet}{q}_{\mathbb{1}}, \overset{\bullet}{q}_\sigma, \overset{\bullet}{q}_\psi)_{NN}]^T$, we have

$$S = \frac{1}{2}\begin{pmatrix} 1 & d & 1 & & & & & & & & & \\ d & 0 & -d & & & & & & & & & \\ 1 & -d & 1 & & & & & & & & & \\ & & & & & & 1 & d & 1 & & & \\ & & & & & & -d & 0 & d & & & \\ & & & & & & -1 & d & -1 & & & \\ & & & 1 & -d & -1 & & & & & & \\ & & & d & 0 & d & & & & & & \\ & & & 1 & d & -1 & & & & & & \\ & & & & & & & & & -A^2 & -A^2 d & A^2 \\ & & & & & & & & & -A^2 d & 0 & -A^2 d \\ & & & & & & & & & A^2 & -A^2 d & -A^{-2} \end{pmatrix} \tag{85}$$

where we have only listed the non-zero entries. S has two different direct-sum decompositions. First, essentially by construction, it splits into a direct sum over blocks according to spin structures under the S modular transformation. Additionally, we have $S = S_{even} \oplus S_{odd}$, where S_{odd} is the S-matrix acting on ground states with odd fermion parity. This decomposition is always possible, but it will not always match a decomposition based on spin structures. That is, while $S_{odd} = S^{NN\to NN}$ in this theory, spin structure blocks of $S^{NN\to NN}$ will not have a definite fermion parity in general; see Sections 6 and 7 for examples. Also note that $S^4 = \mathbb{1}_{9\times 9} \oplus (-\mathbb{1}_{3\times 3})$ in accordance with $S = S_{even} \oplus S_{odd}$ and $S^4 = (-1)^F \mathbb{1}$.

Now for the T-matrix. In the same quasiparticle basis as before, the T-matrix is

$$T = \begin{pmatrix} & & & 1 & 0 & 0 & & & & & & \\ & & & 0 & A^3 & 0 & & & & & & \\ & & & 0 & 0 & 1 & & & & & & \\ 1 & 0 & 0 & & & & & & & & & \\ 0 & A^3 & 0 & & & & & & & & & \\ 0 & 0 & 1 & & & & & & & & & \\ & & & & & & A^5 & 0 & 0 & & & \\ & & & & & & 0 & 1 & 0 & & & \\ & & & & & & 0 & 0 & -A^5 & & & \\ & & & & & & & & & A^5 & 0 & 0 \\ & & & & & & & & & 0 & 1 & 0 \\ & & & & & & & & & 0 & 0 & -A^5 \end{pmatrix} \tag{86}$$

The T-matrix is not completely diagonalized in the idempotent basis, since it acts non-trivially on the spin structures (although it is diagonalized within each spin structure block).

4 Generalities on fermion condensation and tube categories

The techniques used in Section 2 work more generally. In this section we discuss the general case and some variants thereof.

4.1 General comments on fermion condensation

In this section we will explore fermion condensation in more general settings. In Section 4.1.1 we make some general remarks on fermion condensation in a generic unitary braided fusion category $\mathcal{C}$. In Section 4.1.2 we add the stipulation that the fermion we aim to condense is *transparent*, in that it braids trivially with the other particles in the theory. Section 4.1.3 examines the more general case where the parent category $\mathcal{C}$ is not braided, but the object we want to condense lifts to a fermionic object in the Drinfeld center $\mathcal{Z}(\mathcal{C})$. Finally, Section 4.1.4 sketches a construction in which the braiding of the parent theory is retained after condensation, and spin structure defects are bound to particles that the fermion braids nontrivially with.

First, some preliminary remarks. In what follows we will work with a unitary braided fusion category $\mathcal{C}$ which contains a fermionic object ψ that we aim to condense. We require that ψ satisfy the following conditions:

- $\psi \otimes \psi \cong \mathbb{1}$
- The Frobenius-Schur indicator of ψ is 1
- The topological twist of ψ is fermionic, i.e. $\theta_\psi = -1$
- The braiding of ψ with itself (see (14)) is equal to -1 times the identity
- The quantum dimension d_ψ of ψ is 1

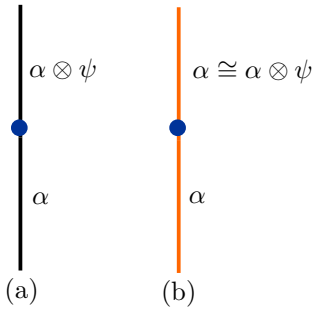

Figure 4.1.1: (a) An m-type particle α. The fermion ψ (blue dot) is an odd map from α to $\alpha \otimes \psi$, with $\alpha \ncong \alpha \otimes \psi$. (b) A q- type particle α with $\alpha \cong \alpha \otimes \psi$, where ψ now acts as an odd endomorphism.

Note that there is some redundancy in this list. For example, in unitary theories we have the spin-statistics relation, and $d_\psi = 1$ can be inferred from $\psi \otimes \psi \cong \mathbb{1}$.

We remark that the above assumptions allow us to endow the object $\mathbb{1} \oplus \psi$ with the structure of a *fermionic commutative algebra object* in $\mathcal{C}$. We can more generally condense any fermionic commutative algebra object φ. In the quotient category $\mathcal{C}/\varphi$, any simple summand of φ becomes isomorphic to $\mathbb{1}$, or perhaps isomorphic to a direct sum of copies of $\mathbb{1}$.

4.1.1 Condensing non-transparent fermions in a braided category

In this subsection we will assume $\mathcal{C}$ is a unitary braided fusion category (UBFC). We will also assume that ψ is non-transparent, meaning that it braids non-trivially with at least one non-trivial object in $\mathcal{C}$. We will examine the case where ψ is transparent in a later subsection.

We will proceed as in Section 2 and define a super pivotal category $\mathcal{C}/\psi$. Since ψ is fermionic in spin and statistics, and since it braids non-trivially with at least one other non-trivial object in $\mathcal{C}$ (from its assumed non-transparency), we must utilize both spin structures and the back wall construction in the condensation procedure.

The objects of $\mathcal{C}/\psi$ are the same as the objects of $\mathcal{C}$. The morphism space assigned to a disk with a boundary condition is the space of all back wall diagrams modulo local relations. (More concretely, the the even part of this morphism space is the corresponding morphism space in the parent category $\mathcal{C}$, and the odd part of this morphism space is (up to isomorphism) the morphism space of $\mathcal{C}$ obtained by adding ψ to the boundary condition.) In order for these relations to make sense, the disk must be equipped with a spin structure. This morphism space is a super vector space, with the $\mathbb{Z}_2$-grading given by the number of ψ endpoints in the diagram modulo 2. Composition of morphisms is given by gluing diagrams together. We can take the domain of the composition map to be the unordered tensor product (see 8.5) of the two morphism spaces we are combining. When doing computations it is necessary to choose an ordering and to take Koszul signs into account.

It follows from our assumptions about ψ that if α is a simple object of $\mathcal{C}$, then $\alpha \otimes \psi$ is also a simple object of $\mathcal{C}$. There are two cases:

- If $\alpha \otimes \psi$ is not isomorphic to α, then α and $\alpha \otimes \psi$ are both m-type objects of $\mathcal{C}/\psi$.

While α and $\alpha\otimes\psi$ represent distinct equivalence classes of simple objects in $\mathcal{C}$, they belong to the same equivalence class in $\mathcal{C}/\psi$. More specifically, α and $\alpha\otimes\psi$ are oddly isomorphic in $\mathcal{C}/\psi$, via a digram with a single ψ dot (see Figure 4.1.1 (a)).

- If $\alpha\otimes\psi\cong\alpha$, then α becomes a q-type simple object in $\mathcal{C}/\psi$. The odd endomorphism from α to itself is as shown in Figure 4.1.1 (b).

We will sometimes use the notation

$$\mathrm{sob}_r(\mathcal{C}/\psi) = \mathrm{sob}_r^m(\mathcal{C}/\psi)\sqcup\mathrm{sob}_r^q(\mathcal{C}/\psi), \tag{87}$$

with $\mathrm{sob}_r^m(\mathcal{C}/\psi)$ a complete set of representatives for m-type simple objects, and $\mathrm{sob}_r^q(\mathcal{C}/\psi)$ a complete set of representatives for q-type simple objects.

$\mathcal{C}/\psi$ is not a braided category, since the back wall used in the condensation procedure prevents us from braiding particles completely around one another. However, it does have the structure of a front-braiding by $\mathcal{C}$, since we are allowed to pass ψ worldlines between other particle worldlines and the back wall. (Another way of saying this is that $\mathcal{C}/\psi$ is a (fermionic) module 2-category for the 3-category $\mathcal{C}$. Yet another way of putting it is that $\mathcal{C}/\psi$ is a codimension-1 defect between $\mathcal{C}$ and the vacuum.)

A particularly simple class of condensed theories obtained from condensing a non-transparent fermion in a braided theory are provided by the $C_{2(n+1)} = A_{4n+3}/\psi$ series, where A_k is the category whose principal graph is the Dynkin diagram of the Lie algebra $\mathfrak{sl}_{k+1}$, and C_k is the category whose principal graph is the Dynkin diagram of the Lie algebra $\mathfrak{sp}_{2k}$. The choice $n=0$ corresponds to the Ising example considered in Section 2.

4.1.2 Condensing transparent fermions in a braided category

In this subsection we make the same assumptions about ψ and $\mathcal{C}$ as in 4.1.1, but we replace the assumption of non-transparency of ψ with the assumption that ψ is transparent in $\mathcal{C}$, meaning that it braids trivially with every other particle in $\mathcal{C}$.

Since ψ is transparent, we do not need the back wall when performing the condensation. We still need a spin structure, however (since $\theta_\psi=-1$), and we also need to keep track of Koszul signs (since ψ has fermionic statistics).

The resulting category $\mathcal{C}/\psi$ is a fermionic braided pivotal category. The absence of the back wall is what allows for $\mathcal{C}/\psi$ to possess a full braiding (rather than the "front-braiding" forced on condensed theories where back walls are needed). We will construct an example of such a theory in Section 6, where we condense a transparent fermion in the $SO(3)_6$ theory.

We note that q-type particles can never arise in the condensed theory if ψ is transparent. To see this, we note that if $\alpha\otimes\psi=\beta$ for α and β simple objects of $\mathcal{C}$, it follows that

$$\theta_\beta = \theta_\alpha\theta_\psi = -\theta_\alpha, \tag{88}$$

where the first equality is because ψ is transparent. It follows that $\alpha\ncong\beta$ in $\mathcal{C}$, and hence α descends to an m-type simple object in $\mathcal{C}/\psi$, since if α were q-type we would have $\alpha\otimes\psi\cong\alpha$.

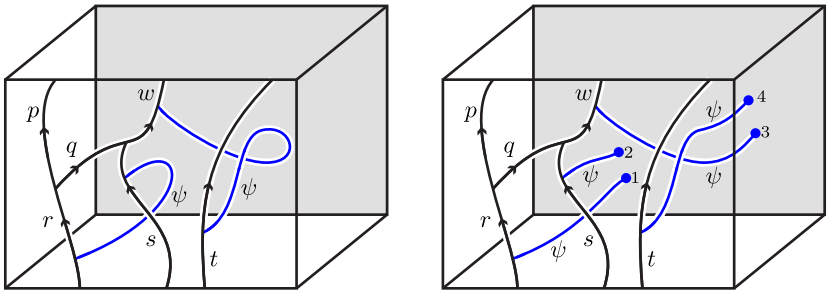

(89)

Figure 4.1.2: On the left we have a 3d box. The front of the box is a 2d boundary on which $\mathcal{C}$ string nets are drawn (viewed as a module for $\mathcal{Z}(\mathcal{C})$). The bulk of the box contains braided nets from $\mathcal{Z}(\mathcal{C})$, which we restrict to ψ. The back of the box can be viewed as a trivial boundary to the vacuum. The right picture shows the box after performing back wall condensation on $\psi \in \mathcal{Z}(\mathcal{C})$. The ψ lines terminate on the back boundary at marked points $1, 2, 3, 4$.

4.1.3 Condensing objects that lift to fermions in the Drinfeld Center

In this section we drop the assumption that $\mathcal{C}$ has a braiding. We will describe how to condense an object y of $\mathcal{C}$ which lifts to a fermion in the Drinfeld center $\mathcal{Z}(\mathcal{C})$. An instance of this construction is the $\frac{1}{2}\mathrm{E}_6$ theory we study in detail in Section 7.

The basic idea is as follows. The tensor category $\mathcal{C}$ can be thought of as a module for the braided category $\mathcal{Z}(\mathcal{C})$. In terms of string net pictures, this means that $\mathcal{C}$ string nets can be thought of as living on the 2d boundary of a 3d bulk of $\mathcal{Z}(\mathcal{C})$ string nets. We can, if we like, restrict the bulk to only contain strings from a subcategory of $\mathcal{Z}(\mathcal{C})$, in particular the subcategory generated by $\mathbb{1}$ and the lift of y. We can now do the back wall construction on the opposite side of the bulk and proceed as before. See Figure 4.1.2.

Now for a few more details.

To condense y, we first need to lift y to $\mathcal{Z}(\mathcal{C})$, which means defining half-braidings for y. For a formal definition of half braid see [22] (Definition 3.1 and Lemma 3.3). A half-braid on an object $y \in \mathcal{C}$ is an isomorphism from $y \otimes r \to r \otimes y$ for each $r \in \mathcal{C}$, the isomorphism being the half-braiding of y with r. We will denote these isomorphisms as $e_y(r)$, and write them diagrammatically as

$e_y(r) =$ 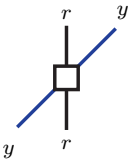 . (90)

One should think of the box braiding y under r. We could equally well think of this as braiding y over r, but since we will use the "back wall condensation" procedure to condense y, it is natural to choose y braiding under r.

Using the semisimplicity of $\mathcal{C}$ we can write $e_y(r)$ as

$e_y(r) =$ 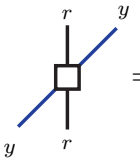 $= \sum_{w \in V_{yr}^{ry}} [e_y(r)]_w$ 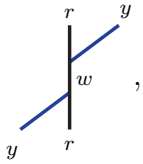 , (91)

Not any isomorphism $e_y(r)$ is allowed; $e_y(r)$ must satisfy some consistency conditions. For example, braiding with the identity object should be trivial (up to unitors):

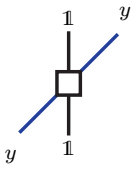

$$= \mathrm{id}_y. \tag{92}$$

The most important property of the braiding isomorphisms is that they commute with fusion, meaning that they can freely slide past the fusion spaces V_c^{ab}:

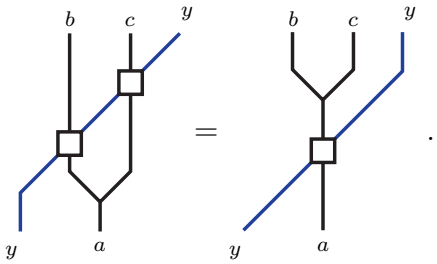

$$. \tag{93}$$

Taking (91) and inserting it into 92 and 93 allows one to find the $[e_y(r)]_w$ defined in (91).

In order to do fermion condensation we require y to lift to a fermionic object. Fermionicity under exchanges means that

$$e_y(y) = -\,\mathrm{id}_y \otimes \mathrm{id}_y. \tag{94}$$

If the quantum dimension of y is 1, then the spin-statistics theorem will imply that the lift of y is also fermionic with respect to twists.

Once a fermion has been defined one can proceed with the techniques of Sections 4.1.1 and 4.1.2. We will provide an example of such a condensation in Section 7.

4.1.4 Condensing non-transparent fermions using spin defects instead of a back wall

In this section, we briefly comment on another way to condense non-transparent fermions through a type of flux attachement, which doesn't make use of the back wall construction and allows the condensed theory to remain braided (for a braided input category). For related ideas, see [18, 30].

The construction proceeds schematically as follows. We allow the ψ worldlines to be absorbed into the vacuum at any point. In this picture the ψ lines end anywhere in 3-space, they are not restricted to terminating on a back wall. In order to resolve problems with the twist and self-statistics of ψ, we must couple the ψ endpoints to a spin structure and introduce Koszul signs, as before. This yields an inconsistent theory if ψ is not transparent (see (15)).

However, this inconsistency is rather mild. A natural way to distinguish the simple objects in $\mathcal{C}$ to use the $\mathbb{Z}_2$ grading inherited from the full braid of objects with ψ. This can be defined by the indicator

$$(-1)^{\nu_x} := S_{a\psi}/S_{a0} \in \{+1, -1\} \tag{95}$$

It is easy to check that this grading is preserved under fusion. Hence we can partition the simple objects in $\mathcal{C}$ as

$$\mathrm{sobj}\,\mathcal{C} = I_0 \cup I_1, \tag{96}$$

where I_k is the set of simple objects x with $\nu_x = k$. Since $I_a \otimes I_b = I_{a+b \bmod 2}$, this is a $\mathbb{Z}_2$ grading of the simple objects. It can be shown that in any UBFC, $\nu_x = 1$ for all q-type objects (those for which $x \otimes \psi \cong x$). Indeed, if x braided trivially with ψ and $x \otimes \psi \cong x$, then it would follow that $\theta_x = \theta_x \theta_\psi = -\theta_x$, a contradiction. Therefore, for a given object $a \in \mathcal{C}$, ψ must either be transparent with respect to a, or be non-transparent only by a minus sign.

We now observe that the problem in (15) would be surmounted if the "box" (the physical fermion attached to the ψ endpoint) had a -1 braiding phase when taken around any anyon with which ψ braids nontrivially. This extra -1 braiding phase cannot be due to the presence of any additional anyonic degrees of freedom, since the physical fermions braid trivially with any emergent anyon. However, there's actually a very natural way to do this: bind spin structure defects to the worldlines of anyons x with which $\nu_x = 1$. If the x worldlines get bound to spin structure defects during the condensation process, then a box will pick up a factor of -1 when traveling around a x line (when it passes through the branch cut), which cancels the -1 sign from the braiding of x and ψ, and solves the transparency inconsistency. The spin structure defects have $\mathbb{Z}_2$ fusion rules, and so this procedure is consistent since the $\mathbb{Z}_2$ grading of objects in (96) is preserved under fusion. This allows the condensation to go through without the use of the back wall construction, which allows us to perform fermion condensation without sacrificing the existence of a braided structure.

This picture also gives us a schematic physical interpretation of how to invert the condensation procedure. To go the other way and un-condense ψ, we just decouple the x lines from the spin structure defects. This gives us a phase consisting of the MTC $\mathcal{C}$ together with a loop gas of spin structure defects. The loop gas of spin structure defects confine free ψ endpoints, forcing all ψ worldlines to be closed and restoring the original phase.

4.2 The tube category of $\mathcal{C}/\psi$

The quasiparticle excitations in a bosonic topological phase obtained from a category $\mathcal{C}$ are given by the simple objects in the Drinfeld center $\mathcal{Z}(\mathcal{C})$ [23]. These excitations are also naturally described by primitive idempotents of a category called the tube category of $\mathcal{C}$ (see e.g. [31, 32, 33, 22, 34, 35, 36], also variously referred to as the tube algebra and the Q-algebra), which we will write as $\mathbf{Tube}(\mathcal{C})$.

The tube category was first introduced by Ocneanu [21] and has since been dubbed "Ocneanu's tube algebra"; it is also referred to as the annular category $\mathrm{Ann}(\mathcal{C})$, or the categorified degree zero Hochschild homology of $\mathcal{C}$. It is closely related to the Drinfeld center: If $\mathcal{C}$ is pivotal then there is a natural isomorphism $\mathrm{Rep}(\mathrm{Ann}(\mathcal{C})) \cong \mathcal{Z}(\mathrm{Rep}(\mathcal{C}))$, and if $\mathcal{C}$ is semisimple then we can drop the Reps and obtain $\mathrm{Ann}(\mathcal{C}) \cong \mathcal{Z}(\mathcal{C})$. With appropriate modifications accounting for spin structure issues, a similar construction holds in the more general fermionic setting considered here.

We will now define two categories $\mathbf{Tube}^B(\mathcal{S})$ and $\mathbf{Tube}^N(\mathcal{S})$ for a string-net TQFT derived from a given super pivotal category $\mathcal{S}$. We will postpone the most general definition of a super pivotal category until Section 8. However, categories obtained from fermion condensation $\mathcal{S} \cong \mathcal{C}/\psi$ all constitute examples of super pivotal categories (and provide all the examples of super pivotal categories discussed explicitly in this paper), and so the reader may substitute $\mathcal{C}/\psi$ for $\mathcal{S}$ in what follows before reading the more general definitions in Section 8.

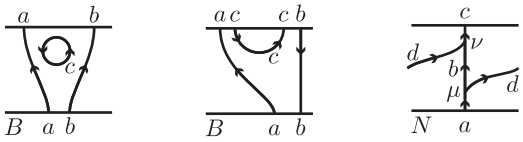

Figure 4.2.1: Some examples of morphisms in $\mathbf{Tube}(\mathcal{S})$, with $\mathcal{S}$ a super pivotal category obtained through a fermionic quotient $(\mathcal{S}/\psi)$ or more generally a category satisfying the assumptions laid out in Section 8. We have written the annulus as a square with (unmarked) left and right sides identified. At the bottom left of each annulus we have denoted the spin structure of the annulus by B (or N) for bounding (or non-bounding). The labels $a, b, c, d \in \mathrm{sob}_r(\mathcal{S})$, and $\nu \in \mathrm{mor}_{\mathcal{S}}(d \otimes b \to c)$, and $\mu \in \mathrm{mor}_{\mathcal{S}}(a \to b \otimes d)$.

The objects of the two spin tube categories $\mathbf{Tube}^B(\mathcal{S})$ and $\mathbf{Tube}^N(\mathcal{S})$ are defined as isomorphism classes of string-net boundary conditions on spin circles with bounding and non-bounding spin structures, respectively. For each spin tube category, we will fix a representative spin circle with which to define its objects. Other possible choices of spin circles are related to the chosen representative by spin diffeomorphisms, and the exact specification of the particular representative will be unimportant in our analysis.

The morphism spaces of the tube category are finite linear combinations of spin annuli decorated with different string-net configurations. Again, we will fix a particular representative spin annulus for each spin structure to use when defining morphisms, with other choices being related by spin diffeomorphisms. Figure 4.2.1 shows some examples of morphisms in the tube category.

Up to isomorphism, every object in the tube category is isomorphic to a direct sum of objects with a exactly one string net endpoint on the circle. Put another way, the full subcategory spanned by such one-endpoint objects is Morita equivalent to the entire category. This means that for purposes of, for example, enumerating equivalence classes of minimal idempotents or computing Hilbert spaces (ground states), we can restrict our attention to the one-endpoint subcategory. And indeed we will usually do so without comment. (Note however that it is sometimes convenient to work in the larger category; see e.g. 5.2.)

In the one-endpoint subcategory, morphism spaces can be presented as

$$\mathrm{mor}(\mathbf{Tube}^X(\mathcal{S})) \;=\; \mathbb{C}\left[\right. \quad \left.\right] \tag{97}$$

where a, b, c, d are simple objects in $\mathcal{S}$ and $X \in \{B, N\}$ denotes the spin structure of the annulus. The multiplicity indices μ, and ν are collective indices that denote the vector in the fusion space V_a^{db} and $V_b^{c\bar{d}}$, as well as the ordering of the tensor product $(V_a^{db} \otimes V_b^{cd^*}$ or $V_b^{cd^*} \otimes V_a^{db})$ which forms the Hilbert space of the tube.

We define the *full* tube category $\mathbf{Tube}(\mathcal{S})$ to be the direct sum

$$\mathbf{Tube}(\mathcal{S}) \cong \mathbf{Tube}^B(\mathcal{S}) \oplus \mathbf{Tube}^N(\mathcal{S}). \tag{98}$$

In what follows we will mostly think of $\mathbf{Tube}(\mathcal{S})$ as the fundamental category of interest.

This is because in what follows we will be led to consider a $\otimes$ structure on $\mathbf{Tube}(\mathcal{S})$, which mixes the two spin components (we defer a discussion of this to Section 4.4).

Composition of morphisms in $\mathbf{Tube}(\mathcal{S})$ is defined by stacking tubes together. Graphically,

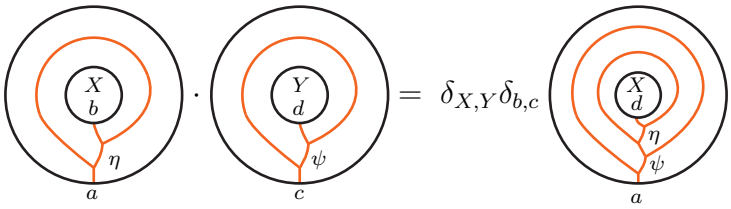

(99)

The δ functions ensure that if the string labels of the two tubes don't agree on the boundary on which they are being glued (i.e. if $b \neq c$), or if the spin structures of the two tubes disagree, the two tubes compose (or multiply) to zero.

Before moving on, we briefly remark on the physical interpretation of the tube category. In Section 9 we will define a Hamiltonian whose ground state wave functions assign amplitudes to string nets in such a way that equivalent string nets receive equal amplitudes. (In other words, the ground states are naturally identified with the string net TQFT Hilbert space $Z(Y;c)$, where Y is a spin surface and c is a boundary condition.) Let S be a boundary component of Y, which we will think of as a puncture. We can act on the space of string nets of of Y (a.k.a. $A(Y;c)$) by gluing morphisms of the tube category (which are string-net-decorated spin annuli) to Y at S. Dually, we get an action of the tube category on the ground state vector spaces $Z(Y;c)$ (for various values of c). If we like, we can think of this action of the tube category as a scale transformation; see [35]. We can also think of it as a generalized symmetry of the Hamiltonian. The collection of ground states $Z(Y;c)$ can be decomposed as a direct sum of irreducible representations of the tube category. The irreducible representations of the tube category are thus identified with the elementary particles (i.e. anyons) of the theory. Using the usual correspondence between minimal idempotents and irreducible representations, we can also identify the minimal idempotents of the tube category with anyons. See the end of Section 9.3.3 for slightly more detail.

4.2.1 Traces and inner products

Recall that a trace on a super linear category $\mathcal{T}$ is an even linear function from endomorphisms to $\mathbb{C}$, satisfying

$$\mathrm{tr}(fg) = \mathrm{tr}(gf), \tag{100}$$

for all $f \in \mathrm{mor}(x \to y)$ and $g \in \mathrm{mor}(y \to x)$. (Note that $\mathrm{tr}(f) = 0$ if f is odd, since tr is an even function. Note also that there is no Koszul sign in (100).)

All of the categories we consider have a reflection structure[9] (more specifically, a pin+ reflection structure), which is an order 2 antilinear antiautomorphism of $\mathcal{T}$ (i.e. $\mathrm{mor}(x \to y)$ is sent to $\mathrm{mor}(y \to x)$, for all objects x and y). We will denote the image of a morphism f under reflection as $\bar{f}$. The antiautomorphism property has the usual Koszul sign

$$\overline{fg} = (-1)^{|f||g|}\bar{g}\bar{f}. \tag{101}$$

[9]Usually called a $*$-structure, but we are already committed to denoting the pivotal structure in tensor categories by $*$.

A trace is equivalent to a collection of sesquilinear inner products on $\mathrm{mor}(x \to y)$ satisfying

$$\langle fg, h\rangle = (-1)^{|g||h|}\langle f, h\bar{g}\rangle \quad \text{and} \quad \langle fg, h\rangle = (-1)^{|f||h|}\langle g, \bar{f}h\rangle \tag{102}$$

The trace and inner products are related by

$$\mathrm{tr}(f) = \langle f, \mathrm{id}_x\rangle \quad \text{and} \quad \langle g, h\rangle = \mathrm{tr}(g\bar{h}) \tag{103}$$

for $f \in \mathrm{mor}(x \to x)$ and $g, h \in \mathrm{mor}(x \to y)$. A trace is called nondegenerate if the corresponding inner product is nondegenerate in the usual sense (on each morphism space individually).

We now recall two facts about TQFTs. The first is that we can define a nondegenerate pairing on the predual Hilbert space $A(Y; a_1, \ldots, a_k)$, where Y is a spin surface with k disjoint boundary components and the a_i are tube category idempotents, satisfying $\bar{a}_i = a_i^*$, which specify boundary conditions at each boundary component. The nondegenerate pairing is defined via

$$\langle u, v\rangle = Z(Y \times I)(u \cup \bar{v}), \tag{104}$$

where the bar denotes the reflection map from $A(Y; a_1, \ldots, a_k)$ to $A(-Y; a_1, \ldots, a_k)$. Here we are using the "pinched boundary" condition for $Y \times I$, so that $\partial(Y \times I) = Y \cup -Y$. In other words, we glue together the string nets u and $\bar{v}$ to get a string net on $\partial(Y \times I)$, and then we evaluate the path integral of $Y \times I$ with the $u \cup \bar{v}$ string net as the boundary condition.

The second fact concerns the path integral of 3-manifolds of the form $Y \times S^1_B$ or $Y \times S^1_N$. Let c be a string net on $(\partial Y) \times S^1$ (with either spin structure on S^1). $(\partial Y) \times S^1$ is a disjoint union of tori, and we can cut these tori open into a disjoint union of annuli. Let c' denote the cut-open string nets on the annuli. Note that c' is not uniquely determined by c; c' depends on where we cut the tori. The string net c' determines a linear map

$$g(c') : A(Y; a_i) \to A(Y; a_i), \tag{105}$$

given by gluing the c' annuli on to the boundary of a string net on Y. The gluing rules for the path integral imply that

$$Z(Y \times S^1_B)(c) = \mathrm{tr}(g(c')) \tag{106}$$

and

$$Z(Y \times S^1_N)(c) = \mathrm{str}(g(c')), \tag{107}$$

where str denotes the supertrace, which is the trace weighted by the fermion parity operator, i.e. $\mathrm{str}(f) = \mathrm{tr}((-1)^F f)$. The association of the trace (supertrace) with the B (N) spin structure was also noticed in [25]. Note that the partition functions above are independent of the details of the cutting procedure; any choice of cutting curves and any choice of c' will yield the same answer on the RHS above.

We now apply the above to the case where Y is an annulus to obtain a nondegenerate trace on the tube category. In what follows we will continue to let $\mathcal{S}$ be a super pivotal fusion category satisfying the assumptions of Section 8 (e.g. one coming from a fermionic quotient). Letting $t \in \mathbf{Tube}^W(\mathcal{S})$ and writing $\mathrm{tr}(t)$ for the trace of t, we can use (103) to write

$$\mathrm{tr}(t) = \langle t, \mathrm{id}\rangle = Z((S^1_W \times I) \times I)(t \cup \overline{\mathrm{id}}) = Z(S^1_W \times D^2)(t \cup \overline{\mathrm{id}}) = Z(S^1_W \times D^2)(\mathrm{cl}(t)). \tag{108}$$

Diagrammatically we can write the evaluation of the partition function on the right hand side of (108) as the trace of a matrix, through

$\langle t, \mathrm{id}\rangle =$ 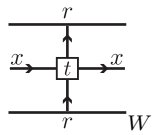 $= \mathrm{tr}_W$, (109)

where we have made use of the graphical representation of the endomorphism t in the first equality. The solid cylinder in the third equality provides a linear map from the disk at the origin of the x line to the disk at the end of the x line, with each disk possessing a single marked point on its boundary labeled x. The subscript W denotes that the solid cylinder was found by cutting open a cycle with spin structure W. From (106) and (107), we see that tr_W will be a trace if W is bounding, and a super trace if W is non-bounding. The source and target of this linear map is $\mathrm{mor}(\mathbb{1} \to x)$, which we write as the vector space assigned to a disc with one marked point labeled x:

$$A\left(\left(\right)_{x}\right) \cong \mathrm{mor}(\mathbb{1} \to x) = \bigoplus_i \mathbb{1} \xrightarrow{\mu_i} x, \tag{110}$$

with μ_i denoting a complete basis of morphisms for $\mathrm{mor}(\mathbb{1} \to x)$ We allow for $x \cong a_1 \otimes a_2 \otimes \cdots \otimes a_k$ so that a basis of $\mathrm{mor}(\mathbb{1} \to x)$ could be relatively large. Often x will denote a simple object and so $\mathrm{mor}(\mathbb{1} \to x)$ will be zero or one dimensional:

$$A\left(\left(\right)_{x}\right) = \begin{cases} \mathbb{C}^{1|0} & \text{if } x \text{ is evenly isomorphic to } \mathbb{1} \\ \mathbb{C}^{0|1} & \text{if } x \text{ is evenly isomorphic to } \psi \\ 0 & \text{otherwise} \end{cases}. \tag{111}$$

The linear map induced by the cut on these basis elements is given by

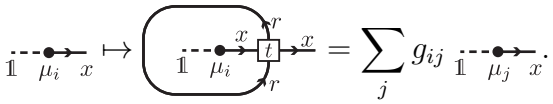 $= \sum_j g_{ij}$ 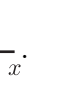 . (112)

The coefficients g_{ij} are found by reducing the middle diagram using local relations. As usual, the trace is basis independent and any basis of $\mathrm{mor}(\mathbb{1} \to x)$ will do.

Let us introduce the notation

$$s(X) = \begin{cases} 1 & \text{if } X = B \quad \text{Bounding} \\ -1 & \text{if } X = N \quad \text{Non-bounding} \end{cases} \tag{113}$$

Explicitly, (109) is then given by

$$\mathrm{tr}_W(g) = \sum_j g_{jj} s(W)^{|\mu_j|}. \tag{114}$$

If W is bounding then $s(W) = 1$ and (114) is just $\mathrm{tr}(g)$. On the other hand, if W is non-bounding then $s(W) = -1$, and (114) is the super trace $\mathrm{str}(g)$.

This trace is defined for the tube category of any super pivotal category satisfying the assumptions of Section 8. The inner product obtained from the trace is even, in the sense that $\langle v, w\rangle = 0$ if $|v| \neq |w|$.

In summary, the trace on the tube category is obtained as follows. Start with a string net t on the annulus $S^1_W \times I$. Cut t along an interval to obtain a string net on a square. Rotate this square $\pi/2$ and then reglue (with bounding spin structure) to obtain a new annular string net $\mathrm{rot}(t)$ on $S^1_B \times I$. Gluing $\mathrm{rot}(t)$ to the boundary of a disk induces a linear map r_t on disk string nets. If $W = B$ then $\mathrm{tr}(t) = \mathrm{tr}(r_t)$, where the tr on the RHS is the usual linear algebra trace. If $W = N$ then $\mathrm{tr}(t) = \mathrm{str}(r_t)$, where the str on the RHS is the usual linear algebra super trace. Note that $\mathrm{rot}(t)$ and r_t depend on the choice of initial cut, but $\mathrm{tr}(r_t)$ and $\mathrm{str}(r_t)$ are independent of this choice.

We now compute some traces that illustrate the techniques described in this section, and which will also be of use to us later.

First we compute the norm squared of a single strand on an annulus with empty boundary conditions. We denote by $\mathrm{cl}_B(x)$ the closure of $x \in \mathrm{sob}_r(\mathcal{S})$ on an annulus with bounding spin structure:

$$\mathrm{cl}_B(x) \;=\; \tag{115}$$

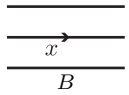

The the norm squared of $\mathrm{cl}_B(x)$ is

$$\langle \mathrm{cl}_B(x), \mathrm{cl}_B(x) \rangle = \mathrm{tr}_B\{\mathrm{id} : \; \mathrm{mor}(\mathbb{1} \to x \otimes x^*) \to \mathrm{mor}(\mathbb{1} \to x \otimes x^*)\}. \tag{116}$$

Since $\mathrm{mor}(\mathbb{1} \to x \otimes x^*) \cong \mathrm{mor}(x \to x) \cong \mathrm{End}(x)$, we get

$$\langle \mathrm{cl}_B(x), \mathrm{cl}_B(x) \rangle = \dim \mathrm{End}(x) = \begin{cases} 1 & \text{if } x \text{ is m-type} \\ 2 & \text{if } x \text{ is q-type} \end{cases}. \tag{117}$$

We can also compute the quantum dimensions d_{e_j} of the minimal idempotents in $\mathbf{Tube}(\mathcal{S})$. The un-normalized quantum dimension $\tilde{d}_{e_j}$ is defined by the trace of the idempotent:

$$\tilde{d}_{e_j} = \mathrm{tr}(e_j), \tag{118}$$

The normalized quantum dimension d_{e_j} is then given by $\tilde{d}_{e_j}/\tilde{d}_{e_0}$, where e_0 is the trivial idempotent. For example, in the C_2 theory, we can use this approach to obtain $\tilde{d}_{m_{\mathbb{1}/\psi}} = 1/2, \tilde{d}_{m^+_\sigma} = \tilde{d}_{q_{\mathbb{1}/\psi}} = 1/\sqrt{2}, \tilde{d}_{q_\sigma} = 1$. Normalizing so that $d_{m_{\mathbb{1}}} = 1$, we obtain the normalized quantum dimensions listed in Table 3.1.2.

The total squared dimension $\mathcal{D}^2$ of the theory is defined to be $\langle S^2_\phi, S^2_\phi \rangle$, the inner product of the empty diagram on the 2-sphere with itself. We can then compute

$$\langle S^2_\phi, S^2_\phi \rangle = Z(S^2 \times I)(\overline{S^2_\phi} \cup S^2_\phi) = \sum_{x \in \mathrm{sob}_r(\mathcal{S})} \frac{Z(B^3, \mathrm{cl}(x)) Z(B^3, \overline{\mathrm{cl}(x)})}{\langle \mathrm{cl}_B(x), \mathrm{cl}_B(x) \rangle}, \tag{119}$$

where B^3 is the 3-ball and $Z(B^3, \mathrm{cl}(x))$ denotes the partition function of a 3-ball with a closed x loop on its surface. To obtain the second equality, we have written $S^2 \times I$ as a union of two manifolds homeomorphic to B^3 glued along a bounding annulus and have made use of the gluing axioms of TQFT. We can compute $Z(B^3, \mathrm{cl}(x)) = Z(B^3, \overline{\mathrm{cl}(x)}) = d_x$ by definition of the quantum dimension, and hence the total squared dimension is given by

$$\mathcal{D}^2 = \sum_{x \in \mathrm{sob}_r(\mathcal{S})} \frac{d_x^2}{\dim \mathrm{End}(x)}. \tag{120}$$

A similar derivation recovers (40), where we pointed out that $\mathrm{cl}_N(\beta)$ is zero. Let us see how this works out in the tube category $\mathbf{Tube}(\mathcal{S})$. Let $x \in \mathrm{sob}_r(\mathcal{S})$, it follows that

$$\langle \mathrm{cl}_N(x), \mathrm{cl}_N(x) \rangle = \mathrm{tr}_N\{\mathrm{id} : \ \mathrm{mor}(\mathbb{1} \to x \otimes x^*) \to \mathrm{mor}(\mathbb{1} \to x \otimes x^*)\} = \begin{cases} 1 & \text{if } x \text{ is m-type} \\ 0 & \text{if } x \text{ is q-type} \end{cases} \tag{121}$$

The last equality follows from $\mathrm{mor}(\mathbb{1} \to x \otimes x^*) \cong \mathrm{End}(x)$ and that tr_N is the super trace of $\mathrm{id} : \ \mathrm{End}(x) \to \mathrm{End}(x)$. More explicitly, if x is m-type then as a vector space $\mathrm{End}(x) \cong \mathbb{C}$ and $\mathrm{str}\{\mathrm{id} : \ \mathbb{C} \to \mathbb{C}\} = 1$. On the other hand, if x is q-type then as a vector space $\mathrm{End}(x) \cong \mathbb{C}^{1|1}$ and

$$\mathrm{str}\{\mathrm{id} : \ \mathbb{C}^{1|1} \to \mathbb{C}^{1|1}\} = \mathrm{tr}\{(-1)^F : \ \mathbb{C}^{1|1} \to \mathbb{C}^{1|1}\} = 1 - 1 = 0 \tag{122}$$

Hence q-type idempotent closed up to an annulus with non-bounding spin structure has norm zero. Similarly, one can show that $\langle \mathrm{cl}_N(\gamma), \mathrm{cl}_N(\gamma) \rangle = 2$ when x is q-type and gamma is an odd endomorphism such that $\gamma^2 = \mathrm{id}$.

We now show that closing up a q-type idempotent of $\mathbf{Tube}(\mathcal{S})$ onto a torus results in a state with norm $\sqrt{2}$. Let x be a minimal idempotent of $\mathbf{Tube}(\mathcal{S})$, and $\mathrm{cl}_W(x) \in A(T^2)$ be the string net found by closing x onto a torus with spin structure W along the newly closed cycle. First consider the case where $W = B$. The norm squared of $\mathrm{cl}_B(x)$ is

$$\langle \mathrm{cl}_B(x), \mathrm{cl}_B(x) \rangle = Z(T^2 \times I)(\overline{\mathrm{cl}_B(x)} \cup \mathrm{cl}_B(x)) = Z((S^1 \times I) \times S^1_B)(\overline{\mathrm{cl}_B(x)} \cup \mathrm{cl}_B(x)). \tag{123}$$

In the third equality we have rewritten the torus in a form where we can readily apply equation (106) or (107). The role of Y is played by $S^1 \times I$, an annulus with spin structure determined by x. Further, we can assume a boundary condition given by the idempotent x on each boundary component of the annulus. We will also assume that $\bar{x} = x$. The linear map we need to take the matrix (super) trace of is just the identity map, so

$$\langle \mathrm{cl}_B(x), \mathrm{cl}_B(x) \rangle = \dim \mathrm{End}(x) \tag{124}$$

A similar calculation for the non-bounding torus yields the same answer, however the q-type idempotents need to be closed with an odd endomorphism. We can now justify the mysterious normalization factor introduced in (76) when closing up q-type idempotents on the torus. A complete orthogonal basis for the torus is given by closing up a complete set of representatives of minimal idempotents. To find a unitary S-matrix we require each of the basis states to have unit norm, hence we divide closed up q-type idempotents by $\sqrt{2}$.

Lastly we point out a useful relation between the total dimension of a pivotal fusion category $\mathcal{C}$ and its fermionic quotient $\mathcal{C}/\psi$. Let $\mathcal{C}$ be a pivotal fusion category, $\psi \in \mathcal{Z}(\mathcal{C})$ a fermion with $\psi \otimes \psi \cong \mathbb{1}$, and $\mathcal{C}/\psi$ the fermionic quotient of $\mathcal{C}$, then

$$\mathcal{D}^2_{\mathcal{C}} = 2\mathcal{D}^2_{\mathcal{C}/\psi} \tag{125}$$

if in addition we assume that $\mathcal{C}$ is a modular tensor category we also have,

$$\mathcal{D}^2_{\mathbf{Tube}(\mathcal{C}/\psi)} = \mathcal{D}^2_{\mathcal{C}}\mathcal{D}^2_{\mathcal{C}/\psi} \tag{126}$$

To show (125), we simply note

$$\mathcal{D}_{\mathcal{C}}^2 = \sum_{x \in \mathrm{sob}_r(\mathcal{C})} d_x^2 = \sum_{x \in \mathrm{sob}_r^m(\mathcal{C}/\psi)} d_x^2 + d_{x\otimes\psi}^2 + \sum_{q \in \mathrm{sob}_r^q(\mathcal{C}/\psi)} d_x^2. \tag{127}$$

Since $d_{x\otimes\psi} = d_x d_\psi = d_x$ we can write

$$\mathcal{D}_{\mathcal{C}}^2 = 2 \sum_{x \in \mathrm{sob}_r^m(\mathcal{C}/\psi)} d_x^2 + \sum_{x \in \mathrm{sob}_r^q(\mathcal{C}/\psi)} d_x^2 = 2 \sum_{x \in \mathrm{sob}_r(\mathcal{C}/\psi)} \frac{d_x^2}{\dim \mathrm{End}(x)} = 2\mathcal{D}_{\mathcal{C}/\psi}^2 \tag{128}$$

hence, (125). For the C_2 theory, this works out as $\mathcal{D}_{C_2} = \sqrt{2} = \mathcal{D}_{\mathrm{Ising}}/\sqrt{2}$. Using (125) and specializing to the case where $\mathcal{C}$ is a modular tensor category then $\mathbf{Tube}(\mathcal{C}/\psi) \cong \mathcal{C} \times (\mathcal{C}/\psi)$ (a result that we prove in Section 5.3), and we have

$$\mathcal{D}_{\mathbf{Tube}(\mathcal{C}/\psi)} = \mathcal{D}_{\mathcal{C}} \mathcal{D}_{\mathcal{C}/\psi}. \tag{129}$$

For example, in the C_2 theory this is verified by $\mathcal{D}_{\mathbf{Tube}(C_2)} = \sqrt{8} = \sqrt{2}(\sqrt{2})^2 = \sqrt{2}\mathcal{D}_{C_2}^2$.

4.2.2 The sum-of-squares formula

When analyzing tube categories, we are often presented with a collection of non-simple objects $x_1, x_2, \ldots$ (e.g. single string net endpoints), together with the super dimensions of the vector spaces $\mathrm{mor}(x_i \to x_j)$. From this we want to deduce a complete set of minimal idempotents $\{e_\alpha\}$, together with isomorphisms

$$x_i \cong \bigoplus_\alpha W_{i\alpha} \cdot e_\alpha \tag{130}$$

where the $\{W_{i\alpha}\}$ are supervector spaces. We will show in (322) how to compute morphism spaces between objects that are of the form of those in the RHS of (130). Applying (322) yields

$$\mathrm{mor}(x_i \to x_j) \cong \bigoplus_\alpha \mathrm{Hom}(W_{i\alpha} \to W_{j\alpha}) \otimes_{\mathbb{C}} \mathrm{End}(e_\alpha). \tag{131}$$

When $i \neq j$, this is merely an isomorphism of supervector spaces, but when $i = j$ this is an isomorphism of super algebras.

It is frequently possible, given the left hand side of (131) and a small amount of additional information, to solve for the things on the right hand side: the idempotents $\{e_\alpha\}$, their types, and the coefficients $W_{i\alpha}$. This is useful since the morphisms that constitute the left hand side are often very easy to enumerate: they are simply the different tubes in $\mathbf{Tube}_{x_i \to x_j}$. In terms of super dimensions, setting $i = j$ we have

$$\dim(\mathrm{mor}(x_i \to x_i)) = \sum_\alpha \dim(\mathrm{End}(W_{i\alpha})) \dim(\mathrm{End}(e_\alpha)). \tag{132}$$

This is a fermionic "sum-of-squares" formula since $\dim \mathrm{End}(W_{i\alpha})$ will always be the square of an integer.

For example, we can consider the space $\mathrm{mor}^X(\mathbb{1} \to \mathbb{1})$ in the C_2 theory. Letting $X = B$ we see immediately from (38) that $\mathrm{mor}(x_i \to x_i)$ has super dimension $2|0$, meaning that there must be two summands on the RHS of (132), and hence two minimal idempotents in $\mathbf{Tube}^B_{\mathbb{1}\to\mathbb{1}}$. Letting $X = N$ we read off a super dimension of $1|1$, which implies that

there is only one q-type idempotent in $\mathbf{Tube}^N_{\mathbb{1}\to\mathbb{1}}$. Similarly from (38) one verifies that the super dimensions of $\mathrm{mor}^X(\beta \to \beta)$ are each $2|2$, meaning that each sector must contain either one m-type idempotent with $\dim \mathrm{End}(W_\alpha) = 2^2$ or two q-type idempotents e_α with $\dim \mathrm{End}(W_\alpha) = 1$ (although the latter is ruled out if $X = B$ since $\mathbf{Tube}^B$ can host no q-type idempotents). Thus, one can learn a good deal about the number of minimal idempotents and their type in the tube category simply from a list of the non-zero linearly independent tubes.

In Section 7.4 we will see a further example of these techniques.

4.3 Ground states on the torus

In what follows, we will let T_{XY} with $X, Y \in \{B, N\}$ denote the torus with spin structure XY (with spin structure X along the meridional cycle and Y along the longitudinal cycle), and $A(T_{XY})$ the Hilbert space of ground-state string-net configurations on T_{XY}. As before, we will also let $\mathbf{Tube}^B$ denote the bounding tube category and $\mathbf{Tube}^N$ denote the non-bounding tube category.

We have the following theorem, valid for any super pivotal category, which allows us to determine the ground states on a torus from the tube category:

Theorem 4.3.1. *Let X equal B or N. The Hilbert space $A(T_{XB})$ is purely even, with an orthogonal basis given by closed-up idempotents $\{cl(e_i)\}$, where e_i runs through a set of representatives of the minimal idempotents of $\mathbf{Tube}^X$. The Hilbert space of T_{XN} is isomorphic to $\mathbb{C}^{p|q}$, where p is the number of m-type idempotents of $\mathbf{Tube}^X$ and q is the number of q-type idempotents of $\mathbf{Tube}^X$. An orthogonal basis is given by $\{cl(e_i)\}$, where e_i runs through a set of representatives of the minimal m-type idempotents of $\mathbf{Tube}^X$, union $\{cl(\gamma_j)\}$, where γ_j runs through a set of representatives of odd endomorphisms of the minimal q-type idempotents of $\mathbf{Tube}^X$.*

The proof of the above claim consists of a sequence of fairly simple observations:

1. Let c be an object of $\mathbf{Tube}^X$ and let $f \in \mathrm{End}(c)$. Recall that f is a linear combination of string nets on the annulus (with spin structure X), with boundary conditions c on both boundary components of the annulus. We can therefore glue up f to obtain a new string net $\mathrm{cl}(f)$ (the closure of f) on either T_{XB} or T_{XN}. This map is clearly linear, so we have a linear map $\mathrm{cl}_c : \mathrm{End}(c) \to A(T_{XY})$, where Y is either B or N. (For future reference, we will call the image of the boundary of the annulus in the torus K.)

2. Taking (finite) sums over different boundary conditions, we have a linear map

$$\mathrm{cl} : \bigoplus_c \mathrm{End}(c) \to A(T_{XY}), \tag{133}$$

   where c ranges over all possible boundary conditions. (Note that even though c ranges over an uncountable set, the direct sum consists only of finite linear combinations; there are no convergence issues.)

3. The map cl is surjective. This is because any string net on the torus is, after a small isotopy, transverse to the gluing locus K. But cl is very far from being injective, so our next task is to characterize the kernel of cl.

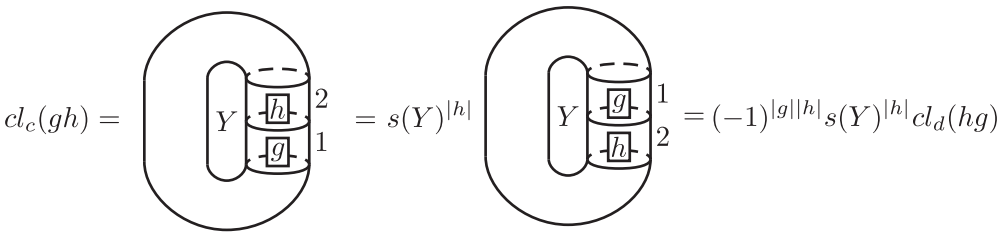

Figure 4.3.1: A graphical illustration of how to interchange morphisms in the tube category. The labels 1 and 2 denote the order in which the morphisms g and h appear in tensor products. The factor of $s(Y)$ comes from transporting h around the torus, and the factor of $(-1)^{|g||h|}$ is the usual Koszul sign.

4. One way of constructing elements in the kernel of cl is as follows. Let c and d be two objects of $\mathbf{Tube}^X$. Let $g : c \to d$ and $h : d \to c$. Then $gh \in \mathrm{End}(c)$ and $hg \in \mathrm{End}(d)$. We have

$$\mathrm{cl}(gh) = (-1)^{|g||h|} s(Y)^{|h|} \mathrm{cl}(hg), \tag{134}$$

where $s(B) = -1$ (antiperiodic) and $s(N) = 1$ (periodic). This follows from the fact that the two string nets $\mathrm{cl}(gh)$ and $\mathrm{cl}(hg)$ are isotopic via a "shift" isotopy which pushes h past the gluing locus K. The factor of $(-1)^{|g||h|}$ is the usual Koszul sign. The factor of $s(Y)^{|h|}$ comes from sliding h past the spin structure branch cut at K; see Figure 4.3.1. It follows that elements of the form

$$gh - (-1)^{|g||h|} s(Y)^{|h|} hg \in \bigoplus_x \mathrm{End}(x) \tag{135}$$

are in the kernel of cl.

5. In fact, elements of the form (135) generate all of the kernel of cl. In the bosonic case, this is a standard fact (see [24]). The proof for the fermionic case is exactly the same, except that we have to keep track of Koszul signs and signs coming from the spin structure. The key idea of the proof is that any isotopy of the torus can be decomposed into (a) isotopies which are fixed near K, and therefore can be lifted to isotopies of the annulus, and (b) a "shift" isotopy as described above. In summary,

$$A(T_{XY}) \cong \left(\bigoplus_x \mathrm{End}(x) \right) / \left\langle gh - (-1)^{|g||h|} s(Y)^{|h|} hg \right\rangle. \tag{136}$$

6. In the semisimple case, the expression (136) can be greatly simplified. Let $\{e_i\}$ be a complete set of minimal idempotents for $\mathbf{Tube}^X$. Any endomorphism f can be written as a sum of endomorphisms of the form $f' e_i f''$. Using (135), we see that the subspace (of the big direct sum)

$$\bigoplus_i \mathrm{End}(e_i) \tag{137}$$

maps surjectively to $A(T_{XY})$. Furthermore, because the minimal idempotents are orthogonal (in the sense that $e_i f e_j$ is zero for any f unless $i = j$), the only relations we have to consider are of the form

$$gh - (-1)^{|g||h|} s(Y)^{|h|} hg \tag{138}$$

where both g and h are endomorphisms of e_i. The theorem now follows.

If e_i is m-type, then (138) is always zero and we get a summand of $\mathbb{C}^{1|0}$ in $A(T_{XY})$. If e_i is q-type and Y is B, then any odd endomorphism is of the form (138) and we get a summand of $\mathbb{C}^{1|0}$. If e_i is q-type and Y is N, then any even endomorphism is of the form (138) and we get a summand of $\mathbb{C}^{0|1}$.

A useful corollary of Theorem 4.3.1 is that all the idempotents of $\mathbf{Tube}^B$ must be m-type. Since T_{BN} is spin diffeomorphic to T_{NB}, we can compute the Hilbert space for these spin surfaces in two different ways, one using idempotents of $\mathbf{Tube}^B$ and the other using idempotents of $\mathbf{Tube}^N$. By the first part of the theorem, the Hilbert space of T_{NB} is purely even. By the second part of theorem, the dimension of the odd part of the Hilbert space of T_{BN} is given by the number of q-type idempotents of $\mathbf{Tube}^B$. Since the two Hilbert spaces are isomorphic, there can be no q-type idempotents in $\mathbf{Tube}^B$.

A similar argument shows that the total number of (equivalence classes of) minimal idempotents of $\mathbf{Tube}^B$ must equal that of $\mathbf{Tube}^N$.

4.4 Fusion rules

In this subsection, we will define the fusion (tensor product) of representations of the tube category.

We begin with some general observations. Let Y be a spin surface with k boundary components, denoted by $S_1, \ldots, S_k$. Let T_i denote the tube category corresponding to the circle S_i. Each T_i is (non-canonically) isomorphic to either $\mathbf{Tube}^B$ or $\mathbf{Tube}^N$. (In order to make the isomorphisms canonical, we must choose a spin framing in each boundary component.) Given objects c_i of T_i, for $1 \leq i \leq k$, we have a super vector space $A(Y; c_1, \ldots, c_k)$ consisting on string nets on Y, modulo local relations, with boundary conditions c_i at S_i.

We can then glue morphisms of T_i (tubes) onto S_i to obtain a new string net with (possibly) different boundary condition. A concise way to describe this algebraic structure is to say that the collection of super vector spaces $\{A(Y; c_1, \ldots, c_k)\}$ (for all possible values of $c_1, \ldots, c_k$) affords a representation of the category $T_1 \times \cdots \times T_k$. We will denote this representation by $A(Y)$.

To define the fusion rules of excitations, we take Y to be the pair of pants (a.k.a three-punctured sphere), which we will denote as P.

There are four spin structures on P. In one of them, all three boundary components have a bounding spin structure, while in the remaining three, two out of the three boundary components have a non-bounding spin structure. We will choose a standard representative for each of these spin pairs of pants, so that each boundary component is equipped with a spin diffeomorphism to a standard copy of S^1_B or S^1_N.

Let T_a, T_b and T_c denote the three copies of the tube category associated to the boundary components of P. Given representations ρ_a and ρ_b of T_a and T_b, we can define a new representation of T_c, denoted $\rho_a \otimes \rho_b$, via

$$\rho_a \otimes \rho_b = (\rho_a \boxtimes \rho_b) \otimes_{T_a \times T_b} A(P). \tag{139}$$

Here $\rho_a \boxtimes \rho_b$ denotes the "outer" tensor product (so that $\rho_a \boxtimes \rho_b$ is a representation of $T_a \times T_b$), and $A(P)$ is the trimodule defined above, built out of vector spaces of string-net configurations (modulo local relations) on P with all possible boundary conditions. Informally, $\rho_a \otimes \rho_b$ is found by taking a superposition of tubes carrying ρ_a and ρ_b (which

is the outer product $\rho_a \boxtimes \rho_b$) and gluing them onto a pair of pants (given by $A(P)$). The algebraic implementation of gluing is the tensor product $\otimes_{T_a \times T_b}$.

If ρ is the representation (i.e. module) determined by an idempotent e (as described at the start of 3.2), then the above association of ρ to a boundary component is equivalent to imposing e as a boundary condition in a annular neighborhood of that boundary component.

Note that the spin structure grading of the tube category (and its modules) is respected by the above tensor product:

$$B \otimes B = B \qquad B \otimes N = N \qquad N \otimes N = B \tag{140}$$

where B (N) is shorthand for the bounding (non-bounding) sector of the tube category.

4.5 Dimension formula

In this subsection we give a Verlinde-type formula for the super dimension of the Hilbert space of a surface Y.

4.5.1 The formula

Let Y be a spin surface with boundary components $U_1, \ldots, U_k$. Each U_i inherits either a bounding (a.k.a. antiperiodic or non-vortex) spin structure or a nonbounding (a.k.a. periodic or vortex) spin structure.

Let $a_1, \ldots, a_k$ be a set of labels for ∂Y. Each a_i is a minimal idempotent in the tube category $\mathbf{Tube}^{U_i}(\mathcal{C})$ (which is isomorphic to either $\mathbf{Tube}^{B}(\mathcal{C})$ or $\mathbf{Tube}^{N}(\mathcal{C})$); either a non-vortex anyon or a vortex anyon (according to the spin structure on U_i). The predual Hilbert space of string-net configurations on Y with boundary conditions determined by the a_i is $A(Y; a_1, \ldots, a_k) \cong \mathbb{C}^{p|q}$ for some integers p, q. Our goal is to compute p and q.

Let S_{ab} denote the normalized, unitary S-matrix. The indices a and b are closed-up idempotents on a spin torus. They are specified by giving an idempotent (either bounding or nonbounding) together with the way the annulus was glued to obtain the torus (again either bounding or nonbounding, independent of the bounding/nonbounding status of the idempotent). The idempotent a is glued up in a (non)bounding way if b is a (non)bounding idempotent, and vice versa.[10] If the idempotent is q-type, it is rescaled by $1/\sqrt{2}$ to obtain a unit vector in $A(T^2)$, the vector space of string-net configurations modulo local relations on the torus (see 4.2.1). (Note that there is still some ambiguity for entries in the S-matrix corresponding to odd vectors in T^2_{NN}, but the formulas below will not use these S-matrix entries.)

Let S'_{ab} be S_{ab} if a is m-type and $\sqrt{2} \cdot S_{ab}$ if a is q-type. Note that S'_{ab} is asymmetric in a and b; we're undoing the normalization for a but not for b. The idempotents we will be summing over fall into three classes: B_m (bounding and m-type), N_m (non-bounding and m-type), and N_q (non-bounding and q-type). Recall (from the discussion at the end of 4.3) that bounding idempotents are always m-type; in other words the potential fourth class B_q is empty.

We can now state the dimension formula: We have

$$p + q = \sum_{x \in B_m} {S_{1x}}^{\chi(Y)} \prod_i S'_{a_i x} \tag{141}$$

[10] This is because spin structure on the cutting circle of one torus must match the spin structure of the circle perpendicular to the cutting circle of the other torus.

where $\chi(Y)$ is the Euler characteristic of Y. If any of the a_i are q-type, then we know that $p = q$ and we are done, since in that case $\mathbb{C}^{p|q}$ has an odd isomorphism coming from the action of an odd element of $\mathrm{End}(a_i)$.

Now assume that none of the a_i are q-type. In this case we have

$$p - q = \sum_{x \in N_m} {S_{1x}}^{\chi(Y)} \prod_i S'_{a_i x} \quad + \quad (-1)^{\mathrm{Arf}(Y)} \sum_{x \in N_q} {S_{1x}}^{\chi(Y)} \prod_i S'_{a_i x}. \tag{142}$$

Where $\mathrm{Arf}(Y)$ is the Arf invariant of Y. If Y is closed, then $\mathrm{Arf}(Y) = 0$ if Y has a bounding spin structure and $\mathrm{Arf}(Y) = 1$ if Y has a nonbounding spin structure. For a torus, the BB, BN and NB spin structures are bounding and the NN spin structure is nonbounding. $\mathrm{Arf}(Y)$ for a higher genus spin surface can be determined by writing Y as a connected sum of spin tori, and using the fact that $\mathrm{Arf}(Y)$ is additive under connected sums.

If Y has non-empty boundary and each boundary component has a bounding spin structure, we define $\mathrm{Arf}(Y)$ to be the Arf invariant of the closed surface obtained by capping each boundary component off with a disk.

If Y has a non-bounding boundary component, say U_1, then by assumption the label a_1 is m-type. It follows that $S'_{a_1 x} = 0$ if x is q-type, so there is no need to define $\mathrm{Arf}(Y)$ in this case. We can see that $S'_{a_1 x} = 0$ because the torus basis vector corresponding to x is odd (odd endomorphism of x glued up periodically), while the basis vector corresponding to a_1 is even (the idempotent a_1 glued up periodically), and S is an even operator. This can be observed, for example, the NN block of the S-matrix for the $\frac{1}{2}\mathrm{E}_6/\psi$ theory, (296).

Note that the formula for $p + q$ above does not depend on the Arf invariant of Y, while the formula for $p - q$ does. Thus the total dimension of the Hilbert space is not sensitive to the spin structure of Y, but the even and odd Hilbert space dimensions do depend on the spin structure.

4.5.2 Sketch of proof

In this subsection we sketch the proof of the above dimension formula.

Let Z denote the 2+1-dimensional TQFT associated to the super pivotal category $\mathcal{C}$. Let Y be a closed spin surface with Hilbert space $Z(Y)$, and let $p|q = \dim(Z(Y))$. Then we have

$$p + q = \mathrm{tr}(\mathrm{id} : Z(Y) \to Z(Y)) = Z(Y \times S^1_B) \tag{143}$$

and

$$p - q = \mathrm{tr}((-1)^F : Z(Y) \to Z(Y)) = Z(Y \times S^1_N). \tag{144}$$

More generally, if Y has nonempty boundary and the boundary components are labeled by $a_1, \ldots, a_k$ (minimal idempotents of the tube category), then

$$\begin{aligned} p + q &= \mathrm{tr}(\mathrm{id} : Z(Y; a_1, \ldots, a_k) \to Z(Y; a_1, \ldots, a_k)) && (145)\\ &= Z(Y \times S^1_B)(\mathrm{cl}_B(a_1) \sqcup \cdots \sqcup \mathrm{cl}_B(a_k)) && (146) \end{aligned}$$

and

$$\begin{aligned} p - q &= \mathrm{tr}((-1)^F : Z(Y; a_1, \ldots, a_k) \to Z(Y; a_1, \ldots, a_k)) && (147)\\ &= Z(Y \times S^1_N)(\mathrm{cl}_N(a_1) \sqcup \cdots \sqcup \mathrm{cl}_N(a_k)). && (148) \end{aligned}$$

Here $\mathrm{cl}_X(a_i)$ denotes the element of $Z(T^2_{UX})$ obtained by closing up the idempotent a_i, and U is the spin structure (B or N) on the i-th boundary component. Note that if a_i is q-type, then $\mathrm{cl}_N(a_i) \in Z(T^2_{NN})$ is zero. But in this case we also know that $p - q = 0$, since the odd endomorphism of a_i maps the even part of $Z(Y; a_1, \ldots, a_k)$ isomorphically to the odd part.

Recall that we can define reduced 1+1-dimensional TQFTs $Z_{S^1_B}$ and $Z_{S^1_N}$ via

$$Z_{S^1_B}(M) = Z(M \times S^1_B) \qquad Z_{S^1_N}(M) = Z(M \times S^1_N), \tag{149}$$

where M is a manifold of dimension 0, 1 or 2. Combining the above we have, for closed spin surfaces Y,

$$p + q = Z_{S^1_B}(Y) \tag{150}$$

and

$$p - q = Z_{S^1_N}(Y), \tag{151}$$

and there are similar formulas when Y has boundary.

We can now outline the remainder of the proof of the dimension formula. We have just seen that the super dimension $p|q$ can be calculated entirely in terms of the reduced 1+1-dimensional TQFTs $Z_{S^1_B}$ and $Z_{S^1_N}$. Because 1 is a small number, we can completely classify 1+1-dimensional spin TQFTs and give an explicit expression for the path integral in terms of basic structure constants of the 1+1-dimensional TQFT. Then all that remains to be done is express the structure constants of the 1+1-dimensional TQFTs in terms of the structure constants of the original 2+1-dimensional TQFT Z. It turns out that the only structure constants we will need are the list of minimal idempotents of the tube category, their types (m or q), and the S-matrix.

Spin 1+1-dimensional TQFTs are determined by two pieces of data: the cylinder category of a point, which is a linear super category C, and a non-degenerate trace on C. The trace is the path integral of the disk D^2; if f is an endomorphism of C, then

$$\mathrm{tr}(f) = Z_{C,\mathrm{tr}}(D^2)(\mathrm{cl}(f)), \tag{152}$$

where, as usual, $\mathrm{cl}(f)$ denotes the closure of f, an element of the (pre-dual) Hilbert space associated to $S^1_B = \partial D^2$. The non-degenerate trace implies that C is semisimple. Up to Morita equivalence, there are only two indecomposable semisimple super categories, the trivial algebra $\mathbb{C}$ and the complex Clifford algebra $\mathbb{C}\ell_1$.

We first consider the case $C = \mathbb{C}$. Let e be the unique minimal idempotent of $\mathbb{C}$ (i.e. $e = 1 \in \mathbb{C}$). Let $\lambda = \mathrm{tr}(e)$. Let Y be a spin surface with k boundary components, and let $\mathrm{cl}(e) \sqcup \cdots \sqcup \mathrm{cl}(e)$ denote the boundary condition given by placing $\mathrm{cl}(e)$ on each boundary component of Y. The the path integral for the TQFT determined by $(\mathbb{C}, \lambda)$ is

$$Z_{\mathbb{C},\lambda}(Y)(\mathrm{cl}(e) \sqcup \cdots \sqcup \mathrm{cl}(e)) = \lambda^{\chi(Y)}, \tag{153}$$

where $\chi(Y)$ denotes the Euler characteristic of Y.

Next we consider the case $C = \mathbb{C}\ell_1$. Again let e be the unique minimal idempotent of $\mathbb{C}\ell_1$. Let $\lambda = \mathrm{tr}(e)$. Let Y be a spin surface with k boundary components. We will assume that each boundary component of Y has the bounding spin structure, since that is the only case we will need for the dimension formula. Let

$$\hat{e} = \frac{1}{\sqrt{2}}\, e \tag{154}$$

be the normalized idempotent. (The norm of $\mathrm{cl}(\hat{e})$ in $A(S^1_B)$ is 1.) The the path integral for the TQFT determined by $(\mathbb{C}\ell_1, \lambda)$ is

$$Z_{\mathbb{C}\ell_1,\lambda}(Y)(\mathrm{cl}(\hat{e}) \sqcup \cdots \sqcup \mathrm{cl}(\hat{e})) = (-1)^{\mathrm{Arf}(Y)} \left(\frac{\lambda}{\sqrt{2}}\right)^{\chi(Y)}, \tag{155}$$

where $\chi(Y)$ denotes the Euler characteristic of Y, and $\mathrm{Arf}(Y)$ is the Arf invariant of Y with its boundary components capped off by disks.

A general 1+1-dimensional spin TQFT is a direct sum of instances of the two theories described above.

All that remains to be done is to write the reduced theories $Z_{S^1_B}$ and $Z_{S^1_N}$ as a direct sum of the $(\mathbb{C}, \lambda)$ and $(\mathbb{C}\ell_1, \lambda)$ theories described above.

The first task is to obtain a list of the idempotents (and their type, m or q) of the minimal idempotents of $Z_{S^1_B}$ and $Z_{S^1_N}$. This is easily done: the category which $Z_{S^1_B}$ assigns to a point is $\mathbf{Tube}^B$, and the category which $Z_{S^1_N}$ assigns to a point is $\mathbf{Tube}^N$. The m-type idempotents correspond to $(\mathbb{C}, \lambda)$ theories, and the q-type idempotents correspond to $(\mathbb{C}\ell_1, \lambda)$ theories.

The second task is to determine, for each idempotent a in $\mathbf{Tube}^B$ and $\mathbf{Tube}^N$, the number λ above (path integral of the disk evaluated on a closed-up idempotent). This is exactly the S-matrix entry S_{1a} if a is m-type. If a is q-type, then (since we have normalized the S-matrix) S_{1a} is equal to $\lambda/\sqrt{2}$, but this is the value we need for (155).

The third and final task is to convert the $\mathrm{cl}(a_i)$ boundary conditions from the beginning of 4.5.1 to the $\mathrm{cl}(e)$ and $\mathrm{cl}(\hat{e})$ boundary conditions appearing in (153) and (155). Both of these boundary conditions are (after undoing the dimensional reduction along S^1_B or S^1_N) vectors in $A(T^2)$, and both boundary conditions are closed-up idempotents (possibly normalized with a factor of $1/\sqrt{2}$). But the $\mathrm{cl}(a_i)$ boundary condition cuts the torus along a longitude, while the $\mathrm{cl}(e)$ and $\mathrm{cl}(\hat{e})$ boundary conditions cut the torus along a meridian. So we need to apply the S-matrix (actually S', because $\hat{e}$ is normalized while a_i is not) to change basis:

$$\mathrm{cl}(a_i) = \sum_x S'_{a_i x} \mathrm{cl}(\hat{x}), \tag{156}$$

where for convenience we have defined $\hat{x} = x$ if x is m-type.

Combining (150), (151), (153), (155), and (156) yields the dimension formula.

4.5.3 Sample calculations

There are three specific S matrices calculated in this paper, for the TQFTs based on the C_2, $SO(3)_6/\psi$, and $\frac{1}{2}\mathrm{E}_6/y$ theories. Note that all three of these theories have just one non-trivial simple object. Plugging the S-matrix entries into the above dimension formula, we find, for closed surfaces of genus g and specified Arf invariant, the results in Figure 4.5.1.

If we take Y to be a 3-punctured sphere (with various spin structures), then we can use the dimension formula to compute the fusion rules of the tube category. For example, the fusion rules of Table 7.4.5 were computed using the dimension formula. Explicitly, we have

$$\dim_{\mathrm{even}}(V^{abc}) = \frac{\sqrt{n_a n_b n_c}}{2} \left(\sum_{x \in B_m} \frac{S_{ax} S_{bx} S_{cx}}{S_{1x}} + \sum_{x \in N_m \cup N_q} \frac{S_{ax} S_{bx} S_{cx}}{S_{1x}} \right) \tag{157}$$

	C_2	$SO(3)_6/\psi$	$\frac{1}{2}\mathrm{E}_6/y$
$g=1, \mathrm{Arf}=0$	3 | 0	4 | 0	3 | 0
$g=1, \mathrm{Arf}=1$	0 | 3	2 | 2	1 | 2
$g=2, \mathrm{Arf}=0$	10 | 0	40 | 24	19 | 8
$g=2, \mathrm{Arf}=1$	0 | 10	32 | 32	11 | 16
$g=3, \mathrm{Arf}=0$	36 | 0	1184 | 1120	281 | 232
$g=3, \mathrm{Arf}=1$	0 | 36	1152 | 1152	241 | 272
$g=4, \mathrm{Arf}=0$	136 | 0	51328 | 51072	5755 | 5504
$g=4, \mathrm{Arf}=1$	0 | 136	51200 | 51200	5531 | 5728
$g=5, \mathrm{Arf}=0$	528 | 0	2368000 | 2366976	126449 | 125056
$g=5, \mathrm{Arf}=1$	0 | 528	2367488 | 2367488	125137 | 126368

Figure 4.5.1: Hilbert space dimensions for closed surfaces in various theories.

and

$$\dim_{\mathrm{odd}}(V^{abc}) = \frac{\sqrt{n_a n_b n_c}}{2}\left(\sum_{x\in B_m}\frac{S_{ax}S_{bx}S_{cx}}{S_{1x}} - \sum_{x\in N_m\cup N_q}\frac{S_{ax}S_{bx}S_{cx}}{S_{1x}}\right). \tag{158}$$

Recall that n_a is defined to be $\dim(\mathrm{End}(a))$, i.e. 1 if a is m-type and 2 if a is q-type.

We remark that the dimension formula is a useful check on S-matrix accuracy. Mistakes in calculating the S matrix typically lead to non-integer outputs from the dimension formula.

5 More on fermion condensation in modular tensor categories and the tube category

In this section we investigate $\mathbf{Tube}(\mathcal{C}/\psi)$ when $\mathcal{C}$ is a modular tensor category. If $\mathcal{C}$ is a MTC, it is a well known theorem that $\mathbf{Tube}(\mathcal{C}) \cong \mathcal{C}\times\overline{\mathcal{C}}$ as braided tensor categories (see for example Theorem 7.10 of [22]). In the this section we will prove an analogous theorem for the super pivotal categories resulting from fermion condensation on MTCs. Specifically, if $\mathcal{C}$ is a MTC we prove that

$$\mathbf{Tube}(\mathcal{C}/\psi) \cong \mathcal{C}\times\overline{\mathcal{C}/\psi} \tag{159}$$

as tensor categories. (Neither side of this equivalence is braided in the usual sense.)

The analogous result when ψ is a boson is a special case of Corollary 4.8 of [37] (see also the 1998 announcement by Ocneaunu referred to therein).

To begin, we remind the reader of this known result for $\mathbf{Tube}(\mathcal{C})$. We then turn our attention to super pivotal categories of the form $\mathbf{Tube}(\mathcal{C}/\psi)$ and make the necessary modifications.

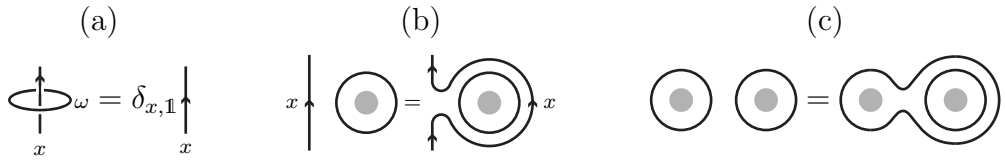

Table 5.1.1: All unlabeled lines in the above figures are ω loops as defined in (160). For a modular theory, the ω loop projects onto the vacuum as shown in part (a) (agreeing with the interpretation of ω as the minimal idempotent in the solid torus corresponding to the trivial object of $\mathcal{C}$). Part (b) shows that arbitrary string-net lines can be deformed across any ω loop. Part(c) shows the same move as in part (b) but with an ω loop, rather than a single simple object x.

5.1 ω loops

An essential tool in what follows will be the the ω loop [26]. We take $\mathcal{C}$ to be a MTC and $\mathrm{sob}_r(\mathcal{C})$ be the set of the simple objects of $\mathcal{C}$. The ω loop is defined by

$$\omega = \frac{1}{\mathcal{D}^2} \sum_{x \in \mathrm{sob}_r(\mathcal{C})} d_x \cdot \mathrm{cl}(x), \tag{160}$$

where as before, $\mathrm{cl}(x)$ denotes a closed loop labeled by x, i.e. the closure of x inside a solid torus.

One way to think of the ω loop is as follows. In any premodular category, string nets in the solid torus (with the empty boundary condition) form a semisimple commutative algebra (isomorphic to the fusion ring of the premodular category). Therefore this vector space has a basis given by the minimal idempotents of the algebra structure. The S-matrix gives a bijection between these idempotents and $\mathrm{sob}_r(\mathcal{C})$. The ω loop is the minimal idempotent in the solid torus corresponding to the trivial object of $\mathcal{C}$.

Diagrammatically, we will denote the ω loop embedded in an ambient 3-manifold by

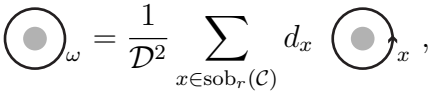

(161)

where the gray disk in the center indicates that this relation holds in the solid torus. If the gray region is empty (i.e. if the solid torus is standardly embedded in the 3-ball), then the ω loop can be shrunk and evaluated using the rules of MTC (since in that case $\mathrm{cl}(x)$ is equal to d_x times the empty diagram), and since $1 = \sum_x d_x^2/\mathcal{D}^2$, the ω loop simply acts as the identity. We summarize all the properties of the ω loop which we will make use of in Table 5.1.1.

For a modular theory, we can easily use part (a) of Table 5.1.1 to see that

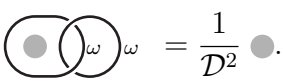

(162)

Note that this is true independent of what is inside the gray disc. In the next section, we will see that this allows us to rewrite elements in the tube algebra in a particularly nice basis.

5.2 Minimal idempotents of Tube($\mathcal{C}$), when $\mathcal{C}$ is a modular tensor category

The starting point for our proof of (159) will be a convenient set of minimal idempotents of **Tube**($\mathcal{C}$) [21]. We will give two constructions for complete sets of minimal idempotents of **Tube**($\mathcal{C}$): one set is more conventional (and appeared first historically), while the second is more suited to the proof of (159).

The first construction of a set of minimal idempotents utilizes annuli that possess only one marked point at each boundary. A basis for the morphism space from a to b in the annular category **Tube**($\mathcal{C}$) is given by

$$\mathrm{mor}\Big(\;\underset{a}{\bullet}\;\to\;\underset{b}{\bullet}\;\Big) = \mathbb{C}\left[\;\;\right] \qquad \text{with} \qquad t \in \bigoplus_r V_a^{rbr^*}, \tag{163}$$

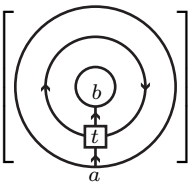

with r in each summand labeling the string wrapping around the annulus. With the help of (162) we can change to a much more convenient basis via

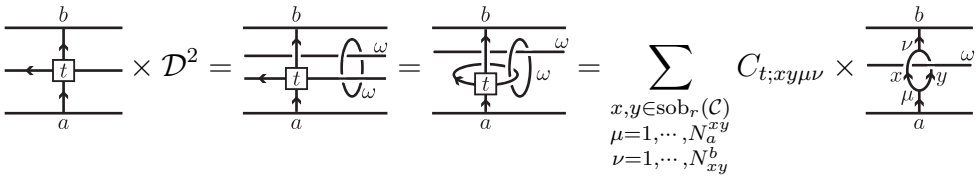

(164)

where we have written the annulus as a rectangle with the left and right (blank) edges identified and the indices μ and ν run over complete orthogonal bases of V_a^{xy} and V_{xy}^b, respectively. The constants $C_{t,xy\mu\nu}$ can be determined by fusing the ω loop into the strand labeled b in the second to last diagram, and then using a series of F and R moves to reduce the diagram to the form of the final diagram on the right. Since $\mathcal{C}$ is assumed to be modular and all transformations shown above are invertible, we have shown that the morphism spaces can be alternatively presented as

$$\mathrm{mor}\Big(\;\underset{a}{\bullet}\;\to\;\underset{b}{\bullet}\;\Big) \cong \mathbb{C}\left[\;\;\right]. \tag{165}$$

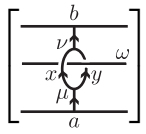

Equivalently, we have shown that

$$\mathrm{mor}\Big(\;\underset{a}{\bullet}\;\to\;\underset{b}{\bullet}\;\Big) \cong \bigoplus_{xy} V_{xy}^b \otimes V_a^{xy}. \tag{166}$$

This basis for the morphism space of **Tube**($\mathcal{C}$) is rather special, and we will see that the diagonal elements (those with $a = b$) are proportional to the minimal idempotents.

Letting μ_i, $i = 1, \cdots, N_{xy}^a$ be a basis of V_a^{xy} and similarly letting ν_i be a basis for V_{xy}^a, we take the normalization convention

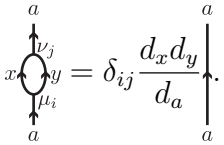

(167)

It then follows that

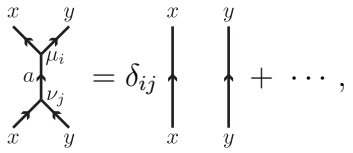

(168)

where the $+\ldots$ represents diagrams that have a nontrivial string connecting the x and y strings (if admissible diagrams of such a form exist). From the properties of the ω loop, we thus have

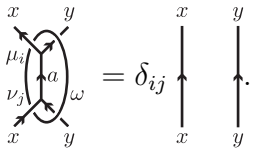

(169)

Our normalization is thus chosen so that there is no numerical prefactor in front of the right hand side of the above equality.

With these conventions, we define a basis of morphisms by

$$f_a^b(x,y,j,i) \;=$$

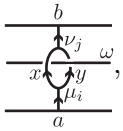

(170)

where ν_j is a basis of V_{xy}^b and μ_i a basis of V_a^{xy}, which are normalized according to (167). It follows that the f_a^b morphisms compose as

$$f_a^b(x,y,j,i) \cdot f_b^c(x',y',j',i') = \delta_{xx'}\delta_{yy'}\delta_{ij'} f_a^c(x,y,j,i'). \tag{171}$$

Therefore, the $f_a^b(x,y,j,i)$ is a basis of matrix units for $\mathbf{Tube}(\mathcal{C})$. Said another way, $\mathbf{Tube}(\mathcal{C})$ (strictly speaking, the subcategory of $\mathbf{Tube}(\mathcal{C})$ spanned by objects with only a single marked point) splits as a direct sum of full matrix categories[11] labeled by pairs of simple objects in $\mathrm{sob}_r(\mathcal{C}) \times \mathrm{sob}_r(\mathcal{C})$:

$$\mathbf{Tube}(\mathcal{C}) \cong \bigoplus_{xy} \mathrm{Mat}(x,y), \tag{172}$$

with the vector space associated to the object a of $\mathbf{Tube}(\mathcal{C})$ at the (x,y) summand being V_{xy}^a, and

$$\mathrm{mor}(a \to b) \cong \bigoplus_{x,y} \hom(V_{xy}^a \to V_{xy}^b). \tag{173}$$

It follows from (171) that the "diagonal" morphisms

$$e(a,x,y,j) = f_a^a(x,y,j,j) \tag{174}$$

are each a minimal idempotent. The idempotents $e(a,x,y,i)$ and $e(b,x',y',j)$ are equivalent[12] if and only if $x \cong x'$ and $y \cong y'$, with the isomorphism given by $e(a,x,y,i) =$

[11] Recall that a full matrix category is one in which each object is a finite-dimensional vector space, and the morphisms between two objects are all linear maps. A full matrix category with only one object is a full matrix algebra. Full matrix categories are Morita trivial; all minimal idempotents within a full matrix category are equivalent to each other.

[12] Two idempotents e and e' are equivalent if $e = uv$ and $e' = vu$ for some u and v.

$f_a^b(x,y,i,j)\cdot f_b^a(x,y,j,i)$ and $e(b,x,y,j) = f_b^a(x,y,j,i)\cdot f_a^b(x,y,i,j)$. This presentation of the minimal idempotents also appeared in [21].

It will be useful to have another complete set of minimal idempotents for $\mathbf{Tube}(\mathcal{C})$ at our disposal. These are the minimal idempotents that live in the annular category with two marked points on each of the circles bounding the annulus (rather than one marked point on each circle). The idempotents are given by

$$e_{xy} = \tag{175}$$

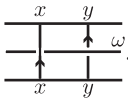

To show that the e_{xy} are a complete set of minimal idempotents, we first show that $e_{xy}\mathbf{Tube}(\mathcal{C})e_{x'y'}$ is zero unless $x = x'$ and $y = y'$, in which case it is 1-dimensional. (This implies that the e_{xy} are minimal and pairwise orthogonal.) Using the spine lemma,[13] a basis for $e_{xy}\mathbf{Tube}(\mathcal{C})e_{x'y'}$ is spanned by

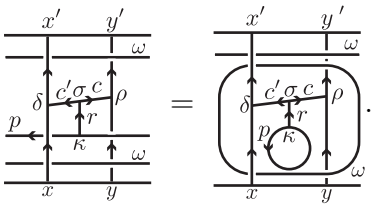

(176)

The RHS is derived from the LHS by first sliding the p loop over the lower ω loop, then sliding the lower ω loop over the upper ω loop. The "no tadpole" axiom implies that the diagram is zero unless $r \cong \mathbb{1}$, and (a) of Table 5.1.1 implies that c (and hence also c') must be $\mathbb{1}$ in any non-zero diagram. This proves the claim.

Completeness of the idempotents follows from the resolution of the identity

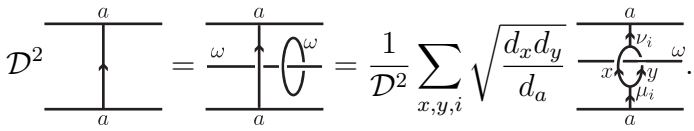

(177)

It is easy to show directly that the idempotents e_{xy} and $e(a,x,y,j)$ are equivalent. Let

(178)

Then we have

$$e_{xy} = g(a,x,y,j)\cdot h(a,x,y,j) \tag{179}$$

and

$$e(a,x,y,j) = h(a,x,y,j)\cdot g(a,x,y,j). \tag{180}$$

The idempotents above can be used to show that $\mathbf{Tube}(\mathcal{C}) \cong \mathcal{C}\times\overline{\mathcal{C}}$. In the following subsection we will state and prove an analogous theorem for $\mathbf{Tube}(\mathcal{C}/\psi)$.

[13] This is a well-known and easy-to-prove folk result which says that arbitrary string nets are equivalent to linear combinations of labeled spines. We don't know a reference for this result.

5.3 Double of the fermionic quotient

In this subsection we prove that $\mathbf{Tube}(\mathcal{C}/\psi) \cong \mathcal{C} \times \overline{\mathcal{C}/\psi}$ as tensor categories when ψ is a fermion satisfying conditions of 4.1.1 and $\mathcal{C}$ is a modular tensor category.

To gain insights on the relation between $\mathbf{Tube}(\mathcal{C}/\psi)$ and $\mathcal{C}$, we will first construct the minimal idempotents of the condensed theory, which are useful objects in their own right. To facilitate this construction, we note that any string net configuration in the parent theory $\mathcal{C}$ descends to a string net configuration in the condensed theory $\mathcal{C}/\psi$. Conversely, we can always take an even morphism in $\mathcal{C}/\psi$ and lift it to $\mathcal{C}$, giving us a way of lifting tubes in $\mathbf{Tube}(\mathcal{C}/\psi)$ to those in $\mathbf{Tube}(\mathcal{C})$. These two facts allow us to find the minimal idempotents of the quotient theory using knowledge of the minimal idempotents of the parent theory. The details of the condensation functor $\mathbf{Tube}(\mathcal{C}) \to \mathbf{Tube}(\mathcal{C}/\psi)$ are important: for example, the image of some of the idempotents may simply be zero, while the images of nonisomorphic idempotents of $\mathbf{Tube}(\mathcal{C})$ may map to the same isomorphism class in $\mathbf{Tube}(\mathcal{C}/\psi)$. These details, as well as minimality and completeness of the idempotents, will have to be addressed carefully. Once this is done, we arrive at the following theorem:

Theorem 5.3.1. *Let $\mathcal{C}$ be a modular tensor category and let ψ be a fermion in $\mathcal{C}$ as in 4.1.1. Let $\mathcal{C}/\psi$ be the super pivotal category resulting from the fermionic quotient. Let $\boldsymbol{Tube}(\mathcal{C}/\psi) = \boldsymbol{Tube}^B(\mathcal{C}/\psi) \cup \boldsymbol{Tube}^N(\mathcal{C}/\psi)$ be the annular category of $\mathcal{C}/\psi$. Then as tensor categories,*

$$\boldsymbol{Tube}(\mathcal{C}/\psi) \cong \mathcal{C} \times \overline{\mathcal{C}/\psi}. \tag{181}$$

In particular, $sob_r(\boldsymbol{Tube}(\mathcal{C}/\psi)) \cong sob_r(\mathcal{C}) \times sob_r(\overline{\mathcal{C}/\psi})$. Let $a \in sob_r(\mathcal{C}/\psi)$ and $\tilde{a} \in sob_r(\mathcal{C})$ be a lift of a. If $\tilde{a}$ is transparent with respect to ψ, then (x, a) is in the bounding sector $\boldsymbol{Tube}^B(\mathcal{C}/\psi)$ of $\boldsymbol{Tube}(\mathcal{C}/\psi)$ (for any $x \in sob_r(\mathcal{C})$). If $\tilde{a}$ is not transparent with respect to ψ, then (x, a) is in the non-bounding sector $\boldsymbol{Tube}^N(\mathcal{C}/\psi)$.

The above result can also be written in terms of the tube category of the parent theory $\mathbf{Tube}(\mathcal{C})$. We first write $\mathcal{C} \times \bar{\mathcal{C}}/\psi \cong (\mathcal{C}/\mathbb{1}) \times (\bar{\mathcal{C}}/\psi) \cong (\mathcal{C} \times \bar{\mathcal{C}})/(\mathbb{1} \times \psi)$. Using the isomorphism $\mathbf{Tube}(\mathcal{C}) \cong \mathcal{C} \times \bar{\mathcal{C}}$, we can embed $\psi \in \mathrm{sob}_r(\mathcal{C})$ into $\mathbf{Tube}(\mathcal{C})$ by $\psi \mapsto \tilde{\psi}$, where $\tilde{\psi} \cong \mathbb{1} \times \psi$. This means that as tensor categories,

$$\mathbf{Tube}(\mathcal{C}/\psi) \cong \mathbf{Tube}(\mathcal{C})/\tilde{\psi}, \tag{182}$$

showing that fermion condensation commutes with constructing the tube category.

We prove the theorem by defining a tensor functor $E : \mathcal{C} \times \overline{\mathcal{C}/\psi} \to \mathbf{Tube}(\mathcal{C}/\psi)$ and showing that it is an equivalence of tensor categories. It is given by

$$E: \quad \mathcal{C} \times \overline{\mathcal{C}/\psi} \longrightarrow \mathbf{Tube}(\mathcal{C}/\psi) \quad ,$$

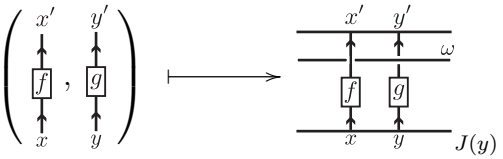

(183)

where $J(y) = B$ if $\nu_y = 0$ and $J(y) = N$ if $\nu_y = 1$, with ν_y the indicator defined in (95). This is clearly a functor; it preserves composition of morphisms in an obvious way. To show that E is a tensor isomorphism we need to show two things:

1. if $\{e_i\}$ and $\{f_j\}$ are a complete set of minimal idempotents for $\mathcal{C}$ and $\overline{\mathcal{C}/\psi}$ respectively, then $\{E(e_i, f_j)\}$ is a complete set of minimal idempotents for $\mathbf{Tube}(\mathcal{C}/\psi)$,

2. E is a tensor functor.

We first establish that $\{E(e_i, f_j)\}$ are a complete set of minimal idempotents for $\mathbf{Tube}(\mathcal{C}/\psi)$. This is done in three parts, first we show completeness, then that the idempotents are non-zero, and finally that they are minimal and orthogonal.

A complete basis of morphisms for $\mathbf{Tube}(\mathcal{C}/\psi)$ is given by

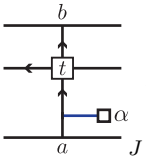

, (184)

with t an even morphism of $\mathbf{Tube}(\mathcal{C}/\psi)$ and $\alpha = \mathbb{1}$ or ψ denotes whether the morphism of $\mathbf{Tube}(\mathcal{C}/\psi)$ has even fermion parity or odd fermion parity. An even parity tube ($\alpha = \mathbb{1}$) has $t \in \bigoplus_x V_a^{xbx^*}$ while an odd parity tube ($\alpha = \psi$) has $t \in \bigoplus_x V_{a\otimes\psi}^{xbx^*}$. Since t is an even morphism in $\mathbf{Tube}(\mathcal{C}/\psi)$, we can (trivially) lift it to $\mathbf{Tube}(\mathcal{C})$, use the completeness relation in (164), and then (trivially) include the morphism back into $\mathbf{Tube}(\mathcal{C}/\psi)$. Hence we have

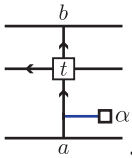

$= \frac{1}{\mathcal{D}^2} \sum_{\substack{x,y\in \mathrm{sob}_r(\mathcal{C}) \\ \nu\in V_{xy}^b \\ \mu\in V_{a\otimes\alpha}^{xy}}} C_{t;xy\mu\nu} \times$
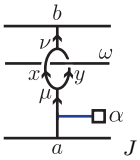

. (185)

for some coefficients $C_{t;xy\mu\nu}$. The morphism on the right hand side of the equation is isomorphic to $E(x, y)$. Making use of the fact that $E(x, y) \cong E(x, y \otimes \psi)$,[14] allows us to replace the sum over $y \in \mathrm{sob}_r(\mathcal{C})$ by a sum over $y \in \mathrm{sob}_r(\mathcal{C}/\psi)$. Therefore, any morphism $t \in \mathbf{Tube}(\mathcal{C}/\psi)$ can be written as

$$t = \sum_k x_k \cdot E(e_{i_k}, f_{j_k}) \cdot y_k, \tag{186}$$

and hence the $\{E(e_i, f_j)\}$ are complete.

We now establish that the the set of idempotents $\{E(e_i, f_j)\}$ are non-zero. We do this using the trace defined Section 4.2.1. We have

$$\mathrm{tr}\,(E(x,y)) = \mathrm{tr}\left(\quad\right) \tag{187}$$
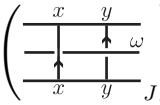

$$= \frac{1}{\mathcal{D}^2} \sum_{r\in\mathcal{C}} d_r\ \mathrm{tr}\left(\quad\right) \tag{188}$$
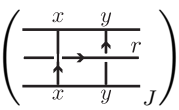

$$= \frac{1}{\mathcal{D}^2}(1 + s(J)(-1)^{\nu_y})d_x d_y. \tag{189}$$

[14] Note that $E(x, y)$ is not isomorphic to $E(x \otimes \psi, y)$, see (211) for more details.

The second line follows from linearity of the trace and the last line from,

$$\text{tr}\left(\quad\right) = \text{tr}_J\left\{\quad : A\left(\quad\right) \to A\left(\quad\right)\right\} \tag{190}$$

$$= (\delta_{r\mathbb{1}} + s(J)(-1)^{\nu_y}\delta_{r\psi})d_x d_y. \tag{191}$$

We have used that when $\text{cl}(\psi)$ is pushed past y the trace picks up the phase $(-1)^{\nu_y}$; see section 4.2.1 for more details on the trace. Hence $\text{tr}\,(E(e_i, f_j))$ is non-zero so long as $s(J) = (-1)^{\nu_{f_j}}$, which is true by definition of the E idempotents (recall (183)).

Now we show that the $\{E(e_i, f_j)\}$ are minimal and orthogonal. We do this by computing the dimension of $E(x, y) \cdot \mathbf{Tube}(\mathcal{C}/\psi) \cdot E(x', y')$. By the spine lemma, a generic element of $E(x, y) \cdot \mathbf{Tube}(\mathcal{C}/\psi) \cdot E(x', y')$ can be written as the LHS of

$$=\quad, \tag{192}$$

with $\delta \in V_{xc}^{x'}$, $\rho \in V_{cy}^{y'\otimes\alpha}$, $\sigma \in V_r^{c'c}$, $\kappa \in V_p^{pr}$. We have suppressed the spin structure index (the spin structure is determined by y; recall (183)). All vector spaces appearing are written in terms of the parent theory, $\mathcal{C}$, and α is either $\mathbb{1}$ or ψ denoting whether the tube is even or odd in $\mathbf{Tube}^J(\mathcal{C}/\psi)$.

The LHS is equal to the RHS by sliding the p strand over the lower ω loop then sliding the lower ω loop over the upper ω loop. On the RHS, the no tadpole axiom guaranties that $r \cong \mathbb{1}$ and consequently that $c^* \cong c'$. The remaining loop labeled p can be removed at the expense of multiplying by its quantum dimension d_p. Using property (a) of 5.1.1 we see that $c \cong \mathbb{1} \cong c'$. Using the orthogonality of the idempotents in the parent theory, we have

$$E(x, y) \cdot \mathbf{Tube}(\mathcal{C}/\psi) \cdot E(x', y') \cong \begin{cases} \mathbb{C}^{1|0} & \text{if } x \cong x' \text{ and } y \cong y' \text{ and } y \ncong y' \otimes \psi \\ \mathbb{C}^{0|1} & \text{if } x \cong x' \text{ and } y \cong \psi \otimes y' \text{ and } y \ncong y' \\ \mathbb{C}^{1|1} & \text{if } x \cong x' \text{ and } y \cong y' \text{ and } y \cong y \otimes \psi \\ 0 & \text{otherwise} \end{cases} \tag{193}$$

Taking $x' = x$ and $y' = y$, it follow that $E(x, y)$ is a minimal m-type idempotent if $y \ncong y \otimes \psi$ and is a minimal q-type idempotent if $y \cong y \otimes \psi$. This also confirms that $E(x, y)$ and $E(x, y \otimes \psi)$ are oddly isomorphic. The orthogonality of the idempotents follows from the fourth line of (193). This completes the proof that $\{E(e_i, f_j)\}$ is a complete set of minimal idempotents.

The tensor structure on $\mathbf{Tube}(\mathcal{C}/\psi)$ is initially defined on $\text{Rep}(\mathbf{Tube}(\mathcal{C}/\psi))$ and then transferred to $\mathbf{Tube}(\mathcal{C}/\psi)$ using semisimplicity ($\mathbf{Tube}(\mathcal{C}) \cong \text{Rep}(\mathbf{Tube}(\mathcal{C}))$ in the semisimple case). Consequently, we only need to show that E induces a tensor functor from $\text{Rep}(\mathcal{C} \times \overline{\mathcal{C}/\psi})$ to $\text{Rep}(\mathbf{Tube}(\mathcal{C}/\psi))$. To establish this, we show that

$$V_{E(c,z)}^{E(a,x),E(b,y)} \cong V_c^{ab}(\mathcal{C}) \otimes V_z^{xy}(\mathcal{C}/\psi), \tag{194}$$

where $V(\mathcal{C})$ denotes the fusion space for $\mathcal{C}$ and $V(\mathcal{C}/\psi)$ denotes the fusion space for $\mathcal{C}/\psi$. This isomorphism is established by the following figure:

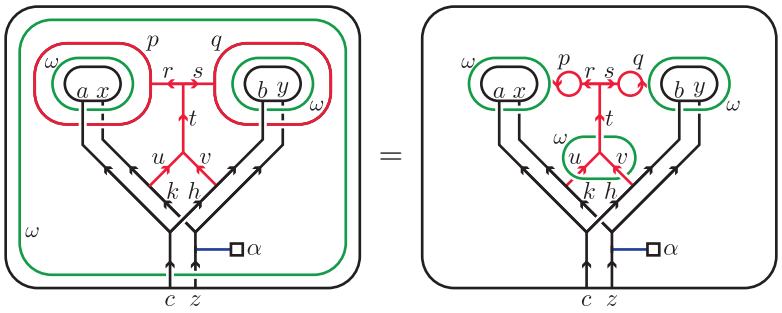

(195)

with $\alpha = \mathbb{1}$ for the even fusion space and $\alpha = \psi$ for the odd fusion space. By the spine lemma, the internal lines (red), labeled $k, h, r, s, t, u, v, p, q$ (multiplicity indices suppressed) span the entire space of net configurations for $V(P)$ with marked points, (a, x), (b, y), and (c, z) living at the boundary circles (as before, P is the pair of pants). Near each boundary circle we have applied the corresponding minimal idempotent to each boundary condition. Using the arguments similar to those following (192) we can simplify the diagram using the ω loop (green) relations of Table 5.1.1 to find the diagram on the right. One finds that $r \cong s \cong t \cong u \cong v \cong \mathbb{1}$, $k \cong x$, $h \cong b$, and the left over p and q loops can be removed by multiplying the picture with their quantum dimensions. The span of the resulting simplified pictures is isomorphic to $V_c^{ab}(\mathcal{C}) \otimes V_z^{xy}(\mathcal{C}/\psi)$. Using semisimplicity, this implies that E is a tensor functor.

5.4 Modular transformations

The explicit representation of the minimal idempotents allows us to compute the modular transformations for the condensed theory.

We first examine the S transformation on bounding spin tori (i.e. the three spin tori that have at least one bounding cycle). The S transformation acts to interchange the longitudinal and meridional cycles of the torus, and so it acts as

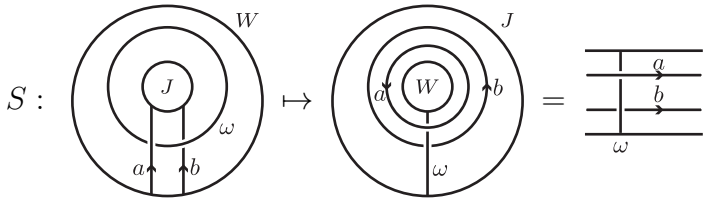

(196)

In the first two pictures we have drawn the torus as an annulus with inner and outer boundaries identified, while in the last picture we have re-written the torus on the plane as a square with the top and bottom as well as left and right edges identified. Additionally, recall that from the way we constructed the idempotents, if the spin structure along the azimuthal direction is bounding, then b must be transparent with respect to ψ, and if the azimuthal spin structure is non-bounding, then b must be non-transparent with respect to ψ. Since we are working with bounding spin tori, and since we always transform to the standard basis of idempotents, the spin structure can be inferred from context, and so we will suppress the labels in some of the diagrams.

We now need to perform a series of manipulations that returns the right hand side of (196) to a linear combination of pictures that are written in the standard basis (the same

as the left hand side of (196) with the spin structures interchanged). We first investigate the part of the diagram with the a string and the ω loop:

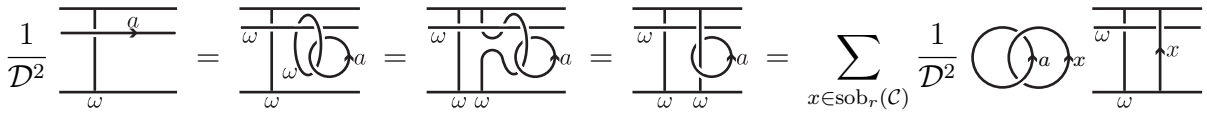

(197)

We can now do the same for the b loop,

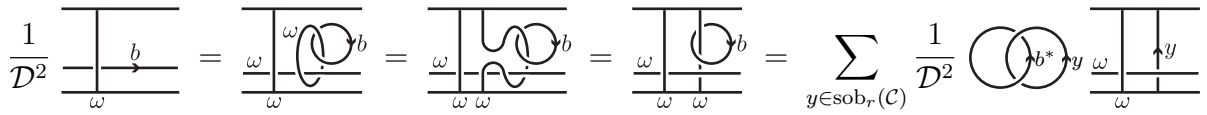

(198)

where we have used that the ω loop is a projector onto the vacuum. In the last summation we need to replace $\sum_{y\in \mathrm{sob}_r(\mathcal{C})}$ with $\sum_{y\in \mathrm{sob}_r(\mathcal{C}/\psi)}$:

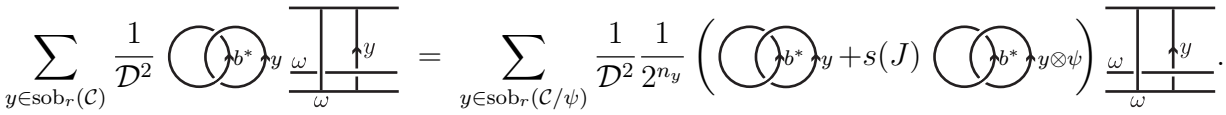

(199)

The factor of $s(J)$ appeared due to $\mathrm{cl}_J(\psi\otimes y) = s(J)\mathrm{cl}_J(y)$, where the subscript J means we close up y around a cycle with spin structure J. The normalization factor $2^{-n_y} = 1/\dim \mathrm{End}(y)$ is inserted so that we don't overcount the q-type simple objects from $\mathrm{sob}_r(\mathcal{C})$ (recall for example, (128)). Using that $S_{b^*(y\otimes\psi)} = (-1)^{\nu_b} S_{b^* y}$, and that $(-1)^{\nu_b} s(J) = 1$ by assumption, the right hand side of (199) can be simplified so that (198) becomes

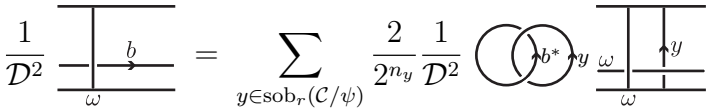

(200)

Putting all calculations together, and removing leftover ω loops (which provide an additional factor of $\mathcal{D}^{-2}$) we find that the matrix elements of the (un-normalized) S-matrix can be written as

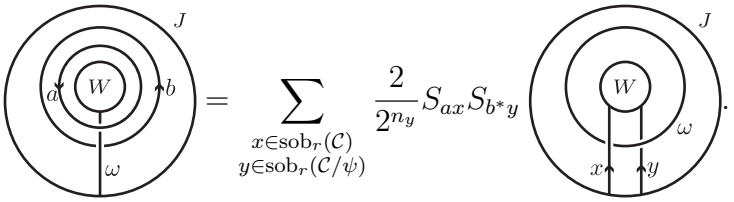

(201)

In the above formula, the S_{ax} and S_{b^*y} are matrix elements of the S-matrix in the original input theory $\mathcal{C}$ (which we assumed to be an MTC). Note that ν_b must be 0 if J is bounding, 1 if J is non-bounding, and similarly for ν_y. The simple object y appearing in S_{b^*y} on the right hand side of (201) is a trivial lift of the y written in the closed up idempotent (recall that the first is a simple object of $\mathcal{C}$, while the latter is a simple object of $\mathcal{C}/\psi$). One can change the representative of the isomorphism class of $y\in\mathcal{C}/\psi$ with an odd isomorphism $\mathrm{mor}(y\to\psi\otimes y)$. Under this odd isomorphism the right hand side of (201) picks up a factor of $s(J)(-1)^{\nu_b}$ which is equal to 1 since $s(J(b)) = (-1)^{\nu_b}$.

In order for the S-matrix to be unitary, we need to normalize each q-type idempotent properly. In the discussion following (193) we pointed out that $E(a,b)$ is q-type if b is q-type. Hence we can normalize our idempotents by re-scaling the q-type idempotents by a factor of $1/\sqrt{2}$. This results in the "pseudo idempotents"

$$\widehat{E}(a,b) = E(a,b)/(\sqrt{2})^{n_b}, \tag{202}$$

which have unit norm. The resulting unitary S-matrix is given by

$$\mathrm{cl}_W(\widehat{E}(a,b)) \xrightarrow{S^{JW\to WJ}} \sum_{\substack{x\in \mathrm{sob}_r(\mathcal{C})\\ y\in \mathrm{sob}_r(\mathcal{C}/\psi)}} \frac{2}{(\sqrt{2})^{n_b+n_y}} S_{ax} S_{b^* y} \mathrm{cl}_J(\widehat{E}(x,y)) \tag{203}$$

Note that $\mathrm{cl}_J(\widehat{E}(x,y))$ on the right hand side of (203) is zero unless y is compatible with the spin structure inherited from the left hand side of (203); explicitly y must satisfy $s(W) = (-1)^{\nu_y}$.

The matrix elements of the S-matrix on the torus with non-bounding spin structure (periodic boundary conditions around both cycles) can be calculated in an analogous way. The first half of the calculation remains the same as in (197). The second half of the calculation changes only if b is q-type, in which case the idempotent $E(a,b)$ is q-type, and has to be closed up on the torus with an odd endomorphism. As discussed in the caption of Figure 3.3.3, closing an idempotent with an odd endomorphism always results in a sign ambiguity for the closed up idempotent. In such a case we have:[15]

$$\frac{1}{\mathcal{D}^2}$$ 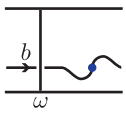 $$= \frac{1}{\mathcal{D}} \sum_{y\in Q} [S^{\psi}]_{yb}$$ 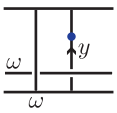 (204)

This completes our calculation of the S-matrix of the condensed theory in terms of the modular data of the input theory.

The T-matrix is found by twisting one boundary of an idempotent by 2π before closing it up. For the annulus, the twisting is implemented by performing a 2π counterclockwise rotation of the inner S^1 with respect to the outer S^1. The matrix elements are given by

$$\mathrm{cl}_W(\widehat{E}(a,b)) \xrightarrow{T^{JW\to J\widetilde{W}}} \theta_a \theta_b^* \mathrm{cl}_{\widetilde{W}}(\widehat{E}(a,b)) \tag{205}$$

where again $J = J(b)$, and where $\widetilde{W}$ can be read off from Figure 3.3.4. The phases θ_a and θ_b are the twists of the lifts of a and b to the parent theory. For example, in the C_2 theory one verifies that $\theta_{m_{\mathbb{1}}} = \theta_{\mathbb{1}}\theta_{\mathbb{1}}^*, \theta_{m_\sigma^+} = \theta_\sigma \theta_{\mathbb{1}}^*, \theta_{q_{\mathbb{1}}} = \theta_{\mathbb{1}}\theta_\sigma^*, \theta_{q_\sigma} = \theta_\sigma\theta_\sigma^*$ and $\theta_\psi = \theta_\psi \theta_\sigma^*$, where $\theta_\sigma = -A^3$.

Note that if $J = B$ then replacing b with $b\otimes\psi$ changes the sign of the twist. Since we can choose either b or $b\otimes\psi$ for the lift, this gives a sign ambiguity in the twist (for the C_2 theory, this is manifested by $\theta_{m_\sigma^+} = \theta_\sigma\theta_{\mathbb{1}}^*, \theta_{m_\sigma^-} = \theta_\sigma\theta_\psi^* = -\theta_{m_\sigma^+}$). This sign ambiguity is expected, since only T^2 has well-defined eigenvalues on idempotents (see the discussion near the beginning of Section 3.3.2).

[15] We have used $(S^z)_{xy} = \frac{1}{\mathcal{D}}$ 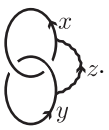 .

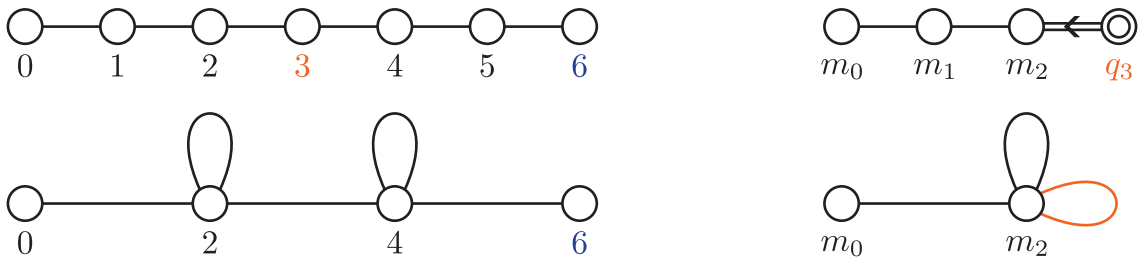

Figure 6.1.1: The upper left diagram is the principle graph of $SU(2)_6$, and the lower left diagram is the principle graph for $SO(3)_6$. On the right we give the principle graphs of the condensed theories $SU(2)_6/\psi$ (top right) and $SO(3)_6/\psi$ (bottom right), both with the identification $\psi = 6$. The naming convention of the condensed theories has been inherited from the parent theories, along with an m or q denoting whether the particle is m-type or q-type. Black links denote even fusion channels, and the red link connecting m_2 to itself denotes an odd fusion channel in accordance with the rule $m_2 \otimes m_2 \cong m_0 \oplus \mathbb{C}^{1|1} m_2$.

6 Fermion condensation in $SO(3)_6$

Here we provide more examples of fermion condensation in two theories which are closely related to each other: $SU(2)_6$ and $SO(3)_6$. Each theory contains a fermion ψ, which we will condense. The main difference between these two theories is that in $SO(3)_6$ the fermion ψ is transparent (i.e. it braids trivially with every other particle in the theory), while in $SU(2)_6$ it is not. This means that when condensing ψ in $SO(3)_6$, we do not need to use the "back wall" construction employed earlier, and the quotient theory will be braided. However, the transparency of ψ also means that the S-matrix in the $SO(3)_6$ theory is degenerate, and hence the theory is not modular. In this case the lack of modularity is fairly benign, $SO(3)_6$ is a subcategory of the modular tensor category $SU(2)_6$. This will allow us to infer the minimal idempotents of $SO(3)_6/\psi$ from the minimal idempotents of $SU(2)_6/\psi$. From the minimal idempotents one can also compute the mapping class group action, which we will work out for the $SO(3)_6/\psi$ example. First we will establish some notation for UBFC's with fermions.

6.1 Fusion theory of $SU(2)_6/\psi$ and $SO(3)_6/\psi$

We will now briefly review $SU(2)_6$ and its connection with $SO(3)_6$. Since these are well known theories we only list out some of their key properties and point the reader to some references for more details: see e.g. [38] and [39]. There are seven objects in $SU(2)_6$, labeled by $0, 1, 2, \cdots, 6$. The principle graph for the theory is shown in the upper left of Fig. 6.1.1. The 0 particle is the trivial object, 6 is a fermion, and we have $6 \otimes x = (6 - x)$. Hence the particle 3 is invariant under fusion with 6, and so under condensation of the 6 particle 3 becomes a q-type simple object in $SU(2)_6/\psi$. Since one m-type particle is always related to another by fusion with ψ and there are six m-type particles, there are only three distinct equivalence classes of m-type particles under fusion with ψ. We can take $\{0, 1, 2\}$ as the complete list of representatives.

We give the principle graph for $SU(2)_6/\psi$ in Fig. 6.1.1 in the upper right, where q_3 is the q-type image of 3 under condensation. The particles $0, 2, 4$, and 6 form a closed sub-category of $SU(2)_6$. The principle graph of this theory is shown in the bottom left of Fig. 6.1.1. This is the subcategory known as $SO(3)_6$, it is a braided theory, with braiding and fusion inherited from $SU(2)_6$, however, it is not modular. The 6 particle

$I_0 \otimes I_0$	m_0	m_2
m_0	m_0	m_2
m_2	m_2	$m_0 \oplus \mathbb{C}^{1\|1} m_2$

$I_0 \otimes I_1$	m_1	q_3
m_0	m_1	q_3
m_2	$m_1 \oplus q_3$	$\mathbb{C}^{1\|1} m_1 \oplus q_3$

$I_1 \otimes I_0$	m_0	m_2
m_1	m_1	$m_1 \oplus q_3$
q_3	q_3	$\mathbb{C}^{1\|1} m_1 \oplus q_3$

$I_1 \otimes I_1$	m_1	q_3
m_1	$m_0 \oplus m_2$	$\mathbb{C}^{1\|1} m_2$
q_3	$\mathbb{C}^{1\|1} m_2$	$\mathbb{C}^{1\|1} m_0 \oplus \mathbb{C}^{1\|1} m_2$

(207)

Table 6.1.1: Fusion rules for $SU(2)_6/\psi$

braids trivially within this subcategory, and is therefore transparent, which breaks the modularity.

We now perform fermion condensation in $SU(2)_6$ and $SO(3)_6$ to obtain two super pivotal categories $SU(2)_6/\psi$ and $SO(3)_6/\psi$. Since ψ is not transparent in $SU(2)_6$, we must perform the back-wall condensation process described earlier. However, since ψ *is* transparent in $SO(3)_6$, condensation of ψ is possible without employing a back-wall (although a spin structure is still needed). The principle graphs of the condensed theories are shown on the right of Fig. 6.1.1. The simple objects of the two theories are given as follows:

$$\begin{aligned} SU(2)_6/\psi: &\quad m_0 \quad m_1 \quad m_2 \quad q_3 \\ SO(3)_6/\psi: &\quad m_0 \qquad m_2 \end{aligned} \tag{206}$$

The particles have a natural grading given by (95) with the even set given by $I_0 = \{m_0, m_2\}$ and the odd set given by $I_1 = \{m_1, q_3\}$, with $I_a \otimes I_b = I_{a+b \bmod 2}$. The closed sub-fusion algebra given by I_0 contains all of the objects in $SO(3)_6/\psi$, which occurs since ψ is transparent in $SO(3)_6$. Note that there are no q-type objects in $SO(3)_6/\psi$.

The non-trivial fusion rules of $SU(2)_6/\psi$ are given in Table 6.1.1.

We note two features of these examples which were not present in our earlier C_2 example:

- Even though m_2 is an m-type particle, $\mathbb{C}^{1|1} m_2$ appears in the tensor product of m_2 with itself. So $SO(3)_6/\psi$ provides us with an example of a theory which has no q-type objects, but which is still fermionic in the sense that its fusion spaces contain both even and odd elements.

- The q-type particle q_3 appears in the tensor product of two m-type particles, namely $m_2 \otimes m_1$. Thus the classification of simple objects as m- or q-type should not be thought of as a $\mathbb{Z}/2$ grading, since the types of a and b in no way constrain the possible types of the simple objects appearing in $a \otimes b$. (In the next section we will also see an example of two q-type particles fusing to another q-type particle.)

The F-symbols of the condensed theories can be deduced from those of the parent theories, so we will not list them here. We now compute the minimal idempotents of the tube category in the condensed theories.

6.2 Primitive idempotents of $SU(2)_6/\psi$

The primitive idempotents of the tube category of $SU(2)_6/\psi$ can be computed directly using the techniques of Section 5. They are given by

$$E(a,b) = \quad , \qquad (a,b) \in \mathrm{sob}_r(SU(2)_6) \times \mathrm{sob}_r(SU(2)_6/\psi), \tag{208}$$

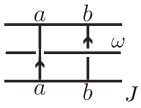

where as before we require that $s(J) = (-1)^{\nu_b}$. It will be useful to recast these idempotents in a form that can be easily used to compute the idempotents for $SO(3)_6$. We first define

$$\widetilde{E}(a,b,\mathrm{cl}(r)) \;=\; \tag{209}$$

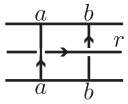

and for $x = \mathbb{1}$ or $x = \psi$ we define the ω_x loop

$$\omega_x = \frac{d_x}{\mathcal{D}^2_{\mathcal{C}/\psi}} \sum_{r \in \mathrm{sob}_r(\mathcal{C}/\psi)} \frac{d_r}{\dim \mathrm{End}(r)} \left(\frac{S_{xr}}{S_{\mathbb{1}r}}\right) \mathrm{cl}(r). \tag{210}$$

The S-matrix above is that of the parent theory, and the labels are trivial lifts from $\mathcal{C}/\psi$. When $x = \mathbb{1}$, $\frac{S_{xr}}{S_{\mathbb{1}r}} = 1$ this is just the standard ω loop, when $x = \psi$, $\frac{S_{xr}}{S_{\mathbb{1}r}} = (-1)^{\nu_r}$ and ω_ψ is a projector onto the ψ strand. The factor $\mathcal{D}^2_{\mathcal{C}/\psi} = \sum_{x \in \mathcal{C}/\psi} d_x^2 / \dim \mathrm{End}(x)$ is the total quantum dimension of the condensed theory in the sense of (120). The minimal idempotents given by $E(a,b)$ in (183) can be re-written as

$$E(a \otimes x, b) \cong \widetilde{E}(a,b,\omega_x), \tag{211}$$

with $a, b \in \mathcal{C}/\psi$ and $x = \mathbb{1}, \psi$. The isomorphism relating the two idempotents is an odd isomorphism if $x = \psi$. Notice that running over all all pairs $a, b \in \mathcal{C}/\psi$ and $x = \mathbb{1}$ or ψ runs over all possible $E(a,b)$. Additionally if $a \otimes \psi \cong a$ then $\widetilde{E}(a,b,\omega_\mathbb{1})$ and $\widetilde{E}(a,b,\omega_\psi)$ are equivalent. This presentation of the idempotents is more symmetric than those discussed in Section 5.

We now write these idempotents so that they have a single strand at the boundary rather than two. We use the fermionic analogue of (178) to write down the single strand idempotents

$$\tilde{e}_{ab}(\omega_x, c, j) \;=\; \tag{212}$$

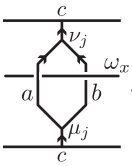

These idempotents are similar to the ones described earlier in (174). The particular representative of the isomorphism class is given by choosing $c \in a \otimes b$, and appropriately normalized vectors $\mu_j \in V_c^{ab}(\mathcal{C}/\psi)$, and $\nu_j \in V_{ab}^c(\mathcal{C}/\psi)$. We will denote the parity of $\mu_j \in V_c^{ab}(\mathcal{C}/\psi)$ by $\sigma_j = 1$ ($\sigma_j = -1$) if the chosen basis vector μ_j in the fusion space $V_c^{ab}(\mathcal{C}/\psi)$ is even (odd). The twists of the idempotents are given by

$$T \cdot \tilde{e}(a,b,\omega_x,c,j) = \begin{cases} \frac{\theta_a}{\theta_b}(-1)^{x(\nu_a+\nu_b)}\sigma_j \; \tilde{e}(a,b,\omega_x,c,j) & \text{if bounding} \\ \frac{\theta_a}{\theta_b}(-1)^{x(\nu_a+\nu_b)} \; \tilde{e}(a,b,\omega_x,c,j) & \text{if non-bounding} \end{cases} \tag{213}$$

type	twist
$m_{00}(\omega_0, c, j)$	1
$m_{10}(\omega_0, c, j)$	$e^{3i\pi/16}$
$m_{20}(\omega_0, c, j)$	i

type	twist
$m_{00}(\omega_\psi, c, j)$	1
$m_{10}(\omega_\psi, c, j)$	$-e^{3i\pi/16}$
$m_{20}(\omega_\psi, c, j)$	i

type	twist $\times \sigma_j$
$m_{30}(\omega_0, c, j)$	$e^{15i\pi/16}$
$m_{32}(\omega_0, c, j)$	$-ie^{15i\pi/16}$

type	twist $\times \sigma_j$
$m_{02}(\omega_0, c, j)$	$-i$
$m_{12}(\omega_0, c, j)$	$-ie^{3i\pi/16}$
$m_{22}(\omega_0, c, j)$	1

type	twist $\times \sigma_j$
$m_{02}(\omega_\psi, c, j)$	$-i$
$m_{12}(\omega_\psi, c, j)$	$ie^{3i\pi/16}$
$m_{22}(\omega_\psi, c, j)$	1

Table 6.2.1: Bounding idempotents for $SU(2)_6/\psi$. Where $c \in a \otimes b$ and j labels the choice of in the fusion space $V_c^{ab}(\mathcal{C}/\psi)$. Some of these labels are determined, e.g., $m_{00}(\omega_0, c, j)$ can be simplified to $m_{00}(\omega_0, m_0, 0)$. The pre-factor σ_j is ± 1 denoting the parity of $\mu_j \in V_c^{ab}$.

We will write $\tilde{e}(a, b, \omega_x, c, j)$ as $m_{ab}(\omega_x, c, j)$ if the idempotent is m-type and $q_{ab}(\omega_x, c, j)$ if the idempotent is q-type. For $SU(2)_6/\psi$ we list a complete set of representatives of minimal idempotents. We find 14 m-type idempotents for the bounding spin structure, and 14 idempotents for the non-bounding spin structure, 7 are m-type and 7 are q-type. Explicitly, the idempotents and corresponding twists are listed in tables 6.2.1 and 6.2.2. Note that if a is q-type, then $\tilde{e}(a, b, \omega_\mathbb{1}, j)$ is isomorphic to $\tilde{e}(a, b, \omega_\psi, j)$ and so we only list one of them. We now turn our attention to the $SO(3)_6$ theory.

6.3 Primitive idempotents of $SO(3)_6/\psi$

Finding the idempotents in the $SO(3)_6/\psi$ theory is more difficult, since the parent theory $SO(3)_6$ isn't modular. However since $SO(3)_6$ is obtained from $SU(2)_6$ by discarding the elements in $SU(2)_6$ that braid nontrivially with ψ, $SU(2)_6$ is a modular extension of $SO(3)_6$ (in fact, it is the minimal modular extension). This fact will allow us to compute the idempotents in the $SO(3)_6/\psi$ theory using our knowledge of the $SU(2)_6$ theory.

Applying (212) directly to $SO(3)_6$ will not yield a complete set of minimal idempotents due to the lack of modularity. Instead we use (212) by taking pairs of simple objects (a, b) from $SU(2)_6/\psi \times SU(2)_6/\psi$ whose tensor product is in $SO(3)_6/\psi$. Additionally, within this subset we need to take an appropriate linear combination of the $SU(2)_6/\psi$ idempotents so that the resulting annulus only has strands labeled by objects in $SO(3)_6/\psi$. This linear combination is given by taking $\tilde{e}_{ab}(\omega_\mathbb{1}, c, j) + \tilde{e}_{ab}(\omega_\psi, c, j)$ which results in the minimal idempotent

$$\widetilde{e}_{ab}(\omega_\mathbb{1} + \omega_\psi, c, j) \in \mathbf{Tube}(SO(3))_6). \tag{214}$$

type	twist
$m_{01}(\omega_0, c, j)$	$-e^{-3i\pi/16}$
$m_{11}(\omega_0, c, j)$	1
$m_{21}(\omega_0, c, j)$	$-ie^{-3i\pi/16}$

type	twist
$m_{01}(\omega_\psi, c, j)$	$-e^{-3i\pi/16}$
$m_{11}(\omega_\psi, c, j)$	1
$m_{21}(\omega_\psi, c, j)$	$-ie^{-3i\pi/16}$

type	twist
$m_{31}(\omega_0, c, j)$	$e^{3i\pi/4}$
$q_{33}(\omega_0, c, j)$	1

type	twist
$q_{03}(\omega_0, c, j)$	$-e^{-15i\pi/16}$
$q_{13}(\omega_0, c, j)$	$e^{-3i\pi/4}$
$q_{23}(\omega_0, c, j)$	$-ie^{-15i\pi/16}$

type	twist
$q_{03}(\omega_\psi, c, j)$	$-e^{-15i\pi/16}$
$q_{13}(\omega_\psi, c, j)$	$e^{-3i\pi/4}$
$q_{23}(\omega_\psi, c, j)$	$-ie^{-15i\pi/16}$

Table 6.2.2: Non-Bounding idempotents for $SU(2)_6/\psi$

where the labels $(a, b) \in I_0/\psi \times I_0/\psi \cup I_1/\psi \times I_1/\psi$.[16] One can show that the procedure creates a complete set of minimal idempotents by direct calculation. The bounding idempotents are found when $(a, b) \in I_0/\psi \times I_0/\psi$, these are the minimal idempotents found from a naive application of (212). The non-bounding idempotents are given by $(a, b) \in I_1/\psi \times I_1/\psi$

We now write down the minimal idempotents of $SO(3)_6/\psi$ and their twists using the same notation as in Section 6.2. In the bounding sector $J = B$, we have 4 m-type idempotents, given by

type	twist
$m_{00}(\omega_{\mathbb{1}} + \omega_\psi, 0, 0)$	1
$m_{02}(\omega_{\mathbb{1}} + \omega_\psi, 2, 0)$	$-i$
$m_{20}(\omega_{\mathbb{1}} + \omega_\psi, 2, 0)$	i
$m_{22}(\omega_{\mathbb{1}} + \omega_\psi, c, j)$	σ_j

(215)

with $c \in m_2 \otimes m_2$ and j labeling a vector in the fusion space $V_c^{m_2 m_2}(\mathcal{C}/\psi)$. Meanwhile the non-bounding idempotents are given by

type	twist
$m_{11}(\omega_{\mathbb{1}} + \omega_\psi, c, j)$	1
$q_{13}(\omega_{\mathbb{1}} + \omega_\psi, 2, j)$	$e^{-3i\pi/4}$
$q_{31}(\omega_{\mathbb{1}} + \omega_\psi, 2, j)$	$e^{3i\pi/4}$
$m_{33}(\omega_{\mathbb{1}} + \omega_\psi, c, j)$	1

(216)

[16] Note that a minimal idempotent of **Tube**$(SO(3)_6/\psi)$ has a trivial lift to an idempotent of **Tube**$(SU(2)_6/\psi)$ but does not remain minimal.

Similarly, $c \in m_1 \otimes m_1$ and j labels a vector in $V_c^{m_1 m_1}$ for m_{11}, and $c \in q_3 \otimes q_3$ and j labels a vector in $V_c^{q_3 q_3}(\mathcal{C}/\psi)$ for m_{33}. Here we've made use of the above observation that only $a \otimes b$ need be in $SO(3)_6/\psi$, and hence the pairs (a, b) in these idempotents are labeled by m_1 and q_3. As the notation suggests m_{33} is not q-type: to see this we note that if it were, then there would be an odd endomorphism of $\mathbf{Tube}(SO(3)_6/\psi)$ with trivial boundary conditions (since $m_0 \in q_3 \otimes q_3$). That would require $SO(3)_6/\psi$ to contain a q-type simple object, but as explained in (88) this is not possible since ψ is transparent in $SO(3)_6$. One can explicitly construct an odd endomorphism for q_{13} by putting a fermion on q_3 and fusing all strands into the annulus; similarly for q_{31}.

6.4 Modular transformations

The modular transformations can be computed directly by manipulating string diagrams. We already have the twists (which are read off from the string-net labels of the idempotents), and the modular T-transformation can be obtained directly from the twists. The modular S-transformation requires a little more work, and so we discuss this in a little more detail.

We first close the minimal idempotents onto the torus. Using the basis above, one finds the image under cl_Y is given by

$$\tilde{e}_{ab}(\omega_{\mathbb{1}} + \omega_\psi, c, j) \xrightarrow{\mathrm{cl}_Y} \tilde{e}_{ab} \;=$$

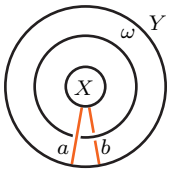

(217)

where a and b label the idempotent as before, X denotes the spin structure of the idempotent which is fixed by b, Y denotes the spin structure around the newly closed cycle, and $\omega = \omega_{\mathbb{1}} + \omega_\psi$. Note that when X is non-bounding, $a, b \in \{m_1, q_3\}$, which lies outside of $SO(3)_6/\psi$. However, $\tilde{e}_{ab} \in \mathrm{cl}_Y \mathbf{Tube}(SO(3)_6/\psi)$ since when the diagram is fused into the torus we find a torus string net labeled with objects only in $SO(3)_6/\psi$, as required.

In this graphical convention, the modular S-transformation acts as

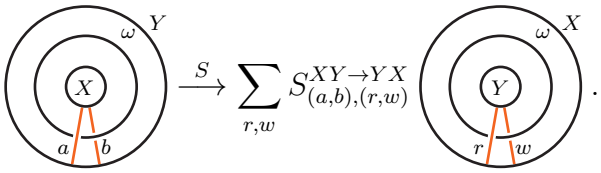

(218)

The matrix elements can be computed explicitly using the S-matrix of $SU(2)_6$. Explicitly, the S-matrix acts on each of the three bounding spin tori as

$$\begin{pmatrix} m_{00} \\ m_{02} \\ m_{20} \\ m_{22} \end{pmatrix}_{BB} \xrightarrow{S^{BB\to BB}} \frac{1}{2\sqrt{2}} \begin{pmatrix} \frac{1}{d} & 1 & 1 & d \\ 1 & -\frac{1}{d} & d & -1 \\ 1 & d & -\frac{1}{d} & -1 \\ d & -1 & -1 & \frac{1}{d} \end{pmatrix} \begin{pmatrix} m_{00} \\ m_{02} \\ m_{20} \\ m_{22} \end{pmatrix}_{BB} \tag{219}$$

$$\begin{pmatrix} m_{11} \\ q_{13} \\ q_{31} \\ m_{33} \end{pmatrix}_{NB} \xrightarrow{S^{NB\to BN}} \frac{1}{2} \begin{pmatrix} 1 & 1 & 1 & 1 \\ 1 & -1 & 1 & -1 \\ 1 & 1 & -1 & -1 \\ 1 & -1 & -1 & 1 \end{pmatrix} \begin{pmatrix} m_{00} \\ m_{02} \\ m_{20} \\ m_{22} \end{pmatrix}_{BN} \tag{220}$$

$$\begin{pmatrix} m_{00} \\ m_{02} \\ m_{20} \\ m_{22} \end{pmatrix}_{BN} \xrightarrow{S^{BN\to NB}} \frac{1}{2}\begin{pmatrix} 1 & 1 & 1 & 1 \\ 1 & -1 & 1 & -1 \\ 1 & 1 & -1 & -1 \\ 1 & -1 & -1 & 1 \end{pmatrix} \begin{pmatrix} m_{11} \\ q_{13} \\ q_{31} \\ m_{33} \end{pmatrix}_{NB} \tag{221}$$

As mentioned earlier, the Dehn twists follow directly from the twists computed above; see (213). Again for the bounding spin tori we find

$$\begin{pmatrix} m_{00} \\ m_{02} \\ m_{20} \\ m_{22} \end{pmatrix}_{BB} \xrightarrow{T^{BB\to BN}} \begin{pmatrix} 1 & & & \\ & -i & & \\ & & i & \\ & & & 1 \end{pmatrix} \begin{pmatrix} m_{00} \\ m_{02} \\ m_{20} \\ m_{22} \end{pmatrix}_{BN} \tag{222}$$

$$\begin{pmatrix} m_{11} \\ q_{13} \\ q_{31} \\ m_{33} \end{pmatrix}_{NB} \xrightarrow{T^{NB\to NB}} \begin{pmatrix} 1 & & & \\ & e^{-3i\pi/4} & & \\ & & e^{3i\pi/4} & \\ & & & 1 \end{pmatrix} \begin{pmatrix} m_{11} \\ q_{13} \\ q_{31} \\ m_{33} \end{pmatrix}_{NB} \tag{223}$$

$$\begin{pmatrix} m_{00} \\ m_{02} \\ m_{20} \\ m_{22} \end{pmatrix}_{BN} \xrightarrow{T^{BN\to BB}} \begin{pmatrix} 1 & & & \\ & -i & & \\ & & i & \\ & & & 1 \end{pmatrix} \begin{pmatrix} m_{11} \\ q_{13} \\ q_{31} \\ m_{33} \end{pmatrix}_{BB} \tag{224}$$

One can verify that $(TS)^3 = \mathrm{id}$, which holds since all three of the spin tori discussed above have even fermion parity (recall that the more general identity is $(ST)^3 = (-1)^F$).

The modular S transformations on the torus with NN spin structure are a little more tedious to calculate. A complete basis of net configurations on the NN spin torus is given by

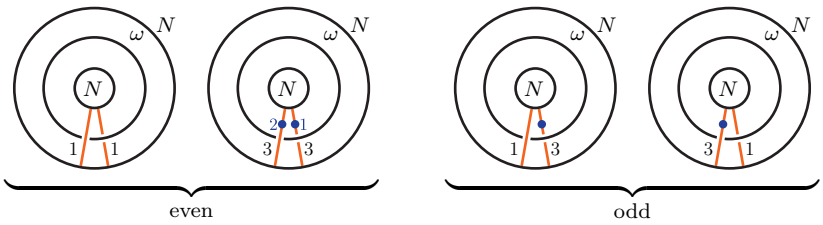

(225)

On the non-bounding torus, m-type idempotents always close up into even parity states, while q-type idempotents close up into odd parity states. The first two vectors have even parity and provide a basis for $\mathrm{cl}_N(m_{11})$ and $\mathrm{cl}_N(m_{33})$, while the second two have odd parity and provide a basis for $\mathrm{cl}_N(q_{13})$ and $\mathrm{cl}_N(q_{31})$. After some calculation one finds that the S and T modular matrices act as

$$\begin{pmatrix} m_{11} \\ m_{33} \\ \bullet \\ q_{13} \\ \bullet \\ q_{31} \end{pmatrix}_{NN} \xrightarrow{S^{NN\to NN}} \begin{pmatrix} 1 & 0 & & \\ 0 & 1 & & \\ & & e^{-i\pi/4} & 0 \\ & & 0 & e^{i\pi/4} \end{pmatrix} \begin{pmatrix} m_{11} \\ m_{33} \\ \bullet \\ q_{13} \\ \bullet \\ q_{31} \end{pmatrix}_{NN} \tag{226}$$

and

$$\begin{pmatrix} m_{11} \\ m_{33} \\ \bullet \\ q_{13} \\ \bullet \\ q_{31} \end{pmatrix}_{NN} \xrightarrow{T^{NN\to NN}} \begin{pmatrix} 1 & 0 & & & \\ 0 & 1 & & & \\ & & e^{-3i\pi/4} & 0 & \\ & & 0 & e^{3i\pi/4} & \end{pmatrix} \begin{pmatrix} m_{11} \\ m_{33} \\ \bullet \\ q_{13} \\ \bullet \\ q_{31} \end{pmatrix}_{NN} \tag{227}$$

As required, the odd part of the S-matrix satisfies $S^4 = -\mathrm{id}$ and $(TS)^3 = -\mathrm{id}$, while the even part satisfies the usual $S^4 = \mathrm{id}$ and $(TS)^3 = \mathrm{id}$.

7 Fermion condensation in $\frac{1}{2}\mathrm{E}_6$

In this section we perform fermion condensation in the category $\frac{1}{2}\mathrm{E}_6$. This provides an example of a super pivotal category with fusion multiplicity. After condensation we will obtain a theory with one non-trivial q-type particle, which we will denote by ρ. ρ obeys the fusion rule

$$\rho \otimes \rho = \mathbb{C}^{1|1}\mathbb{1} \oplus \mathbb{C}^{1|1}\rho, \tag{228}$$

which is similar to the Fibonacci fusion rule but with q-type objects.[17] The nontrivial fusion spaces are $V_\rho^{\rho\rho} \cong \mathbb{C}^{2|2}$ and $V_\rho^{\rho\mathbb{1}} \cong \mathbb{C}^{1|1}$, with the first telling us that the theory has nontrivial fusion multiplicity.

This theory is richer than the examples we have considered previously, and serves as a good case study for the features that appear in phases described by more general super pivotal categories. These more general features include:

- There is a quasiparticle excitation which has a non-bounding spin structure but which is m-type (this also occurs in the $SO(3)_6/\psi$ theory discussed previously) and is oddly self dual.
- The ground state degeneracy on the three spin tori with a bounding cycle (with spin structures BB, BN, and NB) is $\mathbb{C}^{3|0}$, and the ground state degeneracy on the non-bounding torus (with NN spin structure) is $\mathbb{C}^{1|2}$. In particular, the fermion parity of a ground state on the torus is not uniquely determined by the torus' spin structure (this also occurs in the $SO(3)_6/\psi$ theory discussed previously).
- As a fusion category, there is a fusion rule that takes two q-type particles to another q-type particle.[18]

[17] A simpler generalization of the Fibonacci theory to the super pivotal case, with one non-trivial q-type particle and fusion space $V_\tau^{\tau\tau} \cong \mathbb{C}^{1|1}$, does not exist. Indeed, suppose $\mathrm{End}(\tau) = \mathbb{C}\ell_1$ and $V^{\tau\tau\tau} \cong \mathbb{C}^{1|1}$. $\gamma \in \mathrm{End}(\tau)$ denote the odd endomorphism in $V^{\tau\tau\tau}$. Then we can write down three anti-commuting operators $\gamma \otimes \gamma \otimes 1$, $\gamma \otimes 1 \otimes \gamma$ and $1 \otimes \gamma \otimes \gamma$ which are each even and as such preserve the grading on $V^{\tau\tau\tau}$. However, the even and odd subspaces of $V^{\tau\tau\tau}$ are one dimensional, and so these operators cannot be represented. Hence a theory with a single q-type particle with Fibonacci-like fusion rules must have nontrivial fusion multiplicity. In the $\frac{1}{2}\mathrm{E}_6$ theory we have $V^{\tau\tau\tau} \cong \mathbb{C}^{2|2}$, which is big enough to represent all three of the above operators.

[18] Note that fusion products of this type cannot appear in the tube category of a fermionic theory since two idempotents in the tube category with non-bounding spin structure must fuse to an idempotent with bounding spin structure, which can never be q-type.

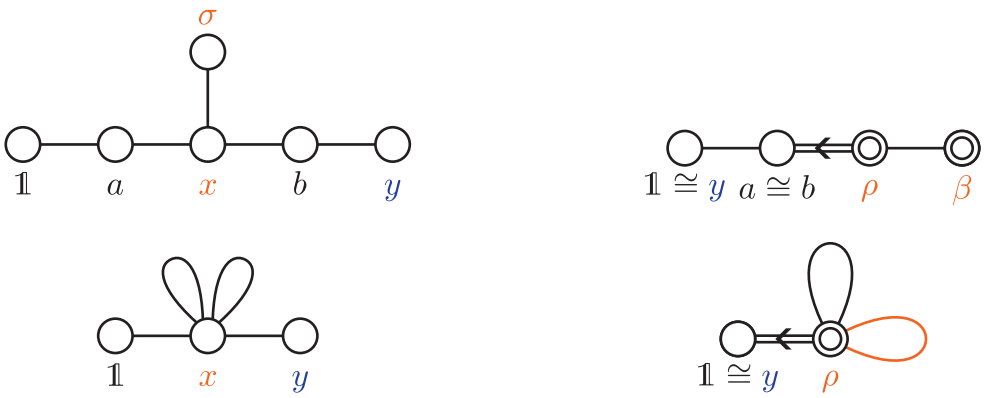

Figure 7.1.1: On the upper left we have the E_6 Dynkin diagram. The E_6 fusion theory has two closed fusion subcategories whose simple objects are $\{\mathbb{1},\ \sigma,\ y\}$ and $\{\mathbb{1}, x, y\}$. The first satisfies the Ising fusion rules while the second satisfies those of $\frac{1}{2}\mathrm{E}_6$ given in (229). The figure on the upper right denotes the principal graph of the theory after condensing y (after first lifting y to the Drinfeld center). On the bottom left we have drawn the $\frac{1}{2}\mathrm{E}_6$ principal graph. The figure on the bottom right is the principal graph of $\frac{1}{2}\mathrm{E}_6/y$ studied in this section. The fermionic quotient of the $\frac{1}{2}\mathrm{E}_6$ fusion subcategory reduces the particle content to $\{\mathbb{1}, \rho\}$.

Performing the condensation requires one additional step that did not appear in the previous examples. This is because the category $\frac{1}{2}\mathrm{E}_6$ is not braided, and so doesn't have a fermion to condense. However, as described in Section 4.1.3, it suffices to lift a particle in $\frac{1}{2}\mathrm{E}_6$ to a fermion in the Drinfeld center of $\frac{1}{2}\mathrm{E}_6$.

In what follows, we will first introduce the fusion theory of $\frac{1}{2}\mathrm{E}_6$ and its properties that are pertinent to the rest of the section. We will then compute the half braid for the emergent fermion, and condense it in the same way we did in the previous examples. Following this, we will compute the idempotents in the condensed theory, as well as the modular S and T matrices.

7.1 Fusion theory of $\frac{1}{2}\mathrm{E}_6$

The E_6 fusion category is the fusion category whose principle graph is given by the E_6 Dynkin diagram, shown to the left in Figure 7.1.1. The E_6 fusion category has two subcategories: one subcategory has the fusion rules of the Ising theory, while the other is known as $\frac{1}{2}\mathrm{E}_6$ [40] and has more complicated fusion rules.

The fusion category $\frac{1}{2}\mathrm{E}_6$ has three particles, $\mathbb{1}$, x, and y. The non-trivial fusion rules are

$$y \otimes y \cong \mathbb{1} \qquad y \otimes x \cong x \otimes y \cong x \qquad x \otimes x \cong \mathbb{1} \oplus 2x \oplus y, \tag{229}$$

and the quantum dimensions are given by

$$d_{\mathbb{1}} = 1 \qquad d_x = 1 + \sqrt{3} \qquad d_y = 1. \tag{230}$$

Note that one of the fusion spaces (V_x^{xx}) has dimension greater than 1. Note also that x is invariant under fusion with y, and that y has quantum dimension 1. If the theory were

braided, and y were fermionic, then condensing y would lead to a super pivotal fusion theory with only two objects, $\mathbb{1}$ and ρ, the image of x under condensation of y. This theory however is not braided, and so we will have to do more work to condense y, as discussed in the next subsection (see also the discussion in Section 4.1.3).

We now to lay out some of the basic data of $\frac{1}{2}\mathrm{E}_6$ which will be useful to us in the following sections. Specifically we will give all information required to manipulate the y line, which will be useful knowledge to have on hand when we condense y.

From looking at (229) we notice that all particles are self dual, and therefore we must specify their Frobenius-Schur indicators. In this case both Frobenius-Schur indicators are equal to 1. These can be found from the associators $\kappa_x = d_x \left[F_x^{xxx}\right]_{\mathbb{1}\mathbb{1}}$, and similarly for y. We list all the F-symbols (as found in [41, 42]) in App. D.1. Using the F-symbols in App. D.1 we can check that, in this gauge, y has nice pivotal properties:

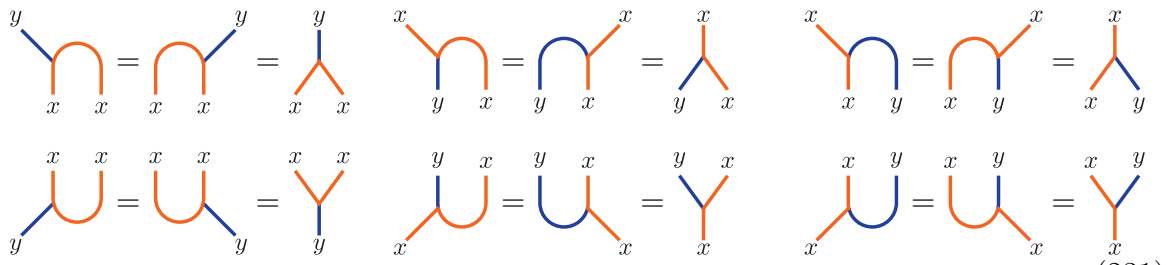

(231)

The fact that these diagrams are trivially pivotal is a reflection of the gauge choice used for the splitting spaces.

Next, we look at what happens when we slide a y line past a V_x^{xx} fusion space. Since $\dim V_x^{xx} = 2$ the fusion space requires a multiplicity index labeling the independent vectors spanning this vector space. We denote them v_1 and v_2, and diagrammatically label them with an index at the fusion vertex:

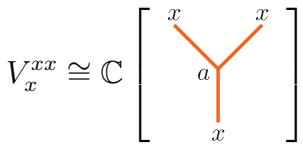

$$a = 1, 2. \tag{232}$$

The next three relations show what happens when y shifts past the fusion space V_x^{xx}:

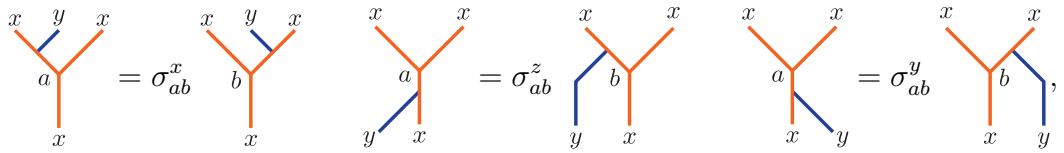

(233)

where the σ^w, $w = x, y, z$ are the standard Pauli matrices.[19] When we condense y, these sliding moves will determine the action of $\mathrm{End}(\rho) \otimes \mathrm{End}(\rho) \otimes \mathrm{End}(\rho)$ on $V_\rho^{\rho\rho}$.

[19] Explicitly $\sigma^x = \begin{pmatrix} 0 & 1 \\ 1 & 0 \end{pmatrix}$ $\sigma^y = \begin{pmatrix} 0 & -i \\ i & 0 \end{pmatrix}$ $\sigma^z = \begin{pmatrix} 1 & 0 \\ 0 & -1 \end{pmatrix}$

Lastly, we have

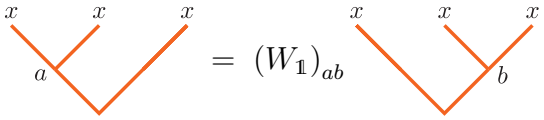

$$W_{\mathbb{1}} = \frac{e^{-7i\pi/12}}{\sqrt{2}} \begin{pmatrix} 1 & -i \\ 1 & i \end{pmatrix} \tag{234}$$

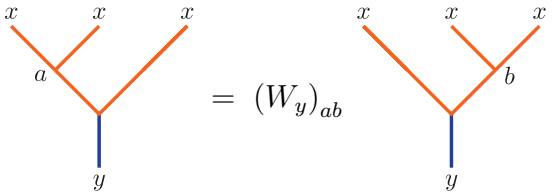

$$W_y = \frac{e^{-7i\pi/12}}{\sqrt{2}} \begin{pmatrix} 1 & -i \\ -1 & -i \end{pmatrix} \tag{235}$$

These will be of use to us when we specify the pivotal properties of $\frac{1}{2}\mathrm{E}_6$ after condensing y; see Section 7.2.1 for more details. The only data left to specify is the associators for the V_x^{xxx} fusion space, which we list in Appendix D.1.

7.2 Fermion condensation in $\frac{1}{2}\mathbf{E}_6$

In this subsection we will describe the procedure for condensing the y particle in $\frac{1}{2}\mathrm{E}_6$. As mentioned earlier, $\frac{1}{2}\mathrm{E}_6$ is not braided, and so when we say condense y, we actually mean that we lift y to the Drinfeld center (where it is an emergent fermion), and condense the lift of y. Since the center of $\frac{1}{2}\mathrm{E}_6$ has been computed in several places [40, 43, 37] we will not provide all details.

The lift of y to the Drinfeld center can be found by solving (91) subject to the constraints (92) and (93). Using the fusion theory of $\frac{1}{2}\mathrm{E}_6$ defined above in Section 7.1 one readily finds the unique solution,

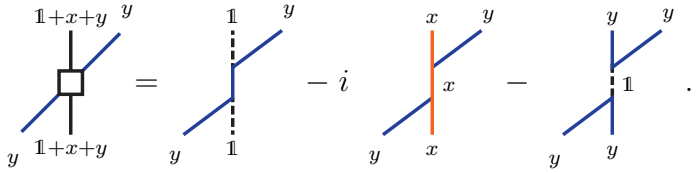

(236)

The negative sign on the last term makes the statistics and twist of (the lift of) y fermionic.

We are now in a position to condense y. Since x is invariant under fusion with y after condensation it becomes a q-type simple object, which we will denote by ρ:

$$x \xrightarrow{\text{condense } y} \rho \qquad \mathrm{End}(\rho) \cong \mathbb{C}\ell_1 \tag{237}$$

ρ is the only non-trivial simple object in the condensed theory. Furthermore, since x has fusion multiplicity in the parent theory, ρ has fusion multiplicity in the condensed theory. This is captured by the fusion space

$$V_\rho^{\rho\rho} \cong \mathbb{C}^{2|2}. \tag{238}$$

The nontrivial fusion rule of the condensed theory is

$$\rho \otimes \rho = \mathbb{C}^{1|1} \cdot \mathbb{1} \oplus \mathbb{C}^{1|1} \cdot \rho. \tag{239}$$

The fusion rule coefficients $\Delta_\rho^{\rho\rho} = \Delta_{\mathbb{1}}^{\rho\rho} \cong \mathbb{C}^{1|1}$ appearing in the above formula are determined by the relation $V_c^{ab} \cong \Delta_c^{ab} \otimes \mathrm{End}(c)$ and the knowledge of the fusion spaces $V_\rho^{\rho\rho} \cong \mathbb{C}^{2|2}, V_\rho^{\rho\mathbb{1}} \cong \mathbb{C}^{1|1}$.[20]

[20] We could have also taken $\Delta_\rho^{\rho\rho} \cong \mathbb{C}^{2|0}$ or $\mathbb{C}^{0|2}$.

7.2.1 Pivotal structure

Since $\mathrm{End}(\rho) \cong \mathbb{C}\ell_1$, $\mathrm{End}(\rho)$ possesses an odd endomorphism which we will denote as f. We will denote the even basis vectors of $V_\rho^{\rho\rho}$ as v_1 and v_2, so that the odd basis vectors are fv_1 and fv_2, where the fv_i are obtained by acting with f on the bottom leg of the fusion space. Diagrammatically we can denote this vector space by

$$V_\rho^{\rho\rho} \cong \mathbb{C}\left[\ \rho\ \rho\ a\ \rho\ ,\ \rho\ \rho\ a\ \rho\ \right] \qquad a = 1, 2, \tag{240}$$

where f is represented graphically by the blue dot. We can then use our knowledge of local relations in the parent $\frac{1}{2}\mathrm{E}_6$ theory and the lift of y to derive the following relations in the condensed theory:

$$\rho\ \rho\ a\ \rho = \sigma^z_{ab}\ \rho\ \rho\ b\ \rho \qquad \rho\ \rho\ a\ \rho = \sigma^y_{ab}\ \rho\ \rho\ b\ \rho \qquad \rho\ \rho\ a\ \rho = -i\sigma^x_{ab}\ \rho\ \rho\ b\ \rho\ , \tag{241}$$

where the σ^w are the standard Pauli matrices (compare (233)). We can also obtain the following pivoting moves:

$$\rho\ \rho\ a\ \rho = P_{ab}\ \rho\ \rho\ b\ \rho \qquad P = \frac{e^{7i\pi/12}}{\sqrt{2}}\begin{pmatrix} 1 & 1 \\ i & -i \end{pmatrix} \tag{242}$$

$$\rho\ \rho\ a\ \rho = \dot{P}_{ab}\ \rho\ \rho\ b\ \rho \qquad \dot{P} = \frac{e^{7i\pi/12}}{\sqrt{2}}\begin{pmatrix} i & -i \\ -1 & -1 \end{pmatrix} \tag{243}$$

Note that we have $P^3 = \mathbb{1}, (\dot{P})^3 = -\mathbb{1}$, which is consistent with the fact that P acts on even vectors while $\dot{P}$ acts on odd ones (so that $(\dot{P})^3$ rotates an odd vector by 2π, which produces a minus sign).

7.3 The tube category and the torus

7.3.1 Tube category morphism spaces

In this subsection we compute bases for tube category morphism spaces. We will make use of the notation $s(X)$ defined in (113). Using the relations

$$\circledX = s(X)\ \circledX \qquad \circledX = -s(X)\ \circledX \tag{244}$$

we see that a complete basis of morphisms from trivial (empty) boundary to the empty boundary is listed in Table 7.3.1. (The relations are found by taking two fermions out of the vacuum and sliding them around the annulus.)

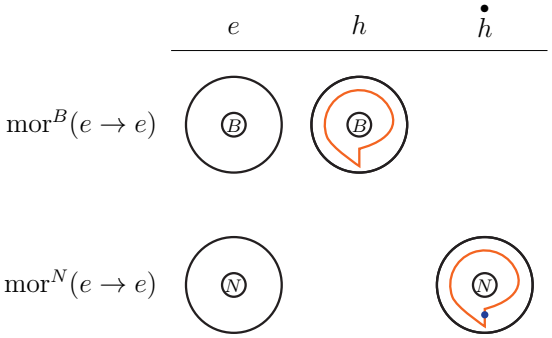

Table 7.3.1: A complete basis of morphisms for $\mathrm{mor}^B(e \to e) \in \mathbf{Tube}(\frac{1}{2}\mathrm{E}_6/y)$. The labels above each tube are short-hand for that tube: e – empty tube; h – tube with horizontal ρ line. The dot above h denotes that the morphism is an odd morphism.

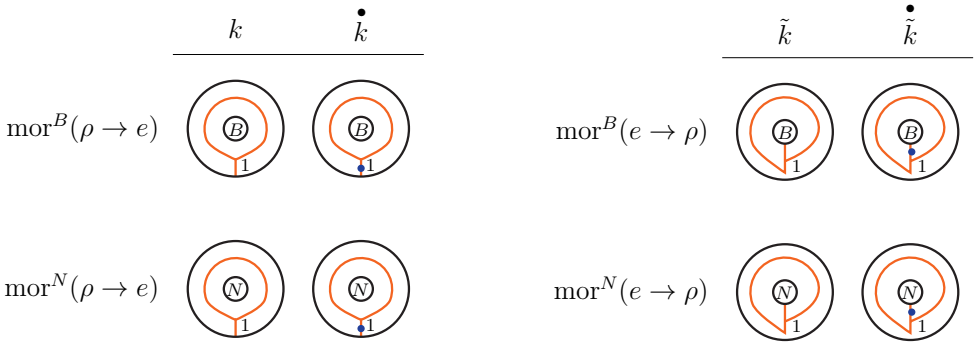

Table 7.3.2: A complete basis of morphisms $\mathrm{mor}(\rho \to e) \in \mathbf{Tube}(\frac{1}{2}\mathrm{E}_6/y)$ and $\mathrm{mor}(e \to \rho) \in \mathbf{Tube}(\frac{1}{2}\mathrm{E}_6/y)$. We have denoted these by k, $\dot{k}$ $\tilde{k}$, and $\dot{\tilde{k}}$.

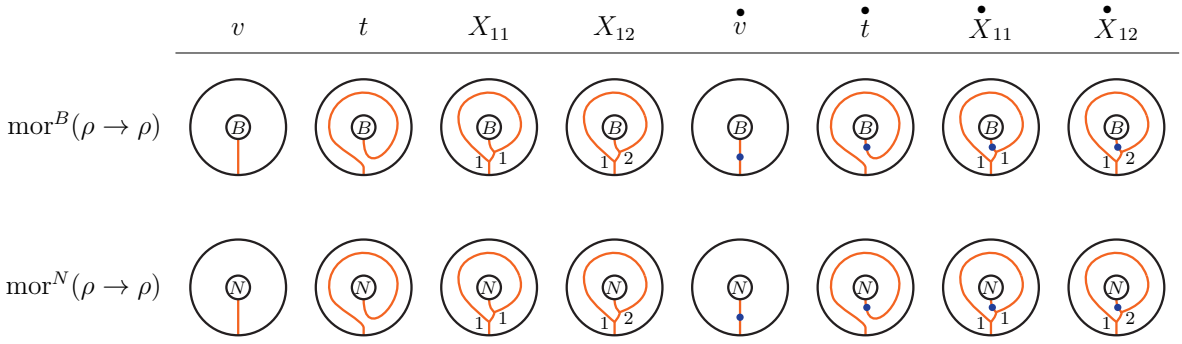

Table 7.3.3: A complete basis of morphisms for $\mathrm{mor}(\rho \to \rho) \in \mathbf{Tube}(\frac{1}{2}\mathrm{E}_6/y)$. The labels above each tube are shorthand for that tube: v – tube with vertical ρ strand; t – tube with ρ strand wrapping both cycles; X – tube with all labels given by ρ. As before, a dot denotes an odd vector.

Similarly, we have

(245)

Hence some of these states are linearly dependent, and so a complete basis of morphisms is found if we fix the fusion space, and also consider the action of the odd endomorphism. The basis we choose is listed in Table 7.3.2.

The morphisms of $\mathrm{mor}(\rho \to \rho)$ satisfy

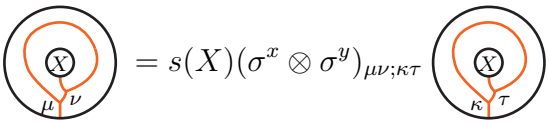

(246)

and also

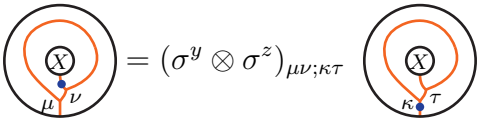

(247)

We can use these results to obtain a basis for $\mathrm{mor}(\rho \to \rho)$, which is given in Table 7.3.3.

7.3.2 Bases for tori

In this subsection we compute bases for the Hilbert spaces of spin tori. We could of course do this using knowledge of tube category idempotents and 4.3.1, but it's an instructive exercise to also compute bases using more elementary means. In addition, when computing S and T matrices, it will be useful to have a topologically simple basis at our disposal.

On the torus there are four spin structures. We will first investigate the local relations on the three bounding tori which have spin structure $(X, Y) = (B, B), (N, B), (B, N)$. Then we will consider the (N, N) torus separately. We use the same notation as in Section 3.3.

Depending on the spin structure, some of the annular tubes become zero after identifying the boundaries to form tori. Since there is always one cycle with bounding spin structure, an odd tube is identified with zero for the same reason as discussed in 3.3.1. For another example, due to (244) we have

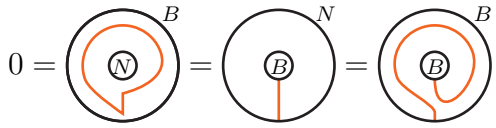

(248)

We also get another local relation from (246) after closing up the annulus to a torus, namely

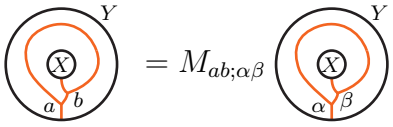

$$M = s(X)\sigma^x \otimes \sigma^y, \quad s(Y)\sigma^y \otimes \sigma^z \tag{249}$$

The two relations above can be multiplied to find a third:

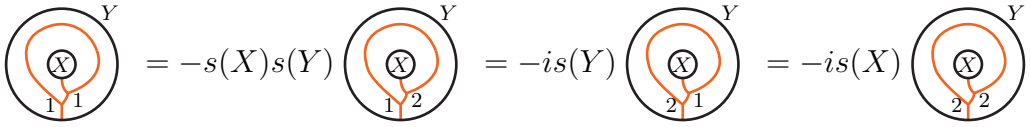

(250)

We take the state with $(a, b) = (1, 1)$ as the representative of this set of linearly dependent vectors.

There is one additional useful linear relation to be found. This relation comes from nucleating a ρ loop and extending it around the torus before fusing it back into the canonical basis:

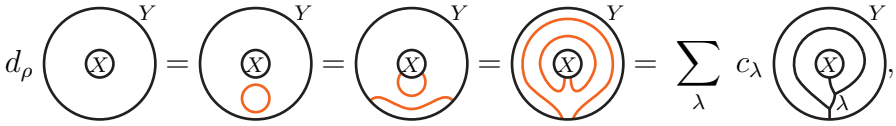

(251)

where c_λ are coefficients that depend on the F-symbols. The string of equalities gives an additional local relation, in particular, it allows us solve for the tubes in (250) above in terms of the other non-zero tubes. Explicitly in the three sectors $(B, B), (B, N)$, and (N, B) we have,

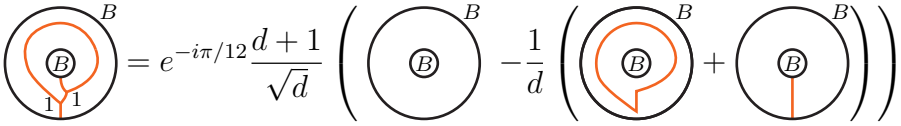

(252)

(253)

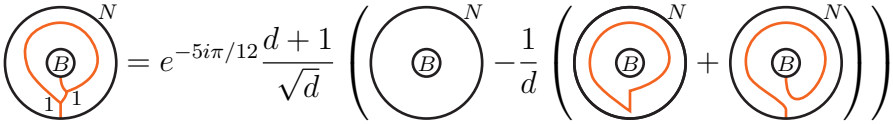

(254)

(255)

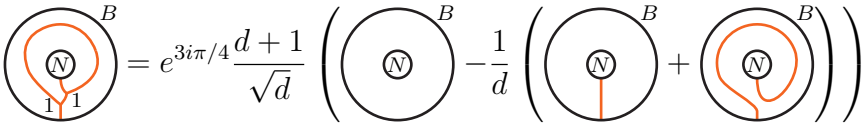

(256)

We now move on to the torus where the spin structure is non-bounding along both cycles. We first notice that

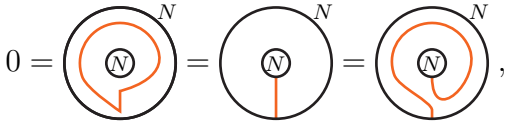

(257)

which can be seen by nucleating two fermions out of the vacuum along each ρ line and dragging one of them along the entire ρ line before fusing them back to the vacuum. Furthermore, the same calculation as (251) implies that the the empty tube is identified with zero:

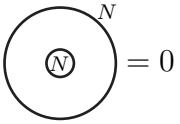

(258)

The only non-zero tube with even parity is given by

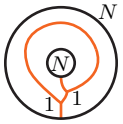

(259)

and those which are proportional to it are given by (250).

As one may expect from the Ising example, there are odd tubes which are non-zero. Indeed we can find four of them,

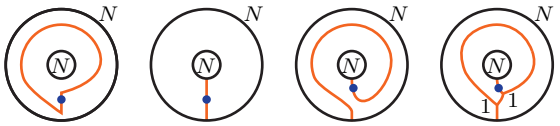

(260)

However, these four tubes are not linearly independent. There are two independent linear relations that can be found between them by multiplying the tadpole-like diagrams in two different ways,

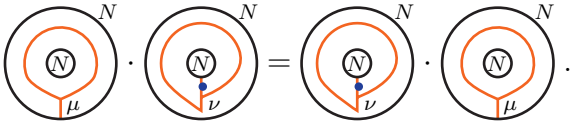

(261)

This is an instance of the familiar relation $cl(a \cdot b) = cl(b \cdot a)$. Despite the indices μ and ν varying over four distinct values, this yields only two linearly independent relations on the torus. They are given by

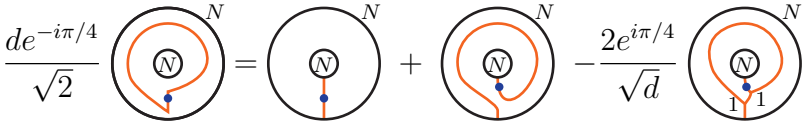

(262)

and[21]

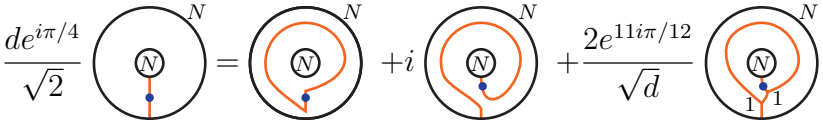

(263)

We can now solve for any two of the above four states. We choose

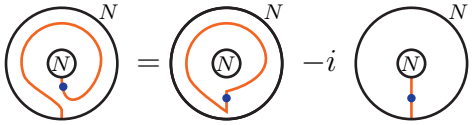

(264)

(265)

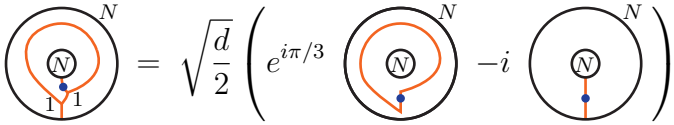

(266)

[21] One can check that the second relation follows from the first by performing an S transformation.

In summary, the Hilbert spaces on each of the different spin tori are poo

$$
\begin{aligned}
A(T^2_{BB}) &\cong \mathbb{C}^{3|0} = \mathbb{C}\Big[\\
A(T^2_{BN}) &\cong \mathbb{C}^{3|0} = \mathbb{C}\Big[\\
A(T^2_{(NB)}) &\cong \mathbb{C}^{3|0} = \mathbb{C}\Big[\\
A(T^2_{NN}) &\cong \mathbb{C}^{1|2} = \mathbb{C}\Big[
\end{aligned}
$$

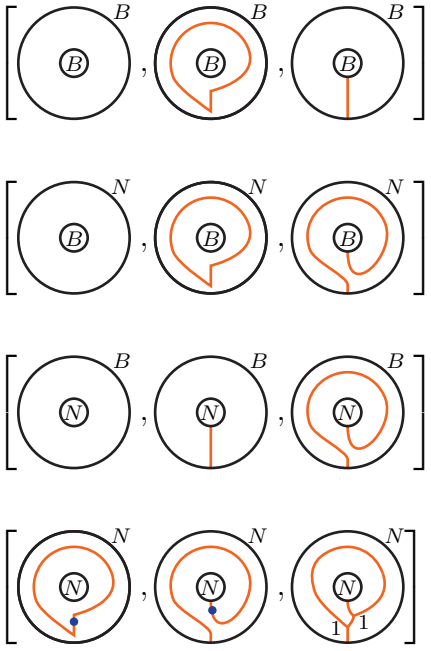

(267)

7.4 The tube category of $\frac{1}{2}\mathbf{E}_6/y$

In this subsection we compute the minimal idempotents of the tube category of $\frac{1}{2}\mathrm{E}_6/y$. The tube category is somewhat exotic, and highlights many of the non-trivial features which arise when studying fermionic theories. We start by analyzing the idempotents from a purely algebraic point of view using only the dimensions of the morphism spaces, which can be inferred from Tables 7.3.1–7.3.3. We also provide explicit representations of the idempotents, which are given in Tables 7.4.1 – 7.4.3.

We begin by examining the bounding tube category. A basis for the morphism space $\mathrm{mor}^B(e \to e)$ is given in Table 7.3.1. As a vector space $\mathrm{mor}^B(e \to e)$ is isomorphic to $\mathbb{C}^{2|0}$, and (as we have seen before in (46)) there is only one possible super algebra structure on $\mathbb{C}^{2|0}$, given by $\mathbb{C} \oplus \mathbb{C}$. (As before $\mathbb{C}$ is shorthand for the trivial 1-dimensional algebra.) Therefore this subcategory contains two inequivalent minimal idempotents. One is the trivial idempotent which we denote m_1, the other we denote m_2. Explicit representations of these idempotents are given in Table 7.4.1. The trivial idempotent is the usual one, just given by the quantum dimensions. The non-trivial idempotent m_2 is easily computed from the constraint $m_1 + m_2 = \mathrm{id}_e$ and is also listed in Table 7.4.1.

Next we look at $\mathrm{mor}^B(\rho \to e)$, a basis for which is listed in Table 7.3.2. As a vector space $\mathrm{mor}^B(\rho \to e) \cong \mathbb{C}^{1|1}$. This implies that $\mathrm{mor}^B(\rho \to \rho)$ contains a two by two matrix algebra $M(1|1)$. One may think that it could just have easily been $Q(1) \oplus Q(1)$, but we know that the bounding tube category does not admit q-type simple objects; see the discussion at the end of Section 4.3. Thus we find two minimal idempotents in $\mathrm{mor}^B(\rho \to \rho)$, both isomorphic to m_2 (they cannot be isomorphic to m_1 due to the no tadpole axiom.). One of these minimal idempotents is evenly isomorphic to m_2 which we denote m_2^+, the other is oddly isomorphic and denoted m_2^-. The two isomorphic idempotents are explicitly written in Table 7.4.2. (They are proportional to $k \cdot m_2 \cdot \tilde{k}$ and $\overset{\bullet}{k} \cdot m_2 \cdot \overset{\bullet}{\tilde{k}}$.)

We now look at $\mathrm{mor}^B(\rho \to \rho)$ and ask which part of it has not been accounted for.

We see from Table 7.3.3 that $\mathrm{mor}^B(\rho \to \rho) \cong \mathbb{C}^{4|4}$ as a vector space. An $M(1|1)$ matrix algebra has been accounted for by $m_2^{\pm}$. Thus the only consistent super algebra structure is $\mathrm{mor}^B(\rho \to \rho) \cong M(1|1) \oplus M(1|1)$. The remaining $M(1|1)$ contains two equivalent oddly isomorphic minimal idempotents, which we label as m_3^+ and m_3^-.

The super algebra structure of the non-bounding tube category is more exotic but equally well tamed by the classification of semisimple super algebras. We begin by looking at $\mathrm{mor}^N(e \to e) \cong \mathbb{C}^{1|1}$. There is a unique simple algebra structure on $\mathbb{C}^{1|1}$ given by $Q(1)$. We denote the corresponding q-type minimal idempotent by q_1.

Next we look at $\mathrm{mor}^N(e \to \rho)$ which is isomorphic to $\mathbb{C}^{1|1}$ as a vector space. It follows that $\mathrm{mor}^N(\rho \to \rho)$ contains a $Q(1)$ summand, and a minimal idempotent isomorphic to q_1 which we denote q_1', and list in Table 7.4.3.

We now turn to $\mathrm{mor}^N(\rho \to \rho) \cong \mathbb{C}^{4|4}$. A $\mathbb{C}^{1|1}$ dimensional subalgebra has been accounted for by q_1. Hence we only need to look at complement of this subalgebra, which as a vector space is isomorphic to $\mathbb{C}^{3|3}$. There are two possible super algebra structures available: either three copies of $Q(1)$ or one copy of $Q(1)$ and one copy of $M(1|1)$. However, $\mathbf{Tube}^B$ and $\mathbf{Tube}^N$ must contain the same number of non-isomorphic minimal idempotents, as shown at the end of Section 4.3. Since $\mathbf{Tube}^B(\frac{1}{2}\mathrm{E}_6/y)$ has three non-isomorphic minimal idempotents, so must $\mathbf{Tube}^N(\frac{1}{2}\mathrm{E}_6/y)$. Hence the algebra structure on the remaining $\mathbb{C}^{3|3}$ must be $Q(1) \oplus M(1|1)$. Correspondingly we find one q-type minimal idempotent which we label q_2, and two oddly isomorphic m-type minimal idempotents which we label m_4^+ and m_4^-. These idempotents are given explicitly in Table 7.4.3.

It is useful to write the isomorphisms between the idempotents in a standard form. Namely, if e and e' are isomorphic we can write $e = u \cdot v$ and $e' = v \cdot u$ for some u and v. In an obvious notation we have,

$$m_2 = \frac{e^{i\pi/4}}{2}\sqrt{\frac{d}{3}}$$  $$= \frac{e^{-i\pi/4}}{2}\sqrt{\frac{d}{3}}$$ 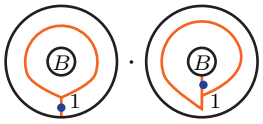 (268)

which can be used to track the isomorphisms across the three representatives m_2, m_2^+ and m_2^-. Similarly we have,

$$q_1 = \frac{e^{i\pi/4}}{\sqrt{d}}$$ 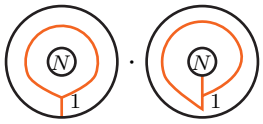 (269)

Lastly we note that $m_3^+ \cdot \overset{\bullet}{v} = \overset{\bullet}{v} \cdot m_3^-$, and $m_4^+ \cdot \overset{\bullet}{v} = \overset{\bullet}{v} \cdot m_4^-$ where $\overset{\bullet}{v}$ is listed in Table 7.3.3. Consequently we have,

$$m_3^+ = \lambda^{-1}(m_3^+ \cdot \overset{\bullet}{v}) \cdot (\overset{\bullet}{v} \cdot m_3^+) \qquad m_3^- = \lambda^{-1}(\overset{\bullet}{v} \cdot m_3^+) \cdot (m_3^+ \cdot \overset{\bullet}{v}) \tag{270}$$

and similarly,

$$m_4^+ = \lambda^{-1}(m_4^+ \cdot \overset{\bullet}{v}) \cdot (\overset{\bullet}{v} \cdot m_4^+) \qquad m_4^- = \lambda^{-1}(\overset{\bullet}{v} \cdot m_4^+) \cdot (m_4^+ \cdot \overset{\bullet}{v}). \tag{271}$$

The twists and quantum dimensions of the idempotents can be computed with the techniques developed in previous sections; we list the results in Table 7.4.4.

We also note that an idempotent of the parent tube category can always be included into the tube category of the condensed theory. As in Section 5.2 the inclusion can

type	twist	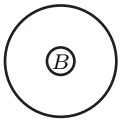	
m_1	1	$\frac{1}{d\sqrt{3}}$	$\frac{1}{2\sqrt{3}}$
m_2	1	$\frac{d}{2\sqrt{3}}$	$\frac{-1}{2\sqrt{3}}$

Table 7.4.1: Quasiparticles of $\frac{1}{2}\mathrm{E}_6$ with bounding spin structure and trivial boundary condition. The particle is a linear combination of the tubes shown at the top of the table multipled by the coefficients in the row.

type	twist	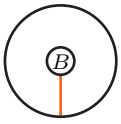		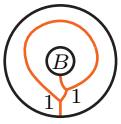	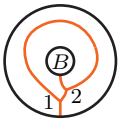
m_2^+	1	$\frac{1}{2\sqrt{3}}$	$\frac{1}{2\sqrt{3}}$	$\frac{e^{i\pi/4}}{2\sqrt{d}}$	$\frac{-e^{-i\pi/4}}{2\sqrt{3d}}$
m_2^-	-1	$\frac{1}{2\sqrt{3}}$	$\frac{-1}{2\sqrt{3}}$	$\frac{e^{-i\pi/4}}{2\sqrt{3d}}$	$\frac{-e^{i\pi/4}}{2\sqrt{d}}$
m_3^+	$e^{i\pi/3}$	$\frac{1}{2+d}$	$\frac{e^{-i\pi/3}}{2+d}$	$\frac{-e^{i\pi/12}}{\sqrt{3d}}$	
m_3^-	$-e^{i\pi/3}$	$\frac{1}{2+d}$	$\frac{-e^{-i\pi/3}}{2+d}$		$\frac{e^{i\pi/12}}{\sqrt{3d}}$

Table 7.4.2: Quasiparticles of $\frac{1}{2}\mathrm{E}_6$ with bounding spin structures, and boundary condition ρ. The tube with a single ρ line is a direct sum of four simple objects, two of which we name m_2^+ and m_3^+. The other two are oddly isomorphic to m_2^+ and m_3^+, and we denote them m_2^- and m_3^-

be non non-trivial: some of the idempotents may become isomorphic, or even equal to zero. In Appendix D.2, we compute the minimal idempotents of $\mathbf{Tube}(\frac{1}{2}\mathrm{E}_6)$ and track their images under the inclusion into $\mathbf{Tube}(\frac{1}{2}\mathrm{E}_6/y)$. This also provides an additional crosscheck on the minimal idempotents given in tables 7.4.1 – 7.4.3.

The fusion rules in the condensed theory can be calculated using (141) and (142) as well as the S-matrix which we compute in the next section. We list the fusion rules in Table 7.4.5. A particularly noteworthy fusion rule is:

$$m_4^+ \otimes m_4^+ \cong \mathbb{C}^{0|1} m_1 \oplus m_2 \oplus m_3^+. \tag{272}$$

The odd vector space coefficient of the trivial object m_1 implies that m_4^+ is oddly self dual. Let's show explicitly that $\mathrm{mor}(\mathbb{1} \to m_4^+ \otimes m_4^+) \cong \mathbb{C}^{0|1}$. We first note the following linear relations,

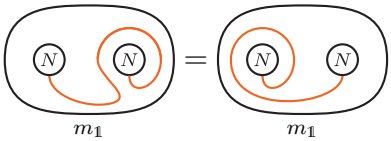

(273)

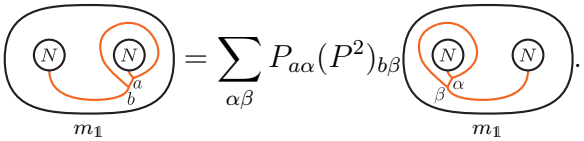

(274)

type	twist	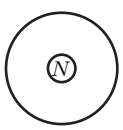
q_1	1	1

type	twist	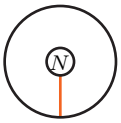			
q_1'	1	$\frac{1}{d}$	$\frac{1}{d}$	$\frac{-e^{i\pi/4}}{d\sqrt{d}}$	$\frac{-e^{i\pi/4}}{d\sqrt{d}}$
q_2	$-i$	$\frac{1}{2+d}$	$\frac{i}{2+d}$	$\frac{i\gamma}{\sqrt{2+d}}$	$\frac{i\gamma}{\sqrt{2+d}}$
m_4^+	$e^{5i\pi/6}$	$\frac{1}{2+d}$	$\frac{e^{-5i\pi/6}}{2+d}$	$\frac{-\alpha e^{5i\pi/6}}{\sqrt{2+d}}$	$\frac{\beta e^{5i\pi/6}}{\sqrt{2+d}}$
m_4^-	$e^{5i\pi/6}$	$\frac{1}{2+d}$	$\frac{e^{-5i\pi/6}}{2+d}$	$\frac{\beta e^{5i\pi/6}}{\sqrt{2+d}}$	$\frac{-\alpha e^{5i\pi/6}}{\sqrt{2+d}}$

Table 7.4.3: Quasiparticles of $\frac{1}{2}E6$ with vortex (periodic) spin structures. Two are q-type, and one is m-type. The m-type particle is two-dimensional, consisting of of two smaller simple modules. Π is an odd isomorphism, and $\alpha = \frac{1}{2}\left(1 + 1/\sqrt{2d+1}\right)$, and $\beta = \frac{1}{2}\left(1 - 1/\sqrt{2d+1}\right)$.

particle	m_1	m_2	m_3^+	q_1	q_2	m_4
quantum dimension	1	$1+d$	d	$2+d$	d	d
twist	1	1	$e^{-i\pi/3}$	1	i	$e^{-5i\pi/6}$

Table 7.4.4: The $\frac{1}{2}\mathrm{E}_6$ quantum dimensions and twists. We have normalized the quantum dimensions by the quantum dimension of the trivial idempotent. The total quantum dimension is given by $\mathcal{D} = d\sqrt{6}$.

The boundary is labeled by $m_{\mathbb{1}}$ and allows us to treat the pair of pants as if it were a sphere with two disks removed each with one marked point labeled ρ. Indeed (273) follows directly from this observation, while (274) also requires some pivots. After plugging in the coefficients and using (246), one finds that

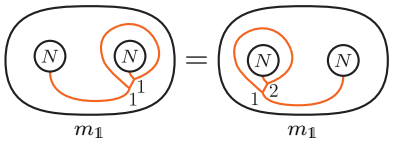

(275)

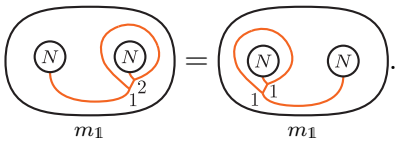

(276)

Under interchanging X_{11} with X_{12}, we see that m_4^+ is interchanged with m_4^-. It follows that inserting the m_4^+ idempotent on the right hand side of the pair of pants is equivalent to inserting m_4^- on the left hand side of the pair of pants. Using that $\overset{\bullet}{v} \cdot m_4^- = m_4^+ \cdot \overset{\bullet}{v}$, a basis for $V_{\mathbb{1}}^{m_4^+ m_4^+}$ is generated by a single odd vector:

$$V_{\mathbb{1}}^{m_4^+ m_4^+} = \Big\langle$$

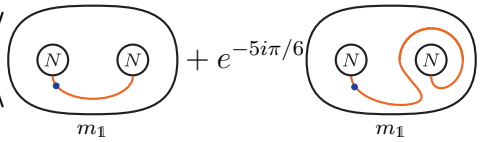

$$+ e^{-5i\pi/6}$$

$$- \alpha\sqrt{2+d}e^{5i\pi/6}$$

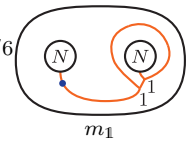

$$+ \beta\sqrt{2+d}e^{5i\pi/6}$$

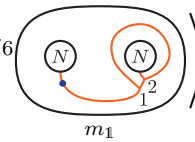

$$\Big\rangle,$$

(277)

and so $V_{\mathbb{1}}^{m_4^+ m_4^+} \cong \mathbb{C}^{0|1}$.

7.5 Modular transformations

7.5.1 Topological and idempotent bases

There are two natural bases on the torus. One is the topological basis, corresponding to (267), the other is the idempotent basis (or quasiparticle basis) given in Tables 7.4.2 and 7.4.3. We will compute the modular transformations in the topological basis first, and then change over to the idempotent basis.

We define the shorthand notation for the tubes as in Tables 7.3.1–7.3.3 We will then denote the spin structure by a subscript, for example,

$$h_{BN} =$$

(278)

Every state on the torus can be expanded in terms of the above states, as long as we are also careful to use the relations provided in Section 7.3.2. Hence one can directly compute the change of basis by taking the particles in Tables 7.4.1, 7.4.2, and 7.4.3 and projecting them onto the torus, and then modding out by the relations described in Section 7.3.2. The change of basis matrices in the spin sectors with at least one bounding

$\mathcal{A}\otimes\mathcal{A}$	m_1	m_2	m_3^+
m_1	m_1	m_2	m_3^+
m_2	m_2	$m_1\oplus\mathbb{C}^{1\|1}m_2\oplus\mathbb{C}^{1\|1}m_3^+$	$\mathbb{C}^{1\|1}m_2\oplus\mathbb{C}^{0\|1}m_3^+$
m_3^+	m_3^+	$\mathbb{C}^{1\|1}m_2\oplus\mathbb{C}^{0\|1}m_3^+$	$m_1\oplus\mathbb{C}^{0\|1}m_2\oplus m_3^+$

$\mathcal{V}\otimes\mathcal{A}$	m_1	m_2	m_3^+
q_1	q_1	$\mathbb{C}^{1\|1}q_1\oplus q_2\oplus\mathbb{C}^{1\|1}m_4^+$	$q_1\oplus q_2\oplus\mathbb{C}^{1\|1}m_4^+$
q_2	q_2	$q_1\oplus\mathbb{C}^{1\|1}m_4^+$	$q_1\oplus q_2$
m_4^+	m_4^+	$q_1\oplus q_2\oplus\mathbb{C}^{0\|1}m_4^+$	$q_1\oplus\mathbb{C}^{0\|1}m_4^+$

$\mathcal{V}\otimes\mathcal{V}$	q_1	q_2	m_4^+
q_1	$\mathbb{C}^{1\|1}m_1\oplus\mathbb{C}^{2\|2}m_2\oplus\mathbb{C}^{1\|1}m_3^+$	$\mathbb{C}^{1\|1}m_2\oplus\mathbb{C}^{1\|1}m_3^+$	$\mathbb{C}^{1\|1}m_2\oplus\mathbb{C}^{1\|1}m_3^+$
q_2	$\mathbb{C}^{1\|1}m_2\oplus\mathbb{C}^{1\|1}m_3^+$	$\mathbb{C}^{1\|1}m_1\oplus m_3^+$	$\mathbb{C}^{1\|1}m_2$
m_4^+	$\mathbb{C}^{1\|1}m_2\oplus\mathbb{C}^{1\|1}m_3^+$	$\mathbb{C}^{1\|1}m_2$	$\mathbb{C}^{0\|1}m_1\oplus m_2\oplus m_3^+$

Table 7.4.5: $\frac{1}{2}\mathrm{E}_6$ fusion rules. We define $\mathcal{A}=\{m_1,m_2,m_3^+\}$ and $\mathcal{V}=\{q_1,q_2,m_4^+\}$ as the set of non-vortex and vortex quasiparticles, respectively. The $\mathbb{C}^{p|q}$ denote the vector space associated with Δ_c^{ab} which is related to the fusion space through $V_c^{ab}=\Delta_c^{ab}\otimes\mathrm{End}(c)$. Notice that m_4^+ is oddly self-dual (the relevant fusion channel is marked in red), and hence it has a Frobenius-Schur indicator of $\pm i$.

cycle are

$$\begin{pmatrix} m_1 \\ m_2 \\ m_3^+ \end{pmatrix}_{BB} = \begin{pmatrix} \frac{1}{d\sqrt{3}} & 0 & \frac{1}{2\sqrt{3}} \\ \frac{d}{2\sqrt{3}} & 0 & -\frac{1}{2\sqrt{3}} \\ -\frac{d}{2\sqrt{3}} & \frac{1}{2} & \frac{1}{2\sqrt{3}} \end{pmatrix} \begin{pmatrix} e \\ v \\ h \end{pmatrix}_{BB} \tag{279}$$

$$\begin{pmatrix} m_1 \\ m_2 \\ m_3^+ \end{pmatrix}_{BN} = \begin{pmatrix} \frac{1}{d\sqrt{3}} & 0 & \frac{1}{2\sqrt{3}} \\ \frac{d}{2\sqrt{3}} & 0 & -\frac{1}{2\sqrt{3}} \\ \frac{de^{2\pi i/3}}{2\sqrt{3}} & \frac{e^{-i\pi/3}}{2} & \frac{e^{-i\pi/3}}{2\sqrt{3}} \end{pmatrix} \begin{pmatrix} e \\ t \\ h \end{pmatrix}_{BN} \tag{280}$$

$$\begin{pmatrix} q_1 \\ q_2 \\ m_4^+ \end{pmatrix}_{NB} = \begin{pmatrix} 1 & 0 & 0 \\ \sqrt{\frac{1+d}{3}}e^{-3i\pi/4} & \frac{e^{i\pi/6}}{\sqrt{3}} & \frac{e^{i\pi/3}}{\sqrt{3}} \\ \frac{e^{7i\pi/12}}{\sqrt{6}} & \frac{e^{-i\pi/6}}{2\sqrt{3}} & \frac{e^{-2i\pi/3}}{2\sqrt{3}} \end{pmatrix} \begin{pmatrix} e \\ v \\ t \end{pmatrix}_{NB} \tag{281}$$

$$\tag{282}$$

For the non-bounding NN spin structure the q-type idempotents need to be closed up into a torus with an odd isomorphism We define $\left[\overset{\bullet}{q}_i\right]^2 = q_i$. This has a $\pm$ ambiguity, we denote the $\pm$ signs by σ_i. We can also change to the idempotent basis with,

$$\begin{pmatrix} \overset{\bullet}{q}_1 \\ \overset{\bullet}{q}_2 \\ m_4^+ \end{pmatrix} = \begin{pmatrix} \sigma_1 e^{-i\pi/4} & 0 & 0 \\ 0 & \sigma_2 e^{-i\pi/4} & 0 \\ 0 & 0 & 1 \end{pmatrix} \begin{pmatrix} \frac{e^{-i\pi/4}}{\sqrt{2}} & 0 & 0 \\ -\frac{e^{-i\pi/4}}{\sqrt{2}} & 1 & 0 \\ 0 & 0 & -\frac{e^{5i\pi/6}}{\sqrt{2+d}} \end{pmatrix} \begin{pmatrix} \overset{\bullet}{h} \\ \overset{\bullet}{v} \\ X \end{pmatrix} \tag{283}$$

The q-type idempotents have norm square of 2 (due to their two-dimensional endomorphism algebras), as opposed to the m-type idempotents that have norm square of 1. To ensure that the modular matrices are unitary, we adjust for this by defining $\widehat{q} = q/\sqrt{2}$. When written in terms of the $\widehat{q}$, the modular matrices are unitary.

7.5.2 S transformation

The S transformation exchanges the longitudinal and meridional cycles of the torus. Since we are drawing the tori as annuli with their boundaries identified, the S transformation looks like

$$S^{XY\to\widetilde{X}\widetilde{Y}}: \quad A(T^2_{XY}) \longrightarrow A(T^2_{\widetilde{X}\widetilde{Y}}) \tag{284}$$

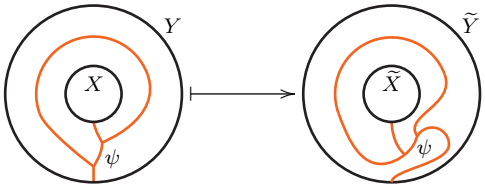

with the transformed spin structure $\widetilde{X}\widetilde{Y}$ being found with the aid of Figure 3.3.4. In terms of the matrix elements of S, we have

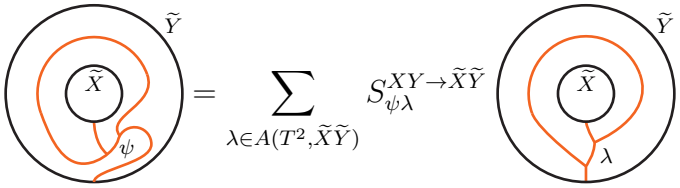

$$= \sum_{\lambda\in A(T^2,\widetilde{X}\widetilde{Y})} S^{XY\to\widetilde{X}\widetilde{Y}}_{\psi\lambda} \tag{285}$$

$$\tag{286}$$

Where we have taken $\psi, \lambda \in \bigoplus_{ab} V_b^{aba^*}$ modulo local relations.

We can now work out the S-matrix for each spin structure in the topological basis, and then change over to the idempotent basis. The calculation is the same in each case, we find the linear map on the in to the topological basis based on (284), and then change back to the particle basis using (281–283).

For the BB spin structure one simply finds that v and h are interchanged so that,

$$\begin{pmatrix} e \\ v \\ h \end{pmatrix}_{BB} \xrightarrow{S^{BB\to BB}} \begin{pmatrix} 1 & 0 & 0 \\ 0 & 0 & 1 \\ 0 & 1 & 0 \end{pmatrix} \begin{pmatrix} e \\ v \\ h \end{pmatrix}_{BB} \tag{287}$$

We can now write down the S-matrix in the idempotent basis using the change of basis in (279)

$$\begin{pmatrix} m_1 \\ m_2 \\ m_3^+ \end{pmatrix}_{BB} \xrightarrow{S^{BB\to BB}} \frac{1}{\sqrt{3}} \begin{pmatrix} \frac{1}{d} & \frac{d}{2} & 1 \\ \frac{d}{2} & \frac{1}{d} & -1 \\ 1 & -1 & 1 \end{pmatrix} \begin{pmatrix} m_1 \\ m_2 \\ m_3^+ \end{pmatrix}_{BB} \tag{288}$$

Next we compute the S-matrix elements that transition between the BN and NB tori. We first find the action of S on the BN torus:

$$\begin{pmatrix} e \\ h \\ v \end{pmatrix}_{BN} \xrightarrow{S^{BN\to NB}} \begin{pmatrix} 1 & 0 & 0 \\ 0 & 1 & 0 \\ de^{-i\pi/6} & e^{5i\pi/6} & e^{2\pi i/3} \end{pmatrix} \begin{pmatrix} e \\ v \\ t \end{pmatrix}_{NB} \tag{289}$$

which can be written in the idempotent basis as

$$\begin{pmatrix} m_1 \\ m_2 \\ m_3^+ \end{pmatrix}_{BN} \xrightarrow{S^{BN\to NB}} \begin{pmatrix} \frac{1}{2} & \frac{1}{2\sqrt{3}} & \frac{1}{\sqrt{3}} \\ \frac{1}{2} & -\frac{1}{2\sqrt{3}} & -\frac{1}{\sqrt{3}} \\ 0 & \frac{1}{\sqrt{3}} & -\frac{1}{\sqrt{3}} \end{pmatrix} \begin{pmatrix} q_1 \\ q_2 \\ m_4^+ \end{pmatrix}_{NB} . \tag{290}$$

Similarly we can work out the S-matrix in the topological basis for the (N, B) torus,

$$\begin{pmatrix} e \\ v \\ t \end{pmatrix}_{NB} \xrightarrow{S^{NB\to BN}} \begin{pmatrix} 1 & 0 & 0 \\ 0 & 1 & 0 \\ de^{i\pi/6} & e^{-5i\pi/6} & e^{-2i\pi/3} \end{pmatrix} \begin{pmatrix} e \\ h \\ t \end{pmatrix}_{BN} \tag{291}$$

And again we can write this in the idempotent basis:

$$\begin{pmatrix} q_1 \\ q_2 \\ m_4^+ \end{pmatrix}_{NB} \xrightarrow{S^{NB\to BN}} \begin{pmatrix} 1 & 1 & 0 \\ \frac{1}{\sqrt{3}} & -\frac{1}{\sqrt{3}} & \frac{2}{\sqrt{3}} \\ \frac{1}{\sqrt{3}} & -\frac{1}{\sqrt{3}} & -\frac{1}{\sqrt{3}} \end{pmatrix} \begin{pmatrix} m_1 \\ m_2 \\ m_3^+ \end{pmatrix}_{BN} \tag{292}$$

Notice that the S-matrix is invertible, but not unitary. This is because we didn't normalize our idempotents appropriately. As mentioned earlier, we write the normalized Q idempotents with a hat, $\widehat{Q}_i = Q_i/\sqrt{2}$. Once doing so we find the appropriately normalized S-matrix is given by

$$\begin{pmatrix} m_1 \\ m_2 \\ m_3^+ \end{pmatrix}_{BN} \xrightarrow{S^{BN\to NB}} \begin{pmatrix} \frac{1}{\sqrt{2}} & \frac{1}{\sqrt{6}} & \frac{1}{\sqrt{3}} \\ \frac{1}{\sqrt{2}} & -\frac{1}{\sqrt{6}} & -\frac{1}{\sqrt{3}} \\ 0 & \sqrt{\frac{2}{3}} & -\frac{1}{\sqrt{3}} \end{pmatrix} \begin{pmatrix} \widehat{q}_1 \\ \widehat{q}_2 \\ m_4^+ \end{pmatrix}_{NB} \tag{293}$$

$$\begin{pmatrix} \widehat{q}_1 \\ \widehat{q}_2 \\ m_4^+ \end{pmatrix}_{NB} \xrightarrow{S^{NB\to BN}} \begin{pmatrix} \frac{1}{\sqrt{2}} & \frac{1}{\sqrt{2}} & 0 \\ \frac{1}{\sqrt{6}} & -\frac{1}{\sqrt{6}} & \sqrt{\frac{2}{3}} \\ \frac{1}{\sqrt{3}} & -\frac{1}{\sqrt{3}} & -\frac{1}{\sqrt{3}} \end{pmatrix} \begin{pmatrix} m_1 \\ m_2 \\ m_3^+ \end{pmatrix}_{BN} \tag{294}$$

Notice that the matrix is symmetric, and unitary.

Lastly, we can work out the S-matrix on the non-bounding torus.

$$\begin{pmatrix} \bullet h \\ \bullet v \\ X \end{pmatrix}_{NN} \xrightarrow{S^{NN\to NN}} \begin{pmatrix} 0 & i & 0 \\ 1 & 0 & 0 \\ 0 & 0 & -i \end{pmatrix} \begin{pmatrix} \bullet h \\ \bullet v \\ X \end{pmatrix}_{NN} \tag{295}$$

In the idempotent basis, this is

$$\begin{pmatrix} \bullet q_1 \\ \bullet q_2 \\ m_4^+ \end{pmatrix}_{NN} \xrightarrow{S^{NN\to NN}} \frac{e^{i\pi/4}}{\sqrt{2}} \begin{pmatrix} 1 & \Sigma & 0 \\ \Sigma & -1 & 0 \\ 0 & 0 & -\sqrt{2}e^{i\pi/4} \end{pmatrix} \begin{pmatrix} \bullet q_1 \\ \bullet q_2 \\ m_4^+ \end{pmatrix}_{NN} \qquad \text{where } \Sigma = \sigma_1\sigma_2. \tag{296}$$

Note that $S^{NN\to NN}$ splits as $S_q^{NN\to NN} \oplus S_m^{NN\to NN}$ into blocks which operate on q-type and m-type particles, as it must: the basis vectors coming from m-type (q-type) idempotents are even (odd), and S preserves fermion parity.

In summary, we have (296) together with

$$\begin{pmatrix} \begin{pmatrix} m_1 \\ m_2 \\ m_3^+ \end{pmatrix}_{BN} \\ \begin{pmatrix} \widehat{q}_1 \\ \widehat{q}_2 \\ m_4^+ \end{pmatrix}_{NB} \\ \begin{pmatrix} m_1 \\ m_2 \\ m_3^+ \end{pmatrix}_{BB} \end{pmatrix} \xrightarrow{S} \begin{pmatrix} & & & \frac{1}{\sqrt{2}} & \frac{1}{\sqrt{6}} & \frac{1}{\sqrt{3}} & \\ & & & \frac{1}{\sqrt{2}} & -\frac{1}{\sqrt{6}} & -\frac{1}{\sqrt{3}} & \\ & & & 0 & \sqrt{\frac{2}{3}} & -\frac{1}{\sqrt{3}} & \\ \frac{1}{\sqrt{2}} & \frac{1}{\sqrt{2}} & 0 & & & & \\ \frac{1}{\sqrt{6}} & -\frac{1}{\sqrt{6}} & \sqrt{\frac{2}{3}} & & & & \\ \frac{1}{\sqrt{3}} & -\frac{1}{\sqrt{3}} & -\frac{1}{\sqrt{3}} & & & & \\ & & & \frac{1}{d\sqrt{3}} & \frac{d}{2\sqrt{3}} & \frac{1}{\sqrt{3}} & \\ & & & \frac{d}{2\sqrt{3}} & \frac{1}{d\sqrt{3}} & -\frac{1}{\sqrt{3}} & \\ & & & \frac{1}{\sqrt{3}} & -\frac{1}{\sqrt{3}} & \frac{1}{\sqrt{3}} & \end{pmatrix} \begin{pmatrix} \begin{pmatrix} m_1 \\ m_2 \\ m_3^+ \end{pmatrix}_{BN} \\ \begin{pmatrix} \widehat{q}_1 \\ \widehat{q}_2 \\ m_4^+ \end{pmatrix}_{NB} \\ \begin{pmatrix} m_1 \\ m_2 \\ m_3^+ \end{pmatrix}_{BB} \end{pmatrix} \tag{297}$$

7.5.3 T transformation

The Dehn twist (T-transformation) corresponds to cutting the torus open along one cycle, applying a full 2π rotation and then gluing the torus back together along that cycle.

$$T^{XY\to\widetilde{X}\widetilde{Y}}: \quad A(T^2_{XY}) \longrightarrow A(T^2_{\widetilde{X}\widetilde{Y}}) \tag{298}$$

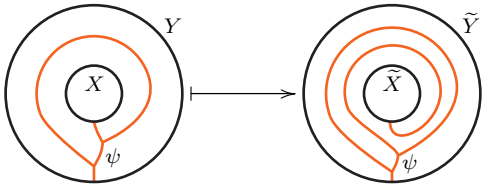

with the spin structure transforming according to Figure 3.3.4. In terms of the matrix elements of T,

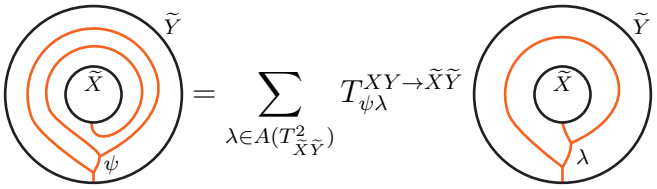

(299)

(300)

Aside from spin structure considerations, all idempotents are eigenstates of the Dehn twist, with T acting diagonally within each spin-structure block.

To find the eigenvalues, we compute the Dehn twist in the topological basis and then change back to the the idempotent basis as usual. We find

$$\begin{pmatrix} \bullet \\ q_1 \\ \bullet \\ q_2 \\ m_4^+ \end{pmatrix}_{NN} \xrightarrow{T^{NN\to NN}} \begin{pmatrix} 1 & 0 & 0 \\ 0 & -i & 0 \\ 0 & 0 & e^{5i\pi/6} \end{pmatrix} \begin{pmatrix} \bullet \\ q_1 \\ \bullet \\ q_2 \\ m_4^+ \end{pmatrix}_{NN} \tag{301}$$

for the NN torus, and

$$\begin{pmatrix} \begin{pmatrix} m_1 \\ m_2 \\ m_3^+ \end{pmatrix}_{BN} \\ \begin{pmatrix} \widehat{q}_1 \\ \widehat{q}_2 \\ m_4^+ \end{pmatrix}_{NB} \\ \begin{pmatrix} m_1 \\ m_2 \\ m_3^+ \end{pmatrix}_{BB} \end{pmatrix} \xrightarrow{T} \begin{pmatrix} & & & & & & 1 & 0 & 0 \\ & & & & & & 0 & 1 & 0 \\ & & & & & & 0 & 0 & e^{i\pi/3} \\ & & & 1 & 0 & 0 & & & \\ & & & 0 & -i & 0 & & & \\ & & & 0 & 0 & e^{5i\pi/6} & & & \\ 1 & 0 & 0 & & & & & & \\ 0 & 1 & 0 & & & & & & \\ 0 & 0 & e^{i\pi/3} & & & & & & \end{pmatrix} \begin{pmatrix} \begin{pmatrix} m_1 \\ m_2 \\ m_3^+ \end{pmatrix}_{BN} \\ \begin{pmatrix} \widehat{q}_1 \\ \widehat{q}_2 \\ m_4^+ \end{pmatrix}_{NB} \\ \begin{pmatrix} m_1 \\ m_2 \\ m_3^+ \end{pmatrix}_{BB} \end{pmatrix} \tag{302}$$

for the spin tori with at least one bounding cycle. One can check that the modular matrices defined above satisfy $S^4 = (-1)^F$ and $(ST)^3 = (-1)^F$.

8 Super pivotal categories

In this section we give a more formal (though not completely formal) definition of super pivotal categories. Since the usual bosonic case is well covered in the literature, we will concentrate on the differences between the bosonic case and the fermionic/super case. We will also fix some notation and conventions used elsewhere in the paper.

There are various ways of axiomatizing string nets, including Kuperberg spiders [44], planar algebras [45], disk-like 2-categories [46], and pivotal tensor categories [47].

The first three are better suited to our applications, but the last one is likely the most familiar to a majority or our readers, so we will describe a fermionic/super version of pivotal tensor categories.

So far as we know, the earliest definition of a super pivotal tensor category was given in [46]. In the higher category definition given in that paper, one of the parameters

was the type of balls used to specify morphism spaces. If we take those balls to be 2-dimensional and equipped with spin structures, then one has a definition of a super pivotal 2-category. We can then take a super pivotal tensor category to be a super pivotal 2-category with only one 0-morphism. The more traditional-style definition given below is reverse-engineered to be equivalent with the definition already contained in [46].

Recall from [47] that the data of a pivotal category includes:

- A set of objects $\mathcal{S}^1$.
- A set of morphisms $\mathcal{S}^2$.
- A binary operation $\otimes$ (horizontal composition) on objects and morphisms.
- A binary operation $\circ$ on morphisms.
- A pivotal structure $*$ defined on both objects and morphisms.

The definition of a super pivotal category differs from the usual bosonic case in the following ways:

1. The space of morphisms between two objects has the structure of a super vector space. Morphisms also satisfy the *super interchange law* [10]:

$$(f_1 \otimes f_2) \circ (g_1 \otimes g_2) = (-1)^{|f_2||g_1|}(f_1 \circ g_1) \otimes (f_2 \circ g_2) \tag{303}$$

   where $|f|$ is the parity of the morphism f.

2. There are two distinct types of simple object, "m-type" and "q-type". m-type simple objects have trivial endomorphism algebras $\mathbb{C}$, as is the case in bosonic theories. q-type simple objects have endomorphism algebras isomorphic to $\mathbb{C}\ell_1$, and so their endomorphism algebras contain odd elements in addition to scalars. (See Section 8.1.)

3. In order to keep track of Koszul signs arising from exchanging fermions, we must keep track of a sign-ordering of individual fusion spaces (See 8.5).

4. Fusion spaces V^{abc}, V^{ab}_c, V_{abcd}, etc. are not merely supervector spaces; they come equipped with an action of the endomorphism algebras of the objects being fused. For example, V^{abc} possess an action of $\mathrm{End}(a) \otimes \mathrm{End}(b) \otimes \mathrm{End}(c)$. (See 8.2.)

5. When combining basic 3-valent fusion spaces V^{ab}_c to form fusion spaces of higher valence, we must take tensor products over the endomorphism algebras of the simple objects which connect two fusion spaces. For example, we form the fusion space V^{ab}_{cd} as $V^{ab}_{cd} \cong \bigoplus_e V^{ab}_e \otimes_{\mathrm{End}(e)} V^e_{cd}$. If e is m-type, this is just the usual tensor product over $\mathbb{C}$, as in the bosonic case. But if e is q-type, then we must take a non-trivial tensor product over $\mathbb{C}\ell_1$. (See 8.6.)

6. The square of the pivotal anti-automorphism is the fermion parity functor $(-1)^F$, rather than the identity functor (see 8.3). If $*$ is the pivotal anti-automorphism, then

$$f^{**} = (-1)^{|f|} f. \tag{304}$$

   In order to keep track of minus signs that result from rotating fermions by 2π, we must keep track of a spin-framing at each fusion space.

7. The coherence equations for the basic data of the theory (e.g. the pentagon relations) are modified to incorporate Koszul signs resulting from reordering various fusion spaces. They are also modified to incorporate the tensor products over endomorphism algebras mentioned above. (see 8.7)

8. In order to define an inner product, we need to equip the manifold on which our string-nets are defined with a $pin_\pm$ structure, which is discussed in Appendix B.

8.1 Simple objects

We will assume that our category $\mathcal{S}$ is *idempotent complete* – every idempotent is the identity morphism of an associated object. We also assume that $\mathcal{S}$ is *additive* – we can take direct sums of objects.

An object a of $\mathcal{S}$ is called *simple* if any homogeneous non-zero endomorphism of a is an isomorphism. Equivalently, a is simple if it has no quotient objects. (We also stipulate that the zero object is not a simple object.)

In the usual bosonic, non-super case, the only possible endomorphism algebra for a simple object is the trivial algebra $\mathbb{C}$ (scalars). In the fermionic/super case, there is a second possibility: the complex Clifford algebra $\mathbb{C}\ell_1$, which is the only nontrivial $\mathbb{Z}_2$-graded division algebra other than $\mathbb{C}$. $\mathbb{C}\ell_1$ is generated over $\mathbb{C}$ by the identity (which is even) and an odd element f such that $f^2 = \lambda \cdot \mathrm{id}$ (or $f^2 = \lambda$ for short) for some non-zero complex number λ. Note that by rescaling the odd generator f we can make λ in the definition of $\mathbb{C}\ell_1$ any nonzero complex number.

It follows that simple objects in a super pivotal category fall into two classes, according to whether their endomorphism algebras are $\mathbb{C}$ or $\mathbb{C}\ell_1$. These are the m-type and q-type objects discussed earlier. A simple object is m-type if its endomorphism algebra is $\mathbb{C}$, and q-type if its endomorphism algebra is $\mathbb{C}\ell_1$:

$$\begin{aligned} \mathrm{End}(x) = \mathbb{C} &\longleftrightarrow x \text{ is a simple m-type object} \\ \mathrm{End}(x) = \mathbb{C}\ell_1 &\longleftrightarrow x \text{ is a simple q-type object} \end{aligned} \tag{305}$$

This terminology comes from the notation of [48], which classifies simple super algebras over $\mathbb{C}$ as either $M(p|q) = \mathrm{End}(\mathbb{C}^{p|q})$ or $Q(n)$ (see appendix C). Note that we are using "simple" here in two different (and well-established) senses: any $M(p|q)$ or $Q(n)$ is a simple super algebra (because it has no non-trivial ideals), but the endomorphism algebra of a simple object must be either $M(1|0) \cong M(0|1) \cong \mathbb{C}$ or $Q(1) \cong \mathbb{C}\ell_1$, because all of the larger $M(p|q)$ or $Q(n)$ contain non-invertible elements.

The existence of q-type particles is responsible for much of the novel physics present after performing fermion condensation. q-type objects were also discussed in [9, 15], where they were referred to as "Majorana objects". (We prefer the m-type/q-type terminology, since it makes clearer the relationship to the Morita classification of simple super algebras.)

8.2 Fusion spaces

Arbitrary morphism spaces in a super pivotal category can be built out of basic fusion spaces $V_c^{ab} = \mathrm{mor}(c \to a \otimes b)$, where a, b and c are simple objects (equivalently, minimal idempotents). This is a super vector space of dimension $N_c^{ab} = \dim V_c^{ab} = p|q$, where p is the dimension of the even part of V_c^{ab} and q is the dimension of the odd part of V_c^{ab}.

Alternatively, we can treat a, b and c more symmetrically and define $V^{abc} = \mathrm{mor}(\mathbb{1} \to a \otimes b \otimes c)$, a super vector space of dimension N^{abc}. In most of this paper we use V_c^{ab}, but in Sections 9 and 10 we find it more convenient to use V^{abc}. Elements of the morphism spaces V^{abc} and V_c^{ab} are depicted by

(306)

We call the fusion spaces V^{abc} "pitchforks" because of their graphical depiction. Of course we have $V_c^{ab} \cong V^{abc^*}$ (see 8.3 below).

More generally, we define $V_{cd}^{ab} = \mathrm{mor}(c \otimes d \to a \otimes b)$, $V_{cde}^{ab} = \mathrm{mor}(c \otimes d \otimes e \to a \otimes b)$, $V_{abcd} = \mathrm{mor}(a \otimes b \otimes c \otimes d \to \mathbb{1})$, and so on. In general, we do not require that the objects a, b etc. be simple.

It is very important to note that V_c^{ab} is not merely a super vector space – it also comes equipped with an action of (i.e. module structure for) the endomorphism algebras of a, b and c, and hence admits an action of $\mathrm{End}(a) \otimes \mathrm{End}(b) \otimes \mathrm{End}(c)$. It is impossible to construct the full super pivotal category without knowing this module structure (see 8.6 below), so the module structure is part of the input data. Note that the module structure implies that $N_c^{ab} = n|n$ if any of a, b or c is q-type. This is because any representation of $\mathbb{C}\ell_1$ has equal even and odd dimensions. Acting with the odd (and invertible) element of $\mathbb{C}\ell_1$ gives an isomorphism between the even and odd parts of V_c^{ab}, and hence they must have the same dimension.

The explicit matrix elements of these isomorphisms can be defined in the following way. Let $\psi \in V_c^{ab}$ and suppose that b is a q-type simple object, and let $\Gamma_b \in \mathrm{End}(b)$ be an odd endomorphism. Then

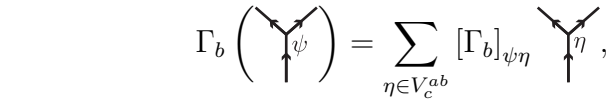

(307)

where the matrix elements are obtained from

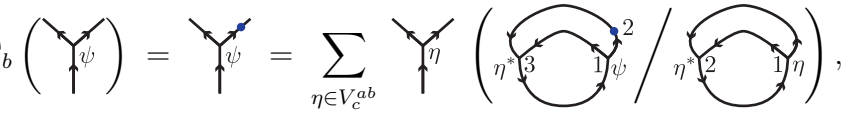

(308)

where the η^* provide a complete orthogonal basis (with respect to the pairing (310)) for $V_{c^*}^{b^*a^*}$. If either a or c are q-type, then Γ_a and Γ_c matrices can be defined in a similar way.

If at least one of a, b, c is q-type, we can simplify the description of V_c^{ab} slightly, which we have done when working out the examples considered earlier. Suppose c is q-type, and that $\{|\psi_i\rangle\} \in [V_c^{ab}]^0, i = 1, \ldots, r$ are the even basis vectors in V_c^{ab}. Then we can define a complete set of odd basis vectors $\{|\eta_i\rangle\}$ for $[V_c^{ab}]^1$ by $|\eta_i\rangle = f|\psi_i\rangle$, where f is the odd element of $\mathrm{End}(c) \cong \mathbb{C}^{1|1}$. When we write $|\eta_i\rangle$ graphically, we will write it as $f|\psi\rangle$, which allows us to "shift the oddness out of the vertex onto the edge" by transferring the fermion residing on the fusion space to the q-type particle c. Graphically, this means

that we are allowed to "displace" dots from trivalent vertices onto q-type worldlines:

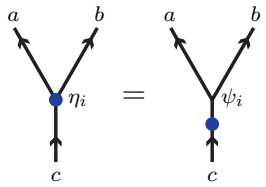

(309)

where the picture on the left is $|\eta_i\rangle$ and the one on the right is $f|\psi_i\rangle$, and c is assumed to be q-type. Although this is not a deep fact, it proves to be helpful when doing graphical manipulations, and operators implementing transformations like (309) will be crucial for writing down the lattice Hamiltonian which realizes the super pivotal version of the Levin-Wen Hamiltonian.

Lastly, we will define a non-degenerate bilinear pairing between vectors in the vector space assigned to a disk with n marked points. We will focus on fusion spaces of the form $V^{x_1 \cdots x_n}$, but the construction for different types of fusion spaces is analogous. The pairing is defined by

$$\mathcal{B} : V^{x_n^* \cdots x_2^* x_1^*} \otimes V^{x_1 x_2 \cdots x_n} \to \mathbb{C} \tag{310}$$

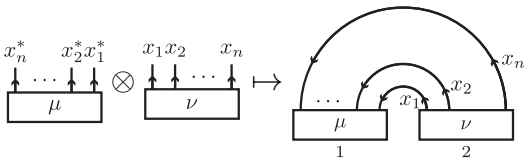

where $\mu \in V^{x_n^* \cdots x_2^* x_1^*}$ and $\nu \in V^{x_1 x_2 \cdots x_n}$. We are working with the convention that the Koszul ordering of the tensor product increases in a left-to-right fashion (indicated by the numbers $1, 2$ in the bottom right of (310)); we will elaborate on this convention in Section 8.5. This bilinear pairing is just the evaluation map, and is $\mathbb{C}$-linear in both its arguments. It is non-degenerate, meaning that if ν_j is a complete basis for the fusion space $V^{x_1 x_2 \cdots x_n}$ and μ_i is a complete basis for the dual fusion space $V^{x_n^* \cdots x_2^* x_1^*}$, then the matrix $\mathcal{B}_{ij} = \mathcal{B}(\mu_i \otimes \nu_j)$ is invertible. Hence we can define a set of vectors $\mu_j^* = \sum_i (\mathcal{B}^{-1})_{ji} \nu_i$ so that $\mathcal{B}(\mu_j^* \otimes \mu_i) = \delta_{ij}$. Alternatively, we will can choose the normalization convention

$$\mathcal{B}(\mu_j^* \otimes \mu_i) = \sqrt{d_a d_b d_c}\, \delta_{ij}, \tag{311}$$

with $\mu_i \in V^{abc}$ and $\mu_j^* \in V^{c^* b^* a^*}$.

8.3 Pivotal structure

The pivotal structure assigns to each object a a dual object a^*. It also provides linear isomorphisms

$$P_L : \mathrm{mor}(a \to b \otimes c) \to \mathrm{mor}(b^* \otimes a \to c) \tag{312}$$

and

$$P_R : \mathrm{mor}(a \otimes b \to c) \to \mathrm{mor}(a \to c \otimes b^*) \tag{313}$$

for any objects a, b and c. These isomorphisms are required to be functorial with respect to a and c. In addition, they are required to be twisted-functorial with respect to b/b^*, where we use the $*$ functor (defined below) to relate morphisms with domain b to morphisms with range b^*.

For objects a, we require that $a^{**} = a$ on the nose (strict pivotal). For morphisms $f : a \to b$, we define $f^* : b^* \to a^*$ by $f^* = P_L(P_R(f))$, diagrammatically by,

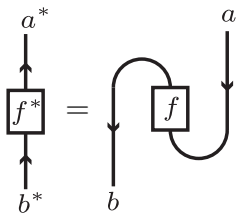

(314)

(We have implicitly added and then removed some tensor units (trivial objects) here appearing in fusion spaces like $V_{\mathbb{1}}^{aa^*}$.) We think of f^* as a $+\pi$ rotation of the morphism f. We have

$$(f \cdot g)^* = (-1)^{|f||g|} g^* \cdot f^*. \tag{315}$$

In other words, $*$ is a contravariant functor if one takes Koszul signs into account.

For (strict) pivotal bosonic categories, one requires that $**$ is the identity functor, but in the fermionic case one requires that $**$ is the spin-flip functor $(-1)^F$. More specifically, we require

$$f^{**} = (-1)^{|f|} f, \tag{316}$$

since f^{**} is a 2π rotation of f.

The part of the pivotal structure most used in calculations is the $+2\pi/3$ rotation on the basic trivalent fusion spaces. We define the "pivot" $P_c^{ab} : V_c^{ab} \to V_{a^*}^{bc^*}$ as $P_R \circ P_L$. In terms of diagrams and matrices, this looks like

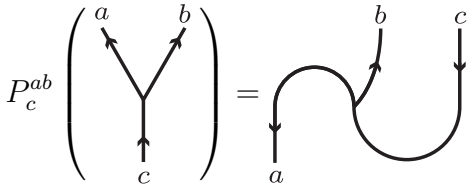

(317)

The Frobenius-Schur indicator κ_a can be computed in terms of pivot maps. If $a \cong a^*$, then κ_a is the eigenvalue of the composite map

$$V_{a^*}^a \xrightarrow{U_r} V_{a^*}^{a1} \xrightarrow{P} V_{a^*}^{1a} \xrightarrow{U_l^{-1}} V_{a^*}^a, \tag{318}$$

where U_r and U_l^{-1} are given by post-composition with the canonical isomorphisms (a.k.a. unitors) $a \xrightarrow{\sim} a \otimes \mathbb{1}$ and $a \xrightarrow{\sim} \mathbb{1} \otimes a$. (If a is q-type then we take the eigenvalue for the even part of $V_{a^*}^a$.)

We also note that the modular S matrix gives the square of the Frobenius-Schur indicator. If $a \cong a^*$ we have $\kappa_a^2 = (S^2)_{aa}$. For a bosonic theory the Frobenius-Schur indicators are ± 1, and this provides no new information. But in fermionic theories the oddly self-dual simple objects have Frobenius-Schur indicators of $\pm i$, and this is detected by the diagonal entries of S^2. The m_4 particle in the $\frac{1}{2}\mathrm{E}_6/y$ theory is an example of this; see (296).

We can similarly define $P^{abc} : V^{abc} \to V^{bca}$. In terms of diagrams,

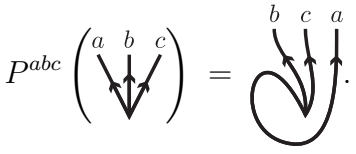

(319)

We will usually write simply P, since the a, b and c are typically clear from context.

Since P^3 acts as a 2π rotation, we have $P^3 = (-1)^F$. Diagrammatically, when acting on V^{abc} this is written

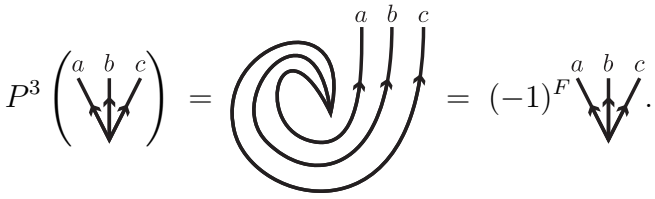

(320)

8.4 Fusion rules and fusion spaces

In this section we elaborate on the differences arising in fermionic theories between fusion spaces and the super vector spaces appearing in the fusion rules.

We assume that our categories are additively complete, which means that it makes sense to multiply objects by super vector spaces. (This is a categorified version of multiplying vectors by scalars. Vectors are promoted to objects and scalars are promoted to vector spaces.) For any collection of super vector spaces $\{W_a\}$ indexed by a finite set of objects $\{a\}$ in our category, we therefore have an object of the form

$$\bigoplus_a W_a \cdot a. \tag{321}$$

Morphisms between these more general objects are calculated as

$$\mathrm{mor}(\bigoplus_a W_a \cdot a \to \bigoplus_b W'_b \cdot b) = \bigoplus_{a,b} \mathrm{Hom}(W_a \to W'_b) \otimes_{\mathbb{C}} \mathrm{mor}(a \to b). \tag{322}$$

Because our category is semisimple, there exists a finite collection $\mathrm{sob}_r(\mathcal{S})$ of mutually non-isomorphic simple objects x such that any object a is isomorphic to one of the form

$$a \cong \bigoplus_{x \in \mathrm{sob}_r(\mathcal{S})} W_x \cdot x. \tag{323}$$

If we want the isomorphism to be canonical, we can take $W_x = \mathrm{mor}(x \to a)$ if x is m-type, or W_x to be the even morphisms in $\mathrm{mor}(x \to a)$ if x is q-type.

Combining (323) and (322), we can compute endomorphisms of objects by

$$\mathrm{End}(a) \cong \bigoplus_{x \in \mathrm{sob}_r(\mathcal{S})} \mathrm{End}(W_x) \otimes_{\mathbb{C}} \mathrm{End}(x). \tag{324}$$

We are now ready to discuss fusion rules. For any a and b, define the vector spaces Δ_c^{ab} by

$$a \otimes b \cong \bigoplus_{c \in \mathrm{sob}_r(\mathcal{S})} \Delta_c^{ab} \cdot c. \tag{325}$$

The Δ_c^{ab} are the fusion rule coefficients.

The fusion spaces V_c^{ab} are defined as the vector space of morphisms from c to $a \otimes b$:

$$V_c^{ab} = \mathrm{mor}(c \to a \otimes b), \tag{326}$$

where a, b, c are simple objects. Decomposing the tensor product and using the simplicity of c, we see that

$$V_c^{ab} \cong \Delta_c^{ab} \otimes \mathrm{mor}(\mathrm{c} \to \mathrm{c}) \cong \Delta_{\mathrm{c}}^{\mathrm{ab}} \otimes \mathrm{End}(\mathrm{c}). \tag{327}$$

Thus, the fusion spaces can be larger than the vector spaces appearing in the fusion rules (in contrast to bosonic theories, where the fusion spaces and fusion rule coefficients are always equal). As examples, in the C_2 theory studied earlier, we have

$$\Delta_{m_\psi}^{q_\sigma q_\sigma} \cong \mathbb{C}^{1|1}, \quad \Delta_{q_\sigma}^{q_\sigma m_{\mathbb{1}}} \cong \mathbb{C}, \tag{328}$$

while

$$V_{m_\psi}^{q_\sigma q_\sigma} \cong V_{q_\sigma}^{q_\sigma m_{\mathbb{1}}} \cong \mathbb{C}^{1|1}. \tag{329}$$

V_x^{ab} is cyclically symmetric (up to isomorphism) in a, b, x (if a and b are simple). Explicitly, this is because

$$\mathrm{mor}(c \to a \otimes b) \cong \mathrm{mor}(\mathbb{1} \to a \otimes b \otimes c^*) \cong \mathrm{mor}(a^* \to b \otimes c^*), \tag{330}$$

which allows us to cyclicly permute the indices of V, so long as we take the duals of any objects that move from subscripts to superscripts, and vice versa. For example, we have $V_c^{ab} \cong V_{a^*}^{bc^*} \cong V_{b^*}^{c^*a}$.

On the other hand, Δ_c^{ab} is *not* cyclically symmetric in a, b, c, as the C_2 theory example shows. Additionally, while V_c^{ab} has an action of $\mathrm{End}(a) \otimes \mathrm{End}(b) \otimes \mathrm{End}(c)$ (as mentioned earlier), Δ_c^{ab} only has an action of $\mathrm{End}(a) \otimes \mathrm{End}(b)$.

8.5 Koszul sign rule and unordered tensor products

We will treat Koszul signs as in [49, Section 1.2]. This approach doesn't really do away with Koszul signs. Rather, it pushes them to the background, where they don't need to be mentioned as frequently. For explicit calculations, they must again be brought to the foreground.

Let I be a finite (and unordered) index set. For each $i \in I$, let W_i be a super vector space. We define the unordered tensor product,

$$\bigotimes_{i \in I} W_i, \tag{331}$$

as follows. For each bijection $f : \{1, \ldots, m\} \to I$ (i.e. for each ordering of I), we have the ordered tensor product

$$T_f = W_{f(1)} \otimes \cdots \otimes W_{f(m)}, \tag{332}$$

generated by elements

$$w_{f(1)} \otimes \cdots \otimes w_{f(m)}. \tag{333}$$

For any two orderings f and g, there is a Koszul isomorphism

$$K_{fg} : T_f \to T_g, \tag{334}$$

characterized by[22]

$$K_{fg} : w_{f(1)} \otimes \cdots \otimes w_{f(k)} \otimes w_{f(k+1)} \otimes \cdots \otimes w_{f(m)} \mapsto \\ (-1)^{|w_{f(k)}||w_{f(k+1)}|} w_{f(1)} \otimes \cdots \otimes w_{f(k+1)} \otimes w_{f(k)} \otimes \cdots \otimes w_{f(m)} \quad (335)$$

when g differs from f by a simple transposition at k, and

$$K_{gh} \circ K_{fg} = K_{fh}. \quad (336)$$

An element of the unordered tensor product is then defined as an assignment to each ordering f of an element $t_f \in T_f$ such that

$$K_{fg}(t_f) = t_g \quad (337)$$

for all orderings f and g. In other words, an element of the unordered tensor product is a collection of elements in all possible ordered tensor products which are related by the usual Koszul sign rules.

Note that to specify an element of the unordered tensor product, it suffices to give an element t_f of one particular ordered tensor product T_f. All of the other t_g are uniquely determined by t_f.

When writing equations involving particular ordered tensor products of fusion spaces, we will adopt the convention that the Koszul ordering is left-to-right on the page, unless explicitly indicated otherwise. If we want to indicate an ordering which departs from this left-to-right convention, we will indicate the ordering explicitly with numerical subscripts, e.g. $V_{c,1}^{ab} \otimes V_{e,2}^{cd}$. This explicit notation is often better suited to our diagrammatic calculus, where we frequently label the Koszul ordering of fermion dots in a way that is not tied to the left-to-right order in which we write down tensor products (this was done throughout Sections 2 and 3, for example).

When drawing diagrams with a particular ordering in mind, we always indicate the ordering explicitly by numbers near each fusion space (i.e. near each vertex in the string net). Another possible convention would be to use the ordering corresponding to (say) bottom-to-top on the page, but this creates opportunities for error when changing diagrams by isotopies, and is not really workable for diagrams drawn on higher genus surfaces.

A map between unordered tensor products

$$\bigotimes_i W_i \ \to \ \bigotimes_j V_j \quad (338)$$

is defined to be a collection of maps between all possible pairs of ordered tensor products. We will call such a collection an "unordered map". These maps are required to commute with the Koszul isomorphisms on either side. To specify such a map, it suffices to give a single map between one particular pair of ordered tensor products. All other maps in the collection are uniquely determined by this choice and the commutativity requirement. This map will be called an "ordered representative" of the unordered map. See 8.8 for a further discussion of the distinction between unordered maps and their ordered representatives.

[22] We should stress that in this section, the left-to-right ordering of tensor factors appearing in equations is tied to their Koszul ordering only, and is independent of the order in which they appear when written down in diagrams. This is in contrast to several other points in the paper, where $a \otimes b$ translates graphically into placing a horizontally next to b on the page.

8.6 Modified tensor product

Let $\mathrm{sob}_r(\mathcal{S})$ be a complete collection of simple objects (minimal idempotents) in some input super fusion category $\mathcal{S}$, one from each equivalence class. (In this subsection, as in most of the paper, we are assuming that our category $\mathcal{S}$ is semisimple with finitely many equivalence classes of simple objects.) For arbitrary objects x and y, we have

$$\mathrm{mor}(x \to y) \;\cong \bigoplus_{a \in \mathrm{sob}_r(\mathcal{S})} \mathrm{mor}(x \to a) \otimes_{\mathrm{End}(a)} \mathrm{mor}(a \to y). \tag{339}$$

Recall that the relative tensor product $\otimes_{\mathrm{End}(a)}$ on the RHS above is defined as the usual tensor product over scalars, modulo elements of the form $\alpha \cdot f \otimes \beta - \alpha \otimes f \cdot \beta$ with $\alpha \in \mathrm{mor}(x \to a)$, $\beta \in \mathrm{mor}(a \to y)$ and $f \in \mathrm{End}(a)$. Clearly such elements are in the kernel of the composition map $\mathrm{mor}(x \to a) \otimes \mathrm{mor}(a \to y) \to \mathrm{mor}(x \to y)$. Our semisimplicity assumption implies that the composition map (summing over all $a \in \mathrm{sob}_r(\mathcal{S})$) is surjective and that such elements generate all of the kernel.

In terms of diagrams, the relative tensor product is responsible for allowing fermionic dots to move across edges labeled by q-type simple objects. Loosely, taking a tensor product over $\mathrm{End}(a)$ when a is q-type allows us to identify diagrams that differ only by the position of a fermionic dot on an a strand.

It follows (though not quite directly) from (339) that we have isomorphisms

$$V_d^{abc} \cong \bigoplus_{x \in \mathrm{sob}_r(\mathcal{S})} V_x^{ab} \otimes_{\mathrm{End}(x)} V_d^{xc} \tag{340}$$

and also

$$V_d^{abc} \cong \bigoplus_{y \in \mathrm{sob}_r(\mathcal{S})} V_d^{ay} \otimes_{\mathrm{End}(y)} V_y^{bc}. \tag{341}$$

Diagrammatically these read,

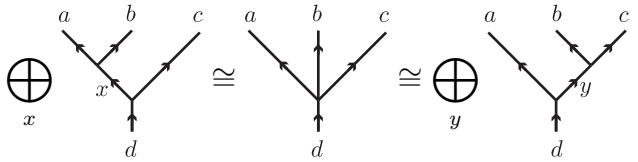

(342)

where the unlabeled trivalent vertices denote the fusion spaces V_x^{ab}, V_d^{xc}, V_d^{ay}, V_y^{bc}, and the unlabeled tetravalent vertex in the middle diagram denotes the fusion space V_d^{abc}. The tensor product over endomorphisms is implicit in the diagram. Similarly,

$$V^{abcd} \cong \bigoplus_{x \in \mathrm{sob}_r(\mathcal{S})} V_x^{ab} \otimes_{\mathrm{End}(x)} V^{xcd}, \tag{343}$$

and using the isomorphism $P_R : V_x^{ab} \to V^{abx^*}$ this becomes

$$V^{abcd} \cong \bigoplus_{x \in \mathrm{sob}_r(\mathcal{S})} V^{abx} \otimes_{\mathrm{End}(x)} V^{x^*cd}. \tag{344}$$

(We are implicitly using the $*$ functor to convert an $\mathrm{End}(x)$ action into an $\mathrm{End}(x^*)$ action.) Alternatively,

$$V^{abcd} \cong \bigoplus_{x \in \mathrm{sob}_r(\mathcal{S})} V_x^{bc} \otimes_{\mathrm{End}(x)} V^{axd} \cong \bigoplus_{x \in \mathrm{sob}_r(\mathcal{S})} V^{axd} \otimes_{\mathrm{End}(x)} V^{x^*bc}. \tag{345}$$

Diagrammatically we have,

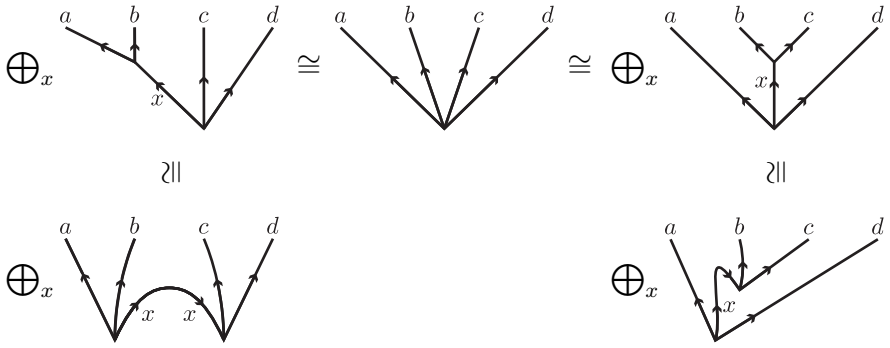

(346)

8.7 F-symbols

It follows from (340) and (341) that there is an isomorphism

$$F_d^{abc} : \bigoplus_{x\in \mathrm{sob}_r(\mathcal{S})} V_x^{ab} \otimes_{\mathrm{End}(x)} V_d^{xc} \to \bigoplus_{y\in \mathrm{sob}_r(\mathcal{S})} V_d^{ay} \otimes_{\mathrm{End}(y)} V_y^{bc}. \tag{347}$$

For the pitchfork version, we instead use (344) and (345) to obtain

$$F^{abcd} : \bigoplus_{x\in \mathrm{sob}_r(\mathcal{S})} V^{abx^*} \otimes_{\mathrm{End}(x)} V^{xcd} \to \bigoplus_{x\in \mathrm{sob}_r(\mathcal{S})} V^{bcx^*} \otimes_{\mathrm{End}(x)} V^{axd}. \tag{348}$$

The tensor products appearing in the above isomorphisms are unordered tensor products. For numerical applications, particular ordered representatives of the tensor products need to be chosen. For the ordered F_d^{abc} isomorphism, we will adopt the convention

$$F_d^{abc} : \bigoplus_{x\in \mathrm{sob}_r(\mathcal{S})} V_d^{xc} \otimes_{\mathrm{End}(x)} V_x^{ab} \to \bigoplus_{y\in \mathrm{sob}_r(\mathcal{S})} V_d^{ay} \otimes_{\mathrm{End}(y)} V_y^{bc}, \tag{349}$$

with implicit sign ordering which increases from left to right on the page. Graphically, and written as a matrix equation, we thus have

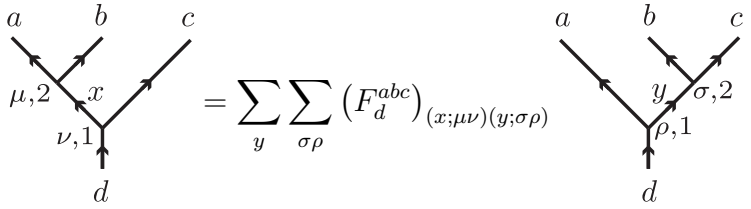

(350)

where the greek indices label particular fusion space basis vectors, with $\mu \in V_x^{ab}, \nu \in V_d^{xc}, \alpha \in V_y^{bc}$, and $\beta \in V_d^{ay}$, and where the first sum is over $y \in \mathrm{sob}_r(\mathcal{S})$. We also stick with the left-to-right ordering convention for the F^{abcd} move:

$$F^{abcd} : \bigoplus_{x\in \mathrm{sob}_r(\mathcal{S})} V^{abx} \otimes_{\mathrm{End}(x)} V^{x^*cd} \to \bigoplus_{y\in \mathrm{sob}_r(\mathcal{S})} V^{ayd} \otimes_{\mathrm{End}(x)} V^{y^*bc}. \tag{351}$$

Which written as a matrix equation is

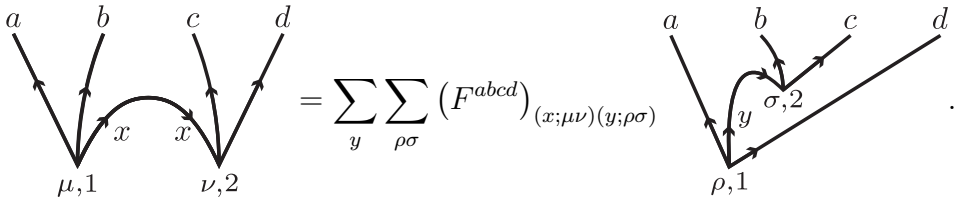

(352)

We will also find the following identity helpful:

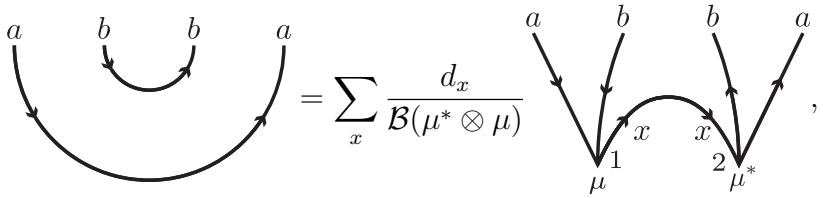

(353)

where the pairing $\mathcal{B}$ is defined in (310).

8.8 Coherence relations

We will not list all coherence relations here. Instead we will give a few examples, in order to highlight how the bosonic case must be changed to take account of Koszul signs and relative tensor products.

We will start with the well-known pentagon equation, in the version that uses the basic fusion spaces V_c^{ab}. If we work in terms of *unordered maps*, with (347) interpreted as an unordered map between direct sums of unordered tensor products, then the fermionic pentagon equation looks just like the bosonic case, namely that the following diagram commutes:

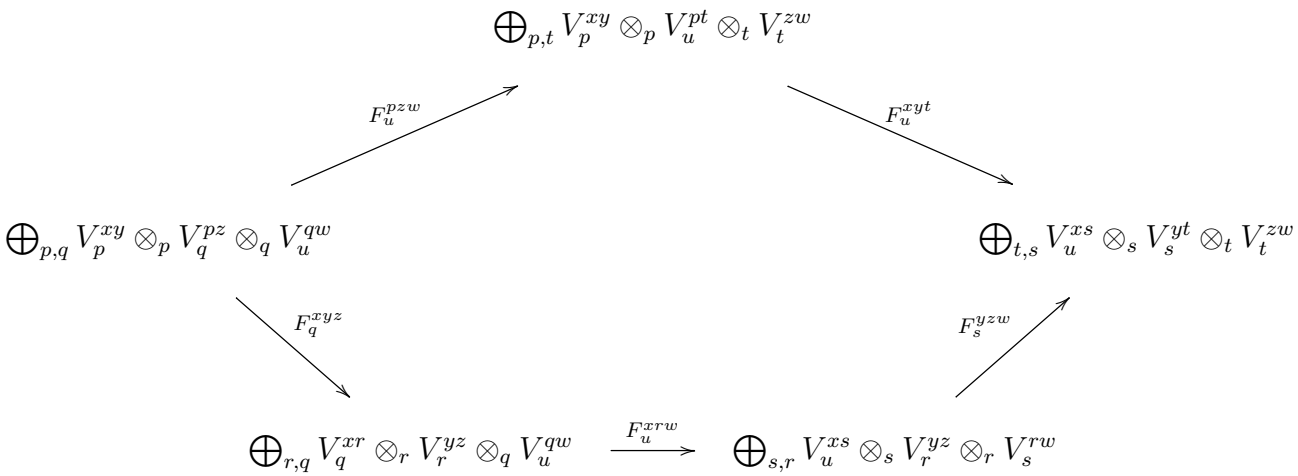

(354)

where all the sums are over a representative set of simple objects and we have used the notation $\otimes_x \equiv \otimes_{\mathrm{End}(x)}$.

However, if we peer under the hood and look at *ordered representatives* (as we would need to do if, for example, we were checking the pentagon equation on a computer), then we see that a Koszul sign appears:

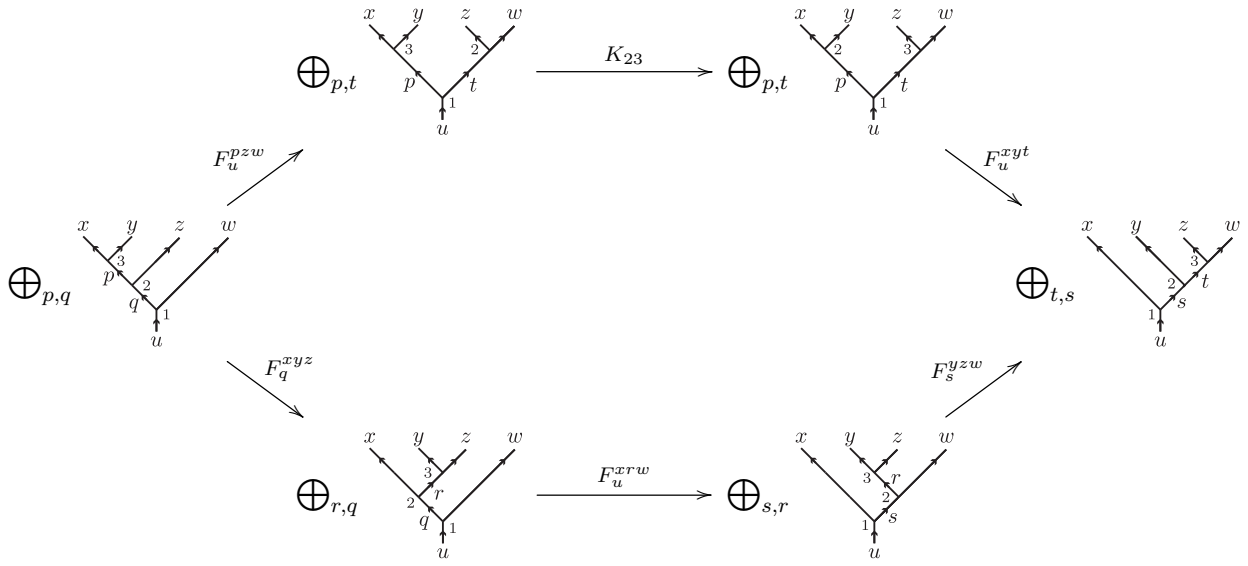

(355)

or equivalently,

$$\begin{array}{ccc} \bigoplus_{p,t}(V_u^{pt}\otimes_t V_t^{zw})\otimes_p V_p^{xy} & \xrightarrow{K_{23}} & \bigoplus_{p,t}(V_u^{pt}\otimes_p V_p^{xy})\otimes_t V_t^{zw} \\ {\scriptstyle F_u^{pzw}}\nearrow & & \searrow{\scriptstyle F_u^{xyt}} \\ \bigoplus_{p,q} V_u^{qw}\otimes_q V_q^{pz}\otimes_p V_p^{xy} & & \bigoplus_{t,s} V_u^{xs}\otimes_s V_s^{yt}\otimes_t V_t^{zw} \\ {\scriptstyle F_q^{xyz}}\searrow & & \nearrow{\scriptstyle F_s^{yzw}} \\ \bigoplus_{r,q} V_u^{qw}\otimes_q V_q^{xr}\otimes_r V_r^{yz} & \xrightarrow{F_u^{xrw}} & \bigoplus_{s,r} V_u^{xs}\otimes_s V_s^{rw}\otimes_r V_r^{yz} \end{array} \tag{356}$$

Here, K_{23} denotes the Koszul isomorphism associated to transposing the second and third tensor factors. Again, we are using the implicit left-to-right Koszul ordering of each tensor product. In terms of the matrix elements of the F-symbols, this reads

$$\begin{aligned} \sum_{r\in \mathrm{sob}_r(\mathcal{S})}\sum_{\sigma\in V_q^{xr}}\sum_{\omega\in V_r^{yz}}\sum_{\eta\in V_s^{rw}} & [F_q^{xyz}]_{(p;\mu\nu)(r;\omega\sigma)}[F_u^{xrw}]_{(q;\sigma\lambda)(s;\eta\gamma)}[F_s^{yzw}]_{(r;\omega\eta)(t;\alpha\delta)} \\ &= \sum_{\beta\in V_u^{pt}}[F_u^{pzw}]_{(q;\nu\lambda)(t;\alpha\beta)}(-1)^{|\mu||\alpha|}[F_u^{xyt}]_{(p;\mu\beta)(s;\delta\gamma)}, \end{aligned} \tag{357}$$

where $\mu\in V_p^{xy}, \nu\in V_q^{pz}, \lambda\in V_u^{qw}, \gamma\in V_u^{xs}, \delta\in V_s^{yt}$, and $\alpha\in V_t^{zw}$. The Koszul sign K_{23} appearing in (356) appears in the above formula as $(-1)^{|\mu||\alpha|}$.

Other coherence relations are modified to take into account Koszul signs. For example, requiring consistency between F-moves and the pivot means that the following diagram

must commute:

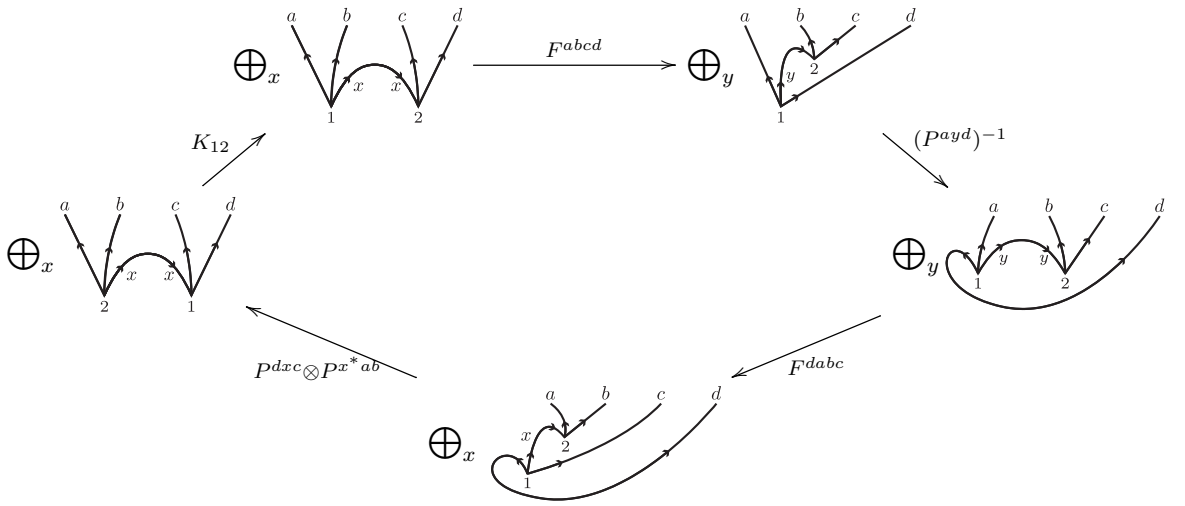

(358)

8.9 Reflection structure

A *reflection structure* on $\mathcal{S}$ is an antilinear anti-automorphism r from $\mathcal{S}$ to itself which preserves (rather than reverses) the the tensor product:

$$\begin{aligned} a &\mapsto r(a) && (359)\\ \alpha : a \to b &\mapsto r(\alpha) : r(b) \to r(a) && (360)\\ r(\lambda\alpha) &= \bar{\lambda} r(\alpha) && (361)\\ r(\alpha\beta) &= r(\beta) r(\alpha) && (362)\\ r(a \otimes b) &= r(a) \otimes r(b) && (363)\\ r(\alpha \otimes \beta) &= r(\alpha) \otimes r(\beta) && (364) \end{aligned}$$

for objects a, b and morphisms α, β. Diagrammatically, the action of r reflects diagrams about the horizontal axis (while acting as complex conjugation on $\mathbb{C}$). Outside of this section, we usually denote r by a bar: $\bar{a} = r(a)$ and $\bar{\alpha} = r(\alpha)$.

For objects, we require that $r(r(a)) = a$.[23] For morphisms, we have two choices. In a pin+ reflection structure, we require r^2 to be the identity functor:

$$r^2 = \mathrm{id}. \tag{365}$$

In a pin− reflection structure, we require r^2 to be the spin flip functor,

$$r^2 = (-1)^F. \tag{366}$$

The main examples of this paper all have pin+ reflection structures.

We require r to be compatible with the other structure maps of $\mathcal{S}$ (pivots, F, etc.).

[23] We also frequently restrict our attention to reflection-invariant objects which satisfy $r(a) = a$, but this is not a requirement for all objects.

For example, we require the following diagrams to be commutative:

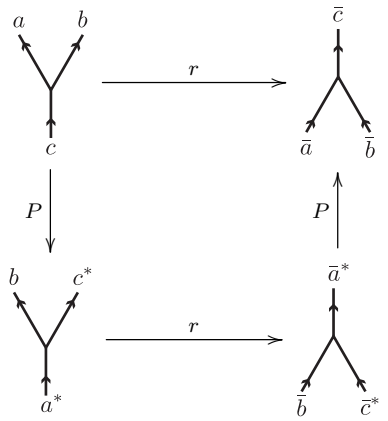

(367)

and

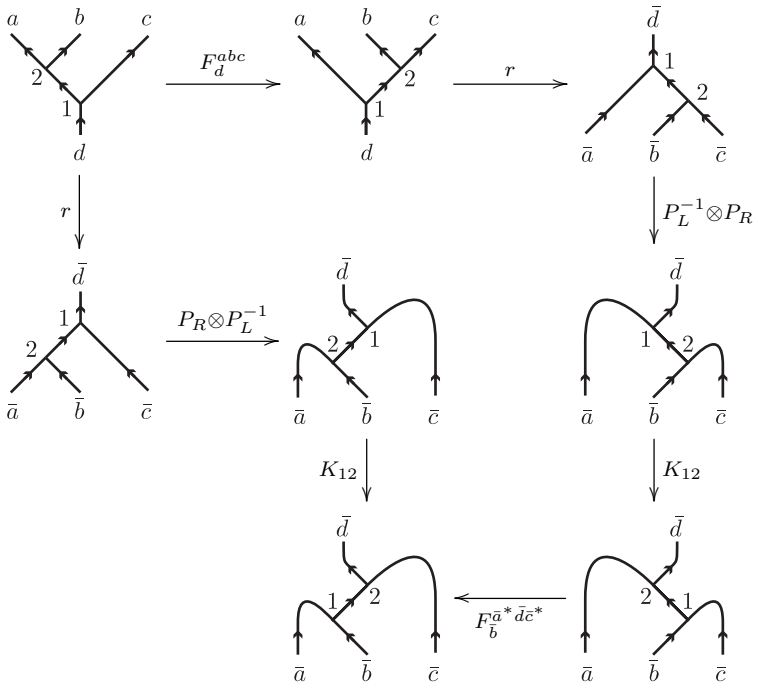

(368)

A pin+ reflection structure on $\mathcal{S}$ allows us to define the action of pin+ diffeomorphisms on $\mathcal{S}$ string nets.

It follows from the "back wall" line bundle construction of Appendix B that super pivotal categories $\mathcal{C}/\psi$ obtained via fermion condensation will have pin+ reflection structures whenever the parent category has an ordinary bosonic reflection structure.

Our main use for pin+ reflections is to define a sesquilinear inner product on the string net space $A(Y;c)$. Let Y be a spin surface and let $-Y$ denote the same underlying surface but with the reversed spin structure. The "identity" map from Y to $-Y$ is not a spin diffeomorphism (as it reverses orientation), but it is a pin+ diffeomorphism. Using the reflection structure on $\mathcal{S}$, we can use this pin+ diffeomorphism to map string nets in $A(Y;c)$ to string nets in $A(-Y;r(c))$. If $r(c) = c^*$, then string nets in $A(Y;c)$ and $A(-Y;r(c))$ can be glued together to get a string net on the closed spin surface $Y \cup_{\partial Y} -Y = \partial(Y \times I)$. Using the path integral $Z(Y \times I) : A(Y \cup_{\partial Y} -Y) \to \mathbb{C}$ now yields a sesquilinear inner product on $A(Y;c)$. Since $A(Y;c)$ is finite-dimensional, we also get an inner product on the dual space $Z(Y;c)$.

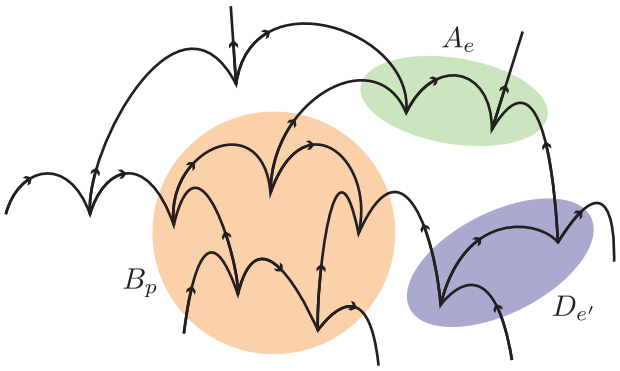

Figure 9.0.1: A cartoon of the support of the operators appearing in a super pivotal Hamiltonian on a section of a generic graph. The motivation for the strange-looking vertices is explained in Section 9.2. Dashed ellipses indicate the support of various terms in the Hamiltonian, on edges e, e' and a plaquette p. The vertex terms A_e act on edges and project onto states with edge colorings that are consistent between adjacent vertices. The edge terms D_e are responsible for sliding fermions along q-type edges. The plaquette terms B_p involve all of the vertices and edges neighboring p. They project onto graph configurations that contain no quasiparticles within the plaquette p.

Let M be a spin 3-manifold. Then the path integrals $Z(M) : A(\partial M) \to \mathbb{C}$ and $Z(-M) : A(-\partial M) \to \mathbb{C}$ are related by

$$Z(-M) = Z(M) \circ R, \tag{369}$$

where $R : A(-\partial M) \to A(\partial M)$ is the antilinear map induced by the orientation-reversing identity map from $-\partial M$ to ∂M. Equivalently, $Z(M) \in Z(\partial M)$ and $Z(-M) \in Z(-\partial M)$ and

$$Z(M) = R(Z(-M)). \tag{370}$$

Let Y_1 and Y_2 be spin surfaces and let M be a cobordism from Y_1 to Y_2 (i.e. $\partial M = Y_2 \cup -Y_1$). Then $-M$ is a cobordism from Y_2 to Y_1. The path integrals can be viewed as maps $Z(M) : Z(Y_1) \to Z(Y_2)$ and $Z(-M) : Z(Y_2) \to Z(Y_1)$. It follows from (370) that $Z(-M)$ is the adjoint of $Z(M)$ with respect to the inner products on $Z(Y_1)$ and $Z(Y_2)$ defined above.

9 Super pivotal Hamiltonian

In this section we will write down a commuting projector Hamiltonian for a generic fermionic topological phase. Since our goal in this section is to be rather general, we will put a fair amount of effort into making our construction mathematically precise – readers who are only interested in the final result may skip to 9.3.

We will follow the same basic construction as in [23], with modifications to take into account the fermionic nature of the phases under consideration. The most important modifications are as follows: First, we will need to fix a spin structure on the manifold on which we are working. This spin structure affects the details of the local projections which constitute the Hamiltonian, and is a necessary feature of any fermionic lattice model. Additionally, we will need to allow the local degrees of freedom that constitute the

Hilbert space for our lattice model to be super vector spaces, rather than the regular vector spaces in bosonic models. Finally, we will need to add a new term in the Hamiltonian with support on the edges and pairs of neighboring vertices in the lattice that allows fermions to fluctuate across edges that host q-type strings.

To begin the construction of the lattice model, we will thus need the following data:

1. a super pivotal fusion category $\mathcal{C}$,
2. a spin surface Σ,
3. and a graph $\mathcal{G}$ embedded in Σ (more precisely, a cell decomposition of Σ) which inherits information about the spin structure.

In the following subsections we define the Hamiltonian explicitly in terms of the above data.

We will write a frustration-free Hamiltonian as a sum of local projectors, which fall into three classes. Two of these classes of projector are the fermionic analogues of the plaquette and vertex terms from the usual Levin-Wen Hamiltonian, while the third is an edge term which allows fermions to fluctuate across edges hosting q-type strings. The Hamiltonian takes the form

$$H = \lambda_p \sum_{p \in \mathcal{F}} (1 - B_p) + \lambda_e \sum_{e \in \mathcal{E}} (1 - D_e) + \lambda_v \sum_{e \in \mathcal{E}} (1 - A_e), \tag{371}$$

where the sums are over the plaquettes (faces) $\mathcal{F}$ and edges $\mathcal{E}$ of the graph, and the $\lambda_p, \lambda_e, \lambda_v$ are positive constants. As in the bosonic case, we require a hierarchy in the couplings of $\lambda_v \gg \lambda_e \gg \lambda_p$.[24] This is because the operators appearing in the plaquette terms are not well-defined unless the edge term energies are minimized, and in turn the terms appearing in the edge operators are not well-defined unless the terms involving A_e are minimized. Thus, the projectors associated with k-cells are only defined on the ground states of the projectors associated with l-cells, for all $l < k$. In Fig. 9.0.1 we illustrate the support of each operator appearing in the Hamiltonian with dashed circles, where we have drawn a section of the graph $\mathcal{G}$ embedded in the plane for the sake of visualization. For simplicity, we will assume that all vertices in $\mathcal{G}$ are trivalent.[25]

9.1 Hilbert space

We will locate all all degrees of freedom (spins) at the vertices of the graph $\mathcal{G}$, so the big Hilbert space on which the Hamiltonian is defined is

$$\mathcal{H}_{\mathcal{G}} = \bigotimes_{v \in \mathcal{V}} \mathcal{H}_v. \tag{372}$$

We are making use of the unordered tensor product defined in Section 8.5.

[24] This makes the low energy spectrum consist purely of "flux" excitations: the "charged" idempotents always violate both the plaquette and A_e term, which with this hierarchy of coefficients costs a large amount of energy. One way to put charge and flux excitations on an energetically more equal footing is to add "tails" to each plaquette that host the charge degrees of freedom, as in [36]. Alternatively, we could modify the Hamiltonian so that $B_p \to B_p \prod_{e \in p}(1 - D_e) \prod_{v \in p}(1 - A_v)$, and $D_e \to D_e \prod_{v \in e}(1 - A_v)$.

[25] Any surface possesses a cell decomposition with trivalent vertices. Such cell decompositions are Poincaré dual to triangulations.

The vertex Hilbert spaces $\mathcal{H}_v$ will depend on three sets of choices. First, we must choose an orientation of each edge of $\mathcal{G}$. This is because of the possibility of non-trivial Frobenius-Schur indicators; see below. Second, we must choose an ordering of the edges incident to each vertex, consistent with with the intrinsic cyclic ordering of those edges coming from the embedding of $\mathcal{G}$ in the oriented surface (so if the vertex is r-valent, there are r possible orderings). Finally, we must choose a spin framing at each vertex.

In order to make the choice of cyclic ordering manifest in diagrams, and in order to simplify spin-structure-related aspects of our construction, we will choose to draw our graphs in a way such that all of the edges at each trivalent vertex are "on the same footing". This is in contrast to the conventions in the physics literature and in the earlier sections of this paper, where vertices are drawn with one edge extending below the vertex and two edges extending above, since in this convention the edge extending below is distinguished from the two other edges. We will choose a convention in which all three edges at each trivalent vertex extend above the vertex: with this choice, each vertex resembles a pitchfork.

We must also choose a spin framing at each vertex, consistent with the "pitchforkization" convention. The pitchforkization and spin framing are needed in order to define an unambiguous isomorphism between local degrees of freedom at v is standard vector spaces V^{abc}. Without this standardization, the local Hilbert spaces would be ambiguous up to automorphisms. The standardization procedure is nothing more than fixing a convenient choice of gauge in the way we present our fusion diagrams.

If all the edges incident to a vertex v point out of the vertex, we define the vertex Hilbert space at v by

$$\mathcal{H}_v = \bigoplus_{a,b,c} V^{abc} \qquad \text{ 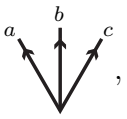 } \tag{373}$$

where the sum is over the simple objects of $\mathcal{S}$. If the first edge points in and the other two point out, then we define

$$\mathcal{H}_v = \bigoplus_{a,b,c} V^{a^*bc} \qquad \text{ 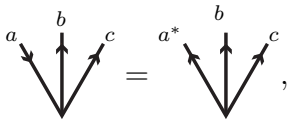 } \tag{374}$$

and so on for all eight possible patterns of in/out of the three incident edges.

This completes the definition on the big Hilbert space for the Hamiltonian. Impatient readers should now skip to the next subsection, but readers who are puzzled by some of the choices we made above are encouraged to read on.

Why are there no spins on edges, as in the original Levin-Wen Hamiltonian? Levin and Wen explicitly assume that V^{abc} is at most 1-dimensional. This is true for theories based on Temperley-Lieb or $Rep_q(sl_2)$, but it is not true in general, so we need to add spins on vertices. But each basis vector in $\bigoplus_{a,b,c} V^{abc}$ "knows" the labels on the adjacent edges, so once we have these vertex degrees of freedom the edge degrees of freedom become redundant and can be eliminated.[26]

[26] An argument in favor of edge degrees of freedom is that they can lead to smaller local Hilbert spaces, at least for simple theories. For example, one can write a Hamiltonian for the C_2 theory which has a (2|0)-dimensional Hilbert space at each edge and a (1|1)-dimensional Hilbert space at each vertex. The general Hamiltonian we are now discussing, specialized to the C_2 theory, would assign a (4|3)-dimensional Hilbert space to each vertex (but no Hilbert spaces for edges).

Why must we choose an orientation of each edge? The short answer: because of the possibility of non-trivial Frobenius-Schur indicators. Now for the longer answer. If the edges are not oriented, then we would assign vertex Hilbert spaces as above, but with all edges point out at each vertex. This means that each edge sees two inward pointing edges.

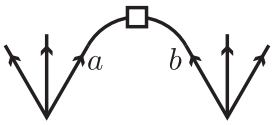

(375)

If the two labels coming from the two adjacent vertices are a and b (which we will assume are both m-type, for simplicity), then the associated vector space for the edge is V_{ab}, which is 0-dimensional unless $a \cong b^*$. If a is not self-dual, or if a is evenly self-dual with FS indicator 1, then there is a canonical identification of V_{ab} with $\mathbb{C} = \mathbb{C}^{1|0}$ and we can ignore it.

But if a is evenly self-dual with FS indicator -1, then there is a sign ambiguity in identifying V_{aa} with $\mathbb{C}$, and we will have to keep careful track of this sign when defining the Hamiltonian. Even worse, if a is *oddly* self-dual (and a is m-type), with FS indicator $\pm i$ (as occurs in the $\frac{1}{2}\mathrm{E}_6$ theory studied earlier), then V_{aa} is an odd vector space, non-canonically isomorphic to $\mathbb{C}^{0|1}$. Keeping track of these odd vector spaces would entail even more bookkeeping.

Overall, we think the least annoying solution to the above problems is to orient each edge of the graph. This allows us to treat a and a^* as distinct objects, even when they happen to be isomorphic. Now, instead of V_{aa}, we have $V_{aa^*} \cong \mathrm{End}(a)$, which has a canonical element $id : a \to a$, even when Frobenius-Schur indicators are nontrivial.

Why the pitchforks? As alluded to earlier, rotations by $2\pi/3$ can act non-trivially on V^{aaa}, and so it is helpful to choose a vertex configuration where every outgoing edge is placed on the same footing. This is true even in the bosonic case.

Why the spin framings? Because V^{abc} has a spin-flip automorphism, and also because we need to enhance the graph $\mathcal{G}$ with information related to the spin structure of the ambient manifold in order to write the edge terms, as explained below.

9.2 Spin structure considerations and the standardization of the graph

To derive the Hamiltonian (371) and explain the nature of the B_p, D_e, and A_v operators, we will first need to describe how the graph inherits spin structure data from the ambient spin manifold on which it is defined.

Recall that we have a graph $\mathcal{G}$ embedded in an orientable spin surface Σ. In order to define the super pivotal Hamiltonian we will need to equip $\mathcal{G}$ with information about the spin structure σ. In order to talk about the spin structure data at the vertices and edges of $\mathcal{G}$, we will thicken the cell decomposition to a handle decomposition of Σ. A handle decomposition is essentially a fattened version of a graph; see Fig. 9.2.1 for an illustration. The handle decomposition can be obtained by expanding each vertex of the graph into a disk (0-handle) and each edge into a thickened strip (1-handle). The remaining faces constitute the 2-handles, which are homeomorphic to disks.

Recall from Section 9.1 that in order to define the local vertex degrees of freedom we choose an orientation for each edge, a "pitchforkization" for each vertex, and a spin

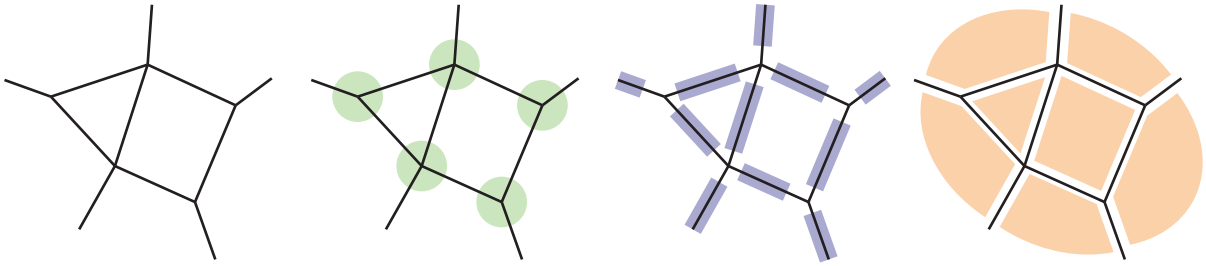

Figure 9.2.1: A handle decomposition obtained from the graph on the far left. The 0 handles (green disks) are neighborhoods of the vertices, the 1-handles (purple strips) are neighborhoods of the edges, and the 2 handles (orange polygons) which are the compliment of the union of the 0- and 1-handles.

framing at each vertex. These choices are analogous to choosing a gauge – different choices lead to isomorphic Hamiltonians and ground states.

The choices of pitchforkization and spin framing are equivalent to choosing a spin diffeomorphism from a 0-handle to a standard model for a 0-handle. We define a spin diffeomorphism φ_v from a generic 0-handle v to a disk in $\mathbb{R}^2$ with its standard spin structure, so that the attaching regions for the 1-handles terminating on v are all located on the top part of the disk. That is, we use the spin diffeomorphisms to turn each 0-handle into a "standardized 0-handle", where the configuration of the 1-handles terminating on each 0-handle means that that each 0-handle looks like a pitchfork. The spin diffeomorphism φ_v that maps a generic 0-cell v to a standardized 0-cell (thereby implementing the pitchforkization procedure) is defined pictorially by

$$\varphi_v : \quad D_v \longrightarrow D(n) \tag{376}$$

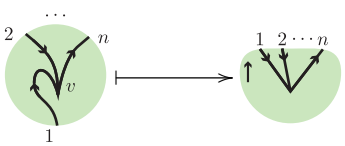

where n is the number of edges which terminate at v and the black arrow in the picture on the right hand side denotes the fermion framing of the 0-handle, which is constant throughout the 0-handle. When writing down the Hamiltonian we always take $n = 3$ without loss of generality, but when discussing tensor network constructions of these phases it is helpful to let n be unspecified. Using the pitchforkization map φ_v we can pull back the standard spin framing of $\mathbb{R}^2$ to the 0-handle. This results in a spin framing which is parallel to the outgoing edges at the top of the 0-handle.

Just as we do for the 0-handles, we will "standardize" the 1-handles so that they all assume the same form. After standardizing our 0-handles, 1-handles will always enter/exit from a 0-handle "vertically" (see Figure 9.2.2), and so our standardized 1-handles will look like

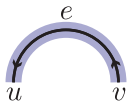

(377)

For theories with q-type particles, the Hamiltonian will contain terms that allow fermions to fluctuate across a 1-handle from vertex to vertex. The spin structure on a 1-handle (relative to the two attaching intervals) will determine what phase factor a fermion picks up when it moves across a 1-handle.

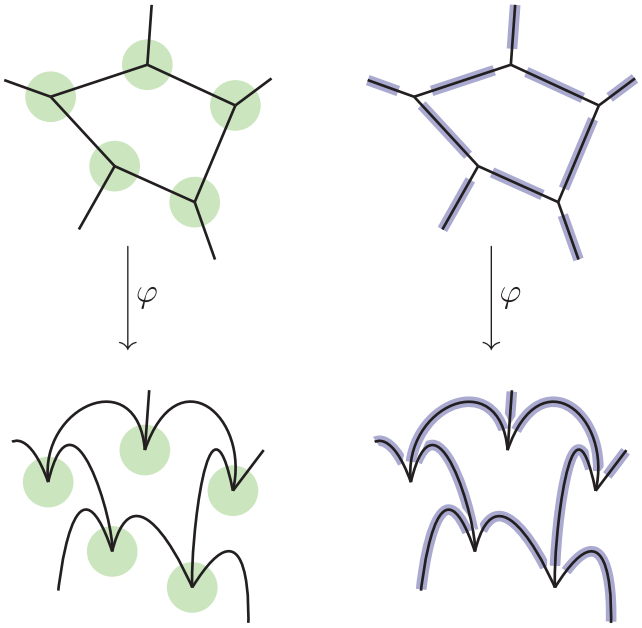

Figure 9.2.2: The mapping φ that maps a generic handle decomposition (top row) onto a "standardized" handle decomposition in which each 0-handle (green disk) has an identical pitchfork configuration (bottom row).

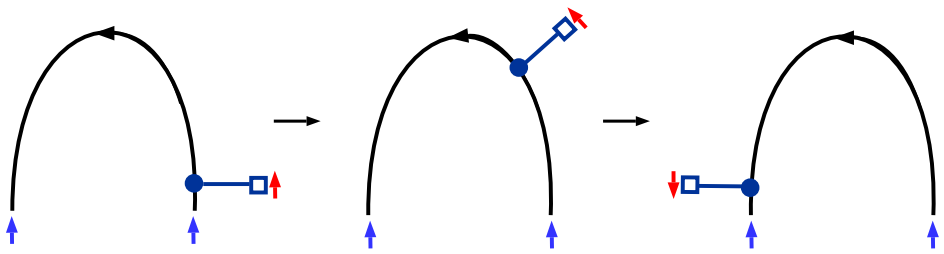

Figure 9.2.3: Parallel-transporting a fermion along a q-type edge, which is oriented as shown. The red arrow keeps track of the fermion framing, which rotates by π when proceeding along the direction of the edge's orientation. The blue arrows at the ends of the edge indicate the fixed framing at each 0-handle at the endpoints of the edge.

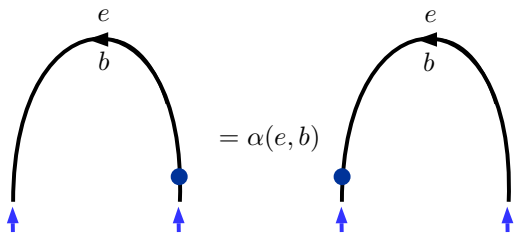

Figure 9.2.4: The action of sliding a fermion across an edge e labeled by the q-type object b is given by $\alpha(e, b)$. The spin framings of the 0-handles on either end of e are denoted by the blue arrows, and the spin framing of the fermion on the right hand side is taken to match that of the left 0-handle.

Once we have chosen coordinates at each vertex, we can associate a spin rotation of $+\pi$ or $-\pi$ to each 1-handle. First, we choose a standard spin framing at the incoming side (recall that each edge is directed) of the 1-handle. A standard choice exists because we have chosen a standard spin framing for the 0-handle at the incoming end of the 1-handle. We then parallel transport the spin framing along the 1-handle, keeping the first basis vector of the spin framing tangent to the core of the 1-handle during the transporting process. This procedure is illustrated in Figure 9.2.3, where the red arrow denotes the first basis vector of the spin framing. When we arrive at the end of the 1-handle, the spin framing we have transported will not agree with the standardized spin framing at the second 0-handle. We can see this from Figure 9.2.3; we have chosen the spin framing to point upwards at each 0-handle, but the red arrow points downward when it reaches the end of the 1-handle, which disagrees with the framing at the 0-handle. These two framings are related by either a $+\pi$ or $-\pi$ spin rotation in $Spin(2)$. We will denote this element of $Spin(2)$ by $\alpha(e)$, where e is the edge corresponding to the 1-handle.

Note that the collection $\{\alpha(e)\}$ is determined by the the spin structure of Σ and the choice of spin framings at each 0-handle. Conversely, any collection $\{\alpha(e)\}$ determines a spin structure on $\Sigma \setminus \{\text{2-handles}\}$. In order for this spin structure to extend to all of Σ, $\{\alpha(e)\}$ must satisfy the constraint that the boundary of each 2-handle has a bounding spin structure; see below.

Let b be a q-type simple object. We want to analyze the effect of sliding a fermionic dot over the edge e when e is labeled by b. At the outset, we will choose an odd element $\gamma_b \in \mathrm{End}(b)$ such that $\gamma_b^2 = \mathrm{id}_b$, and also $\gamma_{b^*} \in \mathrm{End}(b^*)$ such that $\gamma_{b^*}^2 = \mathrm{id}_{b^*}$. The requirement that $\gamma_b^2 = \mathrm{id}_b$ determines γ_b up to sign. Let $r(b) \in \mathbb{C}$ be such that $R_\pi \cdot \gamma_b = r(b)\gamma_{b^*}$, where

$$R_\pi : \mathrm{End}(b) \to \mathrm{End}(b^*) \tag{378}$$

denotes the spin rotation by $+\pi$. It is easy to see that $r(b) = \pm i$. The exact value will depend on the choices of standard generators γ_b and γ_{b^*}. If b is not isomorphic to b^*, then we can always choose γ_b and γ_{b^*} so that $r(b) = i$. But if $b = b^*$ (as happens in the C_2 theory, for example), then $\gamma_b = \gamma_{b^*}$ and the value of $r(b)$ is forced upon us, independent of the choice of γ_b.[27]

We can now, finally, describe the effect of sliding a standard fermionic endomorphism (dot) over an edge e labeled by a q-type particle b. Let $\gamma_b * e$ denote the edge with the

[27] The condition that b is equal to, rather than merely isomorphic to, b^* is in some sense pathological. But for theories build out of unoriented strands, like C_2, it is convenient to allow this pathology.

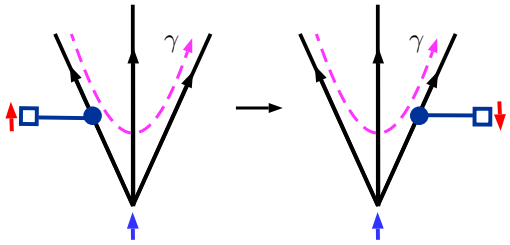

Figure 9.2.5: An illustration of a $+\pi$ spin framing rotation picked up as the path γ (drawn in dashed purple) passes through a 0-handle. If we were to proceed along γ in the opposite direction, we would pick up a $-\pi$ spin framing rotation instead.

standard generator γ_b placed at the incoming end (left side of Figure 9.2.4). Let $e * \gamma_{b^*}$ denote the edge with the standard generator γ_{b^*} placed at the outgoing end (right side of Figure 9.2.4). Then

$$\gamma_b * e = \alpha(e, b) \cdot e * \gamma_{b^*}, \tag{379}$$

where

$$\alpha(e, b) = \begin{cases} r(b) & \text{if } \alpha(e) = R_\pi \\ -r(b) & \text{if } \alpha(e) = R_{-\pi} \end{cases}. \tag{380}$$

This is illustrated in Figure 9.2.4.

Fermionic dots can also be "absorbed" into vertices using the action of $\mathbb{C}\ell_1$ on fusion spaces involving q-type objects, as discussed in Section (8.2). We can do this in analogy with (308) by constructing odd operators Γ_i, $i \in \{1, 2, 3\}$, which map a pitchfork with a standard dot on the i-th outgoing pitchfork edge to a pitchfork without a fermion dot on the i-th leg. Graphically, Γ_1 is defined by

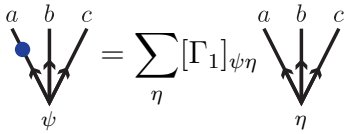

(381)

where ψ, η are basis vectors for V^{abc}, and the fermionic dot has a higher sign ordering than the basis vector it sits on. Γ_2 and Γ_3 are defined similarly:

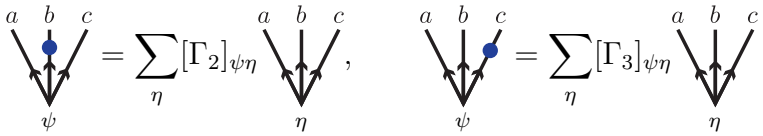

(382)

Since only q-type objects can host fermionic dots, Γ_i is only defined when the i-th leg of the vertex is labeled by a q-type object. Since only q-type objects have odd endomorphisms, Γ_i is only defined when the i-th label of the pitchfork is q-type. The Γ_i are all odd matrices, reversing fermion parity.

We mentioned above that the collection of $\{\alpha(e)\}$ must satisfy some constraints if it is to extend over the 2-cells and give a specified spin structure. Here are the details: let γ be an oriented framed loop in Σ. For simplicity, we will assume that (a) γ is embedded, (b) the framing is the natural one coming from the tangent space of γ, and (c) γ is contained in the union of the 0- and 1-handles. We want to compute the spin rotation, either 0 or 2π, which γ picks up from the spin structure on the 0- and 1-handles. When γ goes

over a 1-handle e, it picks up a rotation of $\alpha(e)$ or $-\alpha(e)$, depending on whether it goes over e with or against the orientation of e. Each time γ passes though a 0-handle, it also picks up a rotation of $\pm\pi$. Suppose γ enters the 0-handle at the i-th 1-handle and exits the 0-handle at the j-th 1-handle.[28] With our ordering conventions, this gives a rotation of $+\pi$ if $i < j$ and a rotation of $-\pi$ if $i > j$ (see Figure 9.2.5). Combining all of these $\pm\pi$ rotations results in a rotation of 0 or 2π. A bounding spin structure on γ yields a 2π rotation (since a 2π rotation acts as multiplication by -1 and produces the requisite anti-periodic boundary conditions), and a non-bounding spin structure corresponds to no rotation. In particular, if γ is the boundary of a single 2-cell/plaquette, then it must correspond to a spin framing rotation of 2π, since we assume that the spin structure around each 2-cell is bounding (which allows the spin structure on the 0- and 1-handles extends to a spin structure on all of Σ). More generally, γ will always get a spin framing rotation by 2π if it is in the trivial homology class of $H_1(\Sigma)$.

9.3 Terms in the Hamiltonian

In this section we will finally write down the Hamiltonian, and then explain the terms appearing in it in detail. As mentioned earlier, the Hamiltonian consists of three kinds of mutually commuting projections:

$$H = \lambda_p \sum_{p \in \mathcal{F}} (1 - B_p) + \lambda_e \sum_{e \in \mathcal{E}} (1 - D_e) + \lambda_v \sum_{e \in \mathcal{E}} (1 - A_e) \tag{383}$$

We'll start with a discussion of the "vertex" term A_e and then address the new edge term D_e, finally ending by describing the plaquette term B_p.

9.3.1 Vertex term

Let v_1 and v_2 be two vertices joined by an edge e. We define

$$A_e(|\psi_1\rangle \otimes |\psi_2\rangle) = \begin{cases} |\psi_1\rangle \otimes |\psi_2\rangle & \text{if } \psi_1 \text{ and } \psi_2 \text{ assign the same label to } e \\ 0 & \text{otherwise} \end{cases} \tag{384}$$

In other words, A_e forces the labels on each end of an edge to agree.

Why do we call these "vertex terms" when they are indexed by edges, and the support is a pair of adjacent vertices, joined by an edge? Because it does the same work as the vertex term of the usual bosonic LW Hamiltonian. If our fermionic category happens to be bosonic (i.e. it lacks fermions), then the ground state of our "vertex" term is isomorphic to the ground state of the vertex term in the usual LW Hamiltonian.[29] If we had chosen to put spins on edges as well as vertices, then we could write a vertex term that was actually indexed by vertices. But its ground state would be isomorphic to the above edge-like vertex term.

Note that vectors in the ground state of the vertex term can be interpreted as string nets. If K is the ground state of the vertex term, we have maps

$$K \to \mathcal{H}(\Sigma \setminus \text{2-cells}) \to \mathcal{H}(\Sigma). \tag{385}$$

[28] Note that i and j refer to the ordering of 1-handle attachments local to the 0-handle, not to some global ordering. The i and j are assigned in the same way as the Γ_i and Γ_j in (381) and (382).

[29] Note that the "admissibility" condition that requires V^{abc} to be in the ground state vector space only if $\mathbb{1} \in a \otimes b \otimes c$ is already satisfied for us, since our local Hilbert spaces at the vertices already have this condition built in.

where $\mathcal{H}(\Sigma \setminus \text{2-cells})$ and $\mathcal{H}(\Sigma)$ are the ground-state Hilbert spaces of $\Sigma \setminus$ 2-cells and Σ, respectively. The job of the edge term (below) will be to pick out a subspace of K on which the first map is an isomorphism. The job of the plaquette term will be to further reduce to a subspace such that the composite map to $H(\Sigma)$ is an isomorphism.

9.3.2 Edge term

The edge terms are the qualitatively new feature of this Hamiltonian, and are a necessary ingredient for the Hamiltonian of any theory possessing q-type particles. They are only well-defined on ground states of the vertex term. They allow fermions to fluctuate across edges of the graph which are labelled by q-type particles, and provide a way of energetically implementing the isotopy relations associated with sliding fermions along the worldlines of q-type particles. In Section 8.6 we solved the same problem in a different context by replacing a tensor product over scalars with a tensor product over the endomorphism algebra of a q-type simple object. The edge term of the Hamiltonian is a stand-in for the tensor product over a non-trivial endomorphism algebra.

The edge term will coherently add and remove fermions at the end points of the q-type bonds, as well as tunnel them across.[30] This term favors an equal-weight (meaning equal up to a phase factor) superposition of fermions across all vertices connected by q-type simple objects with a fixed fermion parity. Since the edge term is responsible for allowing fermions to fluctuate ("hop") across edges labeled by q-type objects, it will be absent in any theory with no q-type objects.

Fermion hopping across q-type edges is implemented by the Γ operators. To do this for an edge e, we can create a pair of fermions near the vertex at the beginning of e, slide one of the fermions along e to the vertex at the end of e, and then use the Γ operators to "absorb" each fermion into their respective vertices. For example, if e hosts a q-type edge label x, then we have

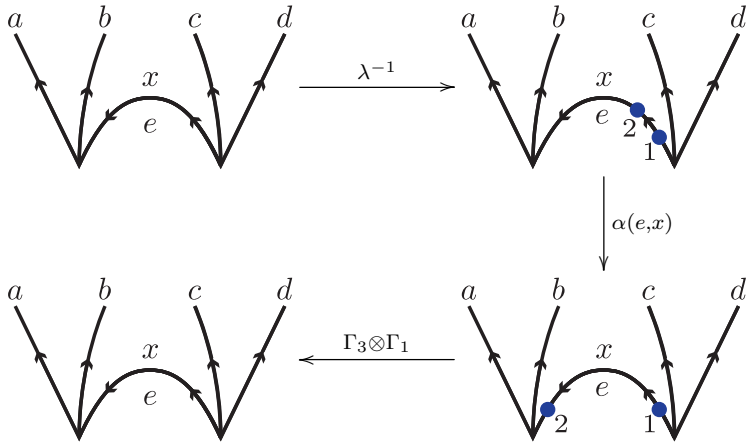

(386)

where we have defined tensor products of Γ operators to act so that operators located further to the left in tensor products absorb fermions with higher order than the operators to their right. Note that although the diagrams in the first and last steps in the above sequence look the same, they are not: the fermion parity of the vectors in the two vertex Hilbert spaces V^{abx^*} and V^{xcd} has been switched.

[30] Heuristically we can think of two adjacent vertices as islands which can hold a number of fermions and whose fermion parity is well defined. If these vertices are connected by a q-type edge, we can think of that edge as a 1D superconductor which coherently couples the two islands together.

For a generic edge e oriented from v_1 to v_2 and colored by a fixed object x the edge term can be written as the projector

$$D_e = \frac{1}{2}(1 + J_e), \tag{387}$$

where J_e acts on vectors $|\psi_1\rangle \otimes |\psi_2\rangle \in \mathcal{H}_{v_1} \otimes \mathcal{H}_{v_2}$ by implementing the local relations coming from $\mathrm{End}(x)$:

$$J_e(|\psi_1\rangle \otimes |\psi_2\rangle) = \begin{cases} \lambda^{-1}\alpha(e,x) \sum_{\eta_1,\eta_2} [\Gamma_i]_{\psi_1\eta_1} |\eta_1\rangle \otimes [\Gamma_j]_{\psi_2\eta_2} |\eta_2\rangle & \text{if } x \text{ is q-type} \\ |\psi_1\rangle \otimes |\psi_2\rangle & \text{if } x \text{ is m-type} \end{cases} \tag{388}$$

Here, we have taken e to be the ith leg of the pitchfork at v_1 and the jth leg at v_2, and $|\eta_1\rangle \otimes |\eta_2\rangle \in \mathcal{H}_{v_1} \otimes \mathcal{H}_{v_2}$. Since D_e acts as the identity on edges colored by m-type objects, edges with m-type edges will automatically lie in the ground state of the edge term.

In summary, including D_e in the Hamiltonian provides a way of energetically enforcing the conditions that the ground states of theories containing q-type particles are realized by superpositions of string-net configurations possessing all possible ways of arranging fermions on the q-type strings. Ensuring that ground states are superpositions of different fermion configurations is tantamount to projecting from the Hilbert space $\mathcal{H}_{\mathcal{G}}$ to the physical Hilbert space $\mathcal{H}_{\text{phys}}$, in which redundant degrees of freedom created by different fermion configurations are modded out.

As mentioned earlier, it can be conceptually helpful to note that a 1D Kitaev wire in the topological phase also exhibits the same behavior as the q-type strings in our theories. However, since generic theories (like the $\frac{1}{2}\mathrm{E}_6$ example considered earlier) can have fusion rules in which two q-type simple objects to fuse to a third q-type simple object, this analogy is not perfect, since at the junction of three Kitaev wires a zero mode is left behind, which does not occur in the $\frac{1}{2}\mathrm{E}_6$ theory.

9.3.3 Plaquette term

As with the vertex term, the plaquette term is essentially the same as the plaquette term in the usual string-net Hamiltonian: it inserts an ω loop into each plaquette, and uses local relations to fuse these ω loops into the boundaries of the plaquettes. Physically it is responsible for the dynamics of net configurations which reside in the ground space of the vertex and edge terms, and it is designed so that two string nets that correspond to the same state vector receive the same amplitude.

Using the definition of the ω loop, we can write B_p as

$$B_p = \frac{1}{\mathcal{D}^2} \sum_{a \in \mathrm{sob}_r(\mathcal{S})} \frac{d_a}{\dim \mathrm{End}(a)} B_p^a, \tag{389}$$

where the operator B_p^a fuses a loop labeled a into the edges and vertices neighboring the plaquette p (note that as discussed earlier, the operator B_p^a is only defined when all vertices and edges neighboring the plaquette p satisfy the corresponding vertex and edge terms).

The matrix elements of B_p^a depend on the choice of cell decomposition and pitchforkization procedure. For a generic cell decomposition it is somewhat tedious to write down these matrix elements, although the procedure is straightforward. To expedite this process we apply yet another standardization procedure. Suppose we are given a plaquette

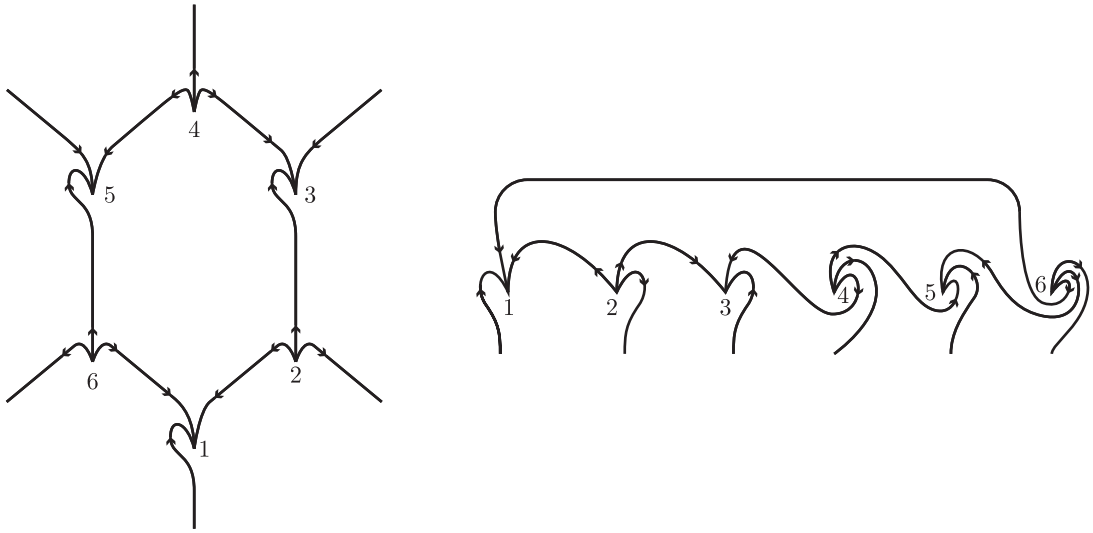

Figure 9.3.1: On the left we have single 2-cell along with its neighboring edges and vertices. Tiling the this 2-cell results in a honeycomb latter. Each vertex has been standardized in to a pitchfork. On the right we have stretched out the 2-cell in preparation for applying the plaquette operator. We can transform it into our standard basis (393) via $R = P \otimes \mathrm{id} \otimes \mathrm{id} \otimes P^{-1} \otimes P^{-1} \otimes P^{-2}$.

p with n neighboring vertices labeled from $1, \cdots, n$ in a counterclockwise fashion with respect to the orientation of Σ, see Figure 9.3.1. The Hilbert space associated to the plaquette p is the subspace of

$$\mathcal{H}_p = \mathcal{H}_{v_1} \otimes \mathcal{H}_{v_2} \otimes \cdots \otimes \mathcal{H}_{v_n} \tag{390}$$

which satisfies the vertex and edge terms. Diagrammatically, states in this space take the form of the figure on the right hand side of 9.3.1. It is useful to apply a number of pivots to vectors in $\mathcal{H}_p$ so that the vector space takes on a standard form which will facilitate the application of B_p^a. Define the operator R_p by

$$R_p : \mathcal{H}_p \to \bigoplus_{\{x_i, z_i\}} V^{x_n^* x_1^* z_1^*} \otimes V^{x_1 x_2 z_2} \otimes \cdots \otimes V^{x_{n-1} x_n z_n} \tag{391}$$

which can be explicitly written as

$$R_p = P_1 \otimes P_2 \otimes \cdots \otimes P_n \tag{392}$$

with each $P_j = \bigoplus_{abc} (P^{abc})^{l_j}$ defined in (319) and with $l_j = -2, -1, 0, 1, 2$ controlling the angle by which the jth vertex is pivoted (if the edges aren't all oriented out of the vertex then the appropriate object in P^{abc} needs to be replaced by its dual). We choose the pivots so that a vector in the image of R_p takes the form

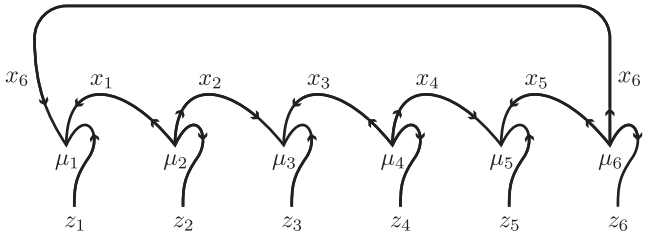

(393)

We now write down the matrix elements of B_p^a in this basis, which we call the *standardized* basis for the plaquette p. We choose an implicit sign ordering which increases from left to right (in particular, the numerical subscripts on x, μ, z, etc. denote string-net labels and not Koszul orders). As with (373) if some of the edges have a different orientation then the object is replaced by its dual.

The following is identical to the standard Levin-Wen plaquette term written in the notation of Section 8. To find the action of B_p^a in the standardized basis of (393) we first insert a closed strand labeled a into the interior of p:

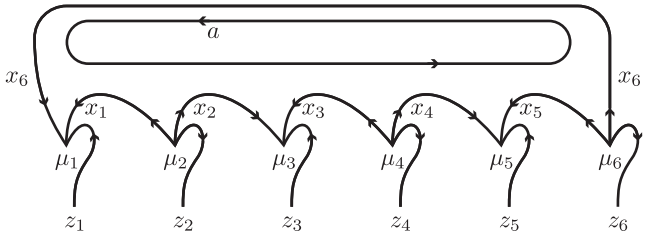

(394)

Next, we begin fusing the strand into the plaquette. We start with the strand labeled by x_6 and use the resolution of the identity (353) on the a and x_6 strands, which gives the picture

$$\sum_{y_6,\sigma_0} \frac{d_{y_6}}{\mathcal{B}(\sigma_0^* \otimes \sigma_0)}$$

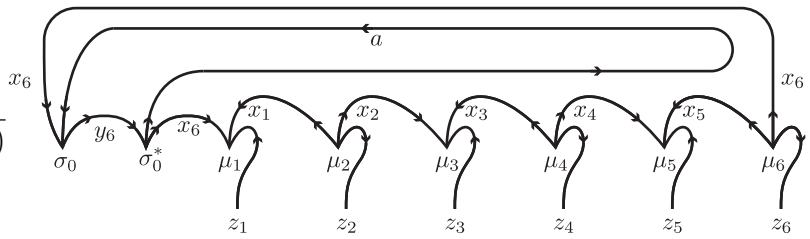

(395)

Next we use the associator (352) to pull the a string over x_6 in the diagram on the right to obtain

$$\sum_{y_1,\sigma_1} (F^{y_6^* a x_1^* z_1^*})_{(x_6;\sigma_0^*\mu_1)(y_1^*;\nu_1\sigma_1)} \times \tag{396}$$

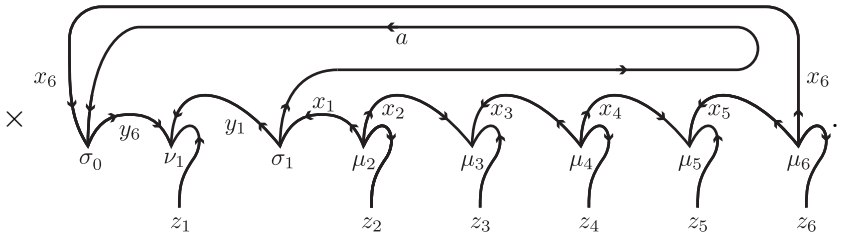

(397)

It will be helpful to use the short hand $(F)_{(\sigma_0^*\mu_1)(\nu_1\sigma_1)}$ for $(F^{y_6^* a x_1^* z_1^*})_{(x_6;\sigma_0^*\mu_1)(y_1^*;\nu_1\sigma_1)}$, which is well-defined so long as $\sigma_0, \mu_1, \sigma_1, \nu_1$ are defined, which will be clear from context. We keep applying F-moves until we are left with

$$\sum_{\substack{\nu_1 \cdots \nu_6 \\ \sigma_1 \cdots \sigma_6}} F_{(\sigma_0^*\mu_1)(\nu_1\sigma_1)} F_{(\sigma_1\mu_2)(\nu_2\sigma_2)} \cdots F_{(\sigma_5\mu_6)(\nu_6\sigma_6)} \times \tag{398}$$

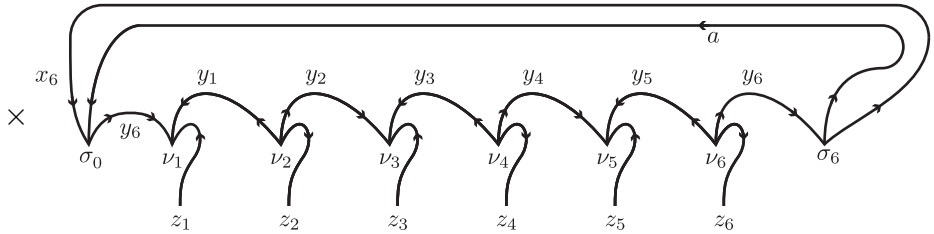

(399)

We note that the sign ordering is increasing from left to right. We now perform one last isotopy and remove the "bubble":

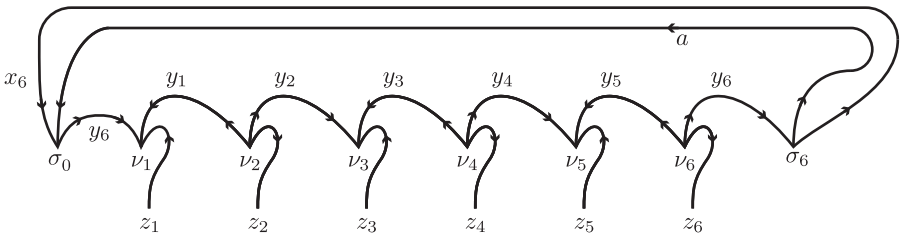

$$= \tag{400}$$

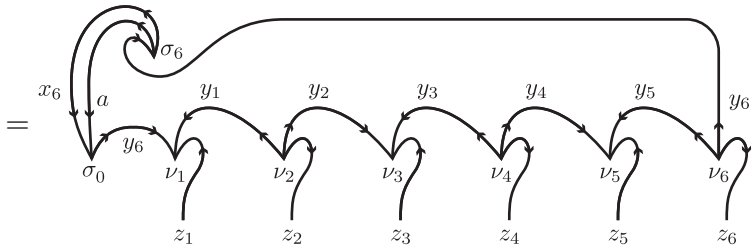

(401)

$$= (-1)^{|\sigma_6|}(-1)^{|\sigma_6|(|\sigma_0|+|\nu_1|+\cdots+|\nu_6|)}\frac{\mathcal{B}(\sigma_6\otimes\sigma_0)}{d_{y_6}}\times \tag{402}$$

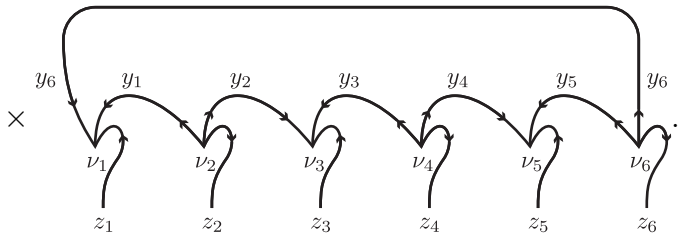

(403)

In the last step, the factor of $(-1)^{|\sigma_6|}$ comes from applying a 2π pivot to the σ_6 vertex and the factor of $(-1)^{|\sigma_6|(|\sigma_0|+|\nu_1|+\cdots+|\nu_6|)}$ is the Koszul sign coming from ensuring that σ_6 is located immediately before σ_0 in the ordering (recall that the pairing $\mathcal{B}$ is only defined on diagrams with a specific Koszul ordering; see (310)). $\mathcal{B}(\sigma_6\otimes\sigma_0)$ is zero unless σ_6 is dual to σ_0, and thus the $\mathcal{B}(\sigma_6\otimes\sigma_0)/d_{y_6}$ factor is cancelled by the factor of $d_{y_6}/\mathcal{B}(\sigma_0^*\otimes\sigma_0)$ introduced in (395). Noting that $|\sigma_6| = |\sigma_0|$, we can write (recall (393)),

$$[B_p^a]_{(\mu_1\cdots\mu_6)(\nu_1\cdots\nu_6)} = \frac{1}{\mathcal{D}^2}\frac{d_a}{\dim \mathrm{End}(a)}\sum_{\sigma_1\cdots\sigma_6} F_{(\sigma_6\mu_1)(\nu_1\sigma_1)}F_{(\sigma_1\mu_2)(\nu_2\sigma_2)}\cdots F_{(\sigma_5\mu_6)(\nu_6\sigma_6)} \times (-1)^{|\sigma_6|(|\nu_1|+\cdots+|\nu_6|)} \tag{404}$$

The plaquette term in the basis $\mathcal{H}_p$ is given by conjugating B_p^a with R_p. Note that due to (358) the pivots commute with the F-moves, and so the computation can be carried out in either basis.

We now briefly remark on surfaces with boundary. Let Y be such a surface and let c be a boundary condition for Y, i.e. a collection of labeled string net endpoints on ∂Y. Choose a graph G in Y such that the "boundary" of G is c and each component of $Y\setminus G$ which does not meet ∂Y is a disk. Given this input, we construct a Hamiltonian similarly to above. There are plaquette terms only for the interior 2-cells. There are edge terms only for interior edges of G. Vertices of G which are adjacent to the labeled points of c will have one or more of their edge labels fixed. The ground state of this Hamiltonian can be identified with $Z(Y;c)$.

We will see in Section 11 that one instance of this construction (with Y a disk and c consisting of two points labeled by a q-type particle and its dual) yields the Kitaev chain Hamiltonian.

Before moving on, we briefly mention a high-level way of understanding the plaquette operator in terms of the tube category. Let $\widehat{\Sigma}$ denote the surface Σ with a disk removed from each 2-cell. Each boundary component of $\widehat{\Sigma}$ corresponds to a plaquette term in the Hamiltonian. There is an obvioud bijection betweent he boundary components of $\widehat{\Sigma}$ and the plaquette terms of the Hamiltonian. For any collections c of labeled string endpoints on the boundary of $\widehat{\Sigma}$, we have the string net Hilbert space $Z(\widehat{\Sigma}; c)$. If c is the empty boundary condition (no labeled endpoints), then this Hilbert space can be identified with the ground state of the vertex and edge terms of the Hamiltonian. The tube categories of each boundary component act on the collection of vector spaces $\{Z(\widehat{\Sigma}; c)\}$, and consequently we can decompose these spaces according to the simple objects of the collective tube category. The summands of this decomposition correspond to the labelings of each boundary component of $\widehat{\Sigma}$ with an anyon of the tube category. Now consider gluing disks to each boundary component of $\widehat{\Sigma}$ to obtain Σ. This has the effect of projecting to the summand corresponding to placing the trivial anyon at each boundary component. Another way of achieving the same effect is to place a copy of the of the trivial tube category idempotent e_0 on an annulus at each boundary component. This is exactly what the plaquette term of the Hamiltonian does. This point of view also explains why the elementary excitations of the Hamiltonian correspond to placing tube category idempotents at 2-cells.

9.4 Excitation spectrum

Finally, we briefly comment on the spectrum of the Hamiltonian (371) and the types of excitations it model supports. Each of the terms in the Hamiltonian enforces one of the local relations of the vector space assigned to Σ by $\mathcal{S}$. As such, the zero-energy ground space is just the vector space assigned to Σ by $\mathcal{S}$. The deconfined anyonic excitations in the model correspond to violations of the plaquette and vertex terms. By construction, these are in one-to-one correspondence with the bounding idempotents of the tube category. This is simply because as discussed earlier, the B_p operator in the plaquette term is the projector $\Pi_{\mathbb{1}}$, which projects onto states containing no quasiparticles in the interior of p. The fusion rules of the excitations can be computed with the tube category methods developed in earlier sections.

One can also consider the excitations corresponding to violations of the edge terms (note that these will only be present in theories with q-type objects). If a given state has a $+1$ eigenvalue under an edge term $(1 - D_e)$, then the fermions traveling across e pick up an additional minus sign relative to the background spin structure. This is illustrated in Figure 9.4.1, where the violated edge e is shown in red, and the two circles marked N denote the vortices created on either side of e. Diagrammatically we denote the additional minus sign with a branch cut (the dashed line in Figure 9.4.1). This implies that violating a single edge term nucleates a pair of vortices (the set of which are in one-to-one correspondence with the non-bounding idempotents of the tube category) on the plaquettes adjacent to the edge e (recall that the plaquette terms are only non-zero in the ground space of the edge and vertex terms). This means that the vortex excitations can only be separated at the expense of a linear increase in energy, and so are linearly confined.

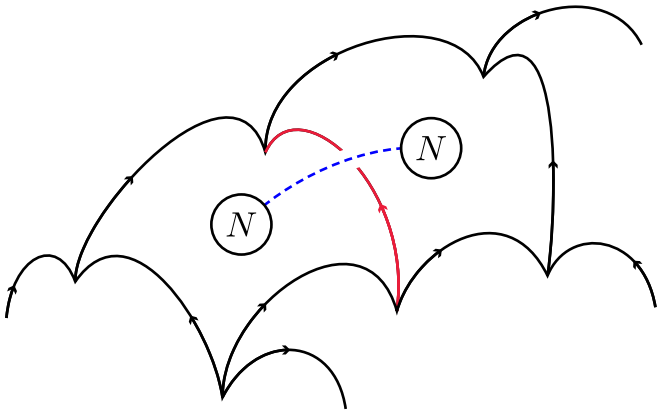

Figure 9.4.1: A region of the graph $\mathcal{G}$ containing two vortex excitations. The two punctures hosting the vortex excitations are marked as circles, with the label N denoting their non-bounding spin structure. The dashed blue line is the spin structure defect connecting the two punctures. The edge colored red intersects the spin structure defect and is excited, violating the edge term D_e in the Hamiltonian.

Alternatively, by modifying the Hamiltonian we can introduce vortices by hand. We remove the plaquette terms where we wish the vortices to reside, and require the corresponding plaquette boundaries to have a non-bounding spin structure. Relative to the un-modified Hamiltonian, the vortices will be connected by spin structure branch cuts. (The edge terms of the modified and unmodified Hamiltonians will differ for edges which intersect these branch cuts.) A ground state of the modified Hamiltonian will be an excited state of the unmodified Hamiltonian, whose energy depends on the choice of branch cut. To deconfine the vortices one needs to give the spin structure dynamics; we leave the study of this possibility to future work.

10 Super pivotal state sums and tensor networks

In this section we describe a version of the Turaev-Viro-Barrett-Westbury (TVBW) state sum [50, 51] for super pivotal fusion categories and a tensor network for the ground state wave function of the Hamiltonian constructed in Section 9. Related work was presented in [16], see also [34]. We first review the TVBW construction for bosonic spherical fusion categories. We then show how to write the state-sum as a tensor contraction on a tensor network. Next we detail the modifications needed for the fermionic versions of the state sum and tensor network. Lastly we use the state sum to write down an explicit wave function for the ground ground state of (371).

Before we begin, we need to establish some terminology regarding cell and handle decompositions. Recall that a handle decomposition for a 3-manifold M is built from a series of k-handles, with $k = 0, 1, 2, 3$, each of which is identified with $D^k \times D^{3-k}$. Handle decompositions can be obtained from cell decompositions by thickening each k-cell into a k-handle. Conversely, each handle decomposition determines a cell decomposition by taking the cores of the handles. (See Section 9.2 for more details.) We will often refer to a k-cell and its associated k-handle with the same letter, since it will be convenient for us to be able to describe things in terms of both handle decompositions and their corresponding cell decompositions. We call $S^{k-1} \times D^{3-k}$ the attaching region (or attaching boundary)

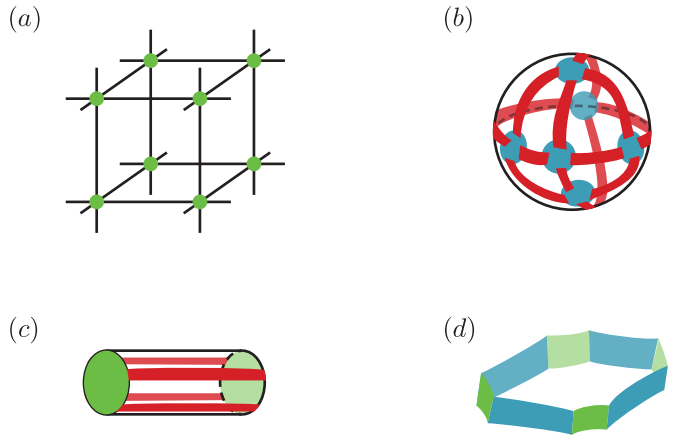

Figure 10.0.1: The handles corresponding to a standard cubic cell decomposition (a). The 0-, 1- and 2-handles are shown in (b), (c) and (d), with colors green, blue and red. In (b) the blue disks on the 0-handle indicate where the 1-handles attach to the 0-handle, and the red rectangles indicate where the 2-handles attach to the 0-handle. In (c) the green disks indicate where the 0-handles attach to the 1-handle and the red rectangles indicate where the 2-handles attach to the 1-handle. Similarly, in (d) the blue and green rectangles indicate where the 2-handles attach to the 0- and 1-handles. We have omitted the 3-handles from the figure.

of the k-handle, and $D^k \times S^{3-k-1}$ the non-attaching boundary. The attaching map of a k-handle is a homeomorphism from the attaching region to a submanifold of the boundary of the union of the lower-dimensional handles. The topology of M is encoded by the various attaching maps. The different types of k-handles are illustrated in Figure 10.0.1.

10.1 Bosonic TVBW state sum

10.1.1 Definition of the state sum

Our first task is to describe the TVBW (bosonic) state sum. The original references are [50, 51]. We will use the form for a general cell/handle decomposition, as described in [24].

Let M be a closed oriented 3-manifold equipped with a handle decomposition $\mathcal{H}$. Choose auxiliary orientations of the 1- and 2-cells of the cell decomposition corresponding to $\mathcal{H}$. Let $\mathcal{H}_i$ denote the set of i-handles ($i = 0, 1, 2, 3$). The state sum has the form

$$Z(M) = \sum_{\beta \in \mathcal{L}(\mathcal{H})} \prod_{c \in \mathcal{H}_3} \mathcal{D}^{-2} \prod_{f \in \mathcal{H}_2} d(f, \beta) \prod_{e \in \mathcal{H}_1} \widetilde{\Theta}(e, \beta)^{-1} \prod_{v \in \mathcal{H}_0} \mathrm{Link}(v, \beta). \tag{405}$$

The next few paragraphs define the notation used in (405).

We use the 2-cell orientations to define an oriented graph (unlabeled string net) on the boundary of each 0-, 1- and 2-handle, as shown in Figure 10.1.1. String-net graphs are assigned to the k-handles as follows:

- On 2-handles, the graph is a single loop along the core of the attaching annulus of a 2-handle. The orientation of the loop is determined by the orientation of the 2-cell.

Figure 10.1.1: Graphs on the boundaries of 0-, 1- and 2-handles, in the case of a cubic cell decomposition. Compare Figure 10.0.1.

Figure 10.1.2: On the left, we have an illustration of four 2-cells meeting a 1-cell. For clarity we have put a small gap between the 1-cell and the four 2-cells. On the right we have the corresponding 1-handle and a particular labeling. We have denoted the corresponding attaching disks by 'i' for initial, and 't' for terminal.

- On 1-handles, the graph is a generalized Θ graph, which we will call a $\widetilde{\Theta}$ graph. The graph has one edge for each 2-handle adjacent to the 1-handle. The middle part of each edge of the graph corresponds to where the cores of the 2-handles meet the boundary of the 1-handle. The two vertices of the graph are on the two attaching disks of the 1-handle. The edges are oriented opposite to the orientations used in the 2-handle loops above.

- On each 0-handle, the graph is determined by the pattern of 2- and 1-handles adjacent to the 0-handle. The graph has one edge for each adjacent 2-handle and one vertex for each adjacent 1-handle. The orientations of the edges are opposite to the orientations of the 2-handle loops. We denote this graph $\mathrm{Link}(v)$.

Recall that we have an orientation of each 1-cell. This allows us to distinguish an "initial" and "terminal" attaching disk for each 1-handle; see Figure 10.1.2. On the initial disk we see a graph with a single vertex in the interior of the disk and k edges connecting the central vertex to the boundary of the disk (where k is the number of 2-handles which cross the 1-handle). For each labeling ℓ of these edges by simple objects in $\mathrm{sob}_r(\mathcal{C})$, we have an associated vector space $V(\ell)$. For example, in the case of Figure 10.1.2 the vector space is isomorphic to $V^{ab^*c^*d}$. Let $B(\ell)$ be some chosen basis of this vector space. For each 1-handle e define $B(e)$ to be the union over all labelings ℓ of $B(\ell)$, and also define $V(e)$ to be the direct sum of all the vector spaces $V(\ell)$.

We define the set of all labelings $\mathcal{L}(\mathcal{H})$ to be the product over all 1-handles e of the basis sets $B(e)$. In other words, we choose (independently, without any compatibility constraints) a labeling by simple objects of the edges of each initial disk graph, then choose a basis vector for each associated vector space.

We also associate a vector space $V^*(\ell)$ to the terminal disk of each labeled 1-handle. In the example, this is isomorphic to $V^{d^*cba^*}$. There is a nondegenerate bilinear pairing between $V(\ell)$ and $V^*(\ell)$, given by evaluating the labeled string net on the boundary of

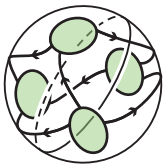

Figure 10.1.3: An example of the surface of a 0-handle on which four 1-handles are attached to. The attaching regions for the 1-handles are marked in green. The coloring β assigns objects to the oriented strands and fusion space basis vectors to the green regions.

the 1-handle (which is a 2-sphere). We will choose a basis of $V^*(\ell)$ such that the pairing matrix is diagonal. (It is sometimes convenient to not insist that the diagonal entries be δ_{ij}.) We also define $V^*(e)$ to be the direct sum (over all labelings ℓ) of $V^*(\ell)$.

We are now ready to define the weights appearing in the state-sum $Z(M)$. Let $\beta \in \mathcal{L}(\mathcal{H})$ and let f be a 2-handle. The labeling β associates a simple object to each intersection of f with a 1-handle. If these simple objects are not all the same, we define $d(f,\beta) = 0$. If they are all equal to the same simple object $a \in \mathrm{sob}_r(\mathcal{C})$, we define the weight $d(f,\beta)$ appearing in (405) by $d(f,\beta) = d_a$.

Let e be a 1-handle. The labeling β associates a basis vector μ to the initial disk of e. Define $\widetilde{\Theta}(e,\beta)$ to be the value of the bilinear pairing evaluated on μ^* and μ. Diagrammatically, $\widetilde{\Theta}(e,\beta)$ is found by connecting the open strings in $V(\ell)$ to their dual counterparts in $V^*(\ell)$ and evaluating the resulting diagram. Continuing with our example in Figure 10.1.2, we have

$$\widetilde{\Theta}(e,\beta) = \tag{406}$$

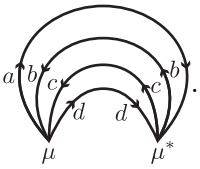

Let v be a 0-handle. The labeling β determines a labeling of the graph $\mathrm{Link}(v)$ as follows. Near each vertex of $\mathrm{Link}(v)$ we place the basis element $\mu^* \in V^*(e)$ (or $\mu \in V(e)$) assigned by β to the corresponding 1-handle if v is attached to the initial (terminal) end of the 1-handle. If these vertex labels are incompatible along edges of $\mathrm{Link}(v)$, we define $\mathrm{Link}(v,\beta) = 0$. If they are all compatible then we define $\mathrm{Link}(v,\beta)$ to be the evaluation of the resulting labeled graph (string net). For cell decompositions dual to a triangulation, the labeled graph is a tetrahedral string net on a sphere. This is illustrated in Figure 10.1.3, which shows an example 0-handle on which four 1-handles terminate.

This completes the definition of the state sum.

It follows from Section 8.2 of [24] that the state sum computes $Z(M)$, independently of the choice of handle decomposition and choice of orientations of 1- and 2-cells.

If M has non-empty boundary, then we choose the cell decomposition so that ∂M lies in the union of the 2-skeleton (union of 0-1, 1- and 2-cells). (An alternative choice would be to require that ∂M is transverse to the 2-skeleton. The two conventions each have strengths and weaknesses.)

The 0- and 1-cells on ∂M will do double duty as the underlying graph of a string net on ∂M. Choose an orientation of each 1-cell on ∂M. (This is analogous to choosing an orientation of the boundary of a 2-cell in the interior of M.) Choose a labeling of these oriented edges by simple objects in $\mathrm{sob}_r(\mathcal{C})$. For each vertex (0-cell) on ∂M, choose an element of the appropriate disk vector space.

We now have a labeled string net g on ∂M. The state sum will evaluate the path integral $Z(M)(g)$ (i.e. the path integral of M with boundary condition given by g). The labelings and weights are defined as before, except that some of the labels are already determined by the string net g on the boundary.

10.1.2 The state sum as a tensor network

Our goal in this subsection is to reinterpret (405) as a tensor network. We will first discuss that case when M is closed, then consider the case when ∂M is non-empty.

If we (temporarily) ignore the factors of $d(f,\beta)$ and $\mathcal{D}^{-2}$ in (405), it is easily seen to compute the contraction of a tensor network. The underlying graph of the tensor network is the union of 0- and 1-cells of the cell decomposition. The vector space associated to each edge e is $V(e)$ as defined above. The matrix elements of the tensor associated to a 0-cell v are the numbers $\mathrm{Link}(v,\beta)$ defined above. The factors of $\widetilde{\Theta}(e,\beta)^{-1}$ arise from the pairing of dual tensor indices.

To incorporate the factors of $d(f,\beta)$ and $\mathcal{D}^{-2}$, we make some ad hoc choices. We consider "dressed" 0-handle weights that incorporate the factors of $d(f,\beta)$ and $\mathcal{D}^{-2}$ for certain adjacent 2- and 3-cells. For each 2-handle f we choose an adjacent 0-handle v_f. For a 0-handle v we modify the associated weight $\mathrm{Link}(v,\beta)$ by multiplying factors of $d(f,\beta)$ for each 2-handle f such that $v = v_f$. Similarly, for each 3-handle we choose an adjacent 0-handle and multiply the associated weight by $\mathcal{D}^{-2}$. Denoting the modified 0-handle weights by $\widetilde{\mathrm{Link}}(v,\beta)$, we define the 0-handle tensors T_v as follows. Let $e_1,\dots,e_k$ be the 1-handles adjacent to the 0-handle v. Let

$$V_i = \begin{cases} V(e_i) & \text{if } v \text{ is adjacent to the terminal end of } e_i \\ V^*(e_i) & \text{if } v \text{ is adjacent to the initial end of } e_i. \end{cases} \tag{407}$$

We define

$$T_v \in V_1^* \otimes \cdots \otimes V_k^* \tag{408}$$

by

$$T_v(w_1 \otimes \cdots \otimes w_k) = \widetilde{\mathrm{Link}}(v, w_1 \otimes \cdots \otimes w_k), \tag{409}$$

where $w_i \in V_i$. In other words, T_v evaluates the link graph with labels determined by $w_1,\dots,w_k$ and multiplied by the factors of $d(f,\beta)$ and $\mathcal{D}^{-2}$ as described above. To obtain the partition function, we trace out the tensor product of all the 0-handle tensors constructed in this way. Because the vector space associated to the region on a 0-handle attached to the terminal end of a 1-handle e is dual to the vector space associated to the corresponding region on the 0-handle attached to the initial end of e, there are precisely as many dual vectors as vectors in the tensor product, and contracting each vector with its associated dual vector computes the complex number $Z(M)$. That is, we have

$$Z(M) = \mathrm{tr}\left(\bigotimes_{v\in\mathcal{H}_0} T_v\right), \tag{410}$$

where the trace tr denotes the tensor contraction. It is easy to see that this tensor network gives the same state sum as (405) and is independent of the way we assign factors of $d(f,\beta)$ and $\mathcal{D}^{-2}$ to the vertex tensors.

In the case where $\partial M \neq \emptyset$, we define the 0-handle tensors T_v as before, but in this case some of the legs of the tensors are unpaired (not contracted). Specifically, there is

one unpaired leg for each 0-cell on ∂M. If $W_1, \ldots, W_n$ are the vector spaces associated to the boundary 0-cells, we have

$$Z(M) = \mathrm{tr}\left(\bigotimes_{v \in \mathcal{H}_0} T_v\right) \in W_1^* \otimes \cdots \otimes W_n^*. \tag{411}$$

Each string net on ∂M (i.e. each labeling of 0- and 1-cells as described above) determines an element of $W_1 \otimes \cdots \otimes W_n$ (the vertex labels). By evaluating (411) on this element we obtain the amplitude of the wave function for the string net.

10.1.3 Standardization procedures

The above tensor network construction is irregular, in the sense that (potentially) every edge vector space is different and every 0-handle tensor is different. There are several standardization procedures that reduce this irregularity.

One standardization procedure is to start with a cell decomposition that is dual to a triangulation. This ensures that there are exactly three 2-handles meeting each edge, and that the vertex graphs $\mathrm{Link}(v, \beta)$ are all tetrahedral. However, this still leaves us with several different types of edge vector spaces and vertex tensors. For example, depending on the choice of 1- and 2-cell orientations, there will be eight possible vector spaces associated to 1-handles, corresponding to V^{abc}, V^{ab^*c}, $V^{a^*b^*c^*}$, etc. (Note that if all Frobenius-Schur indicators are equal to 1, then we can ignore these distinctions.) Similarly, there will be many different tetrahedral vertex tensors, depending on the orientations of the edges of the tetrahedral graph.

We can further standardize the tensor network by choosing a global ordering of the 3-cells of the handle decomposition. (This is equivalent to a global ordering of the vertices of the dual triangulation.) We then choose 2-cell orientations so that the the orientation of a 2-cell together with a normal vector pointing toward the higher-ordered of the two adjacent 3-cells agrees with the orientation of M. We can now choose 1-cell orientations so that the graph on the initial disk of each 1-handle has a trivalent vertex with two outgoing and one incoming edge. With these orientation choices, we have, for every 1-handle e,

$$V(e) = \bigoplus_{a,b,c \in \mathrm{sob}_r(\mathcal{C})} V^{abc^*}. \tag{412}$$

Furthermore, all of the tetrahedral graphs have the same pattern of edge orientations, so all of the 0-handle tensors in the tensor network are of the same form.

However, it is not always convenient to choose a global ordering. For example, our main application is a tensor network associated to $Y \times I$. If Y is a torus, we might hope that the network has translational symmetry, but this is not compatible with the global ordering trick. For this reason, in what follows we will work with a cell decomposition dual to a triangulation, but we will not employ the global ordering trick.

We will find it useful to employ a standardization procedure in which all fusion spaces in the string nets assigned to the 0-handles assume the "pitchfork" form introduced in our treatment of the Hamiltonian. (These vertices are all trivalent since we are now assuming a cell decomposition dual to a triangulation.) In this convention, the T_v tensor weights

are all computed by the evaluation of tetrahedral diagrams:

$$T_v(\alpha \otimes \beta \otimes \gamma \otimes \delta) = \mathrm{Tet}(v, \alpha \otimes \beta \otimes \gamma \otimes \delta) = \tag{413}$$

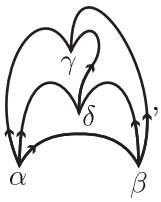

where we have defined the tensor weight by its evaluation of the picture on the right with $\alpha \in \bigoplus_{abc} V^{abc}$, $\beta \in \bigoplus_{abc} V^{a^*bc}$, $\gamma \in \bigoplus_{abc} V^{a^*b^*c^*}$, and $\delta \in \bigoplus_{abc} V^{a^*bc^*}$. The pitchforkization procedure does not entirely fix the form of the T_v tensors above, since the tetrahedral nets associated with each 0-handle will in general have different edge orientations. Since there are $2^6 = 64$ possible choices of edge orientations near a 0-handle, there will be 64 different types of T_v tensors, given by the appropriate diagram evaluation with $\alpha, \beta, \gamma, \delta$ chosen from the appropriate fusion spaces.[31]

In this procedure, we choose standardizations (pitchforkizations) at each 0-handle independently. This means that the two ends of each 1-handle are standardized independently of each other, and the pairing induced from the $\widetilde{\Theta}$ graph on the 1-handle (406) will not necessarily agree with the standard pairing (310). Instead, the 1-handle pairing and the standard pairing will be related by a pivot operation $P_e = P^{l_e}$ for $l_e = 0, 1, 2$, where P is the pivot defined in (319). We define P_e to rotate diagrams counterclockwise relative to the orientation of e. If $l_e \neq 0$, then the pitchforks at the initial and terminal vertices of e are twisted by $2\pi l_e/3$ relative to one another, and this twisting data needs to be incorporated into the 1-handles. The 1-handles now look like

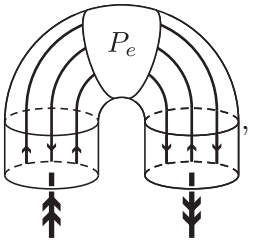

, (414)

where the double arrows designate the orientation of e.

In summary, by standardizing each 0-handle independently, we have managed to make each 0-handle tensor isomorphic to a standard (up to edge orientations) tetrahedral tensor. The price we pay for this is that we have to keep track of the pivots which relate the two ends of each 1-handle. In terms of the tensor network, this means that we either need to insert two-legged pivot/1-handle tensors between each pair or adjacent 0-handle tensors, or we need to further "dress" the 0-handle tensors by merging each such pivot tensor into one of the two adjacent 0-handle tensors. See Figure 10.1.4.

These standardizations also serve to make the original state sum (405) more uniform. We can now write

$$Z(M) = \sum_{\beta \in \mathcal{L}(\mathcal{H})} \prod_{c \in \mathcal{H}_3} \mathcal{D}^{-2} \prod_{f \in \mathcal{H}_2} d(f, \beta) \prod_{e \in \mathcal{H}_1} \Theta(P_e, \beta)^{-1} \prod_{v \in \mathcal{H}_0} \mathrm{Tet}(v, \beta). \tag{415}$$

Here $\Theta(P_e, \beta)$ is a standard pairing as in (310), but modified by the pivot isomorphism P_e. The weight $\mathrm{Tet}(v, \beta)$ is a standard tetrahedral symbol (though there are still variants

[31] Not all these 64 tetrahedra are independent however, as some of them can be transformed into one another by using the pivotal and spherical structure of the input category.

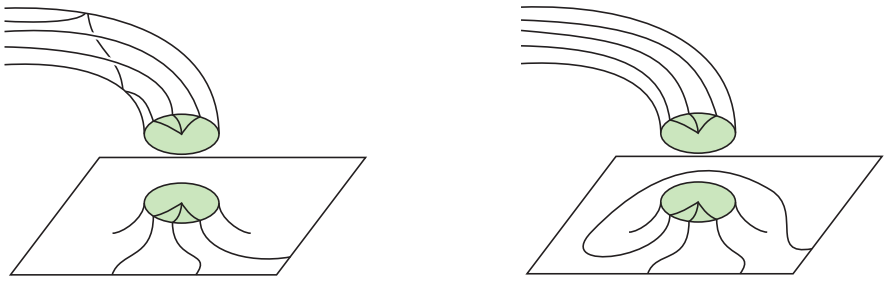

Figure 10.1.4: A 1-handle and its attaching region on an adjacent 0-handle (the plane denotes a section of the surface of the 0-handle). Standardizing the 0-handle attaching regions to be "pitchforks" requires that we either have to add pivots to the 1-handle (left, where one of the strands on the 1-handle is wrapped around the 1-handle) or to the corresponding 0-handle attaching region (right, where one strand on the 0-handle is pivoted around the attaching region). In (415) we choose to include the pivots within 1-handles.

which depend on the orientations of the edges of the tetrahedron). The point is that we have now written the state sum for an arbitrary 3-manifold in terms of a finite number of standard weights.

10.2 The fermionic state sum

10.2.1 Definition of the fermionic state sum

We now extend the bosonic state sum to the fermionic case. We start with two pieces of data: a super pivotal fusion category $\mathcal{S}$, and a spin 3-manifold M possessing a cell decomposition with orientations of 1- and 2-cells. The fermionic version of the state sum is similar to the bosonic version:

$$Z(M) = \sum_{\beta \in \mathcal{L}(\mathcal{H})} (-1)^{\kappa_\beta} \prod_{c \in \mathcal{H}_3} \mathcal{D}^{-2} \prod_{f \in \mathcal{H}_2} \frac{d(f,\beta)}{n(f,\beta)} \prod_{e \in \mathcal{H}_1} \widetilde{\Theta}(e,\beta)^{-1} \prod_{v \in \mathcal{H}_0} \mathrm{Link}(v,\beta). \tag{416}$$

The fermionic version of the state sum differs from the bosonic version in the following ways:

- The the string nets corresponding to the 0- and 1-handle weights require a sign-ordering of their string net vertices. This in turn requires that the partition function is weighted by a Koszul sign $(-1)^{\kappa_\beta}$ which measures the difference between the global sign ordering coming from the 1-handles and the global sign ordering coming from the 0-handles.

- The weights assigned to the 2-handles need to be properly normalized, resulting in a factor of $n(f,\beta) = \dim \mathrm{End}(a)$ if a is the simple object labeling the core of the attaching annulus for the 2-handle f by β.

- The spin structure on M determines how the basis elements which make up the labeling β are inserted into the graphs $\mathrm{Link}(v)$.

As in the previous section, we will now explain the factors appearing in (416).

As before, we use the 2-cell orientations to define an oriented graph (unlabeled string net) on the boundary of each 0-, 1- and 2-handle. String net graphs are assigned to the

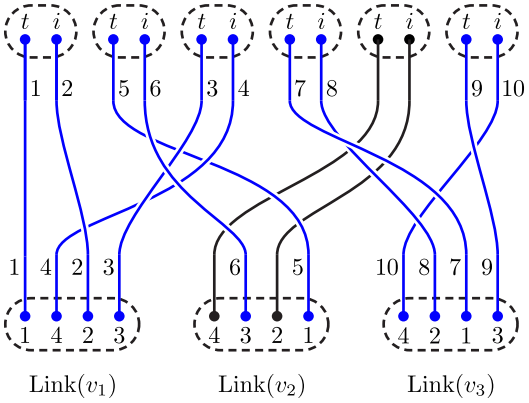

Figure 10.2.1: An example of how to compute the Koszul sign $(-1)^{\kappa_\beta}$ diagrammatically for a graph consisting of three 0-handles and six 1-handles. The lower dashed regions represent the 0-handles, while the upper dashed regions represent the 1-handles (with initial and terminal ends marked as i and t, respectively). The Koszul orderings indicated by the numbers are explained in the text, and κ_β is given by the number of crossings of the blue strands (in this example, $(-1)^{\kappa_\beta} = -1$).

k-handles in the same way as in the bosonic case. The set of all labelings $\mathcal{L}(\mathcal{H})$ is defined as the product over all 1-handles e of the basis sets $B(e)$. For a fixed labeling $\beta \in \mathcal{L}(\mathcal{H})$, the weights are determined as follows.

The 2-handle weight $d(f, \beta)$ is defined in the same way as before. However we now divide by the factor $n(f, \beta) = n_a = \dim \mathrm{End}(a)$, where a the the simple object labeling the boundary of the core of the 2-handle. This factor is necessary because the norm-square of the a-labeled loop is n_a.

The 1-handle weights are determined by the bilinear pairings given by each 1-handle e. When evaluating the graph on the boundary of e, we choose the Koszul ordering which puts the terminal vertex immediately before the initial vertex in the ordering (similar to the convention in (310)).

For each 0-handle v, $\mathrm{Link}(v, \beta)$ is defined in the same way as in the bosonic case: we evaluate a string net determined by the 1- and 2-handles incident on v and the labeling β. There are two subtleties here. First, when mapping a vertex label μ from the initial (terminal) end of a 1-handle to the 0-handle adjacent to the terminal (initial) end of the 1-handle, we must employ the attaching map which connects the terminal (initial) end of the 1-handle to the 0-handle. This attaching map is a spin diffeomorphism, and changing the attaching map by a spin flip changes the sign of the label on the 0-handle by $(-1)^{|\mu|}$. It is here (and only here) that the state sum is sensitive to the spin structure on M. The second subtlety concerns Koszul orderings. In order (pun noticed but not intended) to evaluate the string net on the boundary of the 0-handle, we must choose an (arbitrary) ordering of the string net vertices of the graph on the boundary of the 0-handle. Thus the evaluation $\mathrm{Link}(v, \beta)$ is arbitrary up to a sign. However, we will see that a change of Koszul ordering which changes the sign of $\mathrm{Link}(v, \beta)$ also produces a compensating change in the factor $(-1)^{\kappa_\beta}$, and so the overall state sum is well defined.

The Koszul sign $(-1)^{\kappa_\beta}$ is defined as follows. Consider, for fixed β, the tensor product of the all the super vector spaces associated to the attaching disks on all the 0-handles. If there are k 1-handles, then there are $2k$ tensor factors in this tensor product, one for each 1-handle end. We will compare two different orderings of the tensor factors. In

the first ordering, we place each terminal disk immediately before each initial disk in the ordering. Such an ordering is well-defined up to even permutations. In the second ordering, we choose a global ordering of the 0-handles and then use the above choices of local ordering for the factors associated to each 0-handle. This is again well-defined up to even permutations, since each 0-handle graph evaluates to zero when the total parity at that 0-handle is odd. (It depends on the choice of local orderings but not on the choice of global ordering of the 0-handles.) We then define $(-1)^{\kappa_\beta}$ to be Koszul sign relating these two orderings.

We now describe a convenient way to compute $(-1)^{\kappa_\beta}$ graphically, with an example shown in Figure 10.2.1 for a graph consisting of six 1-handles (upper dashed regions) and 3 0-handles v_1, v_2, v_3 (lower dashed regions). Each 0-handle has four 1-handle attaching regions, which are indicated by the lower small dots and which possess a local ordering relative to one another (indicated by the numbers within the lower dashed regions). Each attaching region can either be even (black) or odd (blue). If it is odd, we assign a Koszul ordering to the attaching region, consistent with the local ordering at the 0-handle. This ordering is indicated by the numbers appearing just outside the lower dashed regions.

Each 1-handle either has two even ends or two odd ends: if it has two odd ends, we assign an ordering to the ends by placing the terminal end immediately before the initial end in the ordering. This ordering is denoted by the top row of numbers below the 1-handles in Figure 10.2.1.

To evaluate $(-1)^{\kappa_\beta}$, we draw a fermion line connecting each odd 0-handle attaching region with Koszul order k to the respective 1-handle end with Koszul order k. $(-1)^{\kappa_\beta}$ is then simply $(-1)^{n_c}$, where n_c is the number of crossing between fermion lines in the resulting diagram. In the example of Figure 10.2.1 we have $n_c = 11$, and so $(-1)^{\kappa_\beta} = -1$.

The case of non-empty ∂M presents one new issue not present in the bosonic version: we must pick a Koszul ordering of the labels corresponding to string net vertices on ∂M. Once this has been done, we can combine that ordering with the ordering coming from the 1-handles. The Koszul sign $(-1)^{\kappa_\beta}$ is now defined to be the sign arising from comparing the 0-handle ordering with the combined ∂M and 1-handle ordering.

10.2.2 The fermionic state sum as a tensor network

We now turn to the task of reinterpreting (416) as a tensor network.

We incorporate the factors of $d(f,\beta)/n(f,\beta)$ and $\mathcal{D}^{-2}$ into the 0-handle weights in the same way as in the bosonic case. As in the bosonic case we denote the dressed 0-handle weights by $\widetilde{\text{Link}}(v,\beta)$. We define the vertex tensor in a similar fashion to (409). Let $e_1, \cdots, e_k$ be the 1-handles adjacent to the 0-handle v with the same ordering as the vertices of the graph $\text{Link}(v)$. Let V_i be defined in the same way as (407) (with the modification that V_i is a super vector space). We define

$$T_v \in V_1^* \otimes \cdots \otimes V_k^* \tag{417}$$

by

$$T_v(w_1 \otimes \cdots \otimes w_k) = \widetilde{\text{Link}}(v, w_1 \otimes \cdots \otimes w_k) \tag{418}$$

where $w_i \in V_i$. In words, T_v evaluates the string-net graph determined by $\text{Link}(v)$ with the ordered vertices labeled by $w_1, \cdots, w_k$ (in the same order), and multiplied by the appropriate factors of $d(f,\beta)/n(f,\beta)$ and $\mathcal{D}^{-2}$.

As in the bosonic case, the partition function is computed as a trace of the T_v tensors:

$$Z(M) = \mathrm{tr}\left(\bigotimes_{v\in\mathcal{H}_0} T_v\right). \tag{419}$$

where the tr denotes contracting dual indices. In practice, to perform the trace, we require that the pair of vectors to be contracted be adjacent in the Koszul ordering (with terminal preceding initial). To make the pair of vectors adjacent in the Koszul ordering we need to apply a number of Koszul isomorphisms. After contracting all vectors we pick up the appropriate factor of $(-1)^{\kappa_\beta}$. Again, $Z(M)$ is independent of the way we assign factors of $d(f,\beta)/n(f,\beta)$ and $\mathcal{D}^{-2}$ to the vertex tensors.

If ∂M is non-empty, we again follow the bosonic prescription in (411) to obtain $Z(M) = \mathrm{tr}\left(\bigotimes_{v\in\mathcal{H}_0} T_v\right) \in W_1^* \otimes \cdots \otimes W_n^*$, where $W_1, \ldots, W_n$ are the vector spaces associated to the boundary 0-cells and we are implicitly making use of the undordered tensor product. When using $Z(M)$ to compute amplitudes of different string-net boundary conditions, care must be taken when performing the tensor contraction on ordered representatives because of Koszul sign issues.

10.2.3 Fermionic standardization procedures

As in the bosonic case, we can standardize the tensor network by choosing a generic cell decomposition (dual to a triangulation) and "pitchforkizing" all trivalent vertices which appear on the boundaries of 0-handles. Note that in this fermionic setting, pitchforkizing includes choosing a spin framing at each trivalent vertex. This standardization procedure results in string net vertices on 0-handles which are standardized independently of their partners at the opposite ends of the 1-handles: the form of a given trivalent vertex at the initial edge of a 1-handle e and the form of the associated vertex on the terminal edge of the 1-handle may be related by a pivot operation. Properly accounting for this requires inserting pivot operators $P_e = P^{l_e}$ into the 1-handles, as in (414). Rather than tacking the spin-structure signs onto the 0-handle weights we incorporate them into the pivots. Indeed, we now have $P_e^3 = (-1)^F$, so that l_e is valued in $\mathbb{Z}_6$ as opposed to $\mathbb{Z}_3$. (Alternatively, we could keep $l_e \in \mathbb{Z}_3$ but insert $(-1)^F \cdot P^{l_e}$ where appropriate.) Note that the spin structure of the underlying 3-manifold is encoded in the edge pivots P_e (and the standardized 0-handles).

The standard tetrahedral string net on each 0-handle must of course incorporate a Koszul ordering in the fermionic case:

$$T_v(\alpha\otimes\beta\otimes\gamma\otimes\delta) = \mathrm{Tet}(v, \alpha\otimes\beta\otimes\gamma\otimes\delta) =$$

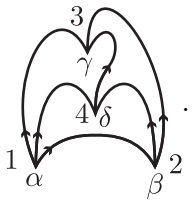

. (420)

Note that there are still multiple versions of the standardized tetrahedral weights Tet differing by choices of the edge orientations. The fermionic analogue of (415) can now be written:

$$Z(M) = \sum_{\beta\in\mathcal{L}(\mathcal{H})} (-1)^{\kappa_\beta} \prod_{c\in\mathcal{H}_3} \mathcal{D}^{-2} \prod_{f\in\mathcal{H}_2} \frac{d(f,\beta)}{n(f,\beta)} \prod_{e\in\mathcal{H}_1} \Theta(P_e,\beta)^{-1} \prod_{v\in\mathcal{H}_0} \mathrm{Tet}(v,\beta). \tag{421}$$

Again, $\Theta(P_e,\beta)$ is a standard pairing as in (310) but modified by the pivot isomorphism $P_e = P^{l_e}$.

10.3 The shadow world and ground state wave functions

In this subsection we construct a state sum and corresponding tensor network that produces the ground state wave function of the Hamiltonian defined in Section 9. In a nutshell, the idea is to apply the general tensor network construction of the previous subsection to the spin 3-manifold $\Sigma \times I$, where Σ is the spin surface which hosts the Hamiltonian.

Recall that the big Hilbert space for the Hamiltonian defined on a cell decomposition $\mathcal{G}$ is

$$\mathcal{H}_{\mathcal{G}} = \bigotimes_{v \in \mathcal{V}} \mathcal{H}_v, \tag{422}$$

where $\mathcal{H}_v$ is defined to be $\bigoplus_{a,b,c} V^{abc}$ if all edges point away from the vertex, with similar definitions of $\mathcal{H}_v$ in the case of other edge orientation arrangements. If a basis vector of $\mathcal{H}_{\mathcal{G}}$ satisfies edge label compatibility for all adjacent pairs of vertices (equivalently, if the basis vector lies in the ground state of the vertex term of the Hamiltonian), then it can be interpreted as defining a string net on Σ. A wave function (not "the" wave function unless the ground state is 1-dimensional) Ψ assigns a weight $\Psi(w)$ to each such basis vector w, in such a way that if $\sum_i c_i w_i$ is equal to zero in $A(\Sigma)$, then $\sum_i c_i \Psi(w_i) = 0$. For basis vectors w which violate edge label compatibility, we have $\Psi(w) = 0$.

Given a string net g on Σ, we can define a wave function Ψ_g via

$$\Psi_g(w) = Z(\Sigma \times I)(\bar{g} \cup w). \tag{423}$$

In other words, we evaluate the path integral $Z(\Sigma \times I)$ with boundary condition $\bar{g}$ on $\Sigma \times \{0\} \cong -\Sigma$ and boundary condition w on $\Sigma \times \{1\} \cong \Sigma$. (Recall that $\bar{g}$ is the reflected version of the string net g on the orientation-reversed surface $-\Sigma$.) Note that as g runs through a basis of $A(\Sigma)$, Ψ_g runs through a basis of the wave functions for the ground state of the Hamiltonian. Our task now reduces to using the techniques of the previous subsection to construct a tensor network which evaluates the RHS of (423).

First we must specify a handle decomposition of $\Sigma \times I$. Let G' be the 1-skeleton of the cell decomposition of Σ associated with $\mathcal{H}_{\mathcal{G}}$, and let G'' be the 1-skeleton of the cell decomposition of Σ underlying the input string net g. (In practice, G' will be as fine a lattice as our computer can handle, while G'' will be as simple as possible subject to the constraint that g can represent a basis of $A(\Sigma)$.) We stipulate that G' and G'' are transverse (i.e., only their 1-cells intersect, and all the intersections are transverse), and are each dual to a triangulation, so that their vertices are all 3-valent. We define the cell decomposition G to be the union of G' and G''. The graph G has three types of vertices: vertices of G', vertices of G'', and vertices corresponding to the points of $G' \cap G''$ which are 4-valent; see Figure 10.3.1.

Our handle decomposition for $\Sigma \times I$ will be a thickened version of G. We have a 0-handle for each vertex of G, a 1-handle for each edge of G, and a 2-handle for each 2-cell of the complement of G. There are no 3-handles. Figure 10.3.2 illustrates this handle decomposition, and also shows how the string nets v and $\bar{g}$ are situated on its boundary.

The next step is to standardize the string nets on the boundary of each 0-handle, by following the procedures outlined in Sections 10.1.3 and 10.2.3. This is illustrated in Figure 10.3.3 for the three different types of 0-handle in our handle decomposition G (one of each type of 0-handle is shown in the rightmost picture of Figure 10.3.2). Note

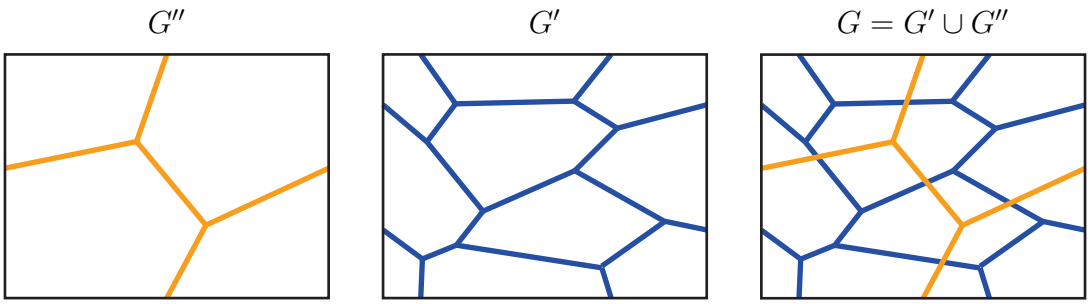

Figure 10.3.1: The cell decompositions described in the text. G'' (left) is the cell decomposition on which the input string-net state is defined, and G' (center) is the decomposition on which the Hamiltonian acts. The union $G = G' \cup G''$ (right) is the cell decomposition we use to construct the ground state wavefunctions.

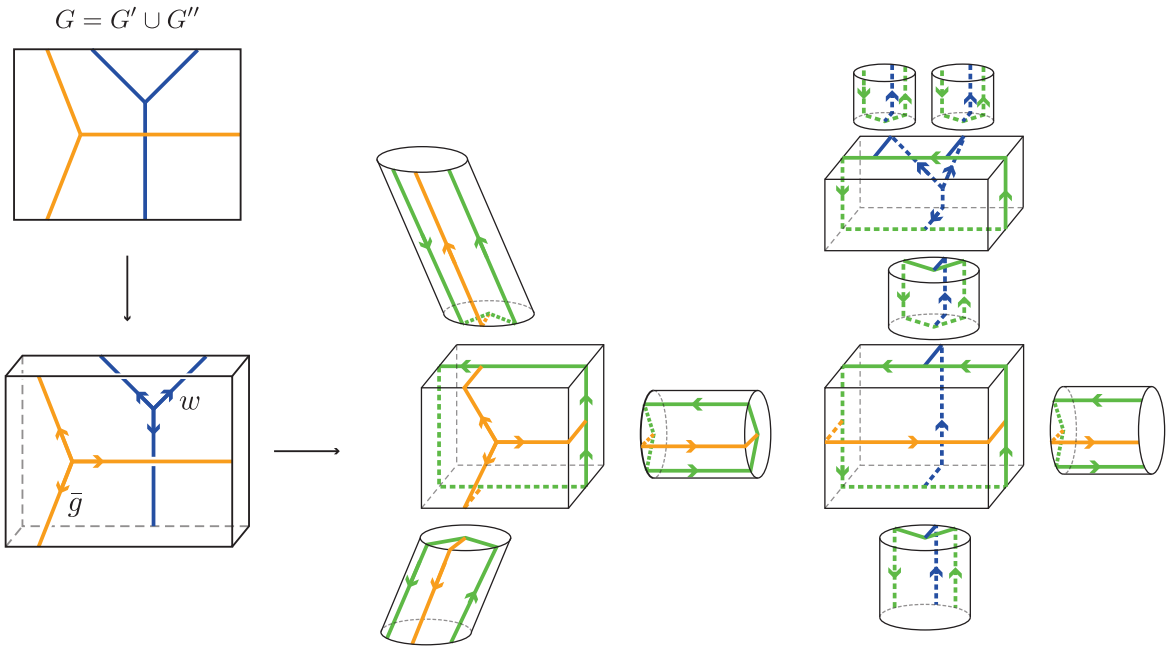

Figure 10.3.2: An example cell decomposition on $\Sigma \times I$. In the upper left figure, we show the cell decomposition G for a given simple choice of G' (blue) and G'' (orange). In the lower left figure, we include the "time direction" in the picture, which thickens it into a box with boundary conditions set by $\bar{g}$ on the initial boundary $\Sigma \times \{0\}$ and boundary conditions set by w on the terminal boundary $\Sigma \times \{1\}$. The right figure shows the full handle decomposition for this setup. Each box shows a 0-handle in the composite cell decomposition G, while each cylinder shows a 1-handle. The green lines denote string nets in the interior of $\Sigma \times I$, which are not fixed by either of the boundary conditions $\bar{g}, v$.

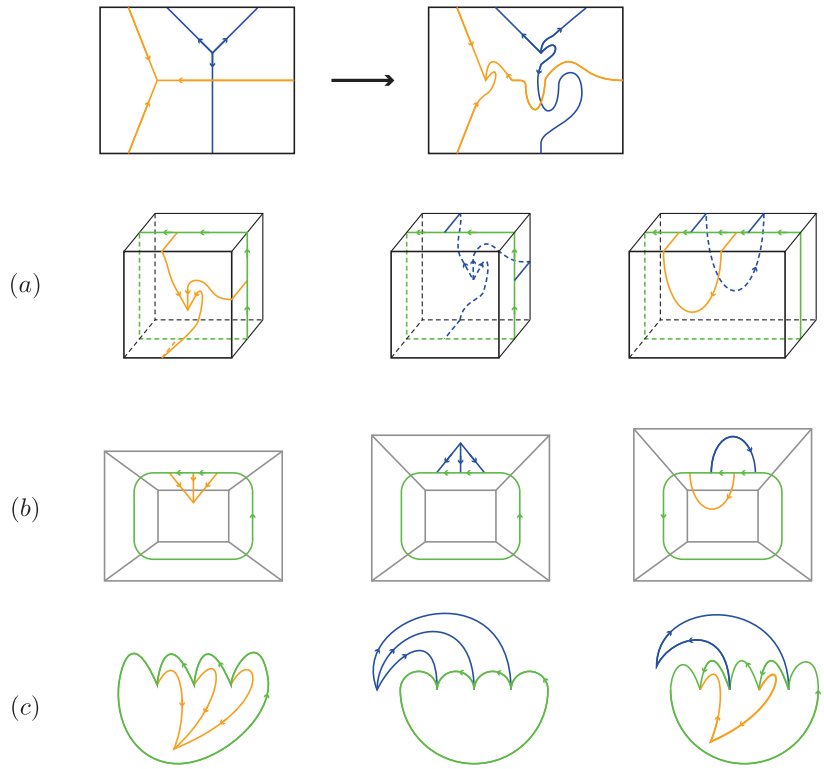

Figure 10.3.3: The different types of 0-handles that appear in the cell decomposition of G. The top picture shows how a simple cell decomposition is standardized by putting each of the trivalent vertices in pitchfork form. In row (a) we show the three different types of standardized 0-cells that can appear in G. The cubes are drawn so that the 0-cells are located in their centers. Orange (blue) lines represent 1-handles in G'' (G'), and green lines represent intersections of 2-cells in G with the cube. In row (b) we show the standardized string nets projected into the plane, and in row (c) we finish the standardization of the diagrams by making each trivalent vertex a pitchfork. The appropriate 0-cell tensors are found by evaluation of these diagrams.

that our conditions on the handle decompositions G', G'' ensure that all three types of 0-handle string nets are tetrahedral.

We are now in a position to apply the state sum and tensor network constructions of the previous subsection. The state sum turns out to be a version of the "shadow world" state sum of [38, 52]. In other words, the shadow world state sum is a special case of the Turaev-Viro state sum. If we fix the (labeled) string net $\bar{g}$ at the outset, the tensor network has an output corresponding to (422).

To compute the tensor network, we just need to know how to assign tensors to the 0-handles in G. This is done by computing evaluations of tetrahedral string-net diagrams, as in previous sections. Explicitly, for a 0-cell v of G consisting of three 1-cells of G'

(middle column of row (a) of Figure 10.3.3), we assign the tensor T_v as follows:

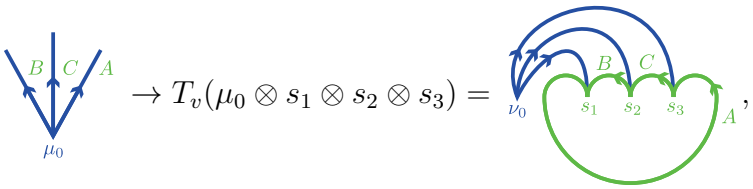

(424)

In the diagrams, the green letters A, B, C denote the labels of the 2-cells in the "interior" of the cell decomposition on $\Sigma \times I$ (those drawn in green in Figure 10.3.2), which will be summed over when computing the amplitude $Z(\Sigma \times I)(\bar{g} \cup v)$. The labels of the blue lines are fixed, and are determined by the labels of the 1-cells in the string-net graph v on $\Sigma \times \{1\}$.

Tensors for the other types of 0-cells in G are determined similarly. For the type of 0-cell in the left column of row (a) in Figure 10.3.3 involving three 1-handles from G'', we assign the tensor

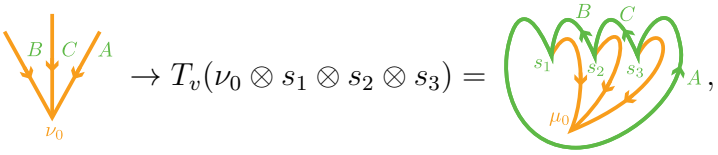

(425)

(426)

where the labels of the orange lines are fixed by the input string-net state $\bar{g}$. Similarly, for the type of 0-cell in the right column (involving the intersection of 1-handles in G' and G'') we assign the tensor

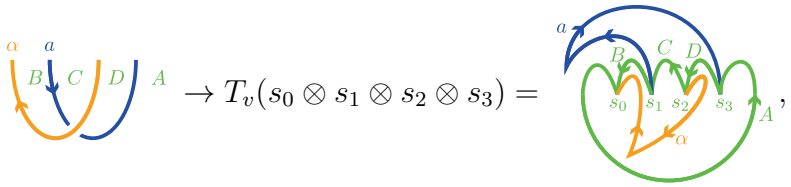

(427)

(428)

which corresponds to a string operator.

Now that we know how to assign tensors to each 0-handle, we can construct the partition function $Z(\Sigma \times I)(\bar{g} \cup v)$ in the same way as in previous sections, namely by performing a tensor contraction over $\bigotimes_{v \in \mathcal{H}_0} T_v$, where the tensor product runs over all 0-cells of G. (The evaluation of this tensor contraction involves the same treatment of Koszul signs and 1-handle pivots as the fermionic state sum discussed in the previous section.)

Instead of fixing a particular input string net g, we can put g and v on more equal footing by constructing a tensor network which computes an operator from $\mathcal{H}_{G''}$ to $\mathcal{H}_{G'}$, where $\mathcal{H}_{G''}$ and $\mathcal{H}_{G'}$ are versions of (422) corresponding to the vertices of g and v, respectively. In particular, we can take G'' to be isotopic[32] to G' and compute a projection from the big Hilbert space to itself. This projection is, of course, the projection onto the ground state of the Hamiltonian of Section 9.

There is one small technical hurdle to overcome before constructing this operator. Previously we adopted the convention that boundaries of 3-manifolds are contained in

[32] We can't take $G'' = G'$ because we require that G' and G'' be transverse.

the 2-skeletons of cell decompositions corresponding to handle decompositions. This is convenient for many purposes, but if we want to glue 3-manifolds along their boundaries (and perform analogous operations with tensor networks), then it would have been more convenient to take the boundaries to be transverse to the cell decompositions. In practice, this means that we must assign some additional factors of $\mathcal{D}^{-2}$ and d_a/n_a to our 0-handle tensors (as described above (407)), corresponding to 3- and 2-cells which straddle the surface along which we are gluing 3-manifolds. Specifically, for each 2-cell of G'' we choose an adjacent 0-cell and assign a factor of $\mathcal{D}^{-2}$ to the corresponding 0-handle tensor, and to each 1-cell of G'' we choose an adjacent 0-cell and assign a factor of d_a/n_a to the corresponding 0-handle tensor. These 2- and 1-cells in Σ correspond to the 3- and 2-cells which straddle the gluing surface when we glue two copies of $\Sigma \times I$ together.

Let H denote the resulting tensor network operator. The fact that $(\Sigma \times I) \cup (\Sigma \times I) \cong \Sigma \times I$ implies that $H \circ H = H$. The fact that $\Sigma \times I \cong -(\Sigma \times I)$ (via a homeomorphism which is the identity on the Σ factor and reverses the I factor) implies that H is self-adjoint (see the end of Section 8.9).

11 Kitaev chain

In this section, we show how the graphical formalism developed in previous sections can be used to capture the salient features of the "Kitaev wire", Kitaev's toy model of a one-dimensional spinless p-wave superconductor [53]. This highlights the connection between Majorana zero modes and Ising anyons and serves as a nice application of the graphical calculus of the C_2 theory. Most of what we say applies beyond the C_2 theory and can be carried out for any theory containing at least one q-type object. The Hamiltonian we write down is a special case of the one constructed in Section 9, for particular choices of cell decompositions of a disk (annulus) with fixed boundary conditions. The associated wavefunctions we construct are the same as those found in, e.g., [54], but presented in a more graphical formalism that serves as a simple example of the techniques discussed in Section 10.

Recall that the C_2 theory has two simple objects, $\mathbb{1}$ and β, with $\beta \otimes \beta \cong \mathbb{C}^{1|1}\mathbb{1}$, and $\mathrm{End}(\beta) \cong \mathbb{C}\ell_1$. We will focus on the β object in the C_2 theory for concreteness, but the analysis can be applied q-type objects q in any theory.

In what follows, we will show that a single strand of β string is a diagrammatic description for the zero correlation length limit of the Kitaev chain. This means that the string-net Hamiltonian in Section 9 based on the C_2 theory describes a phase of fluctuating Kitaev wires, an idea previously investigated in [7, 8, 18].

The basic strategy is to cut a single β strand into pieces and analyze how to glue those pieces back together to recover the uncut strand. Physically, we will implement the gluing by requiring the vectors to be in the ground space of a particular Hamiltonian, which is similar to what we did in Section 9. We first note that the vector space associated to a single interval I with boundary conditions labeled by β can be written graphically as

$$A(I;\beta,\beta) = \mathbb{C}\left[\quad,\quad\right] \cong \mathbb{C}^{1|1}. \tag{429}$$

Now we can consider splitting the interval I into two smaller intervals I_1, I_2, such that $I_1 \cup I_2 = I$. We then can reconstruct the vector space $A(I;\beta,\beta)$ from the vector spaces $A(I_1;\beta,\beta), A(I_2;\beta,\beta)$ by gluing the two intervals I_1, I_2 together. Algebraically, this gluing is implemented by the tensor product. However, we must be sure to make

the proper choice of tensor product to ensure that we don't produce any extra degrees of freedom during the gluing. The standard tensor product $\otimes_{\mathbb{C}}$ doesn't work, since then $A(I_1;\beta,\beta)\otimes_{\mathbb{C}} A(I_2;\beta,\beta)\cong \mathbb{C}\ell_2 \ncong A(I;\beta,\beta)$.

The correct tensor product to use is the relative tensor product $\otimes_{\mathrm{End}(\beta)}$ (a.k.a $\otimes_{\mathbb{C}\ell_1}$) discussed in Section 8.6. With this tensor product, we (rather trivially) have

$$A(I;\beta,\beta)\cong A(I_1;\beta,\beta)\otimes_{\mathrm{End}(\beta)} A(I_2;\beta,\beta), \tag{430}$$

which tells us how to split apart the I interval correctly.

Graphically, the relative tensor product $\otimes_{\mathrm{End}(\beta)}$ is needed to mod out by local relations involving the sliding of fermions along β lines, as was discussed Section 8.6. Utilizing $\otimes_{\mathrm{End}(\beta)}$ is equivalent to performing the regular tensor product $\otimes_{\mathbb{C}}$ and modding out by the equivalence relations

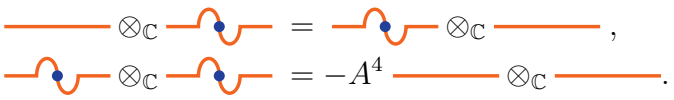

(431)

where we have assumed a Koszul ordering for the fermions which increases from left to right (see Table 2.4.1 for the origin of the phase A^4).

As we did with the string-net Hamiltonian in Section 9, we can implement these equivalence relations energetically, via an appropriately defined Hamiltonian, which will be the same as the edge term in the lattice Hamiltonian defined in (387).

Consider an interval I of β string cut into n segments: $I = I_1 \cup I_2 \cup \cdots \cup I_n$. Each segment I_i will end up mapping to a single physical site in the Kitaev chain. The local Hilbert space at each I_i segment is generated by two basis vectors v_e, v_o, which for convenience we draw as

v_e =  , v_o =  . (432)

The upward-curved ends on each β segment are drawn purely for aesthetic purposes, and exist solely to make drawing the Kitaev chain slightly easier. The local Hilbert space is then

$A(I_i;\beta,\beta) = \mathbb{C}$  $\cong \mathbb{C}^{1|1}$. (433)

The total Hilbert space of the chain is given by tensoring each local Hilbert space together:

$$\mathcal{H}_I = A(I_1;\beta,\beta)\otimes_{\mathbb{C}} A(I_2;\beta,\beta)\otimes_{\mathbb{C}}\cdots\otimes_{\mathbb{C}} A(I_n;\beta,\beta). \tag{434}$$

States in this Hilbert space are expressed graphically as

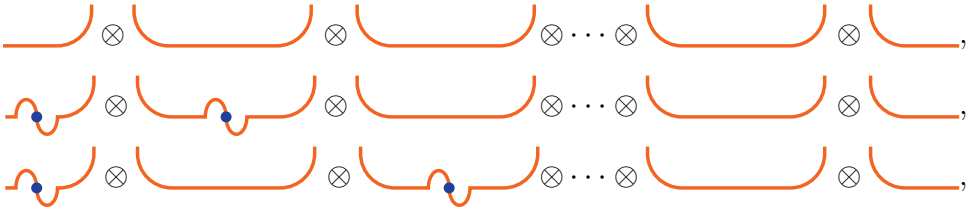
(435)

(436)

(437)

⋮ (438)

and so on. Instead of using the relative tensor product $\otimes_{\mathrm{End}(\beta)}$ to mod out by the equivalence relations (431) we use $\otimes_{\mathbb{C}}$ (abbreviated as $\otimes$ above) and define a Hamiltonian so that the ground space is isomorphic to $A(I;\beta,\beta)$. The Hamiltonian can be written as:

$$H_i = \frac{1}{2}\Big($$ 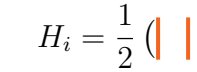 $$\Big)\,,$$ (439)

which have a non-trivial action only on the adjacent Hilbert spaces associated to the intervals I_i and I_{i+1}.[33]

The image of this projector on a pair of adjacent string endpoints is

(440)

so that using $\otimes_{\mathbb{C}}$ and projecting with H is equivalent to using $\otimes_{\mathrm{End}(\beta)}$. Thus, H_i is responsible for gluing together ends of β strands. In terms of electronic operators, H_i implements hopping and pairing between electrons in nearest neighbor sites i and $i+1$.

We form our Hamiltonian from a sum of projectors, H_i, acting between each pair of strands:

$$H = t\sum_{i=1}^{n-1}(1-H_i). \tag{441}$$

This Hamiltonian describes the zero correlation length limit of the Kitaev chain, albeit in a slightly unconventional language. To understand this, we proceed to investigate the ground state wave functions.

We note that the nontrivial term in the Hamiltonian is proportional to the fermion parity measured between adjacent physical sites. Indeed, acting with that term on the vectors v_e, v_o defined in (432), we find

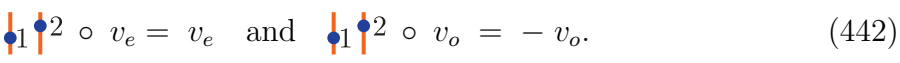

(442)

which is precisely the action of $(-1)^F$ (which can be identified with $i\gamma_1\gamma_2$ in the conventional Clifford algebra language).

It is straightforward to find the ground states of (441). Noting that the non-trivial term in the Hamiltonian is just measuring the parity shared between adjacent "physical" sites, we can do a change of basis using an F-move so that the Hamiltonian is diagonal and annihilates the ground state. In this basis the (un-normalized) ground state wavefunctions take the form

(443)

In this basis the Hamiltonian acts as $(1-(-1)^F)$ on each pair of vertical strands, which is clearly zero.

To better understand the wavefunctions Ψ_e, Ψ_o, we can apply a series of F-moves to change to the physical "on-site" basis.[34] In a Kitaev chain with n physical sites (i.e., n

[33] Note that there are no terms that act on both the right and left ends of a single strand/interval; such a term would perturb us away from the zero correlation length limit. In the language of the Kitaev chain, this corresponds to tuning the chemical potential to zero and the magnitude of the superconducting gap to the hopping amplitude.

[34] Recall the physical Hilbert space is associated to $A(I_i;\beta,\beta)$, whereas the wavefunctions Ψ_e, Ψ_o are expressed in a basis that's "shared" between adjacent sites.

intervals), we recover the well known result

$$\Psi_e = \frac{1}{d^{n-1}} \sum_{\substack{\{v_i\} \\ n_f=\text{even}}} (A^4)^{n_f/2}\, v_1 \otimes v_2 \otimes \cdots \otimes v_n \tag{444}$$

where the sum is over all configurations of $v_i = v_o, v_e$ such that only an even number n_f of odd vectors v_o appear in the tensor product, and where v_e, v_o are defined as in (432). For the odd wavefunction Ψ_o, we find

$$\Psi_o = \frac{1}{d^{n-1}} \sum_{\substack{\{v_i\} \\ n_f=\text{odd}}} (A^4)^{(n_f-1)/2}\, v_1 \otimes v_2 \otimes \cdots \otimes v_n \tag{445}$$

where the sum is now restricted so that only an odd number n_f of odd vectors v_o vectors in the tensor product. From the expressions for Ψ_e, Ψ_o in this basis, we see that they are given by configurations that are coherent sums over all fermion parity even and fermion parity odd states, respectively.

Note that the fermion dot appearing in Ψ_o of (443) has zero energy (since the Hamiltonian does not act on either the beginning of the first strand in the chain or the end of the last strand), while this is not true for fermion dots appearing on the interior cups. Physically, this is due to the presence of a pair of Majorana zero modes localized at the ends of the chain. One can explicitly construct the zero mode operators by considering the odd operators acting on either end of the chain; they commute with the Hamiltonian, anti-commute with one another, anti-commute with $(-1)^{F_{\text{tot}}}$ (the total fermion parity), and up to a pre-factor each square to the identity. These are exactly the properties of a Majorana zero mode. A nice feature of the diagrammatic notation we use is that one can easily see that acting on the left end of the chain with one zero mode operator is equivalent to acting on the right end with the other zero mode operator (up to a phase). To see this, one simply slides the fermionic dot appearing from the zero mode operator along the bottom β strand appearing in the presentation of the wavefunction (see (443)). Physically, this means the ends of the wire share a fermionic mode, and no information about the occupancy of this mode can be detected by local measurements.

By considering the same spin chain but using the regular Ising fusion category A_3 (rather than the condensed A_3/ψ theory), one finds exactly the transverse field Ising model. Fermion condensation provides a map between these two models in the same way the Jordan-Wigner transformation does. Of course, we have only discussed the zero correlation length limit, but on-site terms can be added as well, and the analysis carries through, except that the zero modes are exponentially localized to the boundary (for a small perturbation). In the zero correlation length limit, excited states are easily constructed by putting dots on the intermediate cups.

We now turn our attention to the Kitaev chain defined on a circle. The bulk of the Hamiltonian is constructed from a sum of projectors defined in (439). To "glue" the end points of the interval into a circle, we need to add an additional term across the boundary. There are two ways to do the gluing, differing from one another by a 2π rotation of the spin framing (i.e. a spin flip). These choices correspond to the two spin structures on the circle, S^1_B and S^1_N, corresponding to anti-periodic and periodic fermionic boundary conditions, respectively. To define periodic boundary conditions we define H_{n+1}, the Hamiltonian term which glues the two endpoints of the interval together, by

$H^N_{n+1} =$  (446)

where the leftmost string acts on the left side of I_1 and the rightmost string on the right side of I_n. When closing the interval with anti-periodic boundary conditions (to form the bounding spin structure) we need to apply a spin flip twist to H_n, resulting in an additional minus sign multiplying the nontrivial term in the projector:

$$H^B_{n+1} = \frac{1}{2}\Big($$ 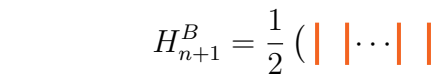 $$(447)$$

We note that these give us explicit matrices for the even linear maps $\mathrm{cl}_B : A(I;\beta,\beta) \to A(S^1_B,\beta)$ and $\mathrm{cl}_N : A(I;\beta,\beta) \to A(S^1_N,\beta)$. In this case we are led to identify cl_B with H^B_{n+1} and cl_N with H^N_{n+1}. To substantiate these identifications we will explicitly compute the ground state wavefunctions.

In Section 3.1 we noted that closing a q-type object along a bounding (non-bounding) spin structure results in an even (odd) parity vector; if the identifications made above are correct, then the ground state of the bounding Hamiltonian should have even parity, and the ground state of the non-bounding Hamiltonian should have odd parity. To see that this is indeed the case, we note that that when acting with the non-trivial term in H^X_{n+1} for $X \in \{B, N\}$ on the the subspace spanned by (443) (with the outer legs now turned up), we need to slide one of the fermions around the full S^1_X. Using this, the fact that the structure of the Hamiltonian is the same as in (439), and using our earlier results (443), we can write the (unnormalized) wavefunctions on the B and N sectors as

$$\Psi_B =$$  $$, \qquad \Psi_N =$$  $$, \qquad (448)$$

where the subscripts denote the spin structure. Although our graphical presentation may give the impression that these pictures are drawn on an interval, they are not: the presence of the H_{n+1} terms, which act on the left-most and right-most strands in the graphical presentation of Ψ_e and Ψ_o are responsible for gluing the interval into a circle.

Note that the other possible candidates for ground-state wavefunctions (an odd-parity version of Ψ_B or an even-parity version of Ψ_N) are identically zero, which can be seen by using the graphical calculus of the C_2 theory (see the discussion around (39)).

The above Hamiltonian can be viewed as a special case of the Hamiltonian in Section 9 as follows. We take the ambient 2-manifold to be a long, thin rectangle (i.e. a disk). We fix a β strand boundary condition at each of the short sides of the rectangle. On the long sides we impose empty boundary conditions. In the interior, the "lattice" contains only 2-valent vertices, as shown in Figure 11.0.1. Applying the general prescription in Section 9 to this case yields essentially the same Kitaev wire Hamiltonian as defined above. The spins at each 2-valent vertex are $V^{\beta\beta} \cong \mathbb{C}^{1|1}$. The vertex terms of the general Hamiltonian do nothing interesting, and there are no plaquette terms. The edge terms of the general Hamiltonian (371), which we recall serve the purpose of allowing fermion dots to fluctuate along q-type strings, are the same as (439). Thus, when acting on single strands of q-type string, the general Hamiltonian (371) reduces to the Kitaev chain Hamiltonian.

We can similarly glue the two ends of the rectangle together (either periodically or antiperiodically) to obtain the Kitaev chain Hamiltonians for spin circles.

We now use the Hamiltonian to construct matrix product operators (MPOs) and their related matrix product states (MPSs) for the ground state wavefunctions (443) of (441). This is a well known result, see e.g. [54, 25, 55]. We write it here as it in some sense gives a "gentler" version of the tensor network discussed in Section 10, and provides a nice application of the graphical calculus developed in the body of the paper.

Figure 11.0.1: A cell decomposition of $I \times I$ with two marked points on the boundary, each labeled β. The interior graph contains n "pitchforkized" 2-valent vertices.

We seek an MPO that projects a given state into the image of the projectors H_i defined in (439). For convenience, we write $H_i = \frac{1}{2}(e_i + f_i)$, with e_i proportional to the identity operator on the junction between the intervals I_i and I_{i+1}, and f_i proportional to the fermion parity operator $(-1)^F$ across the junction. Temporarily putting aside the issue of boundary conditions, to find the MPO we simply act with $\prod_i H_i$ on a given initial vector $V = v_1 \otimes \cdots \otimes v_n$, where $v_i = v_e, v_o$ (graphically, these input vectors look like those appearing in (435)). After expanding the product $\prod_i H_i$, we find an operator which is a sum over all possible configurations of the operators e_i and f_i straddling the junctions between intervals I_i and I_{i+1}. We will denote the resulting state by Ψ.

We now just need to simplify the resulting state Ψ using the local relations of the C_2 theory. Each physical site v_i can be acted on by two terms in the Hamiltonian: H_i (acting on the right strand of v_i) and H_{i-1} (acting on the left strand). Hence, when we simplify Ψ, the phase factor associated with a given physical site v_i will depend on a pair of indices (e,e),(e,f),(f,e), and (f,f), where the left (right) index denotes the term in H_{i-1} (H_i) that contributes to the phase.

Focusing on a single site with input vector v_i, we can succinctly write the action of the Hamiltonian as a matrix $(W^{v_i \to v_i'})_{xy}$, where v_i' denotes the output vector obtained after acting with the Hamiltonian and where $x, y \in \{e, f\}$. These matrices are straightforward to compute using the rules of the C_2 graphical calculus. If the input vector is v_e, we find

$$W^{v_e \to v_e} = \frac{1}{2}\begin{pmatrix} 1 & 0 \\ 0 & 1 \end{pmatrix} \qquad W^{v_e \to v_o} = \frac{1}{2}\begin{pmatrix} 0 & A^4 \\ 1 & 0 \end{pmatrix}, \tag{449}$$

while we get

$$W^{v_o \to v_e} = \frac{1}{2}\begin{pmatrix} 0 & 1 \\ A^4 & 0 \end{pmatrix} \qquad W^{v_o \to v_o} = \frac{1}{2}\begin{pmatrix} 1 & 0 \\ 0 & -1 \end{pmatrix} \tag{450}$$

if the initial input vector is v_o.

We thus obtain an MPO on the interval:

$$W_{b_l b_r} : \mathcal{H}_I \to \mathcal{H}_I \tag{451}$$

$$v_1 \otimes \cdots \otimes v_n \mapsto \sum_{\{v_i'\}} \left(W^{v_1 \to v_1'} W^{v_2 \to v_2'} \cdots W^{v_n \to v_n'} \right)_{b_l b_r} v_1' \otimes \cdots \otimes v_n', \tag{452}$$

where $b_l, b_r \in \{e, f\}$ and b_r are boundary conditions for the interval. If $b_l = f$ ($b_r = f$), an additional fermionic dot is present on the left side of the first interval (right side of the last interval). For example, the diagrammatics allows one to check that W_{ef} is an odd operator which satisfies $W_{ef} = A^4 W_{fe} \circ (-1)^F$.This is a consequence of β having an odd endomorphism. The additional $(-1)^F$ accounts for sliding a fermion past an odd operator.

To obtain an MPS for the ground states, we simply fix an initial vector $v_1 \otimes \ldots \otimes v_n$ and boundary conditions for the MPO. On the interval we can construct the even parity

ground state by

$$\Psi_e = \sum_{\{v_i'\}} \left(W^{v_e \to v_1'} W^{v_e \to v_2'} \cdots W^{v_e \to v_n'} \right)_{ee} \; v_1' \otimes \cdots \otimes v_n' \tag{453}$$

and the odd parity ground state with

$$\Psi_o = \sum_{\{v_i'\}} \left(W^{v_o \to v_1'} W^{v_e \to v_2'} \cdots W^{v_e \to v_n'} \right)_{ee} \; v_1' \otimes \cdots \otimes v_n'. \tag{454}$$

Setting the boundary conditions to be $b_l = b_r = f$ in both cases would provide the same wavefunction up to an overall phase.

Similarly using (106), one can find the (unnormalized) MPS on a bounding spin circle by

$$\Psi_B = \sum_{\{v_i'\}} \mathrm{tr} \left(W^{v_e \to v_1'} W^{v_e \to v_2'} \cdots W^{v_e \to v_n'} \right) v_1' \otimes \cdots \otimes v_n' \tag{455}$$

and by using (107) we find the (unnormalized) MPS on the non-bounding circle:

$$\Psi_N = \sum_{\{v_i'\}} \mathrm{str} \left(W^{v_o \to v_1'} W^{v_e \to v_2'} \cdots W^{v_e \to v_n'} \right) v_1' \otimes \cdots \otimes v_n'. \tag{456}$$

In order to produce a non-zero state we need to choose a even parity initial vector for the bounding spin structure, and an odd parity initial vector for the non-bounding spin structure.

To summarize, we showed that strands of q-type objects are intimately related to the Kitaev chain. One can think of the string net Hamiltonian (defined in Section 8) for the C_2 theory as describing a phase of fluctuating Kitaev wires, a point of view adopted in [7, 8, 18]. We also noted that fermion condensation is closely tied with the Jordan-Wigner transformation, as one With the one-dimensional Hamiltonian at hand, we showed how to explicitly construct the MPS for the ground state wavefunctions in this graphical language, recovering the same MPS as [54, 25, 55].

We also note that the same MPS can be found by employing the shadow world construction outlined in Section 10.3: we work on the 3-manifold $D \times I$ where D is a disk, and fix the string-net graph w on the $D \times \{1\}$ boundary to have two marked β points on the disk boundary and n interior 2-valent vertices (this string-net state is illustrated in Figure 11.0.1, where w is illustrated as being made up of a union of intervals).

12 Outlook

One potentially interesting aspect of the fermionic topological orders we have studied in this paper is their possible quantum information applications, which we now briefly speculate on. We consider a hybrid system with spin structure defects and deconfined anyonic excitations. Each spin structure defect harboring a q-type vortex admits an action by $\mathrm{End}(q)$, and so n such defects admit an action of $\mathrm{End}(q_1) \otimes \mathrm{End}(q_2) \otimes \cdots \otimes \mathrm{End}(q_n) \cong \mathbb{C}\ell_1^{\otimes n} \cong \mathbb{C}\ell_n$. One could then imagine utilizing this action to perform quantum computations. Physically, the action of $\mathbb{C}\ell_n$ is implemented by choosing pairs of vortices q_i and q_j and pumping a charge into q_i and out of q_j. A natural platform for pumping

charge through the q-type vortices is a Kitaev chain. Of course, in addition to the action of $\mathbb{C}\ell_n$, computations can also be performed with the conventional braiding of the deconfined quasiparticles appearing in $q_1 \otimes q_2 \otimes \cdots \otimes q_n$.

It would be useful to make more precise connections between physical entities and some of the mathematical devices we have used to construct the fermionic theories we have studied. In particular, it would be useful to clarify the precise physical meaning of the complex line bundle and the "back wall" that we use to perform fermion condensation. In simple examples like the C_2 theory, the most natural interpretation for these constructs seems to be that they constitute a topological p-wave superconductor. Indeed, the way we treat the physical fermions we use to perform condensation in our models is identical to the behavior of superconductors: they are free fermion states, where wavefunctions that differ by pairs of fermions are related by a phase. The specialization to the p-wave pairing channel is made because of the spinlessness of the fermions we use to induce the condensation, which we assumed from the very beginning. The superconducting nature of the devices we use to perform condensation is forced on us by our assumption that the emergent fermion ψ we condense possesses $\mathbb{Z}_2$ fusion rules, and that in the complex line bundle we construct, pairs of ψ worldline endpoints can be created or destroyed in pairs. Evidence for the presence of a p-wave superconductor is clearly seen in the C_2 theory: restricting our attention to the non-bounding torus with NN spin structure, both the modular S and T matrices factorize as $S = S_{Ising} \otimes S_{p\pm ip}, T = T_{Ising} \otimes T_{p\pm ip}$ (where the choice of $\pm$ is determined by the "angular momentum" of the fermionic dots in our graphical calculus, i.e. the choice of $\pm A^4$ when removing a semicircular fermion worldline), suggesting a possible interpretation of this sector as a stack of the original Ising theory with a topological superconductor. Indeed, this was noticed recently in [8]. Furthermore, the fact that the parity of the ground states on the torus with (N, N) spin structure is always odd agrees with this interpretation, since the fermion parity of a topological p-wave superconductor on such a torus is always odd [56].

In our discussion of the modular S and T matrices in each of the examples we've worked out, we have focused on the modular transformation perspective, rather than on the braiding statistics perspective. For example, we have computed the S-matrix by considering the way it acts to exchange the two cycles of the torus and we have not focused on the statistical picture behind the S-matrix, in which matrix elements S_{ab} correspond to double braids between a and b particles. While we have checked that the computation of double braids reproduces the correct S-matrix for $\mathbf{Tube}(C_2)$, some subtleties involving relative spin structures rear their heads when trying to compute particular braiding data in more general settings. We plan to address these subtleties in future work.

Acknowledgements Ethan Lake and Dave Aasen are grateful to Nick Bultinck, Nicolas Tarantino, Ryan Thorngren, Brayden Ware, and Dominic Williamson for helpful discussions. Dave Aasen thanks Parsa Bonderson for explaining his unpublished work at early stages of this project. Dave Aasen gratefully acknowledges support from the KITP Graduate Fellows Program, the National Science Foundation through grant DMR-1723367 and the Caltech Institute for Quantum Information and Matter, an NSF Physics Frontiers Center with support of the Gordon and Betty Moore Foundation through Grant GBMF1250. Ethan Lake is supported by the Fannie and John Hertz Foundation. Dave Aasen and Ethan Lake acknowledge support by the 2016 Boulder Summer School for Condensed Matter and Materials Physics through NSF grant DMR-13001648. Kevin Walker thanks Zhenghan Wang and Scott Morrison for helpful conversations, and thanks

the Aspen Center for Physics and the Mathematisches Forschungsinstitut Oberwolfach for providing stimulating research environments.

A Spin and pin structures

In this appendix we review basic definitions and properties of spin and pin structures.

Roughly, a spin structure on an oriented n-manifold M is a specification for how fermions pick up phases of -1 as they move around M. Locally, we of course require that fermions pick up a minus sign when rotated through 2π, or when two fermions are exchanged within a small neighborhood of M. But if a fermion moves along a non-contractible loop in M, it is not clear what sign we should assign. A spin structure on M is a consistent set of answers to all possible questions of this form.

More formally, we can define a spin structure on M to be a double covering of the frame bundle $F(M)$, such than on each fiber of $F(M)$ the covering is isomorphic to the standard double covering $Spin(n) \to SO(n)$. Such double coverings correspond to cohomology classes in $H^1(F(M), \mathbb{Z}/2)$ which restrict to the generator of $H^1(SO(n), \mathbb{Z}/2)$ on each fiber. It follows that the difference between any two spin structures is canonically identified with an element of $H^1(M, \mathbb{Z}/2)$; spin structures on M form a $H^1(M, \mathbb{Z}/2)$-torsor. In particular, the number of distinct spin structures on M is given by the number of elements in $H^1(M, \mathbb{Z}/2)$. (Things need to said differently when $n < 2$. One way around this problem is to work with the stabilized frame bundle for 0- and 1-manifolds.)

It is important to note that there is no canonical correspondence between spin structures on M and $H^1(M, \mathbb{Z}/2)$; simply naming a cohomology class does not pick out a spin structure.

One way to specify a spin structure is to specify a framing on the 1-skeleton of a cell decomposition of M. We can think of this framing as an embedded graph in the frame bundle $F(M)$, and the spin structure is uniquely determined by requiring that the double covering of $F(M)$ be trivial when restricted to this graph. We can also think of the 1-skeleton framing as specifying a collection of possible fermion paths which do not pick up a factor of -1.

In this paper, most of the diagrams we draw are embedded in the page/blackboard/$\mathbb{R}^2$. $\mathbb{R}^2$ has a standard framing, so the 1-skeleton of any such diagram inherits a framing, and unless stated otherwise we work in the spin structure associated to that framing. In practice, then means that fermions pick up a minus sign only when their framing rotates with respect to the page.

If we have designated a reference spin structure on M (for example, the blackboard spin struture), then any other spin structure can be specified by giving an element of $H^1(M, \mathbb{Z}/2)$, or equivalently by giving the Poincaré dual element in $H_1(M, \mathbb{Z}/2)$. In this context, we refer to the Poincaré dual homology class as a "branch cut". Fermions obey the rules of the reference spin structure, except that they pick up a -1 whenever they cross the branch cut.

For unoriented manifolds, we must replace $SO(n)$ with $O(n)$ and replace $Spin(n)$ with a $\mathbb{Z}/2$ extension of $O(n)$. There are two such extensions, called $Pin_+(n)$ and $Pin_-(n)$. In $Pin_+(n)$, lifts of reflections in $O(n)$ square to the identity, while in $Pin_-(n)$ such lifted reflections square to the "spin flip" in $Spin(n)$. (When $n = 1$, we have $O(1) \cong \mathbb{Z}/2$, $Pin_+(1) \cong \mathbb{Z}/2 \times \mathbb{Z}/2$, and $Pin_-(1) \cong \mathbb{Z}/4$.) Roughly speaking, in pin+ manifolds reflecting a fermion twice returns us to the same state, while in pin− manifolds reflecting a fermion twice picks op a factor of -1.

None of the examples in this paper have a pin− reflection structure; we only work with pin+ structures.

Specifying pin+ structures in in terms of framings (as we did above for spin structures) is a little awkward. It is usually more convenient to use lifts of classifying maps or, when $n = 2$, quadratic refinements of intersection pairings.

B Constructing the fermion line bundle

Recall our set-up from the end of Section 2.3: We have a back wall B, which is a spin (and therefore oriented) 2-manifold. Associated to B is the configuration space of ψ-ribbon endpoints, $\mathcal{R}(B)$. This configuration space is a disjoint union of pieces $\mathcal{R}(B)_k$, where k is number of ribbon endpoints in a configuration.

Our goal in this subsection is to construct a complex line-bundle-with-flat-connection $F(B)$ over $\mathcal{R}(B)$, satisfying the following six conditions alluded to in Section 2.3:

1. F is functorial with respect to spin diffeomorphisms. That is, if $f : B \to B'$ is spin diffeomorphism, then there is a corresponding bundle isomorphism $F(B) \to F(B')$ which preserves the flat connections and complex structure.

2. F is functorial with respect to orientation-reversing pin_+ diffeomorphisms. That is, if $f : B \to B'$ is an orientation-reversing pin_+ diffeomorphism, then there is a corresponding map $F(B) \to F(B')$ which preserves the flat connections and is complex antilinear on the fibers. (Recall that any spin manifold has an associated pin_+ structure. By "orientation-reversing pin_+ diffeomorphism", we mean a pin_+ diffeomorphism of the associated pin_+ manifolds which reverses the orientations of the underlying oriented manifolds.) This condition is needed in order to define Hermitian/unitary structures.

3. The holonomy around a loop in $\mathcal{R}(B)$ corresponding to a 2π rotation of a ribbon endpoint is -1. This condition is needed to compensate for fermionic twist of ψ.

4. The holonomy around a loop in $\mathcal{R}(B)$ corresponding to an exchange of two ribbon endpoints (inside a fixed disk) is -1. This condition is needed to compensate for the fermionic statistics of ψ.

5. F is local in the following sense. Given a decomposition $B = B' \cup B''$, there is an obvious map $u : \mathcal{R}(B') \times \mathcal{R}(B'') \to \mathcal{R}(B)$, and a corresponding pull-back bundle $u^*(F(B))$ over $\mathcal{R}(B') \times \mathcal{R}(B'')$. We require an isomorphism $u^*(F(B)) \cong F(B') \otimes F(B'')$ which is natural with respect to spin diffeomorphisms.

6. F satisfies a cancellation property. Given a configuration $r \in \mathcal{R}(B)_k$ and a point $x \in B$ distinct from the ribbon endpoints of c, we can create a new configuration $c_+ \in \mathcal{R}(B)_{k+2}$ by inserting a pair of endpoints in a standard configuration near x. We require an isomorphism of fibers $F(B)_c \cong F(B)_{c_+}$ which is compatible with the flat connection as explained below. This condition is needed to allow for well-defined creation and annihilation of pairs of ψ endpoints in line with the fusion rule $\psi \otimes \psi \cong \mathbb{1}$.

To represent an element of $F(B)$, we will choose spin framings at each ribbon endpoint and also assign an ordering to the ribbon endpoints. The main idea is fairly simple, but making this construction compatible with orientation reversal and ribbon endpoint cancellations requires a bit of fussiness with the details.

Recall the group $\mathrm{Pin}_+(1) \cong \mathbb{Z}/2 \times \mathbb{Z}/2$. We will call the non-identity elements of $\mathrm{Pin}_+(1)$ the "spin flip" (the non-trivial element of the kernel of the covering map $\mathrm{Pin}_+(1) \to O(1)$), the "reflection", and the "other reflection" (the latter two reflections map to the single reflection in $O(1)$).

To construct $F(B)$, we will first construct a principal $\mathrm{Pin}_+(1)$ bundle $P(B)$ over $\mathcal{R}(B)$. The construction of $P(B)$ will be independent of reversing the orientation of B. We define the action of $\mathrm{Pin}_+(1)$ on $\mathbb{C}$ as follows: the spin flip sends $z \in \mathbb{C}$ to $-z$; the reflection sends z to the complex conjugate $\bar{z}$; and the other reflection sends z to $-\bar{z}$. Using this action, we can now define $F(B)$ to be

$$F(B) = P(B) \times_{\mathrm{Pin}_+(1)} \mathbb{C}, \tag{457}$$

the associated $\mathbb{C}$ bundle over $\mathcal{R}(B)$. (Recall that this means that elements of $F(B)$ are represented by pairs $(f, z) \in P(B) \times \mathbb{C}$, and that for each element $a \in \mathrm{Pin}_+(1)$, we identify $(f \cdot a, z)$ with $(f, a \cdot z)$.) Since $P(B)$ is a bundle with discrete fibers, it has a canonical flat connection. This induces a flat connection on $F(B)$.

Note that $F(B)$, as defined above, has two different complex-linear structures, one the conjugate of the other. We will see below that the orientation of B picks out one of the two possible complex structures.

We are now ready, finally, to construct $P(B)$. Let $r \in \mathcal{R}(B)_k$ be a configuration of k ribbon endpoints. At each endpoint of r, there is a distinguished unit tangent vector $v \in TB$ pointing in the direction of the front of the ribbon. There are two unit tangent vectors w_1 and w_2 in TB orthogonal to the distinguished vector. The orientation of B allows us to designate one of these two orthogonal vectors as "positive" and the other as "negative". (We call w_i positive if (v, w_i) is a positively oriented frame with respect to the orientation of B.) We will call a collection of framings (v, w_i) at each endpoint "consistent" if they are all positive or all negative. Note that there are exactly two possible consistent collections of framings for each fixed configuration r. We will denote this set of two elements by $cf(r)$. Note that reversing the orientation of B does not change $cf(r)$.[35]

Now define $\widetilde{cf}(r)$ to be the set of all collections of $\mathrm{Pin}_+(2)$-framings (one at each endpoint) which cover an element of $cf(r)$. At each endpoint, there are two possible lifts of an $O(2)$ framing, so $\widetilde{cf}(r)$ is a set with 2^{k+1} elements. Again, $\widetilde{cf}(r)$ does not change if we reverse the spin structure on B.[36]

Let $S(r)$ denote the set of all orderings of the endpoints of r. It is a set with $k!$ elements. Now consider $\widetilde{cf}(r) \times S(r)$, yet another set associated to a ribbon endpoint configuration r. This set has a group of symmetries G which is generated by (a) spin flips acting on any single endpoint, and (b) the symmetric group S_k, acting on the $S(r)$ component. Let $G_e \subset G$ is the subgroup with even total parity, where parity in this context is defined by the homomorphism from G to $\mathbb{Z}/2$ characterized by the condition that is odd for single spin flips and transpositions. Now, finally, define

$$P(B)_r = (\widetilde{cf}(r) \times S(r))/G_e. \tag{458}$$

[35] It is tempting to say that $cf(r)$ depends only on the underlying unoriented manifold of B, but this is not true if B has more than one path component. Reversing the orientation of some but not all of the path components of B would change $cf(r)$.

[36] Reversing a spin structure is analogous to reversing the orientation of an oriented manifold. One way to define it is to extend the Spin bundle E to a Pin+ bundle E_+; the reversed Spin bundle is $E_+ \setminus E$.

We claim that $P(B)_r$ is naturally a torsor for $\mathrm{Pin}_+(1)$. First, let's check the cardinality: $\widetilde{cf}(r) \times S(r)$ has $2^{k+1}k!$ elements, G_e has $2^{k-1}k!$ elements, and G acts freely on $\widetilde{cf}(r) \times S(r)$. Therefore $P(B)_r$ has four elements.

Now we define the action of $\mathrm{Pin}_+(1)$ on $P(B)_r$. The spin flip acts by changing (any) one of the spin framings of $\widetilde{cf}(r)$ by a spin flip. The reflection acts diagonally on all of the spin framings of $\widetilde{cf}(r)$ (i.e. each spin framing is reflected). These two actions are well-defined and commute, so we have an action of $\mathrm{Pin}_+(1) \cong \mathbb{Z}/2 \times \mathbb{Z}/2$. (If $k = 0$ and $r \in \mathcal{R}(B)_0$ is the unique configuration of zero ribbon endpoints, we define $P(B)_r = \mathrm{Pin}_+(1)$ and let $\mathrm{Pin}_+(1)$ act in the obvious way.)

In summary, an element of $F(B)_r$ is represented by a triple $(f, o, z) \in \widetilde{cf}(r) \times S(r) \times \mathbb{C}$. Spin flips, permutations of ribbon endpoints, and reflections act as

- If f and f' differ by a spin flip at a single ribbon endpoint, then $(f, o, z) = (f', o, -z)$.
- If o and o' differ by an odd permutation, then $(f, o, z) = (f, o', -z)$.
- If f and f' differ by reflecting all of the spin framings, then $(f, o, z) = (f', o, \bar{z})$.

To define complex multiplication by $a \in \mathbb{C}$ on $F(B)_r$, we choose a collection of framings f which is positive with respect to the orientation of B and then define $a \cdot (f, o, z) = (f, o, az)$. If we were to reverse the orientation of B, then we would get the conjugate complex structure on $F(B)$. In other words, $F(B)_r = F(-B)_r$ as sets (and even as vector spaces over $\mathbb{R}$), but the identity map from $F(B)_r$ to $F(-B)_r$ is complex antilinear.

We began this subsection with a list of several desiderata for $F(B)$. It is more or less obvious that $F(B)$ has the right sort of functoriality for both orientation-preserving and orientation-reversing spin/pin maps. It should also be clear that $F(B)$ has the desired holonomies for rotations and exchanges. So all that's left to discuss is locality (gluing) and ribbon endpoint cancellation.

We consider locality first. Let $B = B_1 \cup B_2$. Let $r_i \in \mathcal{R}(B_i)$ and let (f_i, o_i, z_i) represent an element of $F(B_i)_{r_i}$. If the spin framing collections f_1 and f_2 are either both positive or both negative, then $f_1 \cup f_2$ is a consistent spin framing in $\widetilde{cf}(r_1 \cup r_2)$, and the triple $(f_1 \cup f_2, o_1 \cup o_2, z_1 z_2)$ represents an element of $F(B)_{r_1 \cup r_2}$. It is easy to check that this map gives a well-defined isomorphism between $u^*(F(B_1)$ and $F(B') \otimes F(B_2)$, both thought of as line bundles over $\mathcal{R}(B_1) \times \mathcal{R}(B_2)$.

Now for cancelations. We want a relation of the type

$$= \lambda \times (\text{vaccuum}), \tag{459}$$

for some $\lambda \in \mathbb{C}$. On the left hand side we have two ribbon endpoints in a disk $D \subset B$ connected by a ribbon in $D \times I$. We have chosen coordinates so that the front of the ribbon always points in the same direction. The spin framings at the two endpoints are chosen to be related by a translation in these coordinates and to both be positive. We have chosen the ordering so that the second vector at endpoint 1 points toward endpoint 2; we will call this a "standard configuration". As indicated, we want this standard picture to be equal to λ times the empty picture.

We will show that in order for this relation to be compatible with reflections, we must have that $\lambda = -\bar{\lambda}$, i.e. λ must be pure imaginary. Note that in order to define the action

of a reflection on string-nets, it is essential that we have defined an action of $\mathrm{Pin}_+(1)$ on $P(B)_r$ (rather than merely an action of $\mathrm{Spin}(1)$). (A $\mathrm{Pin}_-(1)$ structure would also work, but our examples happen to have Pin_+ rather than Pin_- structures.) The existence of a reflection structure also allows us to define inner products of diagrams.

Consider first the RHS of (459). Reflections take the empty picture to the empty picture, and so, since reflections act antilinearly on $F(B)$, the RHS of (459) maps under reflection to $\bar{\lambda}$ times the empty picture.

Now for the LHS of (459). After a reflection (by which we mean an orientation-reversing map), the framings are no longer positive, and so we must reflect them in order to compare to a standard configuration in the target manifold. After the framings are reflected, the second vector at endpoint 1 points away from endpoint 2, so we must swap the ordering in order for it to be a standard configuration. This change of orderings means that under a reflection, a standard configuration map to -1 times a standard configuration. It follows that we must have $\lambda = -\bar{\lambda}$, and so λ must be purely imaginary.

One can show that this cancellation relation satisfies the necessary coherence relations.

C Basic facts about super algebras

In this appendix we briefly recall some of the key mathematical facts about semisimple super algebras; details can be found in [48].

There are two distinct classes of simple super algebras over $\mathbb{C}$. One class is the set of super algebras $M(r|s)$ for $r, s \in \mathbb{Z}_{\geq 0}$, which are $(r+s) \times (r+s)$ matrices whose even and odd subspaces take the form

$$M(r|s)_0 = \text{matrices of the form } \begin{pmatrix} A & 0 \\ 0 & B \end{pmatrix}, \qquad M(r|s)_1 = \text{matrices of the form } \begin{pmatrix} 0 & C \\ D & 0 \end{pmatrix}. \tag{460}$$

In these expressions, A is an $r \times r$ matrix, B an $s \times s$ matrix, C an $r \times s$ matrix, and D an $s \times r$ matrix.

The other class of simple super algebras are denoted by $Q(n)$ for $n \in \mathbb{Z}_{>0}$, which are $(2n) \times (2n)$ matrices with even and odd subspaces of the form

$$Q(n)_0 = \text{matrices of the form } \begin{pmatrix} A & 0 \\ 0 & A \end{pmatrix}, \qquad Q(n)_1 = \text{matrices of the form } \begin{pmatrix} 0 & B \\ B & 0 \end{pmatrix}, \tag{461}$$

where both A and B are $n \times n$ matrices. In particular, $Q(1) = \langle \mathbb{1}, \sigma^x \rangle$ is the first complex Clifford algebra $\mathbb{C}\ell_1$.

Note that all of the $M(r|s)$ are Morita equivalent to the trivial algebra $M(1|0) \cong \mathbb{C}$. All of the $Q(n)$ are Morita equivalent to $Q(1) \cong \mathbb{C}\ell_1$.

If x is an object in a super pivotal category, then $\mathrm{End}(x)$ will be isomorphic to a direct sum of instances of $M(r|s)$ and $Q(n)$.

The form of a general simple super algebra A can be deduced by computing the center $Z(A)$. (An element a is in $Z(A)$ if it super commutes with everything in A, i.e. if $ax = (-1)^{|a||x|}xa$ for all $x \in A$, with $|x|$ denoting the parity of x.) Since the super algebras $Q(n)$ treat even and odd vectors symmetrically, they expect that they will have odd elements in their center, while this will not be true for the super algebras $M(r|s)$. Indeed, we have that if $Z(A) \cong \mathbb{C}^{1|0}$ then $A \cong M(r|s)$ for some r, s, while if $Z(A) \cong \mathbb{C}^{1|1}$ then $A \cong Q(n)$ for some n.

If A, B are super algebras, their tensor product $C = A \otimes B$ is defined as the super algebra such that $C_0 = A_0 \otimes B_0 + A_1 \otimes B_1$, $C_1 = A_0 \otimes B_1 + B_1 \otimes A_0$. The simple super algebras presented above can be tensored together by using the following rules:

$$\begin{aligned} M(r|s) \otimes M(p|q) &\cong M(rp+sq|rq+sp) \\ M(r|s) \otimes Q(n) &\cong Q(rn+sn) \\ Q(n) \otimes Q(m) &\cong M(nm|nm). \end{aligned} \tag{462}$$

Note that all the $Q(n)$ can be generated from $M(n|0)$ and $Q(1)$ according to $Q(n) \cong M(n|0) \otimes Q(1)$.

D $\frac{1}{2}$E6 data

D.1 Associators

There are four solutions to the pentagon equation for $\frac{1}{2}$E6 fusion rules [57]. They split into two sets, one pair has all positive quantum dimensions, while the other has negative quantum dimension on the x particle. The solutions in each set are related by complex conjugation. Here we present one of the solutions with positive quantum dimensions on all particles (they have been extracted from [42]) . Several of the F symbols are trivial,

$$F_y^{yyy} = F_x^{xyy} = F_x^{yyx} = F_y^{xxy} = F_y^{yxx} = F_{\mathbb{1}}^{xyx} = F_{\mathbb{1}}^{xxy} = F_{\mathbb{1}}^{yxx} = 1 \tag{463}$$

Let v_1, v_2 be orthogonal unit vectors for the two-dimensional splitting space V_x^{xx}. We define the F symbols acting on these vectors by $V_x^{xy} \otimes V_x^{xx} = F_x^{xyx} V_x^{xx} \otimes V_x^{yx}$ in the basis $(v_1, v_2)^T$. Explicitly we have,

$$F_x^{xyx} = \begin{pmatrix} 0 & 1 \\ 1 & 0 \end{pmatrix} \quad F_x^{xxy} = \begin{pmatrix} 0 & -i \\ i & 0 \end{pmatrix} \quad F_x^{yxx} = \begin{pmatrix} 1 & 0 \\ 0 & -1 \end{pmatrix} \tag{464}$$

$$\tag{465}$$

$$F_{\mathbb{1}}^{xxx} = c_2^* \begin{pmatrix} 1 & -i \\ 1 & i \end{pmatrix} \quad F_y^{xxx} = c_2^* \begin{pmatrix} 1 & -i \\ -1 & -i \end{pmatrix}, \qquad c_2 = \frac{e^{7i\pi/12}}{\sqrt{2}} \tag{466}$$

Lastly we have the F symbol whose four external legs are all labeled by x. We write this F symbol down in the basis $(0, y, v_1 \otimes v_1, v_1 \otimes v_2, v_2 \otimes v_1, v_2 \otimes v_2)$, where we have

$$F_x^{xxx} = \begin{pmatrix} \frac{1}{d} & \frac{1}{d} & \frac{c_1^*}{\sqrt{2}} & \frac{c_1^*}{\sqrt{2}} & \frac{c_1^*}{\sqrt{2}} & -\frac{c_1^*}{\sqrt{2}} \\ \frac{1}{d} & -\frac{1}{d} & \frac{c_1^*}{\sqrt{2}} & -\frac{c_1^*}{\sqrt{2}} & \frac{c_1^*}{\sqrt{2}} & \frac{c_1^*}{\sqrt{2}} \\ \frac{e^{-i\pi/4}}{\sqrt{d}} & 0 & -\frac{1}{d} & 0 & -ic_4^* & 0 \\ 0 & \frac{e^{i\pi/4}}{\sqrt{d}} & 0 & c_4^* & 0 & \frac{i}{d} \\ 0 & \frac{e^{-i\pi/4}}{\sqrt{d}} & 0 & -\frac{1}{d} & 0 & ic_4^* \\ \frac{e^{i\pi/4}}{\sqrt{d}} & 0 & c_4^* & 0 & -\frac{i}{d} & 0 \end{pmatrix} \tag{467}$$

$$d = 1 + \sqrt{3} \qquad c_1 = \frac{e^{-5i\pi/6}}{\sqrt{d}} \qquad c_4 = \frac{e^{-i\pi/4}}{\sqrt{2}} \tag{468}$$

particle	spin	e	l_x	l_y
$\mathbb{1}$	1	$\frac{1}{2+d^2}$	$\frac{1}{2\sqrt{3}}$	$\frac{1}{2+d^2}$
W	1	$\frac{1}{2}$		$-\frac{1}{2}$
U	1	$\frac{d}{4\sqrt{3}}$	$-\frac{1}{2\sqrt{3}}$	$\frac{d}{4\sqrt{3}}$

Table D.2.1: Minimal idempotents for $\mathbf{Tube}_{\mathbb{1}\to\mathbb{1}}$. We have used the notation e = empty diagram, $l_x = \mathrm{cl}(x)$, and $l_y = \mathrm{cl}(y)$

particle	spin	t_y	$t_y l_x$	v_y
W	1	$\frac{1}{2}$		$\frac{1}{2}$
Y	1/2	$-\frac{1}{2+d^2}$	$e^{\frac{6i\pi}{12}}\frac{1}{2\sqrt{3}}$	$\frac{1}{2+d^2}$
V	1/2	$-\frac{d}{4\sqrt{3}}$	$e^{\frac{-6i\pi}{12}}\frac{1}{2\sqrt{3}}$	$\frac{d}{4\sqrt{3}}$

Table D.2.2: Minimal idempotents for $\mathbf{Tube}_{y\to y}$. We have used the notation $v_y = \mathrm{id}_y \in \mathbf{Tube}_{y\to y}$, $t_y = t_{y\mathbb{1}yy;11}$, and $t_y l_x = t_{yxyx;11}$.

D.2 Idempotents

In this appendix we provide the minimal idempotents of $\mathbf{Tube}(\frac{1}{2}\mathrm{E}_6)$, and give there images under condensation of y. The inclusion is performed by simply condensing fermions off the tubes in $\mathbf{Tube}(\frac{1}{2}\mathrm{E}_6)$ to get tubes in $\mathbf{Tube}(\frac{1}{2}\mathrm{E}_6/y)$. Special care must be taken with respect to spin structure issues, since removing y lines may force a pair of fermions to traverse a cycle of the tube.

The minimal idempotents of $\mathbf{Tube}(\frac{1}{2}\mathrm{E}_6)$ are listed in tables D.2.1, D.2.3, and D.2.2. They were found by brute force on a computer. We also identify the minimal idempotents of $\mathbf{Tube}(\frac{1}{2}\mathrm{E}_6)$ with simple objects of the Drinfeld center $\mathcal{Z}(\frac{1}{2}\mathrm{E}_6)$ listed in [40].[37] Under condensation of y described in Section 7 we find the following maps from idempotents in $\mathbf{Tube}(\frac{1}{2}\mathrm{E}_6)$ to those in in $\mathbf{Tube}(\frac{1}{2}\mathrm{E}_6/y)$:

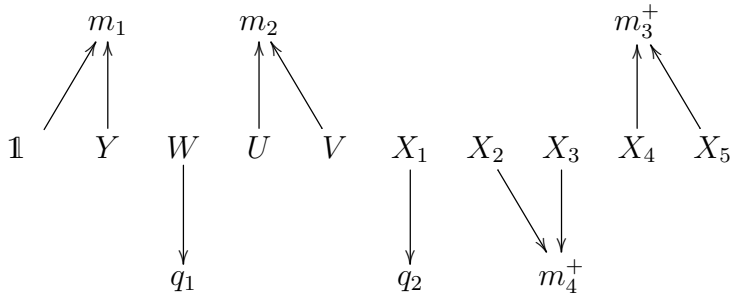

(469)

where the center line lists the idempotents in $\mathbf{Tube}(\frac{1}{2}\mathrm{E}_6)$ and the upper and lower objects are the objects in $\mathbf{Tube}(\frac{1}{2}\mathrm{E}_6/y)$. The identifications are made by taking a minimal idempotent in $\mathbf{Tube}(\frac{1}{2}\mathrm{E}_6)$ and using the inclusion to $\mathbf{Tube}(\frac{1}{2}\mathrm{E}_6/y)$, as discussed in Section 5.3.

Some of the idempotents are isomorphic. For example, W appears in all three tables D.2.1, D.2.3 and D.2.2 (with its boundary condition $\mathbb{1}$, y or x implicit in each table).

[37] Disclaimer: At the level of fusion rules and spins, idempotents X_2 and X_3 are identical and so there is an ambiguity in identifying these minimal idempotents with the simple objects in $Z(\mathcal{C})$ of [40]. The spins here differ from those in [40] by complex conjugation.

particle	spin	t_x	v_x	X_{11}	X_{12}	X_{21}	X_{22}	$v_x l_y$	$t_x h_y$
W	1	$\frac{1}{2d}$	$\frac{1}{2d}$	$e^{\frac{-9i\pi}{12}}\frac{\sqrt{3d-8}}{4}$	$e^{\frac{-9i\pi}{12}}\frac{\sqrt{3d-8}}{4}$	$e^{\frac{9i\pi}{12}}\frac{\sqrt{3d-8}}{4}$	$e^{\frac{-3i\pi}{12}}\frac{\sqrt{3d-8}}{4}$	$e^{\frac{6i\pi}{12}}\frac{1}{2d}$	$e^{\frac{-6i\pi}{12}}\frac{1}{2d}$
U	1	$\frac{1}{4\sqrt{3}}$	$\frac{1}{4\sqrt{3}}$	$e^{\frac{3i\pi}{12}}\frac{1}{4\sqrt{d}}$	$e^{\frac{9i\pi}{12}}\beta$	$e^{\frac{-9i\pi}{12}}\beta$	$e^{\frac{-3i\pi}{12}}\frac{1}{4\sqrt{d}}$	$e^{\frac{-6i\pi}{12}}\frac{1}{4\sqrt{3}}$	$e^{\frac{6i\pi}{12}}\frac{1}{4\sqrt{3}}$
V	1/2	$-\frac{1}{4\sqrt{3}}$	$\frac{1}{4\sqrt{3}}$	$e^{\frac{-3i\pi}{12}}\beta$	$e^{\frac{-9i\pi}{12}}\frac{1}{4\sqrt{d}}$	$e^{\frac{-3i\pi}{12}}\frac{1}{4\sqrt{d}}$	$e^{\frac{-9i\pi}{12}}\beta$	$e^{\frac{-6i\pi}{12}}\frac{1}{4\sqrt{3}}$	$e^{\frac{-6i\pi}{12}}\frac{1}{4\sqrt{3}}$
X_2	$-5/12$	$e^{\frac{-10i\pi}{12}}\frac{1}{2+d^2}$	$\frac{1}{2+d^2}$	$e^{\frac{-2i\pi}{12}}\gamma$	$e^{\frac{10i\pi}{12}}\alpha$	$e^{\frac{4i\pi}{12}}\alpha$	$e^{\frac{4i\pi}{12}}\gamma$	$e^{\frac{6i\pi}{12}}\frac{1}{2+d^2}$	$e^{\frac{8i\pi}{12}}\frac{1}{2+d^2}$
X_1	1/4	$e^{\frac{6i\pi}{12}}\frac{1}{2+d^2}$	$\frac{1}{2+d^2}$	$e^{\frac{6i\pi}{12}}\frac{1}{2\sqrt{6d}}$	$e^{\frac{6i\pi}{12}}\frac{1}{2\sqrt{6d}}$	$\frac{1}{2\sqrt{6d}}$	$-\frac{1}{2\sqrt{6d}}$	$e^{\frac{6i\pi}{12}}\frac{1}{2+d^2}$	$\frac{1}{2+d^2}$
X_3	$-5/12$	$e^{\frac{-10i\pi}{12}}\frac{1}{2+d^2}$	$\frac{1}{2+d^2}$	$e^{\frac{10i\pi}{12}}\alpha$	$e^{\frac{-2i\pi}{12}}\gamma$	$e^{\frac{-8i\pi}{12}}\gamma$	$e^{\frac{-8i\pi}{12}}\alpha$	$e^{\frac{6i\pi}{12}}\frac{1}{2+d^2}$	$e^{\frac{8i\pi}{12}}\frac{1}{2+d^2}$
X_5	1/3	$e^{\frac{8i\pi}{12}}\frac{1}{2+d^2}$	$\frac{1}{2+d^2}$		$e^{\frac{1i\pi}{12}}\frac{1}{2\sqrt{3d}}$	$e^{\frac{7i\pi}{12}}\frac{1}{2\sqrt{3d}}$		$e^{\frac{-6i\pi}{12}}\frac{1}{2+d^2}$	$e^{\frac{-10i\pi}{12}}\frac{1}{2+d^2}$
X_4	$-1/6$	$e^{\frac{-4i\pi}{12}}\frac{1}{2+d^2}$	$\frac{1}{2+d^2}$	$e^{\frac{-11i\pi}{12}}\frac{1}{2\sqrt{3d}}$			$e^{\frac{7i\pi}{12}}\frac{1}{2\sqrt{3d}}$	$e^{\frac{-6i\pi}{12}}\frac{1}{2+d^2}$	$e^{\frac{2i\pi}{12}}\frac{1}{2+d^2}$

Table D.2.3: Minimal idempotents for $\mathbf{Tube}_{x\to x}$. We have used the notation $t_x = t_{x\mathbb{1}xx;11}$, $v_x = \mathrm{id}_x \in \mathbf{Tube}_{x\to x}$, $X_{ij} = t_{xxx;ij}$, $v_x l_y = t_{xxxy;11}$, and $t_x h_y = t_{xyxx;11}$. Where $\alpha = \frac{1}{2}\left(1 + 1/\sqrt{2d+1}\right)$, and $\beta = \frac{1}{2}\left(1 - 1/\sqrt{2d+1}\right)$, $\gamma/\alpha = 1/(2\sqrt{d}3^{1/4})$, and $d = 1+\sqrt{3}$.

As usual, if e and e' are isomorphic idempotents, then we can find morphisms u, v such that $e = u \cdot v$ and $e' = v \cdot u$. In the following we denote the boundary condition of each idempotent by a subscript and similarly for the morphisms, so that, e.g., $W_x = w_{x\mathbb{1}} \cdot w_{\mathbb{1}x} = w_{xy} \cdot w_{yx}$, and $W_{\mathbb{1}} = w_{\mathbb{1}x} \cdot w_{x\mathbb{1}} = w_{\mathbb{1}y} \cdot w_{y\mathbb{1}}$ and so on. We have:

$$w_{\mathbb{1}x} = \frac{i}{\sqrt{2\sqrt{2d}}}(t_{\mathbb{1}xxx;11} - t_{\mathbb{1}xxx;12}) \tag{470}$$

$$w_{x\mathbb{1}} = \frac{-i}{\sqrt{2\sqrt{2d}}}(t_{xx\mathbb{1}x;11} - t_{xx\mathbb{1}x;21}) \tag{471}$$

$$w_{xy} = \frac{1}{(8d)^{\frac{1}{4}}}(t_{xxyx;11} + t_{xxyx;21}) \tag{472}$$

$$w_{yx} = \frac{1}{(8d)^{\frac{1}{4}}}(t_{yxxx;11} + t_{yxxx;12}) \tag{473}$$

$$w_{\mathbb{1}y}\frac{-e^{-i\pi/4}}{\sqrt{2}}t_{\mathbb{1}xyx;11} \tag{474}$$

$$w_{y\mathbb{1}}\frac{-e^{i\pi/4}}{\sqrt{2}}t_{yx\mathbb{1}x;11} \tag{475}$$

$$u_{\mathbb{1}x} = \frac{1}{2}\sqrt{\frac{d}{6}}(t_{\mathbb{1}xxx;11} + t_{\mathbb{1}xxx;12}) \tag{476}$$

$$u_{x\mathbb{1}} = \frac{1}{2}\sqrt{\frac{d}{6}}(t_{xx\mathbb{1}x;11} + t_{xx\mathbb{1}x;21}) \tag{477}$$

$$v_{xy} = \frac{i}{2}\left(\frac{d}{6}\right)^{\frac{1}{4}}(t_{xxyx;11} - t_{xxyx;21}) \tag{478}$$

$$v_{yx} = \frac{i}{2}\left(\frac{d}{6}\right)^{\frac{1}{4}}(t_{yxxx;11} - t_{yxxx;21}) \tag{479}$$

with

$$t_{abcd;\mu\nu} = \quad . \tag{480}$$

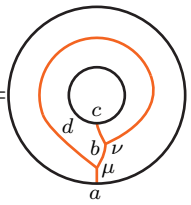

In terms of diagrams, we have

$$W_{\mathbb{1}} \underset{w_{x\mathbb{1}}}{\overset{w_{\mathbb{1}x}}{\rightleftarrows}} W_x \underset{w_{yx}}{\overset{w_{xy}}{\rightleftarrows}} W_y \qquad U_{\mathbb{1}} \underset{u_{x\mathbb{1}}}{\overset{u_{\mathbb{1}x}}{\rightleftarrows}} U_x \qquad V_x \underset{v_{yx}}{\overset{v_{xy}}{\rightleftarrows}} V_y \ . \tag{481}$$

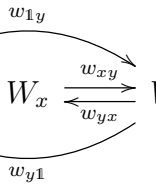

Composing the morphisms in various ways constructs all isomorphic idempotents.

References

[1] K. Walker, "Super planar algebras and D_{odd}." Presented at Subfactors in Maui conference, 2013.

[2] K. Walker, "Domains walls, categorified group actions, and condensing fermions." Presented at "Symmetry in Topological Phases", Princeton, 2014. http://canyon23.net/math/talks/PCTS%20201403%20compressed.pdf.

[3] K. Walker, "Codimension-1 defects, categorified group actions, and condensing fermions." Presented at "Symmetry and Topology in Quantum Matter", Institute for Pure and Applied Mathematics UCLA, 2015. http://www.ipam.ucla.edu/abstract/?tid=12400&pcode=STQ2015.

[4] Z.-C. Gu, Z. Wang, and X.-G. Wen, "Classification of two-dimensional fermionic and bosonic topological orders," *Phys. Rev. B* **91** (Mar, 2015) 125149, arXiv:1010.1517v2.

[5] Z.-C. Gu, Z. Wang, and X.-G. Wen, "Lattice model for fermionic toric code," *Phys. Rev. B* **90** (Aug, 2014) 085140, arXiv:1309.7032.

[6] T. Lan, L. Kong, and X.-G. Wen, "Theory of (2+1)-dimensional fermionic topological orders and fermionic/bosonic topological orders with symmetries," *Phys. Rev. B* **94** (Oct, 2016) 155113, arXiv:1602.05946v2.

[7] N. Tarantino and L. Fidkowski, "Discrete spin structures and commuting projector models for two-dimensional fermionic symmetry-protected topological phases," *Phys. Rev. B* **94** (Sep, 2016) 115115, arXiv:1604.02145v2.

[8] B. Ware, J. H. Son, M. Cheng, R. V. Mishmash, J. Alicea, and B. Bauer, "Ising anyons in frustration-free majorana-dimer models," *Phys. Rev. B* **94** (Sep, 2016) 115127, arXiv:1605.06125.

[9] R. Usher, "Fermionic 6j-symbols in superfusion categories," *arXiv preprint arXiv:1606.03466* (2016) , arXiv:1606.03466.

[10] J. Brundan and A. P. Ellis, "Monoidal supercategories," *Communications in Mathematical Physics* **351** no. 3, (May, 2017) 1045–1089, arXiv:1603.05928.

[11] P. Bruillard, C. Galindo, T. Hagge, S.-H. Ng, J. Y. Plavnik, E. C. Rowell, and Z. Wang, "Fermionic modular categories and the 16-fold way," *Journal of Mathematical Physics* **58** no. 4, (2017) 041704, arXiv:1603.09294.

[12] P. Bonderson, E. C. Rowell, Q. Zhang, and Z. Wang, "Congruence subgroups and super-modular categories," *arXiv preprint arXiv:1704.02041* (2017) . https://arxiv.org/abs/1704.02041.

[13] M. Barkeshli, E. Berg, and S. Kivelson, "Coherent transmutation of electrons into fractionalized anyons," *Science* **346** no. 6210, (2014) 722–725, arXiv:1402.6321.

[14] M. Barkeshli and C. Nayak, "Superconductivity induced topological phase transition at the edge of even denominator fractional quantum hall states," *arXiv preprint arXiv:1507.06305* (2015) , arXiv:1507.06305.

[15] D. Gaiotto and A. Kapustin, "Spin TQFTs and fermionic phases of matter," *International Journal of Modern Physics A* **31** no. 28n29, (2016) 1645044, arXiv:1505.05856.

[16] L. Bhardwaj, D. Gaiotto, and A. Kapustin, "State sum constructions of spin-TFTs and string net constructions of fermionic phases of matter," *Journal of High Energy Physics* **2017** no. 4, (Apr, 2017) 96, arXiv:1605.01640.

[17] L. Bhardwaj, "Unoriented 3d tfts," *Journal of High Energy Physics* **2017** no. 5, (May, 2017) 48, arXiv:1611.02728.

[18] A. Kapustin and R. Thorngren, "Fermionic SPT phases in higher dimensions and bosonization," *arXiv preprint arXiv:1701.08264* (2017) , arXiv:1701.08264.

[19] P. Putrov, J. Wang, and S.-T. Yau, "Braiding statistics and link invariants of bosonic/fermionic topological quantum matter in 2+1 and 3+1 dimensions," *Annals of Physics* (2017) , arXiv:1612.09298.

[20] Y. Wan and C. Wang, "Fermion condensation and gapped domain walls in topological orders," *Journal of High Energy Physics* **2017** no. 3, (Mar, 2017) 172, arXiv:1607.01388.

[21] A. Ocneanu, "Chirality for operator algebras," *Subfactors (Kyuzeso, 1993)* (1994) 39–63.

[22] M. Müger, "From subfactors to categories and topology II: The quantum double of tensor categories and subfactors," *Journal of Pure and Applied Algebra* **180** no. 1, (2003) 159–219, arXiv:math/0111205.

[23] M. A. Levin and X.-G. Wen, "String-net condensation: A physical mechanism for topological phases," *Phys. Rev. B* **71** (Jan, 2005) 045110, arXiv:cond-mat/0404617.

[24] K. Walker, *TQFTs*. 2006. http://canyon23.net/math/.

[25] A. Kapustin, A. Turzillo, and M. You, "Spin topological field theory and fermionic matrix product states," *arXiv preprint arXiv:1610.10075* (2016) , arXiv:1610.10075.

[26] L. H. Kauffman and S. L. Lins, *Temperley-Lieb recoupling theory and invariants of 3-manifolds*. Annals of mathematics studies: no. 134. Princeton, N.J. : Princeton University Press, 1994, 1994.

[27] I. S. Eliëns, J. C. Romers, and F. A. Bais, "Diagrammatics for bose condensation in anyon theories," *Phys. Rev. B* **90** (Nov, 2014) 195130, arXiv:1310.6001.

[28] S. Morrison and K. Walker. In preparation.

[29] J. Cano, M. Cheng, M. Mulligan, C. Nayak, E. Plamadeala, and J. Yard, "Bulk-edge correspondence in (2 + 1)-dimensional abelian topological phases," *Phys. Rev. B* **89** (Mar, 2014) 115116, arXiv:1310.5708.

[30] R. Thorngren, "Framed wilson operators, fermionic strings, and gravitational anomaly in 4d," *Journal of High Energy Physics* **2015** no. 2, (Feb, 2015) 152, arXiv:1404.4385.

[31] A. Ocneanu, "Operator algebras, topology and subgroups of quantum symmetry," *Adv. Studies in Pure Math* (2001) 235–263.

[32] D. E. Evans and Y. Kawahigashi, "On ocneanu's theory of asymptotic inclusions for subfactors, topological quantum field theories and quantum doubles," *International Journal of Mathematics* **6** no. 02, (1995) 205–228.

[33] M. Izumi, "The Structure of Sectors Associated with Longo–Rehren Inclusions I. General Theory," *Communications in Mathematical Physics* **213** no. 1, (2000) 127–179. http://dx.doi.org/10.1007/s002200000234.

[34] N. Bultinck, M. Mariën, D. Williamson, M. Şahinoğlu, J. Haegeman, and F. Verstraete, "Anyons and matrix product operator algebras," *Annals of Physics* **378** (2017) 183 – 233, arXiv:1511.08090.

[35] T. Lan and X.-G. Wen, "Topological quasiparticles and the holographic bulk-edge relation in (2 + 1)-dimensional string-net models," *Phys. Rev. B* **90** (Sep, 2014) 115119, arXiv:1311.1784.

[36] Y. Hu, N. Geer, and Y.-S. Wu, "Full dyon excitation spectrum in generalized levin-wen models," *arXiv preprint arXiv:1502.03433* (2015) , arXiv:1502.03433.

[37] J. Böckenhauer, D. E. Evans, and Y. Kawahigashi, "Longo-rehren subfactors arising from α-induction," *Publications of the Research Institute for Mathematical Sciences* **37** no. 1, (Mar, 2001) 1–35.

[38] A. Kirillow and N. Y. Reshetikhin, "Representations of the algebra $U_q(sl(2))$, q-orthogonal polynomials and invariants of Links," in *Infinite Dimensional Lie Algebras and Groups: Proceedings of the Conference*, vol. 7, p. 285, World Scientific. 1989.

[39] P. H. Bonderson, *Non-Abelian anyons and interferometry*. PhD thesis, California Institute of Technology, 2007.

[40] S.-M. Hong, E. Rowell, and Z. Wang, "On exotic modular tensor categories," *Communications in Contemporary Mathematics* **10** no. supp01, (2008) 1049–1074, arXiv:0710.5761.

[41] K. Okazaki, "The state sum invariant of 3–manifolds constructed from the E6 linear skein," *Algebraic & Geometric Topology* **13** no. 6, (2013) 3469–3536.

[42] K. Suzuki and M. Wakui, "On the turaev-viro-ocneanu invariant of 3-manifolds derived from the E_6-subfactor," *Kyushu Journal of Mathematics* **56** no. 1, (2002) 59–81.

[43] M. Izumi, "The structure of sectors associated with Longo-Rehren inclusions. II. Examples," *Reviews in Mathematical Physics* **13** no. 05, (2001) 603–674.

[44] G. Kuperberg, "Spiders for rank 2 lie algebras," *Comm. Math. Phys.* **180** no. 1, (1996) 109–151, arXiv:q-alg/9712003.

[45] V. F. Jones, "Planar algebras, I," *arXiv preprint math/9909027* (1999) , arXiv:math/9909027.

[46] S. Morrison and K. Walker, "Blob homology," *Geometry & Topology* **16** no. 3, (2012) 1481–1607, arXiv:1009.5025.

[47] A. Joyal and R. Street, "Tortile yang-baxter operators in tensor categories," *Journal of Pure and Applied Algebra* **71** no. 1, (1991) 43 – 51.

[48] T. Józefiak, "Semisimple superalgebras," in *Algebra Some Current Trends*, pp. 96–113. Springer, 1988.

[49] P. Deligne, P. Etingof, D. S. Freed, L. C. Jeffrey, D. Kazhdan, J. W. Morgan, D. R. Morrison, and E. Witten, "Quantum fields and strings: a course for mathematicians, volume 1 and 2," *American Mathematical Society, Providence, RI* (1999) .

[50] V. Turaev and O. Viro, "State sum invariants of 3-manifolds and quantum 6j-symbols," *Topology* **31** no. 4, (1992) 865 – 902.

[51] J. Barrett and B. Westbury, "Invariants of piecewise-linear 3-manifolds," *Transactions of the American Mathematical Society* **348** no. 10, (1996) 3997–4022, arXiv:hep-th/9311155.

[52] V. G. Turaev, *Quantum invariants of knots and 3-manifolds*, vol. 18. Walter de Gruyter GmbH & Co KG, 2016.

[53] A. Y. Kitaev, "Unpaired majorana fermions in quantum wires," *Physics-Uspekhi* **44** no. 10S, (2001) 131, arXiv:cond-mat/0010440.

[54] L. Fidkowski and A. Kitaev, "Topological phases of fermions in one dimension," *Phys. Rev. B* **83** (Feb, 2011) 075103, arXiv:1008.4138.

[55] N. Bultinck, D. J. Williamson, J. Haegeman, and F. Verstraete, "Fermionic matrix product states and one-dimensional topological phases," *Phys. Rev. B* **95** (Feb, 2017) 075108, arXiv:1610.07849.

[56] Y.-Z. You and M. Cheng, "Measuring modular matrices by shearing lattices," *arXiv preprint arXiv:1502.03192* (2015) , arXiv:1502.03192.

[57] T. J. Hagge and S.-M. Hong, "Some non-braided fusion categories of rank 3," *arXiv preprint arXiv:0704.0208* (2007) , arXiv:0704.0208.